UNIVERSITÀ DEGLI STUDI DI PADOVA

Sede Amministrativa: Università degli Studi di Padova

Dipartimento di Ingegneria Idraulica, Marittima, Ambientale e Geotecnica - IMAGE

SCUOLA DI DOTTORATO DI RICERCA IN SCIENZE DELL'INGEGNERIA CIVILE ED AMBIENTALE

INDIRIZZO: IDRODINAMICA E MODELLISTICA AMBIENTALE

XX° CICLO

SEDIMENT BUDGET OF UNSURVEYED RIVERS AT WATERSHED SCALE: THE CASE OF LOWER ZAMBEZI

Direttore della Scuola : Ch.mo Prof. Andrea Rinaldo

Supervisore :Ch.mo Prof. Giampaolo Di Silvio

Dottorando: Paolo Ronco

31 GENNAIO 2008

a Donata

(..) now when I was a little chap I had a passion for maps. I would look for hours at South America, or Africa, or Australia, and lose myself in all the glories of exploration. At that time there were many blank spaces on the earth, and when I saw one that looked particularly inviting on a map I would put my finger on it and say:

'When I grow up I will go there.'

(..) It had got filled since my boyhood with rivers and lakes and names. It had ceased to be a blank space of delightful mystery - a white patch for a boy to dream gloriously over.

It had become a place of darkness.

But there was in it one river especially, a mighty big river, that you could see on the map, resembling an immense snake uncoiled, with its head in the sea, its body at rest curving afar over a vast country, and its tail lost in the depths of the land. And as I looked at the map of it in a shop-window, it fascinated me as a snake would a bird -- a silly little bird.

I went on along Fleet Street, but could not shake off the idea.

The snake had charmed me.

(Heart of Darkness, Joseph Conrad)

AKNOWLEDGEMENTS

This research has been carried on in the framework of the activities of ISI (International Sedimentation Initiative), International Hydrological Programme (IHP) of UNESCO (a special thank to prof. Stevan Bruk) and has been supported by the Italian Ministry of the University (PRIN 2004). A particular acknowledgement to the Mozambican River Authorities DNA and Ara Zambeze as well as to HCB for its precious support in the data collection in Mozambique.

My warmest thanks to prof. Giampaolo Di Silvio that gave me the great opportunity to follow my aspirations and provided me a lot of suggestions and incentives, and to prof. Gerrit Basson for his precious suggestions during the revision of this thesis.

Many thanks to all the wonderful *XX°ciclo* team (TFR congress team, Elisa, Enrico, Giulia, Luca and Martina), for the very good times we had in our headquarter in front of Piovego, that inspired me a lot, especially during the spring time.

A special thought to all the mozambican and italian people that helped and supported me during this long and exciting period. Kanimambo!

Un ringraziamento speciale ai miei genitori, per la pazienza e il sostegno, incondizionato.

To the Club and to the supporters, ACM.

CONTENTS

LIST OF FIGURES

LIST OF TABLES

ABSTRACT

The issue of sustainable management of natural resources, such as water and land, is rising to the attention of the technical and scientific community as a crucial theme of global relevance that asks for a global response both in terms of improved knowledge, better means and specific actions. Earth's erosion and sedimentation processes are of particular interest because they are directly related to human activities, in a bilateral way.

The main constraint is often represented, especially in Developing Countries, by the lack of data and of economic means to collect them. The objective of the present study is trying to integrate the few available data with appropriate and innovative models of sediment transport for simulating the long-term profile evolution of a river and assess at the same time the necessary terms of a sediment balance at watershed scale. The method has been applied to the lower Zambezi river.

In Chapter 1, an overview of recent developments in sediment management and research is presented, underlining the differences in regional approaches, depending upon the respective social and geographical settings. The three basic forms of sediment motion (surface, mass and linear movement, mainly responsible for river processes) and the time- and space-scales of sedimentary systems are considered, underlying the ample variety of features encountered moving along the river from the divide to the coast. A number of morphological models (one, two- and three-dimensional) developed at different time- and space scales and with various degrees of detail and approximation consent to describes these processes.

Soil and water conservation is one of the most critical environmental issues facing many countries, especially in Developing Countries (DC) where the strong impact of climate change, urbanization, deforestation, land degradation, droughts and desertification is increasing conflicts for the use of natural resources. In the various Sections of Chapter 1 a review is made about the present state of research in the field of soil erosion, sedimentation and morphodynamics. The solution of all the related problems, however, require the monitoring of several natural and human induced phenomena. Unfortunately, the capability to collect and manage water and sediment resources-related information remains inadequate in many parts of the world: the African case is particularly dramatic due to the chronic lack of

available data, not only on solid transport but also on the bathymetric and topographic river configuration.

An innovative methodology to better integrate the scanty and sometimes unreliable bathymetric data is presented in Chapter 2. The waterflow and sediment transport equations have been linearized and analytically solved under the hypothesis of quasi-equilibrium conditions. This simplification permits to reconstruct the river bathymetry from planimetric data, the only ones available from satellite images for most of the large rivers of the world, and from averaged altimetric data, usually provided by the available DEM's. The linearized quasi-equilibrium solution provides a criterion to evaluate the accuracy of the approximate (uniform-flow) model, compared to the regular (steady-flow) model, also for non-linear equations in non-equilibrium conditions. The approximate solution presents many advantages which become crucial for long-term morphological computations at watershed scale. The accuracy of the approximate solution appears to improve when the river is schematized with a coarse computational grid although, of course, with a corresponding loss of spatial resolution. A detailed comparative analysis of the accuracy and resolution of both models has been carried out, with an application to the lower Zambezi river in Mozambique.

Finally, with the methodology previously developed, in Chapter 3 we investigated the effects of damming on the morphological evolution of lower Zambezi river. In fact, the few, coarse and non simultaneous data have been integrated with the help of the same simplified model utilized for the morphological analysis. The Zambezi river is the fourth largest river in Africa (after Congo, Nile and Niger) and it is the largest African river flowing into the Indian Ocean. The lower Zambezi in Mozambique is strongly influenced by the presence of two very large reservoirs (Kariba dam and Cahora Bassa dam) that have modified the natural seasonal flows, as well as the sediment balance and morphology of the river. In particular, downstream of the Cahora Bassa reservoir down to the delta, non negligible effects are taking place, such as local scour, bank collapse and shore-line progressive erosion, together with economic and ecologic consequences on shrimp production and biodiversity alteration. In order to assess and possibly mitigate those effects, a quantitative and qualitative analysis of the erosion/sedimentation/sediment transport phenomena along the lower Zambezi is urgently needed. As already mentioned, the main constraint is represented by the scanty and unreliable data available: the Mozambican hydrometric monitoring network is very scarce and no bathymetric survey of the river has been made. Besides the systematic flow records at the dam

sites and few occasional measurements of turbidity and bottom granulometry, only the Digital Elevation Model (DEM) is available. Therefore, the objective of Chapter 3 is investigating the effects of the presence of Kariba and Cahora Bassa dams on the downstream morphology, integrating the few, coarse and non simultaneous data with a simplified model. The results of simulations substantially agree with the celebrated scale of Lane, (quite often invoked to explain the effects of river damming), on the condition that the time- and space-propagation of the disturbances is taken into account. In fact, the reduction of waterflow seems to have an immediate effect downstream by initially fostering the sediment deposition. Subsequently, the total interception of sediment by the dam slowly takes over and inverts this tendency. A larger degradation (or smaller aggradation) with respect to the *natural conditions* (no dams) seems to represent the eventual dominant effect of damming in the long term evolution of the river.

SOMMARIO

La gestione sostenibile delle risorse naturali, tra le quali l'acqua e il suolo rivestono un'importanza fondamentale, sta emergendo in misura sempre maggiore presso la comunità tecnico-scientifica come una tematica di cruciale interesse su scala globale, che esige una serie di risposte urgenti, anch'esse su scala globale, rivolte da un lato all'approfondimento della conoscenza dei processi naturali, dall'altro alla realizzazione di azioni e interventi specifici. I processi di erosione e di sedimentazione rivestono un particolare interesse perché strettamente legati alle attività antropiche, secondo una relazione di causa-effetto biunivoca, o addirittura progressivamente peggiorativa.

In molti stati e in particolar modo nei Paesi in Via di Sviluppo (PVS), l'ostacolo principale è spesso rappresentato, dalla (cronica) carenza di dati e di mezzi economici per poterli raccogliere e gestire. L'obiettivo di questa tesi sarà quindi lo sviluppo di metodologie innovative per l'integrazione dei, seppur pochi, dati e informazioni disponibili con modelli semplificati di trasporto solido, utilizzati per simulare l'evoluzione morfodinamica a lungo termine di un corso d'acqua, a scala di bacino. Questa metodologia è stata applicata al fiume Zambezi, nel suo tratto terminale in Mozambico.

Nel Capitolo 1 viene presentato lo stato dell'arte circa i recenti sviluppi della ricerca nel campo dei processi di evoluzione morfodinamica, le cui implicazioni hanno un carattere fortemente diversificato nelle varie regioni del mondo a seconda delle relative condizioni socio-economiche e climatiche presenti. Dopo una breve descrizione delle principali modalità di trasporto di sedimenti (erosione superficiale, movimento di massa e trasporto lineare nel corso d'acqua) e ad una caratterizzazione dei processi di sedimentazione rispetto alla scala spazio-temporale a cui fanno riferimento all'interno del bacino fluviale (dal versante montano alla zona costiera), vengono esaminate le tipologie di modelli morfologici più utilizzati per la descrizione di tali processi, sottolineandone il grado di dettaglio e le approssimazioni utilizzate per ricavarli. La salvaguardia delle acque, superficiali e sotterranee, e dei suoli rappresenta una delle questioni ambientali più critiche in molti paesi e soprattutto nei PVS dove il pesante impatto socio-ambientale causato dal cambiamento climatico, dall'urbanizzazione crescente, dalla deforestazione, dalla desertificazione e dalle sempre più frequenti siccità, sta esacerbando notevolmente il conflitto per lo sfruttamento delle risorse

naturali. La soluzione di questi problemi, strettamente correlati tra loro, richiede innanzitutto un'adeguata e specifica azione di monitoraggio (raccolta dati) relativamente ai processi naturali coinvolti e agli interventi antropici che insistono sul territorio. Sfortunatamente, la capacità di raccolta e di gestione dei dati riguardanti le tematiche acqua-suolo rimangono inadeguate in molte parti del mondo. Viene quindi esaminato, nella seconda parte del Capitolo 1, il caso del continente africano la cui situazione è particolarmente drammatica a causa della cronica mancanza di strumenti adeguati e informazioni attendibili inerenti il trasporto fluviale di sedimenti e, in particolare, di dati provenienti da rilievi batimetrici e topografici, indispensabili per un inquadramento preliminare dei casi studio.

Nel Capitolo 2 viene esposta una metodologia innovativa per il trattamento e l'utilizzazione dei (pochi) dati planimetrici e topografici a disposizione. Le equazioni della fase liquida e del trasporto di sedimenti sono state linearizzate e risolte analiticamente ipotizzando valide le condizioni di quasi-equilibrio. Questa semplificazione permette di ricostruire la batimetria di un corso d'acqua a partire dalla sua configurazione plani-altimetrica, ricavata elaborando le immagini satellitari e i modelli digitali del terreno (DEM) a medio-bassa risoluzione; facilmente ottenibili anche con un budget limitato. La soluzione linearizzata di quasi-equilibrio fornisce un criterio che permette di valutare l'accuratezza del modello approssimato (a moto uniforme) rispetto al modello regolare (a moto permanente), entrambi uni-dimensionali, anche per le equazioni non lineari in condizioni di non equilibrio. La soluzione approssimata presenta numerosi vantaggi (soprattutto in termini di minor sforzo computazionale richiesto), che risultano essere di fondamentale importanza per lo svolgimento di simulazioni a lungo termine, a scala di bacino. La metodologia sviluppata, che si basa sul concetto di errore teorico relativo tra soluzione approssimata e soluzione regolare, permette di stabilire la dimensione minima della griglia computazionale (*morphological box*), affinché l'utilizzo di modelli approssimati a moto uniforme sia possibile e dia buoni risultati, sia in termini di accuratezza che di risoluzione. I risultati del confronto tra i due modelli, applicati ad un caso studio reale, confermano che l'accuratezza della soluzione approssimata aumenta con le dimensioni della *morphological box*. L'analisi comparativa si è svolta prendendo come caso di studio reale il fiume Zambezi in Mozambico.

Gli strumenti analitici, le metodologie e i modelli semplificati sviluppati nelle sessioni precedenti sono state di seguito utilizzati, nel Capitolo 3, per studiare l'effetto della costruzione di sbarramenti sull'evoluzione morfodinamica del fiume Zambezi in Mozambico,

a partire dai dati e dalle informazioni reperibili (poche e cronologicamente non omogenee). Il fiume Zambezi, quarto per lunghezza in Africa dopo il Congo, il Nilo e il Niger, è il principale corso d'acqua africano che sfocia nell'Oceano Indiano. La costruzione, a monte, di due tra i più grandi invasi artificiali del mondo (Kariba e Cahora Bassa) ha sostanzialmente modificato il ciclo idrologico naturale, il trasporto di sedimenti e la morfologia di questo fiume nel suo tratto finale in Mozambico. In particolare, a valle della diga di Cahora Bassa e per effetto della stessa sono state da alcuni autori segnalate conseguenze non trascurabili sia sulla morfologia fluviale (scavi localizzati, erosione di sponda, arretramento del delta) sia sulle attività economiche (diminuzione della pescosità delle acque) che sulla biodiversità in generale. Al fine di approfondire la dinamica dei processi in atto e di caratterizzare i fenomeni coinvolti (anche in funzione di eventuali successivi interventi mitigatori), si ritiene quindi indispensabile svolgere un'analisi qualitativa e quantitativa dei processi di erosione/trasporto/sedimentazione lungo l'intero corso d'acqua considerato. Come sottolineato in precedenza, l'ostacolo principale è rappresentato dalla scarsità (anche qualitativa) dei dati a disposizione: anche a causa della perdurante situazione di instabilità politico-economica del paese, la rete di monitoraggio idro-morfologico mozambicana è molto precaria e non è mai stato eseguito alcun rilievo topo-batimetrico dai cui poter ottenere le pendenze del fondo del fiume. Gli unici dati di cui si dispone sono alcune misure sistematiche di portata liquida (volumi in ingresso al serbatoio e portate scaricate), occasionali misure di torpidità e di composizione granulometrica del fondo, la planimetria (da immagini LANSAT) e un modello digitale del terreno (DEM) a bassa risoluzione. L'obiettivo del Capitolo 3 è quindi quello di simulare, secondo le schematizzazione e le metodologie sviluppate nei capitoli precedenti, l'evoluzione morfologica del fiume Zambezi per valutare l'effetto della presenza delle dighe di Kariba e Cahora Bassa, sia in termini di modificazione del naturale ciclo idrologico che di riduzione sostanziale dell'apporto di sedimenti a valle. I risultati delle simulazioni confermano nella sostanza quanto previsto dalla bilancia di Lane (utilizzata di frequente per spiegare l'effetto della presenza di sbarramenti sulla morfologia fluviale), soprattutto quando si metta in conto la propagazione spazio-temporale delle perturbazioni idro-sedimentologiche provocate dalle dighe. La riduzione della portata liquida provoca infatti un immediato effetto a valle incoraggiando il deposito di sedimenti; è solo molto dopo a questa fase che la totale intercettazione dei sedimenti da parte dei serbatoi prende il sopravvento invertendo questa tendenza. La maggiore erosione (o minor deposito) rispetto alle condizioni naturali (senza dighe) sembra essere l'effetto dominante della presenza degli sbarramenti nell'evoluzione morfologica a lungo termine del fiume.

Chapter 1

Erosion and Sedimentation: Processes and Data

1.1 INTRODUCTION

Sediment research has been marked by an intensive progress in the last decade. Sediment management has widely been acknowledged as an important aspect of water management and renewed research efforts have been launched in several regions of the world. Research approaches reflect regional priorities, with shifting accents in different regions, as aptly stated by Gordon Grant (2002): “Comparing river problems and strategies for dealing with them in Europe, Japan, the US, and Philippines reveals how strongly water and sediment issues are conditioned by their social and geomorphic settings”. Regional differences have been also appreciated in the meetings between sedimentation specialists of China and the USA (Proceedings of the Workshop on Sediment Transport and Environmental Studies, 2002).

The theme of erosion and sedimentation must be seen as key factor in many different socio-economical environments, but takes special emphasis in the context of the Less

Developed Countries (Africa, Asia, South America) since there are many important problems, both practical and more academic, linked to erosion, transport and deposition of sediment in these countries. For example, soil erosion and associated land degradation are a major problem in many areas of the African continents, and this problem is growing year by year in response to increasing population pressure on agriculture land. Rates of erosion well in excess of rate of soil formation are a recipe for disaster and there is a clear need for improving understanding of soil loss tolerances and for formulation of appropriate soil conservation strategies. These in turn require improved knowledge of erosion processes and the development of effective prediction techniques. Furthermore, the impact of soil erosion will frequently extend beyond the immediate vicinity of erosion fields, because increased sediment yields may introduce serious problems of reservoir sedimentation downstream (Walling, 1984).

The theme of reservoir sedimentation is of particular interest. In fact, in regions where water supply of agriculture and people strongly depends upon surface water stored in reservoirs created by dams, the accent of sediment management is on the preservation of reservoir storage capacity (Bruk, 2003). The current estimate of total reservoir storage worldwide is around 9000 km^3. Between 0.5 and 1 percent of the total storage volume is lost annually as a result of sedimentation (White, 2001). Using the lower figure, this means a loss of 45 km^3 per year. At an average cost of US$ 0.2 /m^3, this would require investments on the order of US$ 9 billion per year, not accounting for the cost of environmental and social issues associated with new dams. Prediction of reservoir sedimentation has high priority where the economic and social consequences of storage loss are alarming (Sumi et al., 2002). Since the most favorable dam sites have already been utilized, sediment management has the goal to extend as much as possible the useful life of existing or new storage reservoirs.

The social risk due to storage loss attains dramatic proportions in the arid and semi arid contexts – North Africa, the Middle East, etc. Failure of water supply may endanger the mere existence of the population. In view of the social and political weight of these regions, this may trigger social crises of global importance. Solutions should be sought in improved, more frugal water uses, with improved technology, combined also with other, non-conventional sources of water, and even making use of the concept of virtual water.

1.2 FORMS OF SEDIMENT MOTION

Removal of sediment from the watershed slopes (erosion) and the subsequent discontinuous motion (dynamics) to the ocean, involve a variety of processes that may be analyzed and classified under different view points, as described in the following.

A middle size watershed of temperate zones (but in fact applying to other climates) is schematically depicted in Fig.(1.1). To give an idea of what usually takes place at different elevations and distances along the water course, the longitudinal dimension is approximately indicated by a logarithmic scale, in such a way as to emphasize the complexity of the problems occurring at the smaller scales (farther and higher areas of the watershed).

Under the action of water (direct: rainfall, overland flow, channeled flow; and indirect: freezing and melting, infiltration, etc.), sediments are removed from the surface of the watershed and conveyed downstream. Depending upon the prevalent extension of the process in three, two or one spatial dimensions, sediment motion assumes three basic forms (*mass, surface and linear*), more or less corresponding, respectively, to (i) landslides, occasionally produced in the steepest slopes of the watershed, even if protected by vegetation; (ii) distributed soil erosion mainly occurring in undulated, scantily vegetated surfaces; and (iii) bedload and suspended transport by waterflow in the stream network. There are also a number of intermediate forms which share some characteristics with the basic ones, as for example: gully development (mass/surface/linear motion) rills erosion (surface/linear movement), debris flow (mass/linear motion). Where rainfall is extremely scarce, as in the desert or in arid zones, wind is often the most effective cause of surface erosion.

Physical phenomena related to sediment motion are therefore extremely numerous and strictly connected with the morphoclimatic conditions under consideration. Moreover, they are traditionally dealt with by different disciplines and professions, very often under a quite “parochial” perspective.

Mass movement, characterized by quick and short displacements of large portions of soil, represent sometimes a risk for human settlement and infrastructures, but also a physiological source of sediments to the rivers in several natural watershed (e.g. in alpine and humid tropical regions). Investigation on mass movement is generally carried on by applied

geologists and, for the structural aspects, by soil mechanics engineers. Mass movement specialists are often barely interested in the final destination of the removed material as sediment yield.

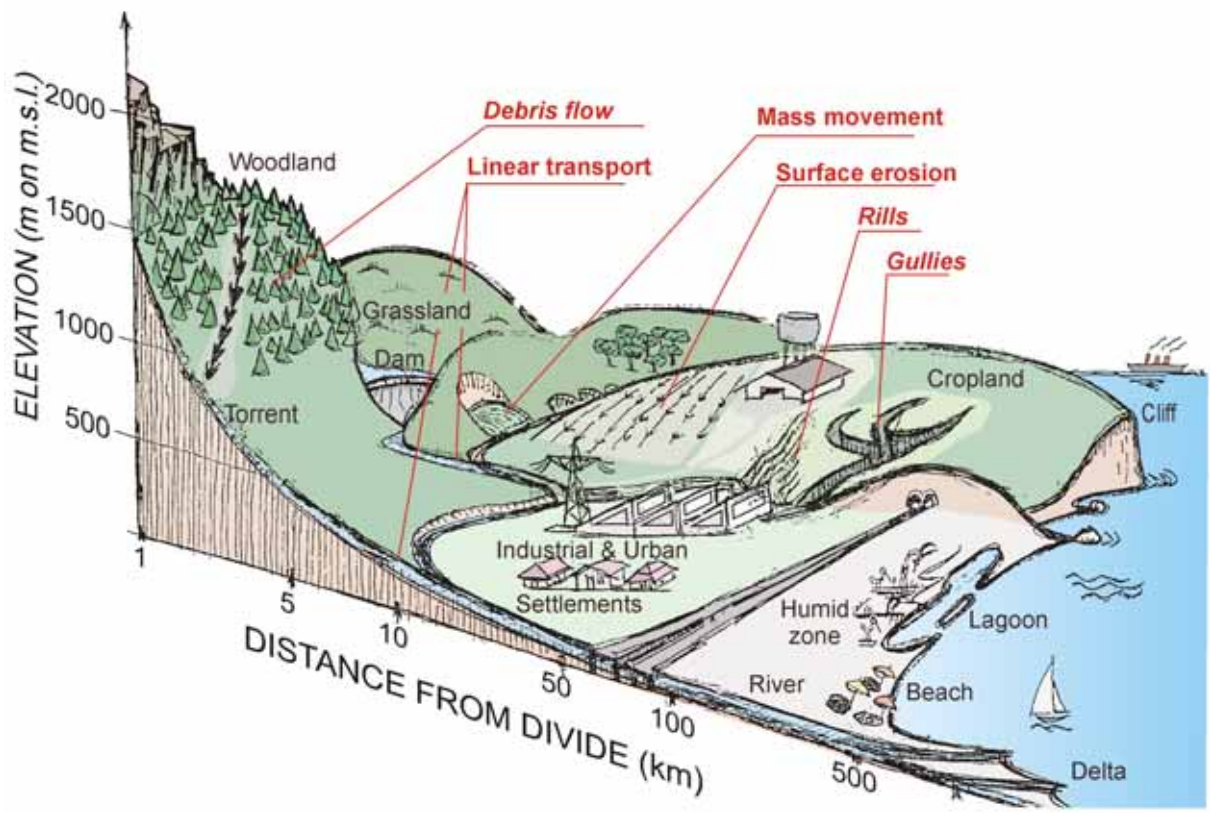

Figure 1.1: Sketch of a watershed in temperate zones: basic forms of sediment motion (Di Silvio, 2006).

Surface erosion, usually as *sheet erosion* but as well as intermediate forms like *rill* and *gully erosion*, for its strict implications with land use and agricultural practices, usually belongs to the province of agronomists and agricultural engineers. It is also investigated however by various scholars of earth science. These forms of erosion constitute a natural source of sediments in arid tropical and temperate regions where rainfall is generally the dominant mechanism of sediment production. On the other hand, surface erosion tends sometimes to be overestimated as a component of sediment yield even in the cases where mass movement prevails.

Finally, *linear transport* is traditionally in the competences of hydrologists and rivers engineers. Bedload and suspended sediment transport convey coarse and fine particles over extremely long distances along the river, down to the estuary, the sea and the adjacent beaches, where they usually pass under the "jurisdiction" of coastal engineers and

oceanographer. While solid transport in the river includes material produced by the entire watershed, little attention is generally paid by fluvial and maritime specialists to the sediments' sources.

A specific disciplinary approach is almost invariably assumed, successfully, to solve most of the engineering problems. However, to understand the behavior of sedimentary systems at relatively large space– and time- scale (see Sect. 1.3) knowledge and experiences from different branches of science and professions should be brought together. This operation is not at all easy, not only between academic disciplines but also between separate ministries and agencies which in each country have competence on sediments.

1.2.1 MASS MOVEMENT

Mass movement corresponds to the detachment of sediments as a bulk from their original position (landslides), when the resisting forces (friction and cohesion) become lesser than the acting force (gravity). Mass movement is an important source of material for many rivers and in same cases the most important one. In *humid tropical forests* as well as in *alpine climates*, for example, the natural thick vegetation cover is such that the direct effect of rainfalls (kinetic energy) on the soil is negligible and the sediment production by surface erosion is practically zero. Yet the sediment transport by mountain rivers may be substantial and even extremely large (up to 10^4 t/km^2/year), due to the contribution of repeated *slope collapses* and occasional big *landslides*. Small and large mass movements from the watershed slopes typically occur during large floods and intense storms and are often associated with *mud-* and *debris flows* in the upper branches of the hydrographic network.

Mud- and debris flows (including ash flow or "lahars", taking place along the steepest channels of volcanoes) are intermediate forms of sediment motion, between mass movement and linear transport, which require a relatively small minimum steepness to be initiated. While their motion depends on particle- and fluid dynamics (similarly to linear transport), their triggering is controlled by static forces, basically depending on friction, cohesion, slope and the degree of saturation of permeable material (as for mass movement). For this reason attempts have been made to model the triggering of both shallow landslides and debris flows by simulating the saturation process of the surface layers of watershed slopes and steep channels (see for instance SHALSTAB and TRGRS models: Montgomery et al., 1994; Baum et al., 2002).

1.2.2 SURFACE EROSION

Surface erosion, prevalently developing over two dimensions, is definitely the most important source of sediment production wherever vegetation does not provide a sufficient cover of the soil from the rainfall impact, and morphological conditions are such as to foster the removal of particle by overland flow. This means that surface erosion is particularly active in cropland areas, especially where the type of soil is more vulnerable while erosion-control measures and correct cultivation practices are not applied. In many temperate countries, extremely high rate of surface erosion took place in historical times, following the rapid expansion of cultivated areas and before sustainable land management was adopted. The most recent episodes of this type occurred about hundred years ago in the U.S.A., where extensive areas of the Midwest were rapidly transformed from natural grassland into cropland. For this reason soil erosion was first investigated at scientific and technical level in this country, with special reference to the undulated landscape and climatic conditions typical of these areas.

The most active institution in this field was certainly the U.S. Department of Agriculture, where the renowned U.S.L.E. model has been proposed. The U.S.L.E. (Universal Soil Loss Equation) was developed since several decades (Wischmeier et al., 1978) by using the U.S.D.A. data base containing a very large number of (plot by experiments) results. The multiplication structure of the formula tries to put into account all the following factors: kinetic energy impact of rainfall combined with the intensity of rainfall, this last proportional to overland flow discharge (*erosivity factor*, *R*); resistance of the soil, quantified by means of descriptive tables (*erodibility factor*, *K*); slope length, also proportional to overland flow discharge (*length factor*, *L*); slope steepness, related to overland flow velocity (*steepness factor*, *S*); protection by vegetation depending on plants, crop and vegetative phase (*cover factor*, *C*); and management practices (*practice factor*, *P*).

The U.S.L.E. has been thoroughly criticized and defended in literature, as well extensively applied even outside the U.S.A., although very often with various “adaptations”. The formula provides, in principle, the values of sediment production at the “plot- or field scale” for a given period of time. For obtaining the corresponding data at catchment scale, the sediment production should be “routed” downhill to the hydrographic network and, eventually, downstream along the river to the closure section of the basin. The routing process that transforms the local *sediment production* into the integral *sediment yield* of the entire watershed is a rather delicate matter (see Sect. 1.5).

Besides the U.S.L.E. equation, more sophisticated models as ANSWERS, WEPP, SHE-SED, EUROSEM etc. have been recently developed for simulating, at catchment level, the detachment of soil particles by rainfall and their subsequent transport by overland flow and by river flow over the entire catchment (Beasley et al., 1980; Nearing et al., 1989; Wicks et al., 1996; Morgan et al, 1998; etc.). In contrast with the so-called "empirical" models (like USLE), the last models are usually called "physically based", since they are constituted by theoretical differential equations (expressing the mass balance of water and sediments) and by appropriate algebraic equations (describing each of the physical processes involved).

Physically based models resemble somehow the erosion- transport- deposition models employed in river morphodynamics (see Sect. 1.4). The physical processes involved in both *water flow* and *sediment motion,* however, are much more complicated on the watershed slopes than in rivers, and therefore much more difficult to be realistically simulated. For this reason, empirical models controlled by few overall coefficients (scarcely recognizable from the physical point of view but quite consistent and confirmed by many and many experiments) frequently give much better results than physically based models controlled by a large number of coefficients (generally unknown and based on hardly plausible physical and geometrical schematizations) which ignore in any case relevant existing interactions.

1.2.3 LINEAR TRANSPORT

Linear transport, namely taking place along one prevailing (longitudinal) direction, is the motion of sediments produced by persistent, channelized water flow. It is mainly responsible for river processes in the hydrographic network.

1.2.3.1 Modes and rate of transport

Linear transport assumes various modes (*bedload*, *suspension* and *intermediate forms*), but attempts have been made towards a conceptual unification of these forms, through the notion of *adaptation length*. The adaptation length expresses the distance required by clear water entering a uniform flow stream flowing over a uniform grainsize bottom to reach the uniform sediment transport conditions. The adaptation length depends on the particle grain size and on the characteristics of the water flow, i.e. more precisely on the ratio between friction velocity u^* and particle settling velocity w_s. When the ratio (u^*/w_s) is very small, the adaptation length has the order of magnitude of 10^2 *grain diameters* and the particles move by sliding and rolling as bedload. When this ratio increases, also the adaptation length correspondingly

increases and the motion passes from saltation to suspension. Adaptation length is practically zero for coarse material moving as bedload, while for fine particles moving in suspension it may reach the value of tens of kilometers.

The *solid discharge* of a natural stream (expressed by the mass or volume of sediments conveyed per unit time through a given cross section) may be somehow evaluated by the so-called *sediment transport formulas.* Most of the formulas have been obtained in laboratory under *uniform conditions (uniform transport by uniform plane flow* and *uniform grainsize* material). In these conditions, the *total solid discharge* can be expressed as a function of the water flow characteristics and the partial diameter, but the total amount may be somehow splitted between bedload and suspended transport. In fact, the distance covered by the particles under the action of the water flow does have a statistical distribution, depending on the ratio (u^*/w_s). This ratio therefore defines the ratio between the number of particles instantaneously subject to different modes of transport, as well as their adaptation length.

When the adaptation length is quite long, the sediment transport rate does not depend solely on the local hydrodynamic and sedimentological characteristics, but also on the conditions upstream. This circumstance in part explains why the suspended transport in a given cross section of a river is often scarcely correlated with the local water flow.

The adaptation length can be evaluated by different approaches (Galappatti et al., 1985; Armanini et al., 1988; Bolla Pittaluga et al., 2003) and its effect should be taken into account, when necessary, in sediment transport computations.

1.2.3.2 Sorted material

In real rivers, particle grainsizes are more or less non-uniformly distributed, with markedly different statistical distributions for *bed material* and *transported material*. In general, bed material appears to be coarser than transported material, and the two distributions can be mutually related by considering the transport of each grainsize class.

When treating different grain size classes, due attention should be paid to the interference of particles of different diameter. In sediment mixtures, in fact, the intrinsic larger mobility of finer particles is somewhat diminished by the presence of the coarser ones (“hiding” effect) while the intrinsic smaller mobility of coarser particles is augmented by their protrusion

("exposure" effect) (Egiazaroff, 1965; Parker et al., 1982; Wu et al., 2000). With very strong water flow in flood periods, the hiding-and-exposure effect may even lead to an "almost equal mobility". In low flow periods, by contrast, the different intrinsic mobility of various diameters strongly prevails on hiding-and-exposure effect (indeed, the coarser particles may even not move at all). In any case, over a long period of time, the transported material (e.g. the material intercepted by a reservoir) appears to be definitely finer than average composition of the river bed.

The "hiding-and-exposure" effect may be taken into account by various empirical coefficients to be introduced in the formulas developed for uniform material. The time evolution of bed- and transport composition is usually modeled by resorting to the *active layer* concept, first proposed by Hirano (1971) and subsequently incorporated in many morphodynamic models. More sophisticated approaches have been developed more recently, either by disaggregating the bottom *active layer* into a *mixing-* and an *intrusion layer* (Di Silvio, 1991), or by considering the bottom a continuous, indefinitely deep layer, statistically described in terms of entrainment capacity (Armanini, 1995, Parker et al, 2000).

1.3 TIME- AND SPACE SCALES OF SEDIMENTARY SYSTEMS

Morphological processes may be seen as the product of repeated succession of three phases of sediment motion: erosion, transport and deposition. In some cases, one of the three phases is definitely dominant. For example, soil removed from short watershed slopes, either by surface erosion or mass movement, may be never replaced by other soil. Conversely, sediment trapped by a deep lake or sea are not entrained and put in motion anymore. In these cases the erosion or deposition process is time-depending but monotone (namely producing either a progressive degradation or a progressive aggradation). In many other cases, by contrast, subsequent phases of erosion, transport and deposition take sequentially place on the same location, giving origin to complicate alternating morphological processes. In this last cases one can only speak of *net* degradation or aggradation of a certain *sedimentary system* over a prescribed *period of time*.

When considering morphological processes, indeed, it is important to have in mind the time- and space scales under consideration. The repeated succession of erosion, transport and deposition, may concern for example: (i) the sliding, rolling and saltation of sediment particles over bed ripples (space scale: boundary layer, say millimeters); (ii) the propagation of dunes (space-scale: river depth, say meters); (iii) the formation of bars and meanders (space scale: river width, say hundreds of meters); (iv) the general aggradation or degradation of a river (space scale: watershed, say up to thousand kilometers). The time-scale of each system may be associated to the corresponding space-scale, *via* a typical process velocity.

It is important to note, in any case, that each system at a given scale may be considered a component (or sub-system) of the system at the larger scale. The morphodynamics of the component does in principle interact with the morphodynamics of the system at larger scale. However, to describe the behavior of a component (e.g. the propagation of dunes along a river reach) it is usually assumed that the system at larger scale (e.g. bars and meanders) remains *stationary* at the time-scale of interest for the component (dunes). At this time-scale, conversely, one assumes that the subsystem at an even smaller scale (e.g. bed ripples), although non-stationary, is in *equilibrium conditions* with the larger system (dunes). This simply means that, during the propagation of the dune, single ripples may appear or disappear, but their statistical distribution (and consequent hydraulic roughness of the dune surface) is exclusively depending on the dune configuration. This assumption is only valid, in principle, when the relevant systems and sub-systems have markedly different scales, but it is implicitly assumed in most morphological models.

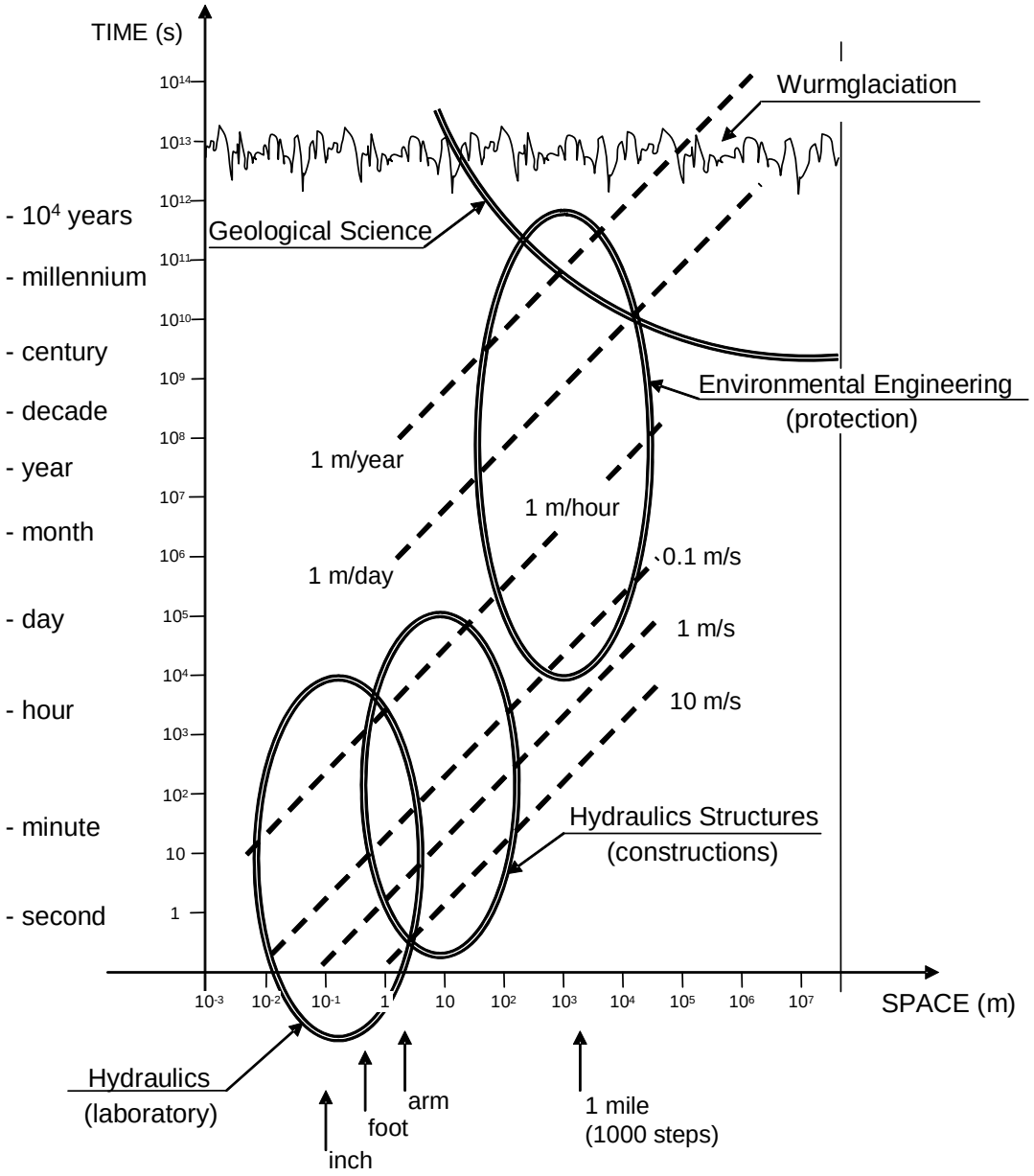

Figure 1.2: Time- and space-scale of sedimentary systems.

The scales of morphological processes extend over several orders of magnitudes ranging from microns to continental sizes (in space) and from seconds to millions of years (in time). The graph of Fig.(1.2) indicates the range of interest for various disciplines interested in sedimentary systems. For *Hydraulic Structures* (*construction prototype)* engineers are generally interested in problems defined (in space) by the "work size" and (in time) by the "event duration", or, at most, by the "project life" of the structure. For *Hydraulic Laboratories (laboratory experiments)* the range of interest is defined by the facility's size and the process' velocity. In basic research (e.g. for analyzing the behaviour of individual sediment particles) the relevant sizes may be extremely small, while for physical models they are generally larger, although obviously much smaller than the size of the corresponding

prototype structure (we may say, in Froude similitude, 100 times less in space and 10 times less in time). However, if the engineer wants to assess the morphological effects of the structure he has designed on the entire river system, he should take into account much larger scales. For example, the presence of the Aswan Dam is already perceived, after several decades since its construction, in the Nile's Delta (subject to erosion) which is thousands of kilometers downstream. Yet, the adaptation process of the entire river Nile system will take an extremely longer time to attain a new quasi-equilibrium configuration. In other words, as shown in Fig.(1.2), the time- and space-scale for *Environmental Engineering (protection)* tend to be much larger than for hydraulic structures and closer to those of the *Geological Sciences*, namely "geological times" and "continental sizes".

As a pure indication, the time axis of the figure is bounded by the end of Würmglaciation, as it is called in Europe the last large climatic change before present, which has interested, with some local variation, both hemispheres and, in terms of sea level change, the entire planet. We may assume, in fact, that at geological scale the climatic forcing after the Würmglaciation was reasonably stationary. By contrast, should we consider a longer period of time, several processes would appear be controlled by non-stationary climatic conditions (sequence of glaciations and consequent sea-level changes), as well as by variable phases of tectonic uplift and subsidence.

However, even by limiting the analysis to the last ten thousand years, a quite large number of time- and space-scales controlling the behavior of sedimentary systems should be considered when developing morphological models (Sect.1.4).

1.4 MORPHOLOGICAL MODELS

A large number of morphological models developed at different time- and space scales and with various degrees of detail and approximation are available in literature. In this section attention will be especially concentrated on the modelling linear transport phenomena (see Sect. 1.2.3).

1.4.1 SMALL SCALE MODELS

Detailed small-scale models have especially been developed for research purpose. Many of these models have the scope to reproduce the movement of individual particles under the action of other particles and water flow and are usually based on a lagrangian approach. They should be able, in principle, to reproduce the behavior of small scale systems (microforms up to the river depth-scale) and may be extremely useful to explain the hydraulic resistance mechanisms (grain and form roughness), to show the validity and limitations of transport formulae, to investigate the dynamics of movable bottom and to describe the motion of hyper-concentrated liquid-solid mixtures.

1.4.2 INTERMEDIATE SCALE MODELS

These models are the most commonly used for practical applications. They are typically extended to the size of a river reach and applied for relatively short time durations (from one single flood event to a few years). As mentioned in Sect.(1.3), during this time all the processes at subsystem scale (microforms, hydraulic resistance, sediment transport rates etc.) are incorporated *via* simple predictors, usually "equilibrium" algebraic equations, as a function of the water discharge. Conversely, all the processes at larger scale (climate, watershed configuration etc.) are supposed to be stationary.

Intermediate scale models are obtained by averaging convection-diffusion equations for sediments are the Reynolds equations for water (in their turn obtained by averaging the water continuity and Navier-Stokes equations over turbulence) over appropriate space dimensions. The most common commercial models are *1-D* (*one-dimensional)*, i.e. averaged over the river cross-section (but possibly disaggregated in a number of sub-sections). One-dimensional models can simulate bottom erosion and deposition along the river (generally the most relevant requested information), somehow "re-distributed" over the cross-section. 1-D models can easily be applied to relatively large portions of the hydrographic network.

Rather common, however, are nowadays becoming *2-D (two-dimensional)* models, i.e. averaged over the river depth, also available as commercial codes developed by several laboratories. Two dimensional models can in principle simulate all the process at the width-scale (migrating and stationary bars, braiding and bifurcations, sediment exchange with flood

plains etc.). Bank collapse and reconstruction can also be incorporated in a 2-D model, which therefore will be able to reproduce meander formation and propagation.

Secondary currents over the cross section are important for localized scouring (piles, groynes etc.) and in meander morphodynamics. Their reproduction require in principle a *3-D* (*three-dimensional)* model but, at bar/meander scale, their local effect can be approximately accounted for by a 2-D model. Reproduction of density currents, often important in certain reservoirs, also requires a 3-D model. In some cases, however, a *vertical 2-D* model (i.e. averaged over the reservoir width) can also be considered.

Intermediate scale models, either 1-D, 2D or 3-D, are extremely sensitive to the *boundary conditions* to be prescribed at the upstream and downstream ands of the river reach under investigation. Correct boundary conditions for morphological models (De Vries, 1993) should be given in terms of sediment input of each grainsize fraction (at the upstream end) and in terms of either water-level or bottom-elevation, respectively for sub-critical and super-critical water flows (at the downstream end). Note that boundary conditions depend in principle on what is going on respectively upstream and downstream the considered reach. For relatively short simulations (years), sediment input upstream can be evaluated by reasonable hypothesis based on "local" quasi-equilibrium conditions; the same can be made for water level or bottom elevation downstream. For longer simulations (centuries), however, the behavior of the entire river system should be explicitly accounted for (Sect. 1.5).

1.4.3 LARGE SCALE MODELS

Although 1-D models have been sometimes applied to relatively large real watersheds for specific flood events, no many examples are available in the literature of morphodynamic modelling at very long (historical or geological) time-scale, except in a few very schematized situations (simple geometry, constant waterflow, uniform grainsize). The effects of geometrical, hydrological and sedimentological *non-uniformities,* invariably present in real systems, have been only in part investigated for long-term, large-scale simulations of actual river and relevant watersheds. In fact, averaging "non-uniformities" of any type in non-linear equations produces "residual terms" which should be properly assessed and eventually modelled with appropriate sub-models (Di Silvio et al., 1996a).

It may be interesting, in this respect, exploring the possibilities offered by *long-term, large-scale morphological models* where averaging is performed on time (year or number of years) and/or space (river reaches of various length). In practice, these models filter the shorter morphological fluctuations and compute only the long-term, large-scale evolution.

1.5 SEDIMENT YIELD AND SEDIMENT PRODUCTION

One of the most difficult problems in establishing a sediment balance at watershed scale is the relation between the sediment removed from the watershed slopes (soil production) and the soil transported by the river (sediment yield). The very same definition of those quantities may present in fact some ambiguities.

A possible, rather unambiguous, definition of *sediment yield is the total amount (mass or volume) of sediments, of any size and origin, transported as bedload or in suspension through a given cross-section during a certain period of time* (year, day, flood event, etc.). Very often, however, sediment transport is disaggregated in two parts: the so-called "bed-material transport" (typically coarser than a conventional grain-size limit, say between 20 and 80 microns) and the so-called "washload" (below that limit). While the transport of bed-material is supposed to be a function of riverbed composition and flow characteristics, washload is assumed to be fed to the river from the watershed slopes and conveyed downstream by the river flow, with the same velocity of the water, i.e. without any interaction with the bottom. In many instances, washload (defined in this way) results to be a very large portion of the total transport, so that "sediment yield" it is assumed to be practically coincident with the corresponding "sediment production" during the same period of time. The distinction between bedload material and washload is obviously made for sake of simplification but it does not have a solid physical foundation. Indeed, even the finer particles have multiple phases of transport, deposition and resuspension and their average motion is by far much slower than the water's. Consequently the sediment yield of the river may be much lesser or larger than the sediment production during the same period of time.

Let us now consider the definition of sediment production. On the analogy of sediment yield, a straightforward definition of *sediment production is the total amount of sediments, of any size and origin, detached by surface erosion and mass movement, from a given location of watershed and transported downhill during a certain period of time (year, month, storm event etc..).* It is apparent that, in this way, sediment production is expressed as entrainment per unit surface but, in practice, it can only be measured as a transport per unit width of the watershed slope at a distance more or less remote from the closest "divide". In fact, although a number of small scale models (see Sect. 1.4.1 and 1.4.2) are available for a theoretical evaluation, it is apparent that a "punctual" measurement of sediment production does not have much sense and that some space-averaging operation should be performed over the slope surface (Di Silvio, 1996b). Experimental data, indeed, are never available point by point, but at "plot" or "field" scale (for cropland) or at "slope" scale (for natural watersheds).

As already observed, however, space-averaging is not at all a banal operation. First of all, except for extremely tiny pieces of slope surface, different transport processes occur at different scales. At a *small scale* (overland flow depth) we may observe that a thin overland flow can not maintain a stable fully two-dimensional aspect but invariably tends to concentrate in a channelized flow. This is very apparent for rills and gullies, but even diffused sheet erosion actually occur though embryonic and intermittent micro-networks, basically controlled by vegetation. For larger and larger sizes, as it conveys larger and larger concentrated waterflow, the micro-network tends to became more stable and well defined and to evolve towards the permanent, morphologically controlled hydrographic network. At an *intermediate scale* (experimental plot, field or natural slope) both the runoff and the sediment transport, actually concentrated along the micro-network, are somehow integrated (i.e. averaged) over the relevant surface. A complete and reliable set of data on sediment production by surface erosion has been formed, over decades, and decades by agricultural engineers on experimental plots in many countries of the world with different soils and different crops. Experimental plots have in general a narrow rectangular surface with no transversal elevation gradient and a uniform longitudinal steepness. These data have been employed in the USA to develop the celebrated Universal Soil Loss Equation (USLE) and elsewhere around the world to adapt this formula to different agricultural and climatic conditions.

As anticipated in Sect (1.2.2), the USLE provides the sediment production, in mass per unit surface, as the product of six factors which include the length of the plot *L* and the steepness *I*. While for an *experimental plot* or even for a regular *cropland field*, ditches clearly show where they initiate and terminate, for a *natural slope* the only apparent boundary is represented by the channels and the divides of the hydrographic network. It is more practical, in this case, to define *the sediment production in a given (preferably small) hydrographic watershed as the portion of sediments, of any size and origin, detached by surface erosion and mass movement, which reaches the hydrographic network during a certain period of time (year, month, storm event, etc..).* Sediment production of the watershed can be computed by applying the same formulations (e.g. U.S.L.E.) calibrated at field scale from experimental plot data, where one assumes for the *length* and *steepness* of the natural slopes respectively the inverse of the basin's *drainage density* and *relief*. In this computation a certain reduction coefficient (*slope delivery ratio*) should be applied for taking into account the trapping effect along the natural slope, especially when the slope is quite long and its profile is undulated.

To transform sediment production in sediment yield, it would now be necessary to route the input of sediment all along the hydrographic network, down to the closure section of the watershed. With the previous definition, a distinction has been made between the intermediate scale (field or slope length) where sediment production takes place and the large scale (watershed or river length) where river processes take place. An even more aggregate definition of *sediment production is the portion of sediments which reaches the closure of the watershed.* In this case, the computation at river scale should be affected by an even smaller reduction coefficient (*overall delivery ratio*), which should take into account also the river processes along the entire hydrographic network.

The concept of "overall delivery ratio" for sediments is somehow analogous to the concept of "runoff coefficient" for water. Yet it is much more elusive to be defined and difficult to be predicted, due to its variability in space and time along the sediment route. In fact the very notion of overall delivery ratio is not much utilized in recent literature. From the early data (Maner, 1958; Roehl, 1962; Williams et al., 1972) it appears that delivery ratio decreases from 1 to a few percents, more or less proportionally to the inverse of the stream length (or square root of the watershed area) but scattering of data appears to be extremely high. Several attempts to have a more accurate prediction of delivery ratio as a function of the watershed

and river morphology (see for instance Walling et al., 1996) did not provide generally valid results.

Similarly to the “runoff coefficient”, the concept of “delivery ratio” is hardly useful when it becomes much smaller than 1 (namely for watersheds larger than 50-100 km^2). The notion of delivery ratio is in fact probably acceptable exclusively at intermediate scale, namely for an overall description of the “monotone” trapping effect the watershed slopes, where very few localized permanent cab only give rise to (averaged) values of the delivery ratio very close to 1.

When river processes become dominant it would probably be better substituting the static concept of "delivery ratio" with a dynamic concept of "response delay", in which the time scale also plays a role (Di Silvio et al., 1997). Indeed, if the watershed is large, it is not correct assuming that the very same particles detached from the watershed slopes during a certain storm can reach the closure section of the basin during the corresponding flood. The sediments moving as bedload or as suspended transport along the river (including the very fine ones, the “washload”), have continuously phases or deposition and re-entrainment with the river bed, banks and floodplains. Repeated deposition and re-entrainment may produce relevant granulometric, altimetric and planimetric changes at different time scale and, in any case, will strongly delay the response of river morphology (and river transport) with respect to the sediment input from the watershed slopes.

An idea about the “response time” and the “attenuation rate” of any perturbation introduced in the fluvial system is given by the analytical solution of the morphological model developed by Fasolato et al.(2007a).

A direct evaluation of sediment yield is possible by utilizing regular (daily) measurements of turbidity and water discharge carried on at some stations along the river. This procedure assumes that there is a direct relationship between “turbidity” usually measured in one single point of the cross section and "transport concentrations" (ratio between total sediment transport and water discharge). This hypothesis is probably acceptable, especially on the long term, but it deserves further theoretical and experimental consideration (Walling et al., 1988).

The most precious and reliable information about sediment yield in terms of both quantity and grainsize composition, however, is given by the progressive sedimentation of existing reservoirs. The surveying technology based on the joint use of remote sensing and Global Positioning System (GPS) (e.g. Lee et al., 1999; Agarwal et al., 2002) has already been applied in similar circumstances. In assessing the sediment volume trapped in a reservoir, the time-depending compaction of the deposited material should be taken into consideration (see for instance Morris et al., 1998). The data collected in existing reservoirs, as well as at measuring stations, may be used for calibrating reliable semi-empirical relationships (even if limited to a specific river configuration) which provide long-term sediment transport as a function of hydrological, geometrical and sedimentological characteristics of the river reach.

1.6 QUALITY OF SEDIMENT DATA IN DEVELOPING COUNTRIES (DC): THE AFRICAN CASE

Soil and water conservation is one of the most critical environmental issues many countries face, Developing Countries (DC) in particular. Water is the source of life and soil is the root of existence. Hence, water and soil resources are the most fundamental materials on which people rely for survival and improving their life conditions. The development of the society is determined by its capacity to use its resources, and some of them may in time become exhausted or deteriorate. Soil has been defined by the International Science Society as “a limited and irreplaceable resource”, and the growing degradation and loss of soil means that the expanding population in many parts of the world is pushing this resource to its limits. In its absence, the biosphere environment of man would collapse, with devastating results for humanity. Soil and water loss causes land resource destruction and reduction in soil fertility, which leads to the deterioration of the environment and the loss of ecological balance, causing natural disasters and constraining the development of agriculture, consequently increasing poverty (Yang, 2005).

Given the uneven magnitude of erosion/sedimentation processes in different geophysical contexts, it is evident that these phenomena are not a global problem but have strong regional connotations. A recently published report by Julien and Shah (2005) for the International

Sedimentation Initiative (ISI) of IHP-UNESCO, provides a summary of major erosion and sedimentation impacts that DC are facing. The countries located in Asia are facing major issues related to soil erosion, droughts, flooding and deforestation. The countries located in Africa are experiencing deforestation, land degradation, droughts and desertification. Also, the increased urbanization and agricultural expansion is constantly affecting the sediment continuity in all the DC.

As WMO (2005) recognizes: "Integrated Water Resources Management (IWRM) calls for an informed participation of different stakeholders concerned with sustainable development. Timely, accurate and comprehensive information about water and sediment resources forms the basis for an effective sustainable management". Agenda 21, the blueprint for sustainable management, recognizes that the monitoring and assessment of water and sediment resources, in terms of both quantity and quality, require adequate hydrological and sedimentological data. Unfortunately, the local capability to collect and manage water and sediment resources-related information remains inadequate in many countries of the world. This situation often arises from lack of adequate financial support from national governments in view of demands from others competitive sectors.

The African case is particularly dramatic due to its political-economical situation and geo-orographical make practically almost impossible the installation, the maintenance and the management of an adequate hydrological and sedimentological monitoring network a particularly prohibitive task. Although measurements of sediment transport by African rivers were initiated over 100 years ago on the River Nile at Cairo by Letheby in 1874 (Baker, 1880) and suspended sediment sampling was included in the national hydrometric network established by the colonial administration in Kenia as early as 1948 (Starmans, 1950), relatively little is currently known about the sediment loads of African rivers. A useful example of some of the uncertainty that has been, and to a large extend is still, associated with this aspect of African hydrology is provided in Fig.(1.3) which portrays the African portions of the global maps of suspended sediment yield produced by Strakhov (1967) and Fournier (1960).

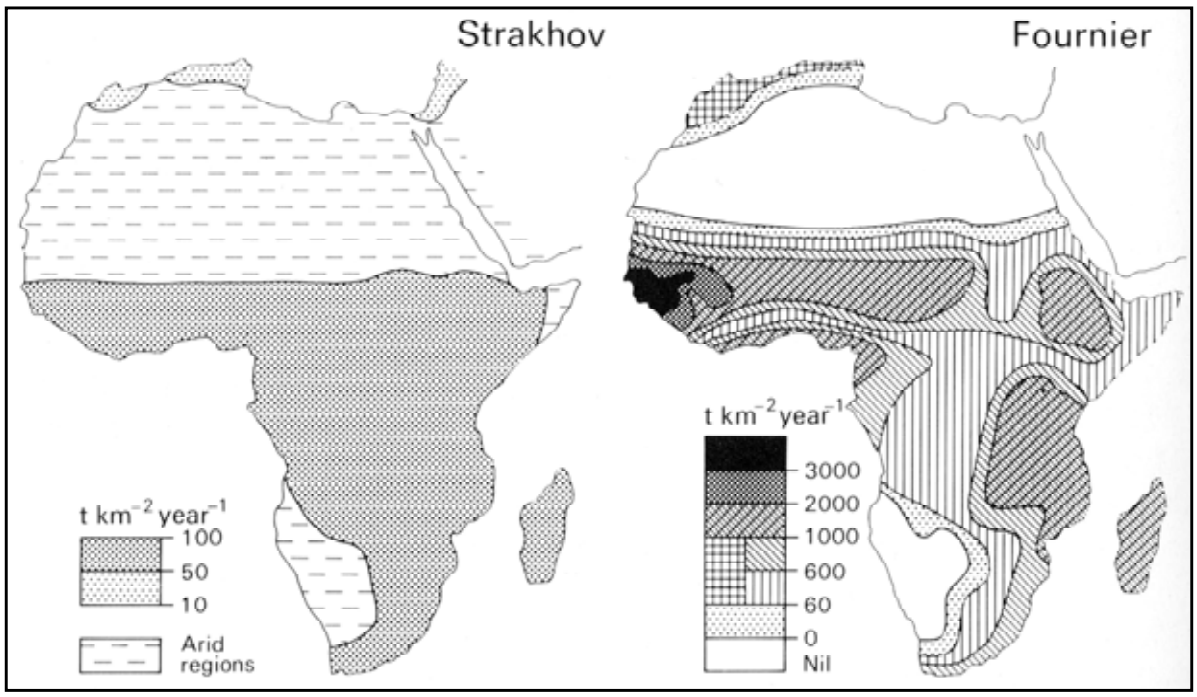

Figure 1.3: Maps of suspended sediment yields within Africa based on the work of Strakhov (1967) and Fournier (1960).

These remain the only continental scale maps of sediment yields in Africa currently available and both the maps and data delivered from them are still cited. A comparison of the magnitude of the sediment yields depicted on the two maps reveals major contrasts: while Strakhov suggests that sediment yields within the range 50-100 t km^2/year, Fournier depicts sediment yields which are an order of magnitude greater with large areas of West and East Africa exhibit suspended sediment yields in excess of 1000 t km^2/year. Both maps were necessary based on meager data, and in Fournier's case no data were available from African rivers to provide a basis for mapping. The map, in fact, was based entirely on extrapolation of relationships between specific sediment yields and basin relief and precipitation regime developed for other areas of the globe.

1.6.1 DATA RELIBILITY AND ACCURACY

Where suspended sediment load data are available, their accuracy should be carefully taken into account (Ferguson et al., 1987). Important factors affecting such accuracy include the equipment and procedures used for collecting samples, the sampling frequency, and the technique used for load calculation (Walling et al., 1988). Likewise, the use of sediment rating curves to estimate suspended sediment loads from infrequent sampling may introduce substantial errors and frequently leads to underestimation. Some indications of the potential

problems associated with data reliability is provided by Fig.(1.4) which depicts the estimates of the mean annual suspended sediment load of the Tana river at Kamburu, Kenia, that have produced a number of studies.

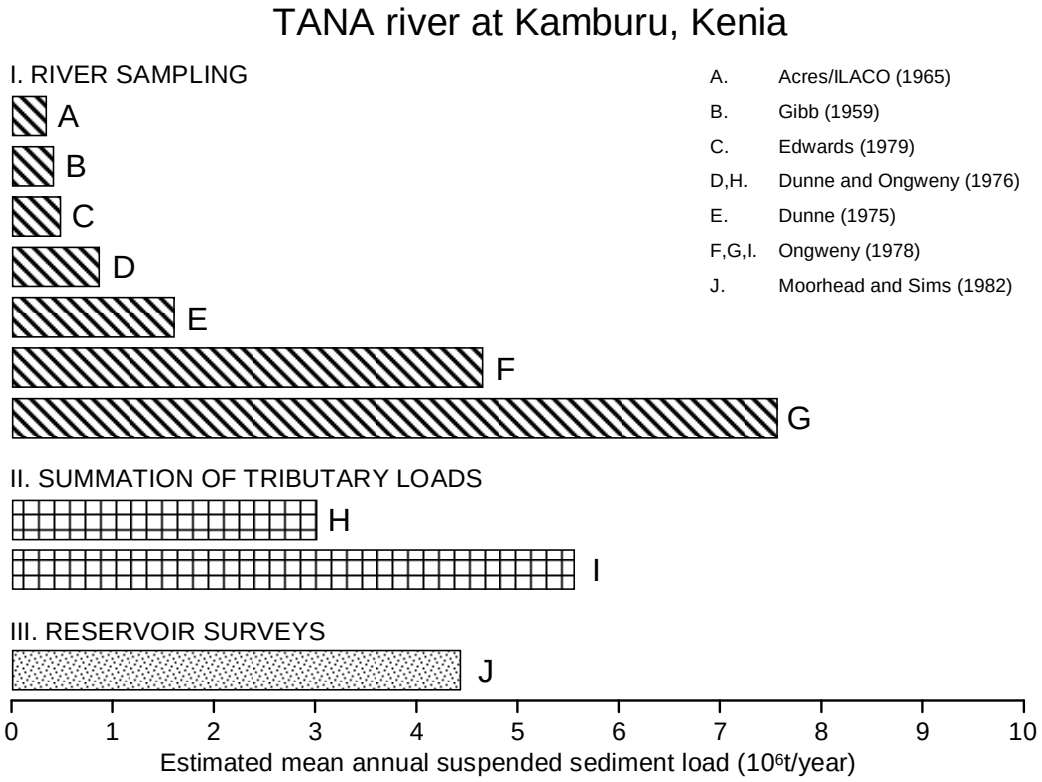

Figure 1.4: Estimates of the mean annual suspended sediment load of the upper Tana river produced by different authors.

Estimates A-E were derived using essentially the same basic flow and sediment concentration data, whereas estimates F and G were based on a new sampling programme. Comparison of their load estimates for the main river with those for the upstream tributaries prompted Dunne et al. (1976) and Ongweny (1978) to suggest that the former were underestimated and to produce revised estimates for the Tana at Kamburu (H and I) by summing and extrapolating the estimates for the individual upstream tributaries. A quite more recent survey of sedimentation rates in Kamburu reservoir by Moorhead and Sims (1982) coupled with and estimated trapping efficiency for the reservoir of 75% provides an alternative approach to estimating the sediment load (J).

These examples clearly evidence the problems that may be encountered in comparing data using different measurement and calculation procedures. Further uncertainties come from the considerable variability an annual sediments loads in many African environments and are in

general associated with the long-term variability and non-stationarity of data. Walling (1984), used the simple standard error statistics to demonstrate the potential deviation of an estimate of mean annual sediment yield, based on short-term records, from the true long term mean, assuming a Cv of 1.0. At 95% level of confidence, a mean based on only 5 years of recording could deviate from the true mean by up to ±80%, and even when based on 25 years of recording this deviation could be ±40%. These estimates clearly demonstrate the problems that may be associated with deriving from short-term records a representative value of the long-term mean annual sediment yield for a drainage basin.

Climatic variations is another factor the could mislead the interpretation of long-term sediment yields by. Lamb (1966) used records of the levels in East African lakes and other hydrological data to conclude that during the early 1960's the atmospheric circulation underwent a significant change, which caused increased rainfall in East Africa. The impact of such a change is evident in the sediment records. Although there is little doubt that the sediment yields of many African rivers have increased over the past few decades in response to forest clearance and other changes in land use, there are few, if any, accurate long-term records of sediment yields which can be used to identify the extent of this non-stationarity.

Definitive analysis of the factors influencing spatial variation in suspended sediment yield is clearly hampered by interdependence amongst variables such as geology, topography, annual runoff, vegetation cover and land use, as well as by sparsity of data. Hopefully improvements in data availability at continental scale as well as the development of national and regional monitoring networks designated to isolate the influence of major controls will provide an improved understanding of this phenomena (Walling, 1984).

The lack of information concerning the magnitude and the detailed pattern of suspended sediment yields within the African continent is paralleled by an even greater sparsity of data concerning the properties and characteristics of the fluvial sediment involved. This situation is particularly unfortunate in view of the current awareness of the importance of sediment properties to the wider environmental significance of suspended sediment transport by rivers. (e.g. Ongley, 1982; Peart et al., 1982; Golterman et al., 1983, Sutherland et al., 2003). Fig.(1.5) provides a representative sample of the limited data existing on the particle size characteristics of suspended sediment transported by African rivers.

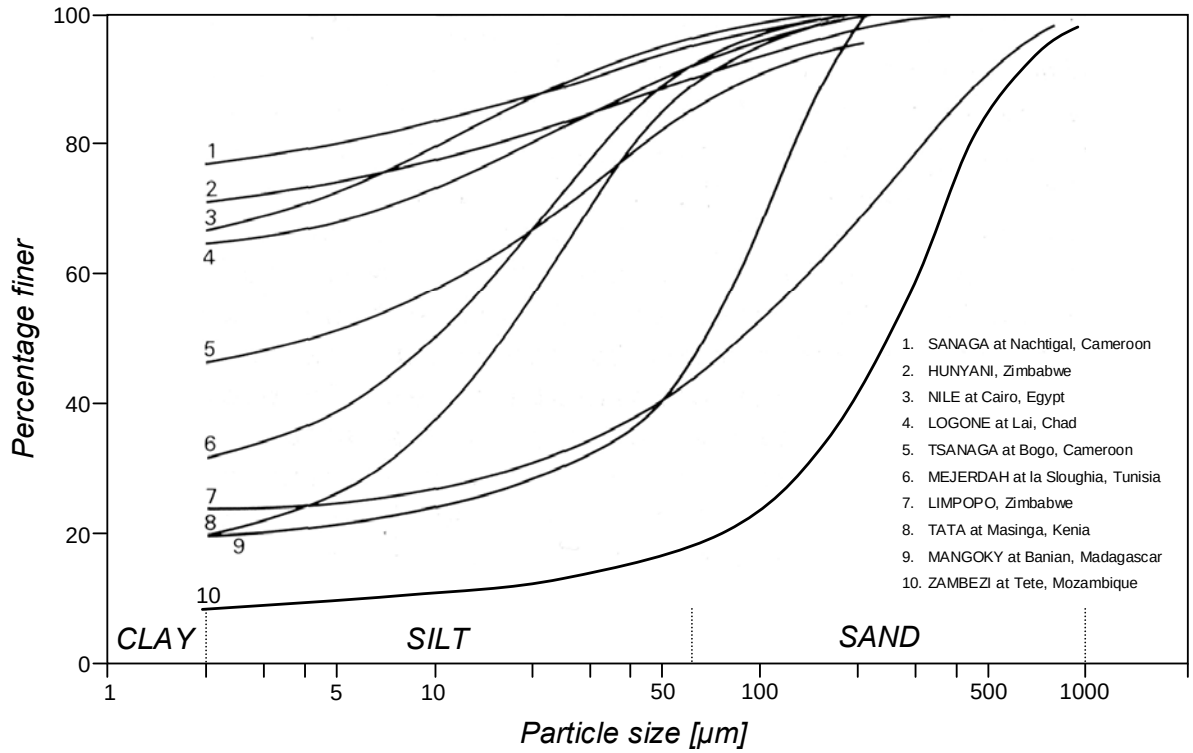

Figure 1.5: The particle size characteristics of suspended sediment transported by a number of African rivers (Walling, 1984).

In some cases the data presented for individual river relate to a single sample and further uncertainties exist as to the comparability of laboratory techniques employed by different workers. Nevertheless, this information suggests that suspended sediment transport is dominated by fine-grained material and that clay and clay + silt frequently account for more than 50% and 80% respectively of the total load. This distribution has important implications for evaluating the trap efficiencies of reservoirs, since clay-sized material may be carried through impounding reservoirs. However, in such evaluation it is important to consider the effective particle size of the sediment, for aggregation may occur naturally during transport. A part very site-specific cases, where single measurement or even episodic surveys has been made in the past (mainly functional to river impoundments, such as dams construction), no information on this aspect of particle size composition would seem to be currently available. Looking in more detail at the individual distributions depicted in Fig.(1.5), it is difficult to account for the contrasts evident. These must reflect variations in soil and bedrock character between the individual river basins and the selectivity of the erosion and conveyance processes operating in these basins. Some authors have also suggested that there is a tendency for the proportion of fine-grained sediment to decline with increasing aridity, but insufficient data are available to confirm such trend.

Few meaningful assessments of bed load transport have been undertaken for African rivers, but available data suggest that suspended sediment dominates the total particulate load in most cases and will commonly account for approximately 90% of the total load.

Moreover, the precise relationship between local rates of erosion and downstream sediment yields, which reflects the sediment delivery processes operating in a drainage basin, remains a major uncertainty in the study of erosion and sediment yields (Walling, 1983). This uncertainty is particularly marked in the case of the African environment, for there have been very few studies of this aspect of drainage basin response and relevant evidence is conflicting. Improved understanding of the relationship between on-site erosion and downstream sediment yield must seen as an important research need in order to that recent advances in the modeling and prediction of soil loss can be translated to the basin scale and that the impact of both land use change and conservation practices on downstream sediment yields can be predicted.

1.6.2 DATA AVAILABILITY AND DATA REQUIREMENTS

The argumentation presented above leads to a critical question to be answered: how can we use simulate and predict the morphological evolution (and therefore the sediment yield) of a river basin, with the scarce and sometimes unreliable data available? A model can be developed and refined using data from carefully monitored and surveyed watershed to produce the most accurate results possible for specific cases. However, since such models are expected to be used mainly in support of policy and conservation efforts, it can be argued that they should be developed in order to produce useful and reliable results using only the limited data that is commonly available to potential users (Renschler et al., 2002).

There is an evident need for models that can produce robust results using readily available data, better if widely accessible through the digital databases that can be easily downloaded form the Internet. This evidently implies the need of *less demanding* models from one side, and innovative methodologies from the other side, that can integrate the data through simple but not simplistic operations (such as interpolation, extrapolation, homogenization, etc.).

Chapter 2

Modelling Morphological Evolution of Unsurveyed Rivers

2.1 INTRODUCTION

Morphological processes in river systems (aggradation and degradation of the bottom and corresponding evolution of grainsize composition) can be described in terms of 1-D (one-dimensional) equations of waterflow (De St.Venant equations) and sediment motion of various granulometric classes (sediment balance equations in the stream and in the bottom layer). Even if 1-D models are relatively simple, they often present a number of problems when are applied in their complete form to long-term simulation at watershed scale. A part from the complexity of the complete non-linear equations, a further problem arises for many rivers (especially in Developing Countries) due to the lack of extended and accurate bathymetric survey of the cross sections. This is the case of the lower Zambezi river, where

the only available data are the planimetric configuration of the river and the slope of the water surface obtained by LANDSAT 7 images and the Digital Elevation Model respectively. In order to integrate the available topographic data with supplementary information, a particular form of 1-D model has been developed, based on the hypothesis that any reasonably short portion of a river can be considered in *quasi-equilibrium condition*. The hypothesis of quasi-equilibrium conditions represents a convenient basis for a theoretical analysis of several problems regarding the optimal use of 1-D models. All these problems are somehow related to the "smoothing" to be performed on the natural irregularities of the watercourses, with an acceptable loss of resolution and loss of accuracy. Appropriate averaging operations, in fact, permit on one side to increase the size of computational steps in space (and consequently in time) with tremendous reduction of numerical effort. On the other side, space averaging over a sufficiently long river reach permits the use of an approximate 1-D model (uniform waterflow) which further reduce the computational time and make possible its application for long-term simulations at watershed scale (Fasolato et al., 2007b). The effects of averaging operations on the spatial irregularities, in terms of accuracy and resolutions, have been investigated for waterflow 2-D models of flood plains (Gee et al., 1990; Bates et al., 1992, 1995; Hardy et al., 1999) and also for the so-called "physically based" models of watershed slopes (Beven, 1989), but no general criterion has been provided to select the most convenient computational grid size. As far as morphodynamic modelling is concerned, interesting analyses have been made about the differences between models at reach- and watershed-scale (e.g. Nicholas and Quine, 2007), with special emphasis to single out the critical physical length (e.g. the river width) which separates the two type of models. Scope of the analysis, however, was mainly the distinction between a "reductionist" approach (based on the averaging of the Navier-Stokes equations) and a "synthesist" approach (based on the inductive development of specific conceptual equations). In this line may also include the discussion of "cellular" models (Coulthard et al., 2007) in their relation with the models obtained in various ways from the Navier-Stokes equations.

In the present Chapter reference is made to the strictly "reductionist" 1-D model (obtained by integrating the Navier-Stokes equations first over turbulence and then over the cross section of the river). The general criterion of *morphological box* has been utilized to recognize the minimum computational steps which should be used if the approximate model (quasi-uniform water flow) is applied instead of the regular 1-D model (quasi-steady water flow) (Ronco et al., 2007b). The criterion has been applied for the schematization of the lower

Zambezi river, obtaining morphological boxes varying from 16 to 76 km as a function of the local Froude number.

A systematic analysis has been subsequently made for comparing the performances of both the approximate and the regular 1-D morphological models in terms of resolution, accuracy and computational time.

2.2 THE ONE-DIMENSIONAL MORPHODYNAMICS MODEL

With reference to the longitudinal distance along the river x^* and time t^*, the complete one-dimensional model is constituted by a system of differential equations expressing, respectively: the water's continuity equation and energy's balance in the stream (De St.Venant equations, eqs. 2.1 and 2.2); the overall sediment balance between the stream and the bottom (Exner equation, eq. 2.3); the sediment balance of each granulometric class present in the mixing layer of the bottom (Hirano equation, eq. 2.4).

$$\frac{\partial Q}{\partial x^*} + \frac{\partial A}{\partial t^*} = 0 \tag{2.1}$$

$$\frac{\partial}{\partial x^*}\left(H + Z + \alpha_c \frac{Q^2}{2gA^2} \right) = -\frac{\beta_c}{g}\frac{\partial U}{\partial t^*} - j \tag{2.2}$$

$$\sum_{k=1}^{N} \frac{\partial P_k}{\partial x^*} = -B\frac{\partial Z}{\partial t^*} \tag{2.3}$$

$$\delta B \frac{\partial \beta_k}{\partial t^*} = -\frac{\partial P_k}{\partial x^*} - B\beta_k^* \frac{\partial Z}{\partial t^*} \tag{2.4}$$

Note that Q is the water discharge, A is the wetted cross section area, H is the local water depth, Z the bottom elevation, g is the acceleration due to gravity, $U=Q/A$ the flow velocity, j the energy slope, P_k is the solid discharge of the k-th class of sediment (k=1,2…N), $B(x)$ the channel width, δ is the thickness of the active-layer, β_k is the percentage of the k-th class d_k present in the active-layer, β_k^s the percentage below the active-layer and β_k^* assuming

different values during the erosion $\left(\beta_k^* = \beta_k^S\right)$ or deposition phase $\left(\beta_k^* = \beta_k\right)$. The coefficients α_c and β_c, accounting for the energy and momentum distribution on the cross-section (Coriolis), are assumed here both equal to 1.

In addition, the following algebraic equations describing, respectively: the hydraulic resistance of the waterflow (Chézy type equation, eq. 2.5); the sediment transport rate of each grainsize class, assuming the immediate adaptation of transport to the local conditions (Engelung-Hansen type equation, eq. 2.6); the hiding/exposure effect for each grainsize class d_k which reduces the larger mobility of smaller particles and vice-versa (Egiazaroff type equation, eq. 2.7).

$$Q = U \cdot B \cdot H = \chi \sqrt{j \cdot H} \cdot B \cdot H \tag{2.5}$$

$$P_k = \alpha_T \cdot \beta_k \cdot \xi_k \frac{Q^m j^n}{B^e d_k^f} \tag{2.6}$$

$$\xi_k = \left(d_k \Big/ \sum_{k=1}^{N} \beta_k d_k \right)^s \tag{2.7}$$

where the coefficient α_T and the exponents *m, n, e, f, s* depend on the category of river under consideration (Di Silvio, 2006).

2.2.1 SIMPLIFICATIONS OF THE WATERFLOW (DE ST.VENANT) EQUATIONS

The continuity equation (eq. 2.1) and the energy equation (eq. 2.2) may be subject to a number of simplifications which can usually be accepted in most rivers, where the flood hydrograph is relatively flat compared with the energy slope *j*. This condition corresponds to assuming the expression:

$$\frac{\partial Q}{\partial x^*} = \frac{2}{3}\frac{1}{U}\frac{\partial Q}{\partial t^*} \tag{2.1'}$$

instead of eq.(2.1) (kinematic wave hypotesis) and to dropping the time-depending term in eq.(2.2) (quasi-steady waterflow):

$$\frac{\partial}{\partial x^*}\left(H + Z + \frac{Q^2}{2gA^2}\right) = -j \qquad (2.2')$$

An even stronger simplification consist in assuming an instantaneous propagation of the waterflow, namely:

$$\frac{\partial Q}{\partial x^*} = 0 \qquad (2.1'')$$

instead of eq.(2.1), and in assuming the equality between the bottom slope and the energy slope (quasi-uniform waterflow):

$$\frac{\partial Z}{\partial x^*} = -j \qquad (2.2'')$$

instead of eq.(2.2).

While eq.(2.1″) is definitely acceptable wherever the distance between two main tributaries of the river is relatively short compared to the floodwave's length, eq.(2.2″) requires some further consideration.

As a matter of fact, eq.(2.2″) can invariably be accepted for a relatively long flood hydrograph provided that the river channel is prismatic and the bottom slope is uniform. By contrast, if the river channel geometry is irregular, we surely cannot assume that in any cross section of the river the local energy slope (which depends on local velocity and hydraulic radius) is equal to the local bottom slope (which in some cases can be even negative). In the last case, however, it may makes sense considering the actual geometric characteristics of the river averaged over appropriate lengths. This procedure has implicitly been applied in many instances by practical river engineers, but, at the authors' knowledge, no theoretical criterion has been developed for indicating whether, where and how the averaging operation can be applied, apart Fasolato et al. (2007b) who have developed a norm for sinusoidal irregularities. An extension of the criterion to natural streams will be set in the following.

2.2.2 THE EQUIVALENT UNIFORM RIVER REACH

For analyzing river morphodynamics at watershed scale it is convenient to introduce the notion of *equivalent uniform river reach.* Let us consider a relatively short portion of a river, say between the confluences of two large tributaries, conveying a water discharge Q. If this portion is much shorter than the flood-wave length, we may assume that the discharge Q is constant along the river reach (eq.2.1). For a given cross-section of the river we may define the water elevation $Y(x^*,t^*)$ with respect to a datum, the corresponding water width $B(x^*,t^*)$, the cross-section averaged bottom elevation $Z(x^*,t^*)$ and the averaged depth $H(x^*,t^*) = Y - Z$. Let us assume now that the (constant) waterflow $\underline{Q}$ is the *equivalent discharge* Q_{eq}, namely the water discharge that conveys the *annually averaged solid discharge* $\underline{P}$ of that reach (see Sect. 3.5.2). For this particular discharge let us define the *equivalent uniform reach*, as the rectangular channel characterized by the *averaged values* along the reach of the water width $\underline{B}$, the water depth $\underline{H}$, the bottom composition β_k and the bottom slope $\underline{i_f} = -\partial \underline{Z}/\partial x^*$. Note that in the equivalent uniform reach the average bottom slope $\underline{i_f}$, water elevation slope $\underline{i_w} = -\partial \underline{Y}/\partial x^*$ and energy slope $\underline{j}$ are equal (Fig.2.1).

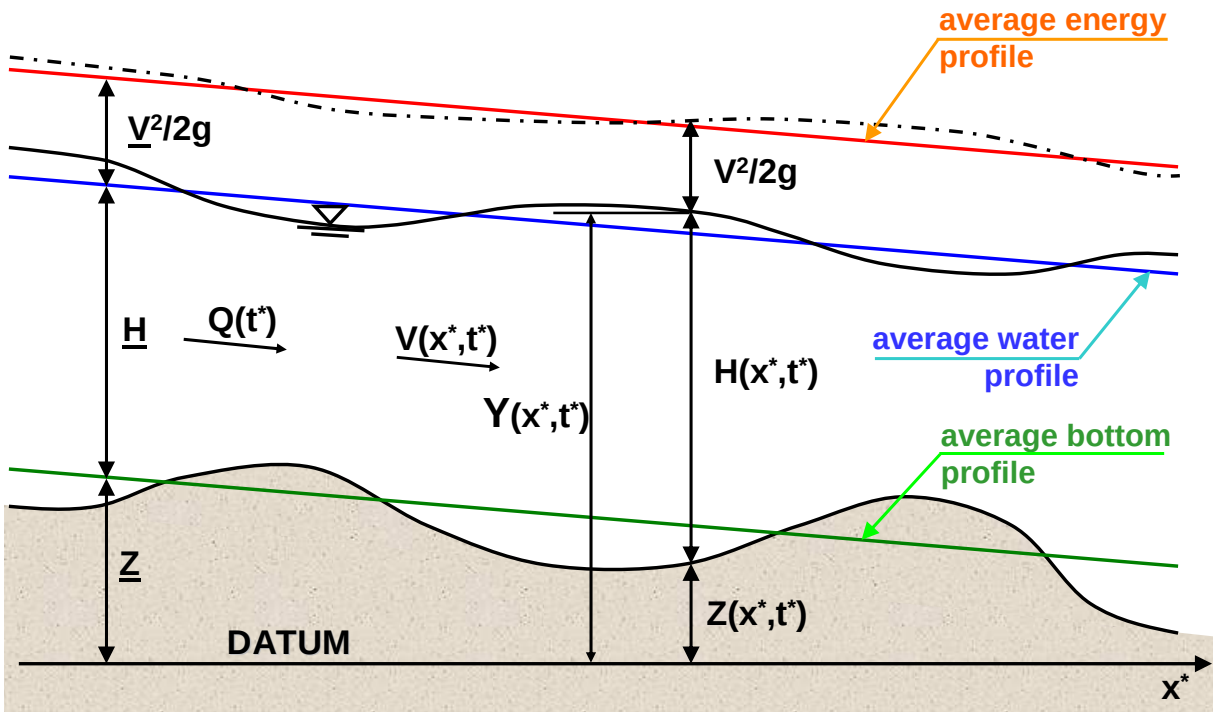

Figure 2.1: Bottom elevation Z, water depth H, water elevation Y and kinetic energy $V^2/2g$ in a given cross-section, compared to the corresponding quantities of the equivalent uniform reach.

The above mentioned quantities are mutually related by the empirical expressions of waterflow (eq. 2.5) and sediment transport (eq. 2.6) as a function of the energy slope:

$$\underline{Q} = \underline{U} \cdot \underline{B} \cdot \underline{H} = \chi \sqrt{\underline{j} \cdot \underline{H}} \cdot \underline{B} \cdot \underline{H} \tag{2.8}$$

$$\underline{P} = \sum_{k=1}^{N} \underline{P}_k = \sum_{k=1}^{N} \alpha_T \cdot \underline{\beta}_k \cdot \xi_k \frac{\underline{Q}^m \underline{j}^n}{\underline{B}^e d_k^f} \tag{2.9}$$

2.2.3 THE LINEARIZED NON-EQUILIBRIUM RIVER

The underlined constant quantities of eqs.(2.8) and (2.9), referring to the *equivalent uniform river reach*, represent a kind of reference conditions. The corresponding quantities with no underline are in general varying in space and time and differ from the previous ones in the following way:

- waterflow: $Q(t) = \underline{Q}\left(1 + q(t)\right)$ (2.10)
- river width: $B(x) = \underline{B}\left(1 + b(x)\right)$ (2.11)
- river depth: $H(x,t) = \underline{H}\left(1 + h(x,t)\right)$ (2.12)
- sediment transport: $P(x,t) = \underline{P}\left(1 + p(x,t)\right)$ (2.13)
- bottom elevation: $Z(x,t) = \underline{Z} + \underline{H} \cdot z(x,t)$ (2.14)
- bottom composition: $\beta_1(x,t) = \underline{\beta_1}\left(1 + \beta_1^0(x,t)\right)$ (2.15)

Note that the, for the sake of simplification, it has been assumed that only 2 grainsize classes (d_1 and d_2) are present and then $P = P_1 + P_2$ and $\beta_1 + \beta_2 = 1$. Moreover it has been assumed that in equilibrium condition the two classes are present in the bottom with the same percentage ($\underline{\beta_1} = \underline{\beta_2} = 0.5$). Finally the exponents in eqs.(2.7) and (2.9) have been rounded off to: $m = n = 1$, $e = f = 2$ and $s=0,8$.

Under the above mentioned hypothesis and assuming the quantities q, b, h, p and β_k^0 much smaller than one, the partial differential equations that describe the time- and space-evolution of the river can be written in the following linearized form (eqs.2.16 - 2.20) , with the non dimensional temporal and spatial coordinates x and t, (with $t = t^* \underline{U}/\underline{H}$ and $x = x^*/\underline{H}$):

$$\frac{\partial q}{\partial x} = 0 \tag{2.16}$$

$$\alpha\frac{\partial h}{\partial x}+\frac{\partial z}{\partial x}-(1-\alpha)\frac{\partial b}{\partial x}=\varepsilon\left(h+\frac{2}{3}b-\frac{2}{3}q\right) \tag{2.17}$$

$$p=6q-6h+\left(\eta^{*}+s\eta\right)\beta_1^0-5b \tag{2.18}$$

$$\frac{\partial z}{\partial t}+\psi\frac{\partial p}{\partial x}=0 \tag{2.19}$$

$$\frac{\partial \beta_1^0}{\partial t}+\frac{\psi}{\Delta}S^{*}\frac{\partial \beta_1^0}{\partial x}+\frac{\psi}{\Delta}\eta^{*}\frac{\partial p}{\partial x}=0 \tag{2.20}$$

where:

- $\alpha=1-F_r^2$ and $F_r^2=\underline{V}^2/g\underline{H}$ is the Froude number (always F_r<1 in our case);
- $\varepsilon=\frac{3}{2}E\,F_r^2$ and E is the resistance coefficient: $E=\frac{2g}{\chi^2}$;
- $\eta=\frac{1-d}{1+d}$ depending exclusively on the ratio $d = d_1/d_2$ between the diameters;
- $\eta^{*}=\frac{1-d^{*}}{1+d^{*}}$ depending on the "hiding-exposure" phenomena through $d^{*} = d^{1-s}$;
- $S^{*}=1-\eta^{*2}=\frac{4d^{*}}{\left(1+d^{*}\right)^2}$
- $\psi=\frac{\underline{P}}{\underline{Q}}$ represents the sediment concentration;
- $\Delta=\frac{\delta}{\underline{H}}$ is the mixing layer.

All the parameters listed above depend on the reference conditions and are supposed to be known constants of each river reach.

The linearized eqs.(2.16 – 2.20) have been analytically solved (Fasolato et al., 2007a) under the hypothesis of sinusoidal spatial and temporal perturbations with respect to the uniform river reach (*harmonic river*).

2.2.4 THE LINEARIZED EQUILIBRIUM RIVER

Particularly simple and interesting is the solution of eqs.(2.16 – 2.20) considering the *morphodynamic stationary conditions* of the river (equilibrium conditions). By putting equal zero all the time-variations of the morphological quantities (Z and $\beta_1{}^0$) one finds immediately:

$$\beta_1^0 = 0 \tag{2.21}$$

$$\frac{\partial q}{\partial x} = \frac{\partial p}{\partial x} = 0 \tag{2.22}$$

$$p = p(t) = 2q(t) \tag{2.23}$$

$$h = h(x,t) = \frac{2}{3}q(t) - \frac{5}{6}b(x) \tag{2.24}$$

$$z = z(x) = \left(1 - \frac{\alpha}{6}\right)b(x) - \frac{\varepsilon}{6}\int_0^x b(x)dx \tag{2.25}$$

The equations above show that the bottom composition β_1 of an equilibrium river remains constant (eq. 2.21), even if the width $b(x)$ and the water discharge $q(t)$ display, respectively, a spatial- variation and a time-variation. Also the sediment transport $p(t)$, in equilibrium with the waterflow $q(t)$, remains constant all over the reach (eq. 2.23). On the other hand the bottom elevation $z(x)$ adjusts its value to the corresponding width (eq. 2.25), while the water depth $h(x,t)$ depends on both the local width $b(x)$ and the water discharge $q(t)$ (eq. 2.24).

For a river in equilibrium (i.e. in morphodynamic stationary conditions) one may also find the solution of eqs.(2.16 – 2.20) if one further assumes (eq. 2.2″) that the local energy slope is equal to the local bottom slope (*uniform waterflow*). The equilibrium solution for the uniform waterflow is given again by eqs.(2.21 – 2.24), while eq.(2.25) is substituted by:

$$z = z(x) = -\frac{\varepsilon}{6}\int_0^x b(x)dx \tag{2.25′}$$

The only difference between the exact solution (steady flow, eq. 2.25) and the approximate solution (uniform flow, eq. 2.25′) consists in the bottom profile, which solely depends on the planimetric distribution of the river width $b(x)$. A thorough discussion of this difference is

reported by Fasolato et al. (2007b), under the hypothesis of a sinusoidal variation of the river width $B(x^*) = \underline{B}(1 + b(x))$ with:

$$b(x) = b_c \cos(\Omega x) \tag{2.26}$$

where $x = x^*/H$, $\Omega = H/\lambda$ and λ is the wavelength of the channel width.

The relative error between the two solutions:

$$Er = \left| \frac{\max|z_{steady}| - \max|z_{uniform}|}{\max|z_{steady}|} \right| \tag{2.27}$$

depends on the parameters $\varepsilon = \frac{3g}{\chi^2} F_r^2$, $\alpha = 1 - F_r^2$ and on the relative wavelength λ/H. By assuming a constant value of $g/\chi^2 = 0.04$, the relative error is provided by Fig.(2.2).

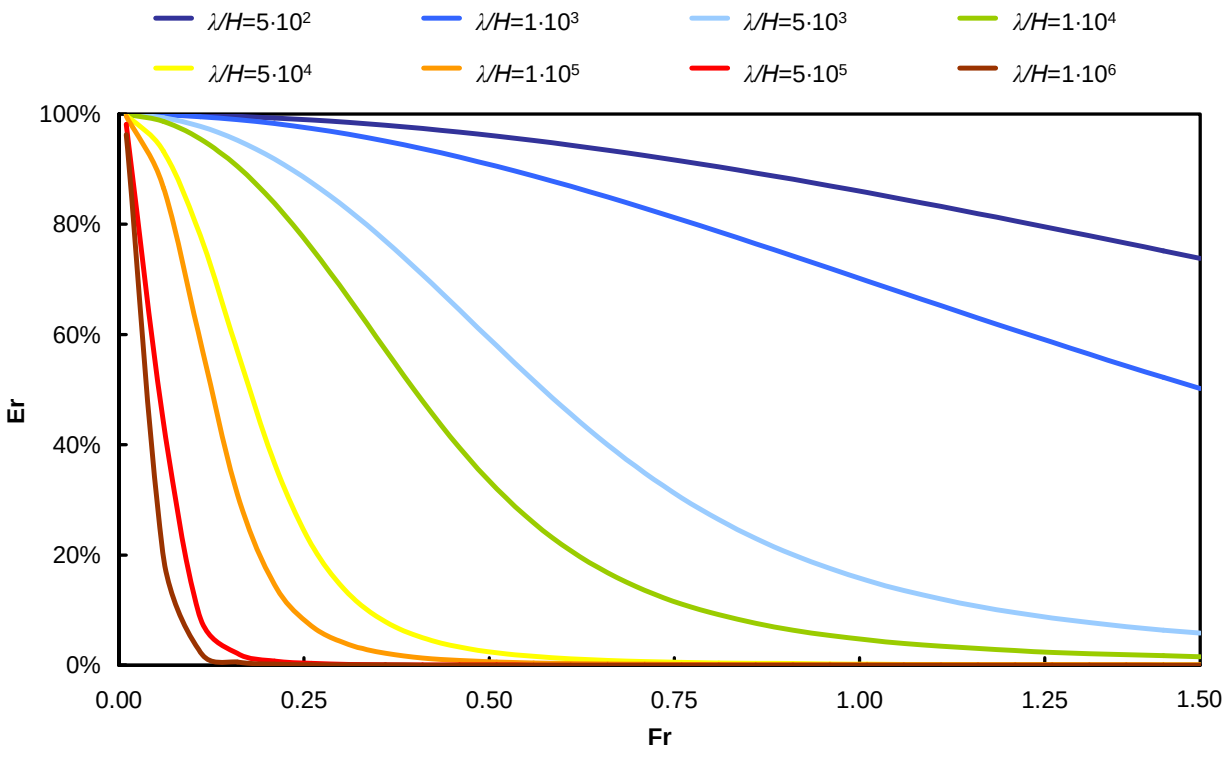

Figure 2.2: Relative error of the approximate solution as a function of the Froude Number, for different values of the relative wavelength λ/H.

2.2.5 BOTTOM PROFILE, WATER SURFACE AND ENERGY LINE

While for the equivalent rectangular river reach in equilibrium conditions, bottom profile, water surface and energy line are three parallel straight-lines, as indicated in Fig.(2.1), the three actual local slopes of the real river may be strongly different. However, if we assume that the river reach is not far from equilibrium, we may compute the three slopes as a function of the channel width *b(x)*, as a proper correction of the unique slope: $\underline{j} = \underline{i}_f = \underline{i}_w = -\partial \underline{Y}/\partial x$, averaged over the reach, which can directly be derived from the river water surface of the Digital Elevation Model (DEM):

$$j(x) = \underline{i}_w \left(1 + \frac{b}{2}\right) \tag{2.28}$$

$$i_w(x) = \underline{i}_w + \frac{1}{6}\underline{H}F_r^2\left(\frac{3}{2}Eb - \frac{db}{dx}\right) \tag{2.29}$$

$$i_f(x) = \underline{i}_w + \frac{1}{6}\left[\varepsilon b - (6-\alpha)\frac{db}{dx}\right] \tag{2.30}$$

Also the quantities *b(x)* and *db/dx* can be evaluated, for each river reach, from the LANDSAT 7 images, which provides both $B(x^*)$ and the average width $\underline{B}$. The average water depth $\underline{H}$ and the other average parameters (α and ε) can also be computed for each river reach by assuming an equivalent discharge $Q_{eq} = \underline{Q}$.

2.2.6 EQUIVALENT DISCHARGE

The notion of equivalent discharge Q_{eq} is again related to the unique slope $\underline{j} = \underline{i}_f = \underline{i}_w = -\partial \underline{Y}/\partial x$ of the equivalent rectangular river reach in equilibrium conditions. Q_{eq} is defined in fact as the constant waterflow $\underline{Q}$ that conveys the solid discharge $\underline{P} = \sum_{k=1}^{N} \underline{P}_k$, corresponding over the time $T_a = 1$ *year* to the annual sediment yield of the reach (eqs. 2.8 and 2.9). For details on the calculation of the *equivalent discharge* see Sect.(3.5.2).

2.3 RIVER SCHEMATIZATION

The concepts developed in the preceding sections have been applied to the lower Zambezi river in Austral Africa, considered as a particularly significant case study because of the great importance and size of this river compared with the great lack of data and information available Ronco et al. (2006 and 2007a). In fact, the only topographical data available are the planimetric configuration of the river and the slope of the water surface obtained by LANDSAT 7 images and the DEM respectively. A more accurate description of the morphoclimatic characteristics of the river basin, hydrology, geology and major structures established within the catchment, together with an in-deep analysis of the available data (both hydrological and sedimentological) and the others boundary conditions of the model is presented in Chapter 3. The calibration of the solid transport formula (eq. 2.9) is provided in Sect.(3.5.6). In this first approach to the river modeling, only a simplified schematization of the lower Zambezi is considered, neglecting the presence of the Luangwa tributary at the upstream boundary but including the other four tributaries downstream Cahora Bassa dam.

2.3.1 RECONSTRUCTING THE RIVER WIDTH AND RIVER BATHYMETRY

The basic river geometrical configuration (width and water slope of the main channel, as well as the ones of the main tributaries) has been reconstructed using different tools, depending on the reach considered, namely discriminating the branch of Zambezi river presently submerged by the Cahora Bassa reservoir - 260 km long - and the river downstream the dam, down to the Indian Ocean, some 600 km long. For the first branch we used the ancient topographic maps, the only available before the inundation of the valley (HCB, 2004), for the rest of the river we used the LANDSAT 7 images and the DEM HYDRO1k Africa. The ancient maps are quite coarse scale (1:50’000), but still acceptable for a preliminary cartographic survey at the base resolution of 1 km. The Orthorectified LANDSAT Enhanced Thematic Mapper (ETM+, bands 7, 4 and 2) mosaic image we used (S-36-15_2000), extends between 15 and 20 degrees south latitude, and span east-west for the full width of the 36 UTM zone. The pixel size is 14.25 meters, that allows for a quite detailed description of the river width configuration.

The hydrographic network dataset of the river basin, which provides for each river reach a basic geometrical description (upper and lower elevation, length, distance from the source and to the sea, etc..) has been extracted from the 1km resolution DEM HYDRO1k Africa that "provides a standard suite of geo-referenced data sets that will be of value for users who need to organize, evaluate, or process hydrologic information on a continental scale" (EROS, 2000). Development of the HYDRO1k database was made possible by the completion of the 30 arc-second digital elevation model at the EROS Data Center of the U.S. Geological Survey in 1996, entitled GTOPO30 (see Fig.2.3). The coarse map scale and data resolution of this model, which can be free downloaded in its entirely or by selecting individual layers (comprising elevation data, compound topographic index, slope, flow direction, streams, drainage basins, flow accumulation, aspect), does not allow a very detailed description of the morphological configuration of the river basin (Cotter et al., 2003), and strongly affects any common hydrological model predictions, both in terms of depth to the water table, streamflow, peakflow and other variables, as well as the representation of the land surface. However, the results of the studies of Wolock et al. (1994) and Zhang et al. (1994) invite the question of "what define an appropriate grid size for simulations of geomorphic and hydrologic processes using topographically driven models"; in fact, they affirm that "the water table configuration may be smoother than the land surface topography and may be related more accurately to a coarse than to a finer resolution DEM" and that "the most appropriate grid size for simulations models is best scaled in reference to the process being modeled". For the purpose of the present study, namely the very long-term simulation of the morphodynamics river process at a watershed scale, the grid size resolution of the HYDRO1k database has only been used for deriving the average slope $\underline{i}_w$ of the water surface, definitely smoother than bathymetry, as eqs. (2.29) and (2.30) indicate. It is seems therefore a reasonable compromise between the overall description of the hydrographic network proprieties, the data handling and the data availability, also considering that the longitudinal configuration of the lower Zambezi river has been reconstructed with a resolution $\Delta x = 1km$ which corresponds to the most frequent width of the river (variable between 0.10 and 5 km) (see Appendix D). It has been assumed that the channel width indicated by the planimetric data (either cartography or satellite images) is independent from the discharge. The water depth below the water elevation provided by the DEM, was established to correspond to the local equivalent discharge Q_{eq} according to eq.(2.5). The local energy slope j was computed by eq.(2.28), under the hypothesis of quasi-equilibrium conditions.

The relative fine bathymetry of the Zambezi river, reconstructed under the hypothesis of quasi-equilibrium conditions (see Fig.2.3), is of course not precisely the real one. Even if virtual, however, the detailed bathymetry has been utilized to compare the performances of the 1-D model, with different approximations (steady and uniform water flow) and different averaging length (fractions of the *morphological "black" box*, as defined in Sect. 2.4.1).

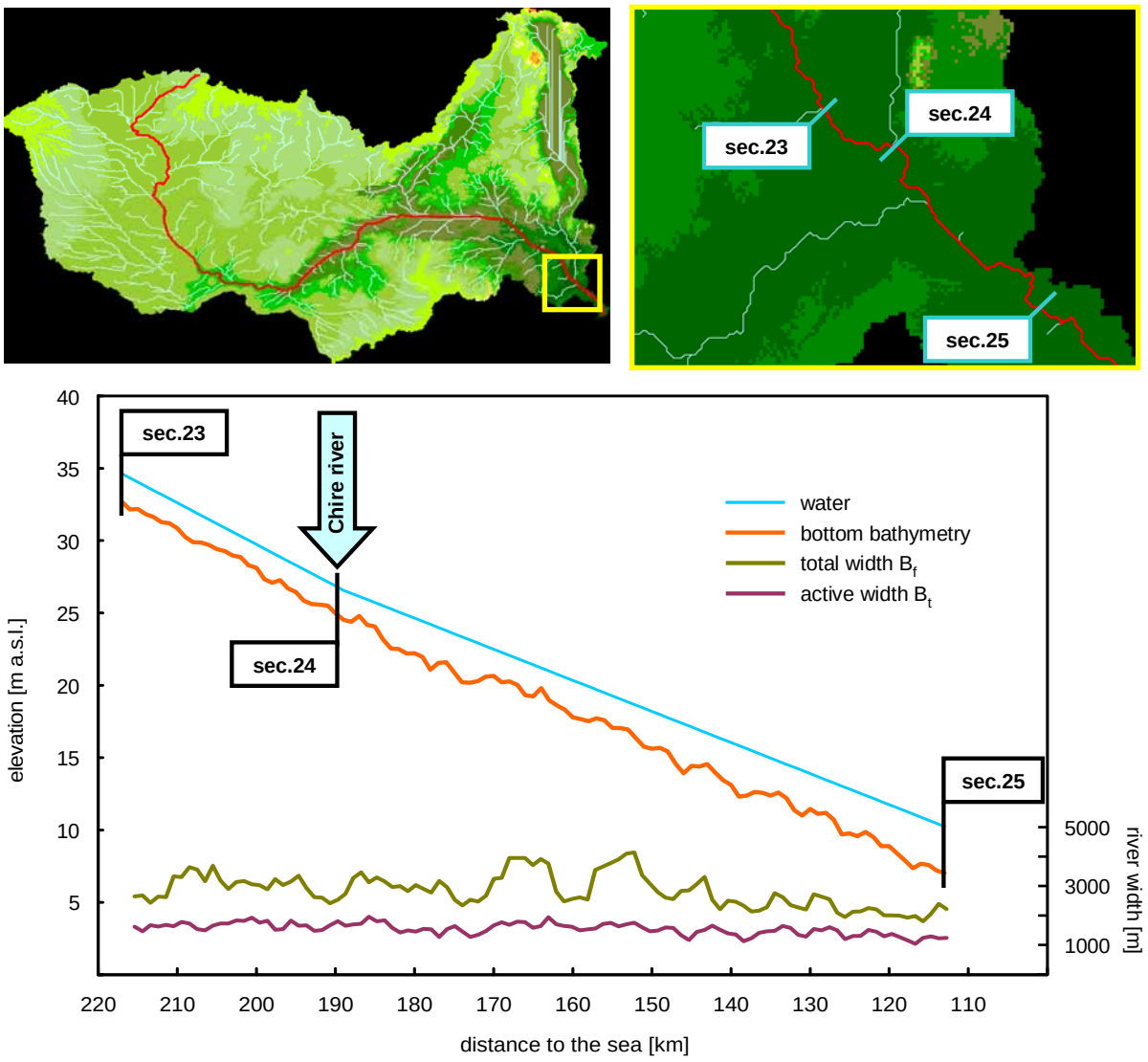

Figure 2.3: An example of reconstruction of the bottom bathymetry from the water slope (provided from the DEM) of part of Zambezi river, in particular between sections 23 and 25 (see *morphological box* schematization, Sect. 2.4.1), including the confluence with the Chire river. The active channel width (B_t) and the total river width (B_f) are also indicated.

2.4 NUMERICAL COMPARISON OF SPATIAL AVERAGING AND SIMPLIFIED MODELS

With reference to the lower Zambezi river, a systematic analysis of the "exact" 1-D morphodynamic model (steady flow, described by eqs. 2.1′, 2.2′, 2.4 and 2.5), will be carried out by changing both the resolution degree of bathymetric data and the size of the computational step. Subsequently a validity assessment of the "approximate" 1-D morphodynamic model (uniform flow, described in eqs. 2.1″, 2.2″, 2.4 and 2.5) will be made by comparison with the "exact" model, by changing again the spatial resolution degree and the computational step. To apply the uniform flow hypothesis to real rivers, bottom elevation shall be averaged over an appropriate *morphological box*.

2.4.1 SIZE OF THE MORPHOLOGICAL BOX

The linearized "exact" solution (steady waterflow) and the linearized "approximate" solution (uniform waterflow) of the 1-D morphodynamic model in equilibrium conditions, have been discussed in Sect.(2.2.4). The relative error between the two solutions, for a prescribed sinusoidal river (eqs. 2.25 and 2.25′), is plotted in the graphs of Fig.(2.2) as a function of the Froude number (Fr) and the non-dimensional wave length (λ/H) of the width perturbation. As it appears from eqs.(2.25 and 2.25′), the relative error (eq. 2.27) does not depends from the amplitude b_c of the width perturbation, and tends to diminish for larger and larger wave lengths λ. If we consider the width of a natural river reach as a combination of a large number of sinusoidal waves, we may assume that the relative error solely depends on the length of each wave. To keep the relative error below a given value ζ, the size of the morphological box L should be larger than $\lambda/4$, being λ the sinusoidal wave length that produces the relative error ζ. This means that within the morphological box $L= \lambda/4$ one can still find both the maximum absolute elevations corresponding to λ, provided by both models, and the corresponding relative error ζ. By contrast, the maximum positive elevation corresponding to shorter waves ($\lambda<4L$) will be averaged, within the box $L= \lambda/4$, with smaller absolute values, producing a substantial reduction of the relative error. On the other hand, longer waves ($\lambda>4L$) will be explicitly and entirely described by the models, but with a relative error E_r smaller than ζ.

In the case of Zambezi river, with reference to the notion of *equivalent uniform river reach* in morphodynamic equilibrium conditions (see Sect.2.2.2 and 2.2.4), a preliminary subdivision of the river in 9 homogeneous *morphological reaches* in quasi-stationary conditions has been made, according to the presence of major morphological "*key factor*", such as: main tributaries, gorges, bifurcations of delta, main structures (dams). For each homogeneous *morphological reach*, the minimum value of the morphological box $L = \lambda/4$ has been singled-out, once a relative error $E_r \cong 20\%$ (average over the entire river) has been selected (see Table 2.1).

River reach	Description	Length [km]	Fr	λ [km]	Morphological box L [km]	E_r theoretical [%]
1	Zumbo – gorges (start)	225	0.29	128	32	19.8
2	gorges (start) – dam site	35	0.52	140	35	12.7
3	dam site – Luia river	32	0.58	64	16	14.2
4	Luia river - gorges (end)	72	0.34	144	36	16.5
5	gorges (end) – Revubue river	31	0.27	124	31	15.9
6	Revubue river – Luenha river	31	0.27	124	31	11.8
7	Luenha river – Chire river	252	0.29	112	28	12.9
8	Chire river – delta bifurcation	153	0.20	304	76	28.5
9	delta bifurcation - sea	36	0.13	72	18	83.6
					average error [%]	**20.8**

Table 2.1: Computation of the wave length and *morphological boxes'* dimension for the lower Zambezi river, assuming an admissible value of the relative error (eq.27) $E_r \cong 20\%$ (average over the entire river)

2.4.2 ANALYSIS OF THE "EXACT" (STEADY FLOW) MODEL

As the flood wave of lower Zambezi is very much longer than the maximum distance between tributaries, the "exact" model which provides the most accurate results is assumed to be the steady waterflow model. On the other hand, the required space- and time-resolution is certainly satisfied by the computational space-step $\Delta x = 1km$ and the corresponding maximum time-step $\Delta t = 100s$. With reference to the most accurate computations carried on in this way, in Fig.(2.4) one can see the effects of averaging these results over different fractions of the morphological box. By expressing the loss of resolution as:

$$\sigma_{\Delta x} = \sqrt{\frac{\sum_{i=1}^{N} \left(z_1^s - z_{1,\Delta x}^s \right)_i^2}{N}} \tag{2.31}$$

one can observe (Fig.2.5) that the mean square error decreases from about 0.80m (for the entire length *L*) to about 0.40m (for a length *L/8*). Correspondingly, in Fig.(2.6) is reported the effects of different computational steps. With reference again to the results obtained with time-step $\Delta x = 1km$, in Fig.(2.7) is reported the increase of accuracy, by using smaller and smaller computational steps:

$$\varepsilon_{\Delta x} = \sqrt{\frac{\sum_{i=1}^{N}\left(z^{s}_{\Delta X} - z^{s}_{1}\right)^{2}_{i}}{N}} \tag{2.32}$$

2.4.2.1 Effects of the different spatial resolution

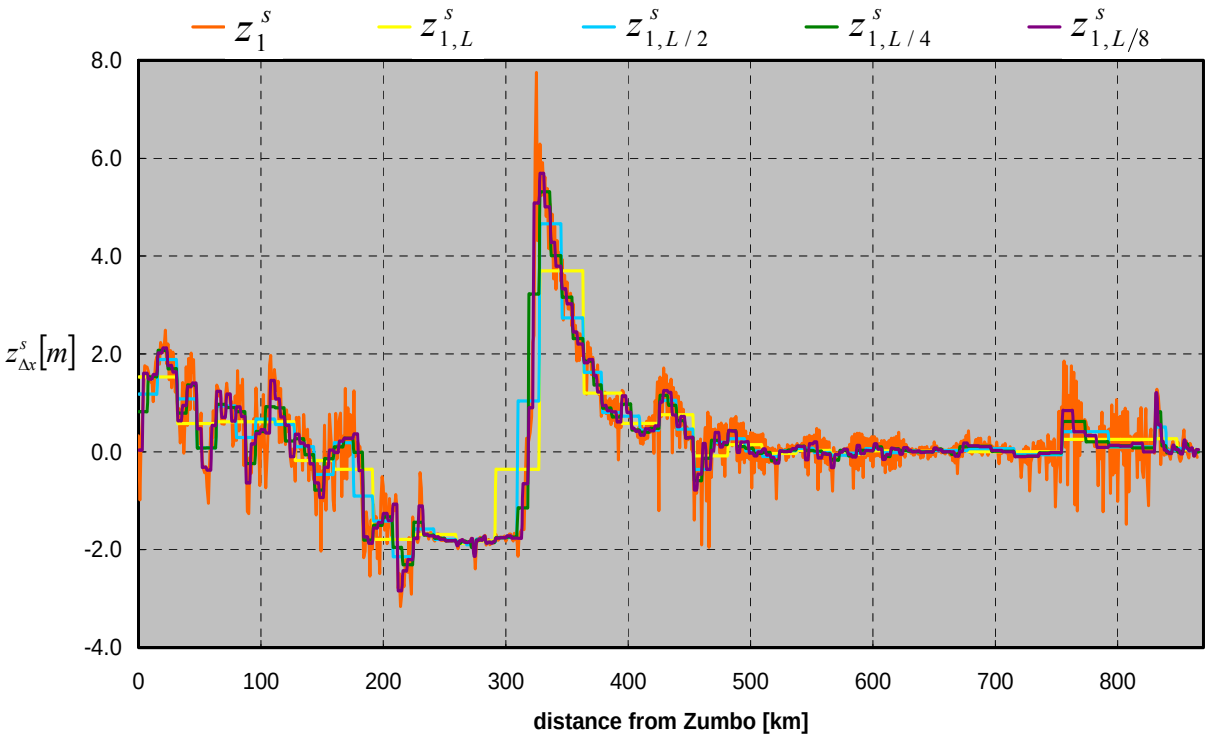

Figure 2.4: Bottom variation of the computed with a space-step of 1km and subsequently averaged within different fractions of the *morphological box* (L, L/2, L/4, L/8).

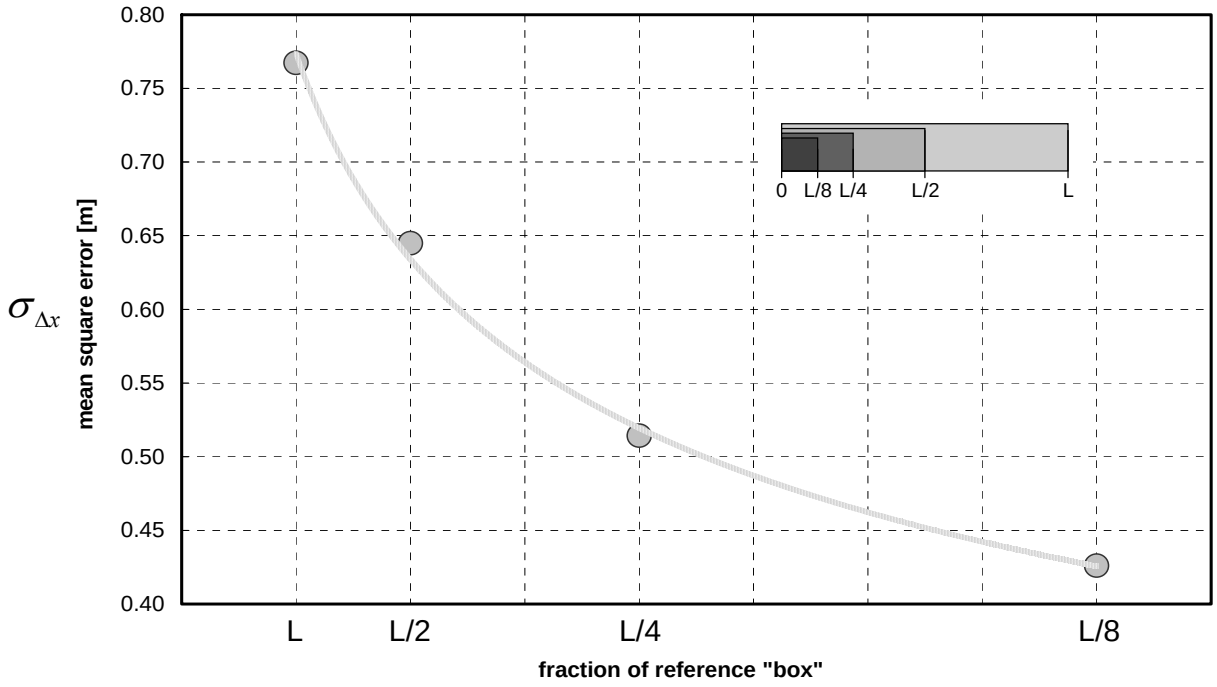

Figure 2.5: Loss of resolution (through the mean square error, eq.2.31) by averaging over smaller and smaller *morphological boxes.*

2.4.2.2 Effects of different computational steps

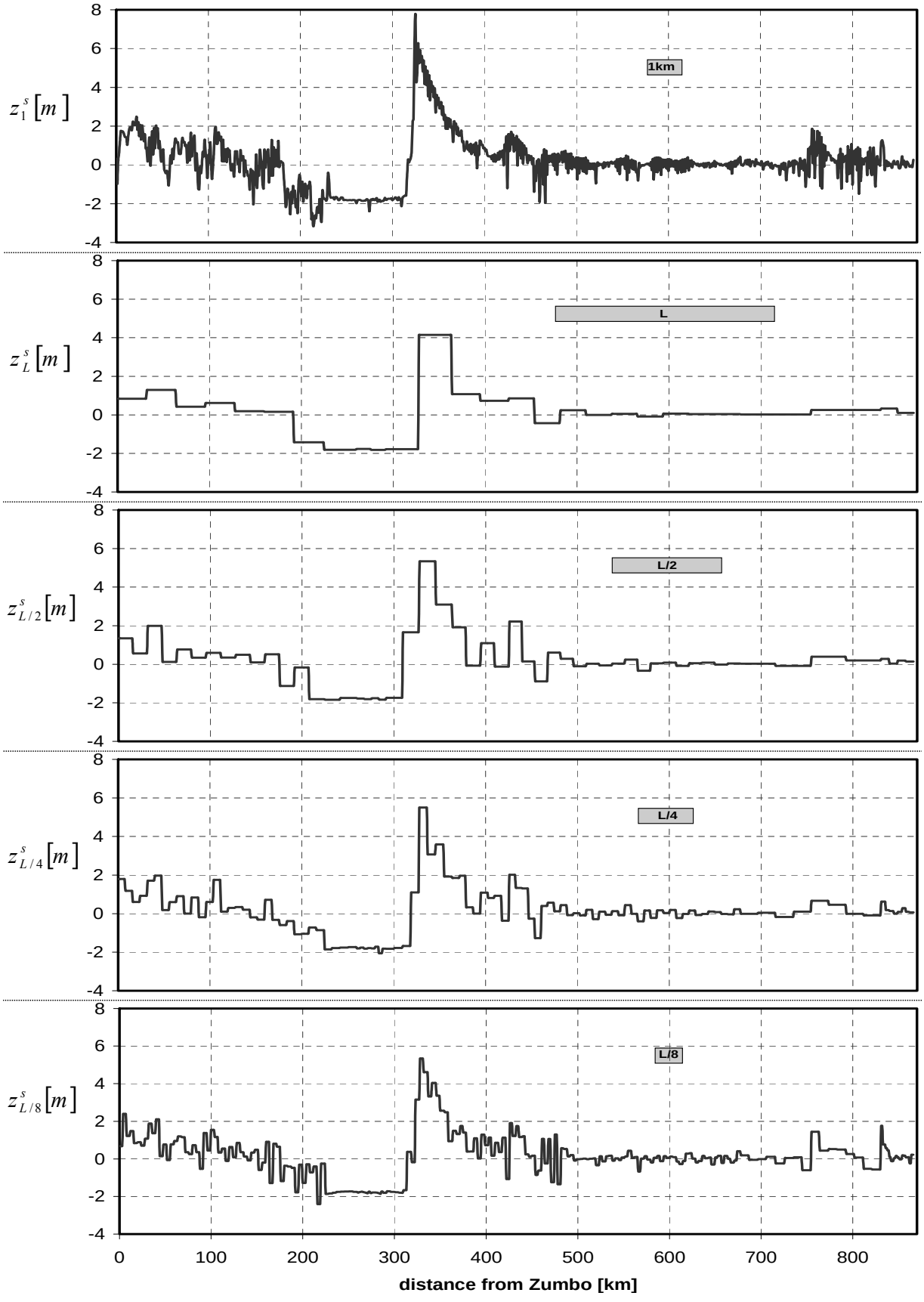

Figure 2.6: Bottom evolution after 10 years simulation, using the 1-D "exact" morphological model, with different computational steps (namely: *1km, L, L/2, L/4, L/8*).

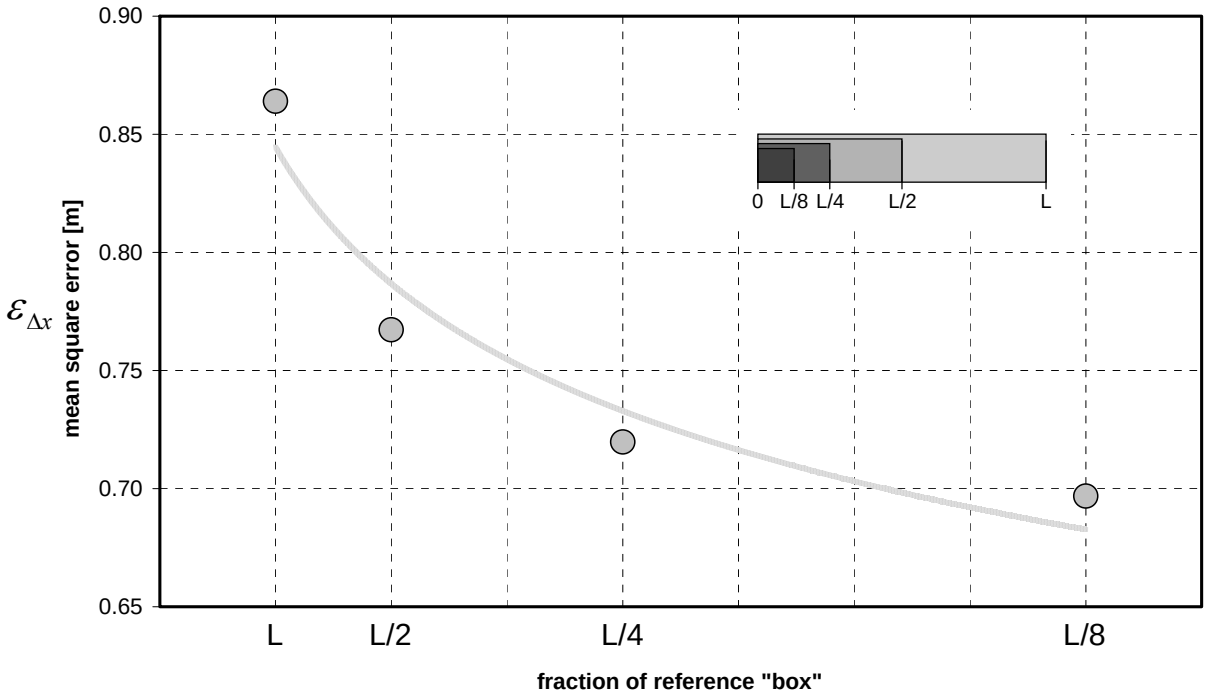

Figure 2.7: Decrease of the mean square error (eq.2.32) by using smaller and smaller computational steps.

As it appears from the graphs, the loss of accuracy is only slightly larger the loss of resolution. In other words the solution provided by the model with a computational space step $\Delta x = L/n$ is not substantially different from the "exact" solution ($\Delta x = 1km$) averaged over the same length L/n.

2.4.3 THE "APPROXIMATE" (UNIFORM FLOW) VS THE "EXACT" (STEADY FLOW) MODEL

The theoretical approach by Fasolato et al. (2007b), under the hypothesis of sinusoidal river in equilibrium conditions, is reasonably confirmed also for the non-equilibrium evolution of a natural river as the lower Zambezi. In Fig.(2.8) the results of the two models after 10 years of evolution are compared by applying different computational steps Δx. Although the results of the two models are altogether quite similar for all the computational steps, the most accurate results of the uniform-flow model have been obtained with the coarser grids. As it appears from Fig.(2.9), the mean square error over the entire river increases from about 18 cm for $\Delta x = L$ (*morphological box*) to about 45 cm for $\Delta x = L/8$. This is also confirmed in Fig.(2.10) by the average relative error along the river, which correspondingly increases from 40% to 135%. As far as the spatial distribution of the relative error is concerned, from Fig.(2.11) one can see that the local relative error provided by the

numerical simulations with $\Delta x = L$ appears rather similar to the theoretical values found as a function of the local Froude number and $\lambda=4L$, (Fig.2.2).

The better resolution obtained with smaller morphological boxes, in conclusion, is inevitably associated to a worse accuracy of the average results. On the other hand, computations performed with larger space steps require of course less computational time as it appears clearly from Fig.(2.12). In relative terms, the required computational effort of the uniform-flow model is 3-6 times faster than steady-flow model.

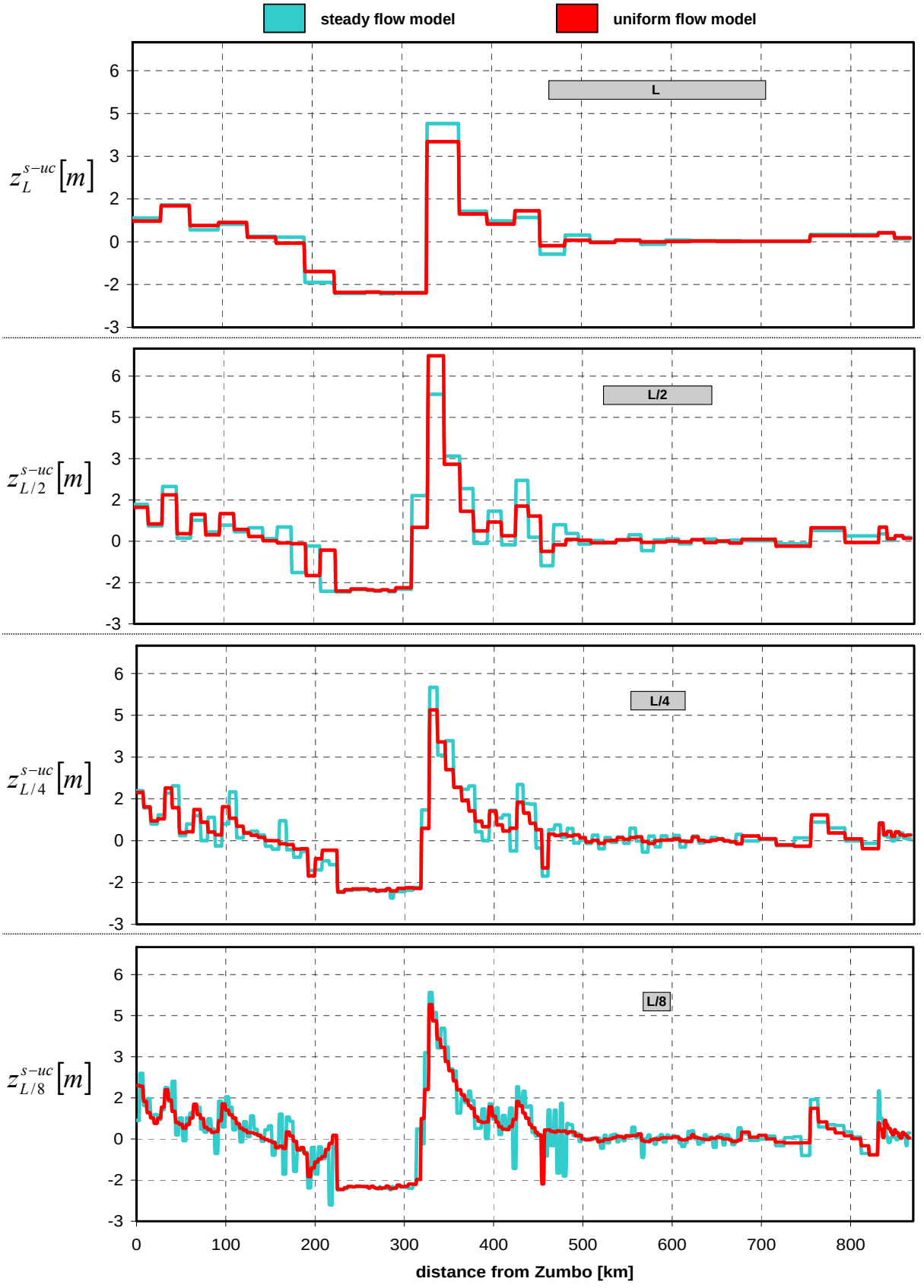

Figure 2.8: Bottom evolution after 10 years simulation, comparing the 1-D "approximate" (*uc*) with the 1-D "exact" (*s*) morphological model, with different computational steps (namely: *L, L/2, L/4, L/8*).

$$\gamma_{\Delta x} = \sqrt{\frac{\sum_{i=1}^{N}\left(z_{\Delta X}^{s} - z_{\Delta x}^{uc}\right)_i^2}{N}} \qquad (2.33)$$

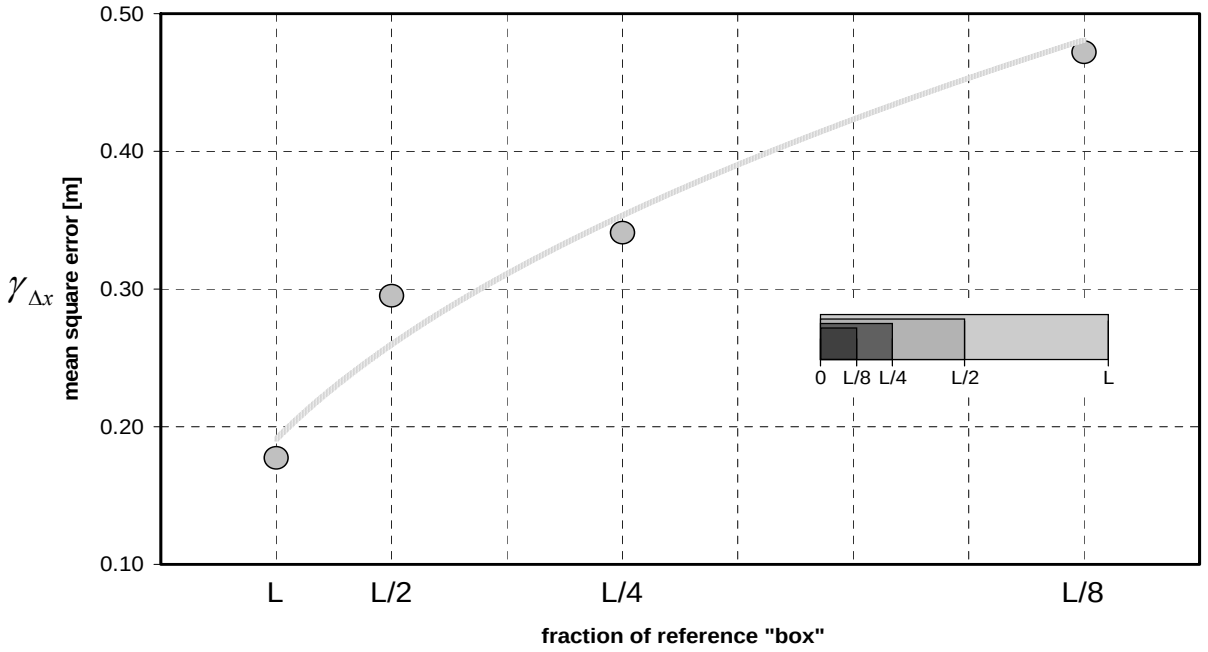

Figure 2.9: Comparison between the "exact" model (steady flow) and "approximate" model (uniform flow). Increase of the mean square error (eq.2.33) by using smaller and smaller computational steps.

$$\lambda_{\Delta x} = \frac{\left|z_{\Delta x}^{s} - z_{\Delta x}^{uc}\right|}{\left|z_{\Delta x}^{s}\right|} \qquad (2.34)$$

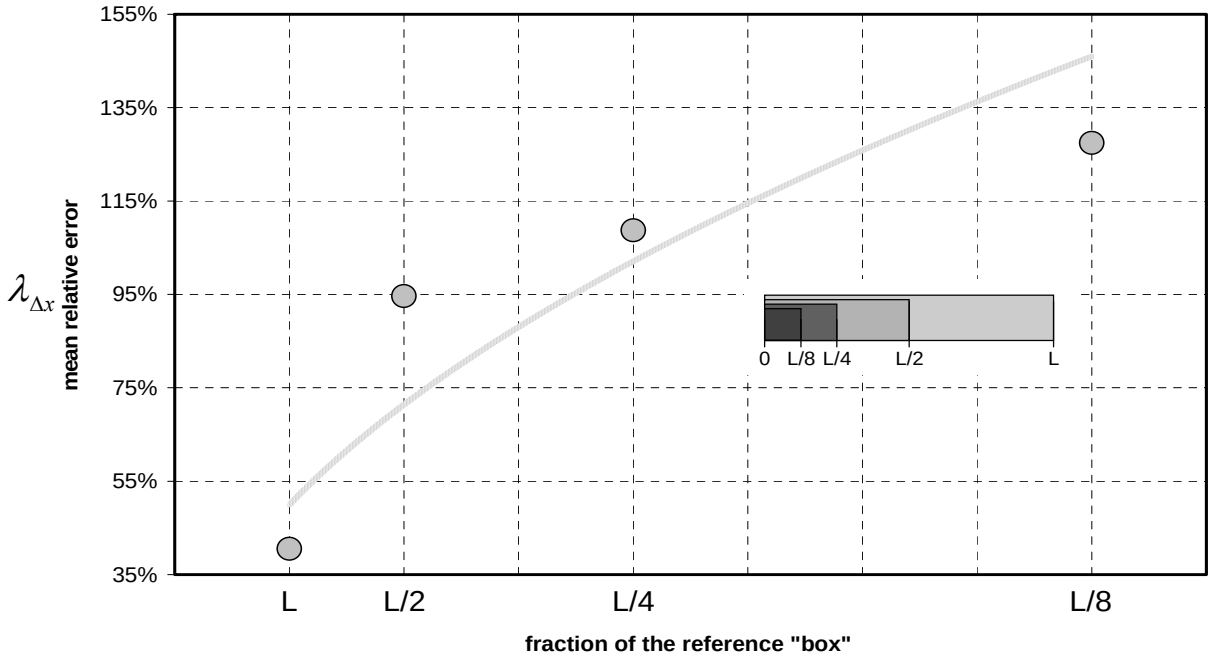

Figure 2.10: Comparison between the "exact" model (steady flow) and "approximate" model (uniform flow). Increase of the mean relative error (eq.2.34) by using smaller and smaller computational steps.

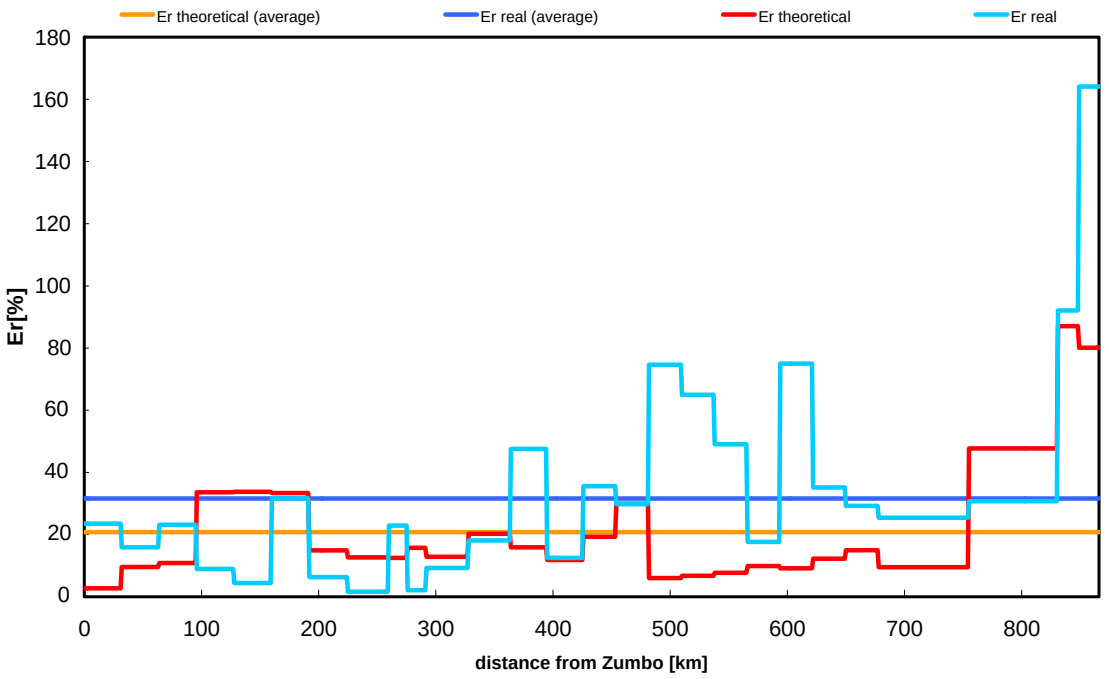

Figure 2.11:Comparison of the relative theoretical and real error (eq.2.27) between approximate (uniform flow) and exact (steady flow) model in lower Zambezi river. Average values over each homogeneous reach (morphological box).

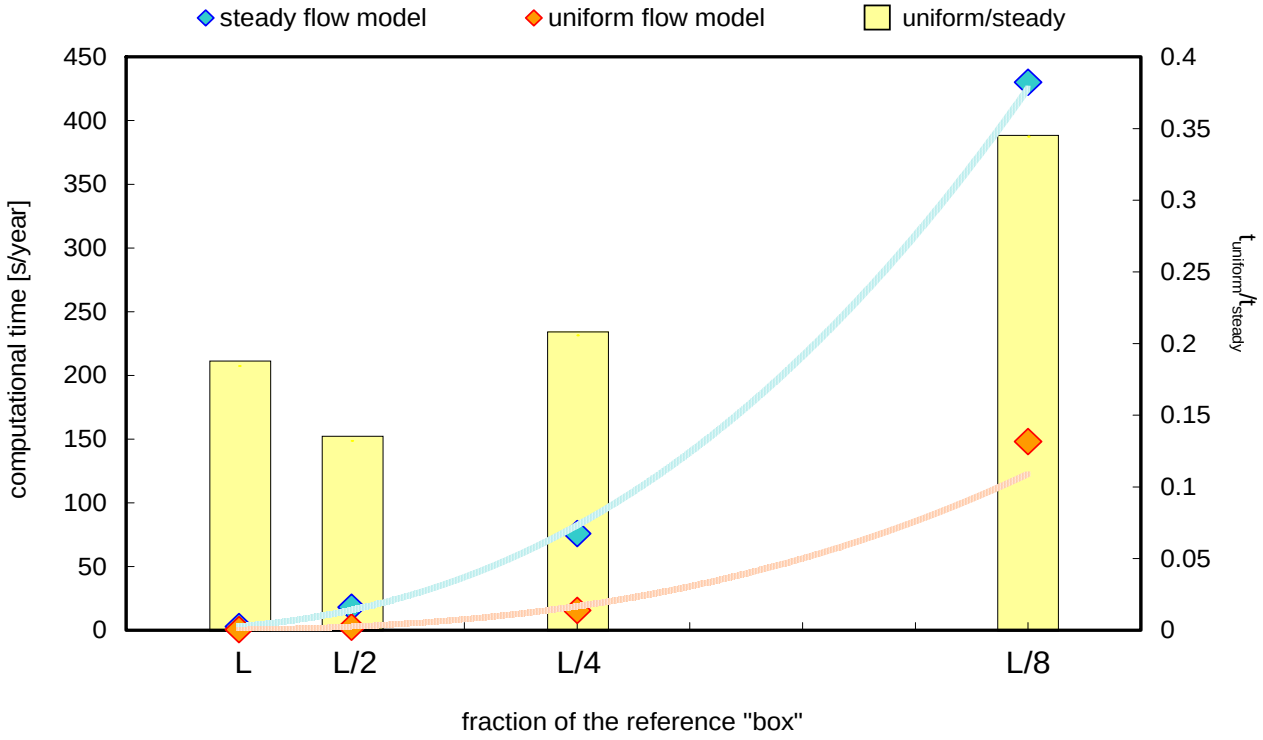

Figure 2.12:Comparison between the “exact” model (steady flow) and “approximate” model (uniform flow) in terms of computational time (seconds per year of simulation), by using smaller and smaller computational steps.

2.5 CONCLUSIONS

A systematic analysis on the lower Zambezi river has been carried out to evaluate the advantages and limitations of the uniform water flow hypothesis in 1-D morphodynamic models. The main advantages of the uniform flow hypothesis is that no detailed bathymetric survey is required by this model. For long-term, large-scale morphodynamic computations, moreover, the same hypothesis requires much less computational time and permits as well a simple estimate of the annual sediment yield in various sections.

The uniform flow hypothesis, in fact, has been always implicitly adopted in river engineering by considering the average value of width and bottom slope of a certain river reach.

This hypothesis is usually considered acceptable provided that the reach appears to be "reasonably regular". A theoretical criterion based on the quasi-equilibrium solution of the morphodynamic equations (Fasolato et al., 2007b), indicates by contrast that the *acceptable length* of the river reach on which the averaging should be made, does not depend on the degree of irregularity but rather on the Froude number, i.e. on the averaged slope of the river reach. As a function of the Froude number (Fig.2.2), the criterion provides the minimum relative length of the river reach ($L= \lambda/4$) to be averaged, in order to keep the relative error between uniform flow and steady flow computation below a prescribed value. This means that within the length L (*morphological "black" box*) we cannot pretend to know the local bathymetric and granulometric details, but, on the other hand, we confide that the averaged values over the box do not differ substantially from the exact computations. While for large and slow flatland rivers, the *morphological "black" box* needs to be at least several tens of kilometres, for small and steep mountain rivers it may be hundred of times short.

The above mentioned criterion has been applied to the lower part of the Zambezi river, characterized by small averaged bottom slope (between $3.6 \cdot 10^{-3}$ and $6.6 \cdot 10^{-5}$, corresponding to Froude number between 0.58 and 0.13). The corresponding lengths of the morphological boxes result to be between 16 and 76 km, for a relative error of about 20%.

For the same 870 km – long river reach, the detailed bathymetry at 1 km distance resolution has been reconstructed, under the hypothesis of quasi-equilibrium conditions, from

the available planimetric data and water surface slopes, as reported in Sect.(2.3.1) (Appendix D). Although the reconstructed bathymetry is only virtual, it has been postulated as real and used to evaluate the accuracy and resolution of the "exact" model (steady flow), as well as to assess the validity of the "approximate" model (uniform flow).

Both the accuracy and the resolution of the "exact" model improve, as expected, by applying smaller computational boxes. By contrast the "approximate" model compares better with the "exact" model when the spatial resolution is relatively coarse and corresponding to the size of the morphological box, selected according to the theoretical criterion.

In conclusion, a relatively course computational grid with a uniform-flow model produces acceptably accurate results with a substantial decrease of computational effort.

Chapter 3

Simulating Effects of Kariba and Cahora Bassa Dams on Lower Zambezi River

3.1 INTRODUCTION

The effects of human-induced change in river systems in general and the one of dams on river geomorphology in particular have been addressed since the beginning of the rapid worldwide development of large reservoirs around the 1950's. A part from the interception of sediments by the reservoir, the other major cause of morphological changes below dams is the substantial reduction of waterflow transport capacity and waterdepth, due to the regulation of water discharge with a virtual disappearance of large and, especially, medium floods. The combination of reduced waterflow and sediment load along the river system produces generalized aggradation and degradation at reach scale, but also important deformations of the cross section at smaller scales (narrowing or widening of the channel width, variation of

braiding/meandering configuration, formation and destruction of fluvial islands and floodplains, etc.), with crucial interactions with riparian vegetation. An interesting updated review of the geomorphological literature on this problem is given by Petts et al., (2005).

Due to the simultaneous reduction of both sediment input and water inflow, it is difficult even to predict the very same direction of the river evolution. As it appears from the renowned "Lane's scale" (1955), indicating the tendencies of a channel change and reported in Fig.(3.1), one cannot in principle foreseen how will react the river reach if one does not know, quantitatively, whether is prevailing the decrease of water or sediment.

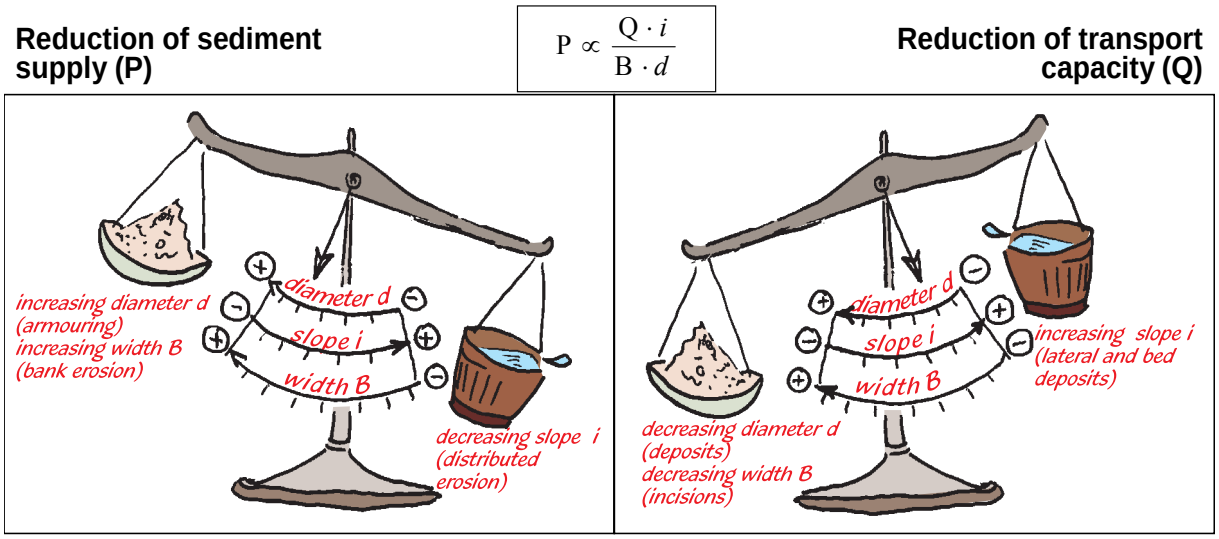

Figure 3.1: Response of a river system to a variation of sediment supply (left) or transport capacity (right). Adapted from Lane (1955).

On the other hand, the entire river system will slowly adapt to the changes of water and sediment produced by the reservoir, starting from the dam location and progressively propagating downstream and up to a point upstream. Several concepts about the adjustment in time and space of the fluvial system towards a new equilibrium configuration, have been proposed in the geomorphological literature since the early work of Shumm (1969). In most of these works (e.g. Gurnell et al., 2002) the Lane's balance principle has been extended and modified to explain reasonable time- and space-variations. Also based somehow on the Lane's scale, Brandt (2000) provides a clever classification of the geomorphological effects downstream of dams in nine different cases, depending on changes in released water flow and sediment load.

It is apparent, however, that the reaction of the river system to the reservoir's perturbation will eventually interest the entire watershed with response times up to millennia. In meantime, other perturbations may subsequently arise in the watershed (new reservoirs, water diversion, reforestation, deforestation, change of land use, erosion control works, sand- and gravel-quarries, etc.). As these perturbations will combine their effects with the first reservoir, waterflow and sediment transport, together with river morphology and bed composition, will vary in an extremely complex way over the hydrographic network, from the divide down to the ocean. It is to be considered, moreover, that many large rivers are still subject to natural evolution, although much slower than anthropogenic one, due to geological conditions (glaciations, tectonics, etc). This is in fact the present situation of all majors rivers in Europe and in many other countries.

Also rivers of Developing Countries, like Zambezi, are subject to large morphological changes, of both natural and anthropogenic origin, covering thousands of kilometres and bound to last for centuries and millennium. The only way of assessing those changes (to possibly mitigate their immediate and long-terms effects) is simulating the erosion/transport/sedimentation processes along the Zambezi with an appropriate morphological model (Ronco et al, 2008).

Morphodynamic models with different degrees of detail have been developed by the hydraulic engineers community since long time (Di Silvio, 2004b). For the purpose represented here a one-dimensional model which would provide the evolution of bottom profile and bottom composition, together with the waterflow and sediment transport rate in any section of the river, would suffice.

Downloaded and commercial versions of one-dimensional models are quite reliable and user friendly. Yet, the "complete" version of one-dimensional model (unsteady waterflow coupled with non-uniform grainsize sediment transport) is hardly applicable to large fluvial systems like Zambezi. The main constraint is represented by the lack of reliable and dense bathymetric surveys as required by the complete model. Moreover, the complete model is extremely demanding in terms of computational time, especially when the simulations should be extended to a basin of $1.4\ 10^6$ km^2 for several thousand years.

As thoroughly described Chapter 2, however, a simplified version of the one-dimensional model is available, based on the local uniform-flow hypothesis, which requires only geometrical data averaged over a relative large distance, called *morphological box*, generally available also for unsurveyed rivers in Developing Countries.

The simplified (uniform-flow) model provides aggradation/degradation rates, sediment transport rate and grainsize composition averaged over the *morphological box*. The width is given for the "active channel" and the for "flooding channel" as a function of the so-called equivalent discharge (see Sect. 3.5.2). The effect of vegetation is empirically accounted in the definition of "active channel" width.

The results of the simplified one-dimensional morphological model may be used to determine the boundary conditions for detailed two-dimensional model, to be applied where local problems should be investigated at very high resolution for short periods of time.

3.2 THE ZAMBEZI RIVER BASIN: AN OVERVIEW

3.2.1 CHARACTERISTICS OF THE BASIN

The catchment area of the Zambezi river basin is 1,385,300 km^2, and it is the fourth largest in Africa after the Congo, the Nile and the Niger (see Fig.3.2). The Zambezi river is approximately 2500 km long. The basin drains from altitudes around 1600 m a.s.l. in northern Zambia and eastern Angola. The upper catchment lies on a vast plateau, the river being contained within a well-defined channel except for two major flood plains known as the Barotse and Chobe swamps. Its descent from this central plateau commences at Victoria Falls (1078 km from sources) where its altitude drops from 978 to 870 m a.s.l. In its natural state the mid course of the river from Victoria Falls to Lupata consisted of narrow rapids and falls in mountainous areas and pen-plains, with an overall fall of 800 m. The river crosses the border into Mozambique near the township of Zumbo at an altitude of 330 m a.s.l. and flows into Cahora Bassa reservoir (1630 km from sources). At the dam site the gorge is very steep sided with a depth of about 600 meters. From the dam, with an altitude of 205 m a.s.l., the river continues in this gorge for a further 60 km before entering the pen plains. The course of the river is only slightly meandering to Lupata, flowing in a well defined channel between

800 and 1000 m wide. After passing a gorge at Lupata at 95 m above datum, the river enter the major flood plain. The final 380 km to the Indian Ocean are characterized by a 1-4 km wide, heavily braided course with ill-defined banks. The delta may be considered to start at Mopeia, 150 km from the Ocean and tidal influence is evident over the last 80 km (SCC Brokonsult, 2001). Major cities within the Zambezi river basin include Lusaka and Harare, the capitals of Zambia and Zimbabwe, respectively. The major African river basin and the Zambezi in particular, are depicted in Fig.(3.2). Table (3.1) provides a summary of the basin area within the numerous nations that share the river basin (SMEC, 2004).

Nation	Area (km^2)	Percentage
Angola	254,600	18.2 %
Zambia	576,900	40.7 %
Namibia	17,200	1.2 %
Botswana	1900	2.8 %
Zimbabwe	215,500	16.0 %
Tanzania	27,200	2.0 %
Malawi	110,400	7.7 %
Mozambique	137,000	11.4 %
Total:	**1,385,300**	**100 %**

Table 3.1: Zambezi river basin area within nations. Southern African Regional Development Corporation.

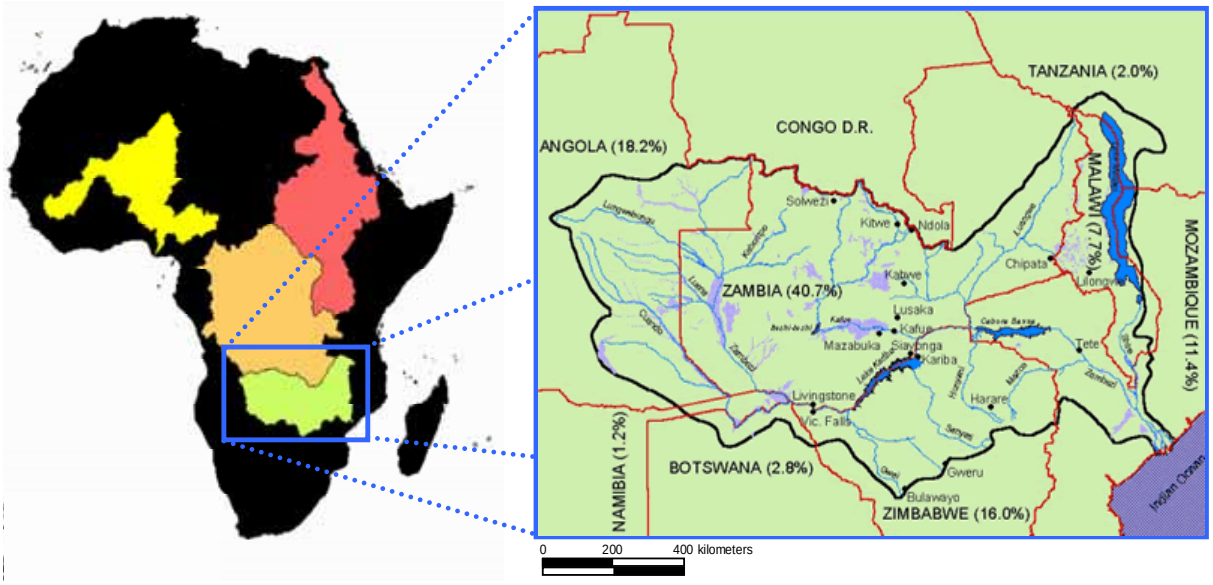

Figure 3.2: Majors river basin in Africa (Nile, Congo, Niger and Zambezi) and the Zambezi river basin.

3.2.2 THE CLIMATE

The climate of the Zambezi basin is typically sub-tropical. The year can be divided in four season:

1. hot season from late August or early September to the beginning of the main rains in October or November;
2. rainy season from October/November to March/April;
3. post rainy season in April and May;
4. cool season from June to early August.

Annual rainfall varies from approximately 1500 mm in the northern part of the catchment to approximately 850 mm in the southern part with the lowest rainfall in the order of 600 to 700 mm occurring in the central Zambezi valley. Maximum rainfall months are December and January with peak discharges at Victoria Falls occurring between the beginning of March and the end of May. The winter rainfall usually account for about 3% of the annual total. With warm sunny conditions prevailing for much of the time in the Zambezi basin (in the lowest areas of the Zambezi valley temperatures can exceed 35°C) insulation is high causing mean annual potential evaporation to be high throughout the area. Class A pan evaporation is typically of the order of 1800 to 2200 mm per annum, with a significant seasonal variation from approximately 200 mm per month between October and March to around 125 mm per month in June e July.(Lahmeyer et al, 2001)

3.2.3 MAJOR STRUCTURES

Completed in 1959 and situated at Kariba gorge between Zambia and Zimbabwe (that receives most of the electricity production), the Kariba dam consists of a double curvature concrete arch dam with a maximum height of about 130 m and a crest length of about 600 m. Six floodgates permit a discharge of 9500 m^3/s. The reservoir has a storage capacity of about 180 km^3 and although the live storage is much less, it is the second largest in Africa and one of the largest of the world. Several other impoundment were established within the Zambezi river catchment in Zimbabwe, among which McIlwaine (reservoir capacity 38.8 km^3) and Ngesi (reservoir capacity 26 km^3). For hydro-electric power purpose, in 1972 a dam was built on the Kafue river and a second dam was built upstream, near Itesitesi. The reservoir of Cahora Bassa in particular is described in detail in Sect.(3.3.1) With all the constructions executed (see Fig.3.3) in Zambezi river, when entering the territory of Mozambique it can be

considered as a regulated river that lost its natural pattern of flow variations in time and in quantity. (Suschka et al., 1986).

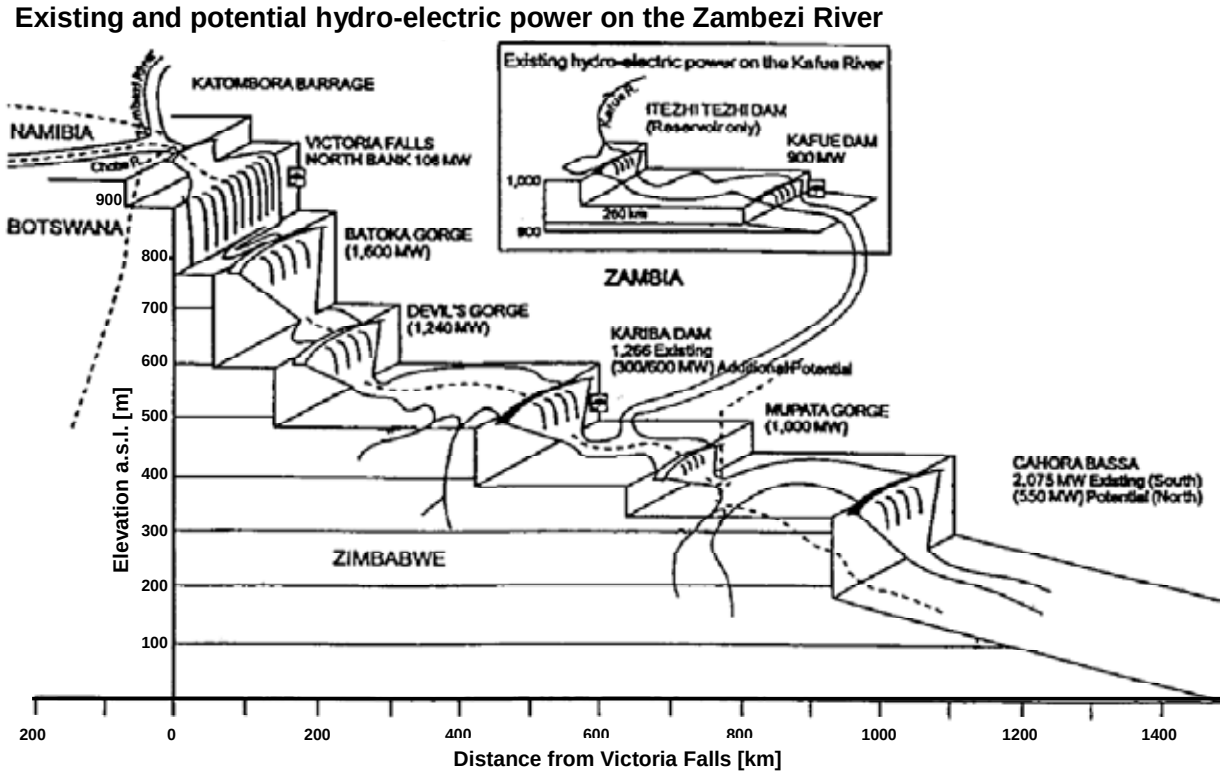

Figure 3.3:Schematic diagram of reservoirs and potential hydro power production of the Zambezi basin (after Chounguiça, 1997).

3.2.4 GEOLOGICAL TEMPLATE

It is not the intention of the present work to supply a complete and in-depth description of the main geological features that characterized the lower Zambezi river and basin. However, it seems necessary to underline some basic aspects of the geo-lithologic configuration of the river basin, for a better understanding of the hydraulic and morphological analysis.

Few studies and publications have been carried on concerning the geological template of the Zambezi basin (Orpen et al., 1989; Nugent, 1990; Thomas et al.,1992; Shoko et al., 1999; Catuneanu et al., 2005) mainly devoted the comprehension of the regional tectonic evolution and implication (uplifting and erosion) on the middle and lower part of the basin.

Focusing our attention on the lower part of the river, the gross architecture of the section of the Zambezi between Cahora Bassa dam and Tambara (some 280 km downstream) is controlled by the West-East trending upper Zambezi graben (that comprises highly resistant

granites and gneisses) and the middle Zambezi graben that causes the river to flow in a NW-SE direction. Between Tambara and the delta zone (some 320 km) the Zambezi river flows predominantly on Quaternary alluvium; this stretch of the river traverses the north-south trending East African Rift valley near Caia (Basson, 2004).

Catuneanu et al., (2005) suggest that " the thickness reflect the tectonic setting, with the rift basins such as mid-Zambezi, Cahora Bassa and the Tanzianian grabens accumulating several kilometres of sediment. Changes from braided coarse-load fluvial system to mixed-load and fine-grained meandering systems can be ascribed to sediment supply rates, reflecting in turn, the interaction of tectonic setting and palaeoclimate". The Karoo sediments lying in lower Zambezi basin have only recently been mapped in details; significant geophysical and geological features make evident that the structure and sedimentology of this part of the basin is dramatically different from the middle Zambezi one, suggesting that a different tectonic setting is enforceable (Orpen et al.,1989). An original and significant description of the geological evolution of the Zambezi river long profile is provided by Nugent (1990) that explains the particular form of the river profile (that not exhibit the characteristics single concave-upwards form (Leopold et al.,1964) forms two concave-upwards sections, with their boundary at the Victoria Falls) by suggesting that "the upper and middle Zambezi evolved and entirely separate river systems, which joined together in comparatively recent times", at the end of the Middle Pleistocene: the major drop in height at the Victoria Falls is seen ad the consequence of the joining of two rivers which were previously graded to different base levels. In terms of Lane' relation (1955), this river capture has an important consequence on the sediment budget evolution because altered the discharge of water and sediment in such way to promote degradation: "it is inferred from the height of recent deposits that the river degraded to bedrock following capture and has not aggraded since, by more than a few tens of centimetres" (Nugent, 1986). Answering to a discussion promoted by Thomas et al.(1992), Nugent infers form alluvial record that the middle Zambezi, after the capture processes, aggraded by about 50 m then degraded to bedrock.

Nothing is know of the geology of the eastern end of the lower Zambezi basin beyond that published on the Mozambique Geological map (1968 and renewed on 1987; Orpen et al.,1989). For the upper part of these part of the basin (namely the Cahora Bassa region), some interesting evaluations, however, could be inferred from the results of the geological survey of the river basin conducted at the end of the '60ies by the Hidrotécnica Portuguesa

(contractor for the construction of the Cahora Bassa dam) with the purpose of determining the most appropriate site for the construction of the impoundment. The geological evolution of this zone could be summarized in three different phases: (i) formation of a very ancient basement complex which went through important metamorphic actions which gave charnockitin facies to the rock; (ii) long tectonic evolution which led to the formation of the depression of the Zambezi valley and which must related the gabbro dykes and lamprophyre dykes; (iii) exhumation of the ancient basement complex in relation to the formations filling that depression, still by the action of an epeirogenic tectonic associated to an important differential erosion, which resulted in the opening of the epigene gorge of Cahora Bassa, which went on along more the one excavation cycle. Overlapping with the Geological Map of Mozambique (ING, 1987), these permits, with a certain approximation, to better locate the widening of the Cahora Bassa gorges, characterized by the strong presence on the river bed of gabbro dykes and lamprophyre dykes, from some 35 km upstream the dam site, close to Chicoa, down to Marara, close to the confluence with Rio Mavuzi some 30 km upstream the capital city of Tete. The total widening of the gorges is approximately 140km long. The river bed in this stretch is cut in granite-gneiss, but (unfortunately) nothing is know about the characteristics of the deposits which can lie over it, so that we remain restricted to conjectures (Hidr. Portug.,1967). The confined rise of the rive bed that is localized just upstream from the dam site seems to be related to differential erosion of the bottom, in relation to the nature of the rocks, and to a certain accumulation of material which was torn away from the bottom which precedes that rise. The survey conducted by Hidrotecnica Portuguesa draws attention to the erosion of the river bed due to the dissipation of energy of the dams's flood discharge admitting as an hypothesis, even if the bedrock configuration downstream of the dam (dam foot) presents particularly favourable conditions for offering high resistance to the water action, that the excavation of the granite-gneiss under the lamprophyre-dyke could reach the tectonic zone, localized at approximately 25m deep. It is to be stressed, however, that this effect seems to be confined at the dam foots and, with this purpose, a downstream cofferdam had been placed. No more information are available on the lower part of the river, downstream of Cahora Bassa gorges. The Geological Map only suggests a firm deposit of sediment from Mepanda Uncua location down to Tete city, but without providing more information on the thickness of this layer.

3.3 THE LOWER ZAMBEZI

3.3.1 THE CAHORA BASSA DAM AND RESERVOIR

Commissioned in the 1959 by the Portuguese Government in Mozambique for promoting the economic development of the lower Zambezi valley through the exploitation of the hydropower potential of the river, the Cahora Bassa dam (where the words "Cahora Bassa" means "the work is finish" in Sena idiom and stems from workers who ferry goods and people for nearly 600 km to Cahora Bassa rapids from the Indian Ocean (Davies et al.,2000). With a storage capacity of 72.5 10^9 m^3, it is one of the most important river impoundments in Austral Africa. With a maximum height of 164 m, a crest length of 303 m, a total discharge capacity of about 14,000 m^3/s through five turbines (2260 m^3/s) and eight sluice gates (see Fig.3.4), it has a power installed of 2075 MW that is mostly sold to South Africa Republic (80%) and Zimbabwe (15%) (HCB, 2004). The 270 km long and 30 km wide reservoir commenced its filling on 5 December 1974 and completed it in approximately six months. The created lake has a reference level of 326 m a.s.l. and a surface area of 2660 km^2; the western end of the reservoir reaches the junction of the Mozambique, Zambia and Zimbabwe frontiers.

Figure 3.4: Cahora Bassa dam and reservoir (HCB,2002).

3.3.2 THE LOWER ZAMBEZI VALLEY

The lower Zambezi in Mozambique could be described as a complex physical system with four macro-scale river zones (Davies et al.,2000), comprising narrow gorges, a transitional zone, braided reaches, and a coastal distributary zone (Fig.3.5). The complexity is due to the regional geomorphology producing a series of distinct valley-floor-trough, river-floodplain associations. In the uplifted mountainous areas which contains the dam of Cahora Bassa, the channel is confined in a narrow wide valley with relatively high gradients. Boulder and bedrock outcrops and high stream energies dominate the instream environment of the gorge zone. Downstream of this zone the valley-floor-trough broadens to several kilometres. With further increases in the width of the valley-floor-trough and a decrease in river channels energies, large floodplains are constructed and a braided sand-river bed dominates. With progressive reduction in bed gradients, the braided stream gives way to a typically coastal distributary deltaic channel network where floodplain widths can reach several hundred kilometres (Davies et al.,2000). In Table (3.2) a summary of the morphological characteristics of the four macro-scale river zones is provided.

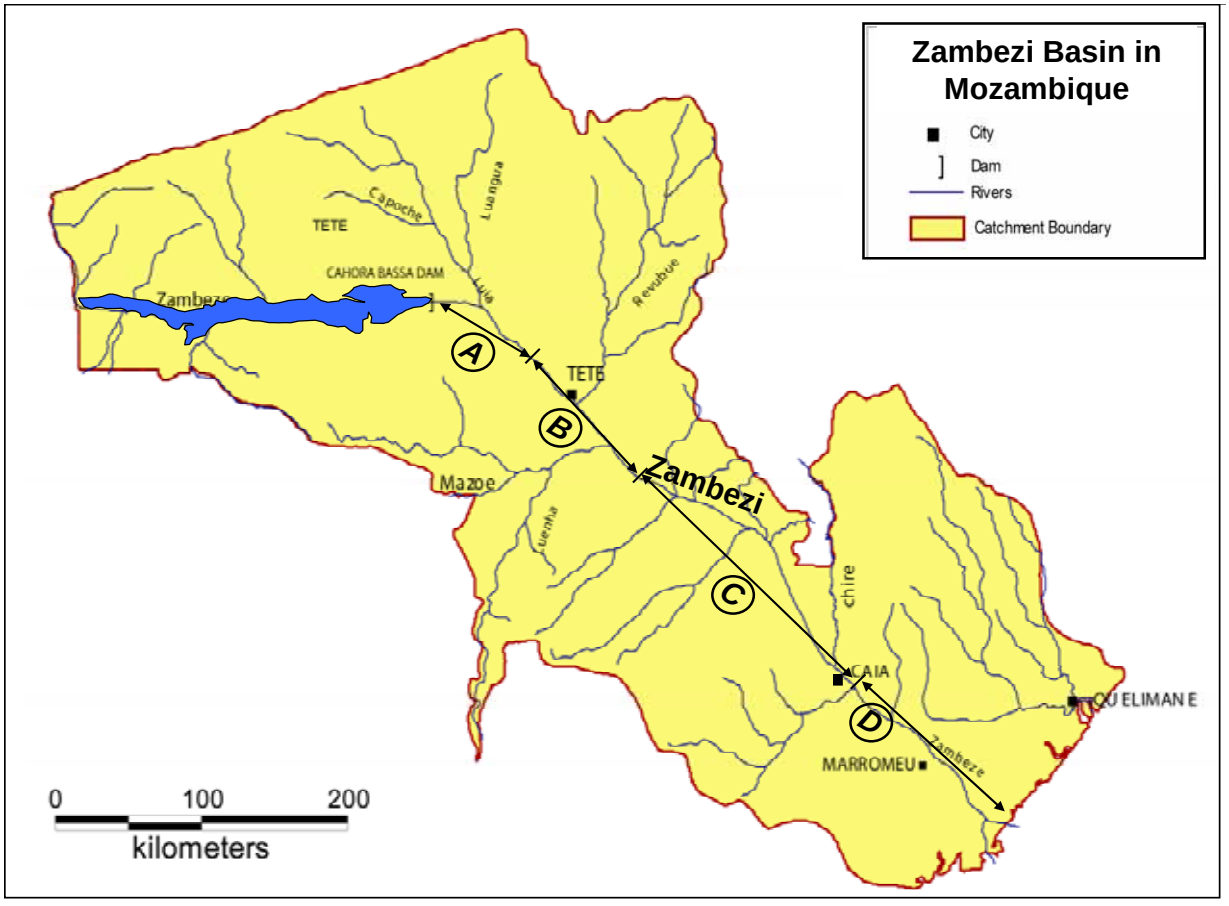

Figure 3.5: The Zambezi river basin in Mozambique, with the four macro-scale river zones. A: gorges zone; B: transitional zone; C: braided zone; D: distributary zone.

Zone	Area [km^2]	Length [km]	Slope	Width [m]
A	38,587	62	$9.26 \cdot 10^{-4}$	191
B	63,132	158	$5 \cdot 10^{-4}$	1090
C	191,159*	225	$1.83 \cdot 10^{-4}$	1301
D	16,273	155	$1.05 \cdot 10^{-4}$	1021

Table 3.2: Morphological parameters (average on the space) of the four macro-scale river zones. * 78,215 km^2 after Lake Niassa

There are many tributaries joining the Zambezi in Mozambique. The first one is the Luangwa river that flows from Luangwa-Malawi watershed in the north-east to south-east of Zambia into Zambezi river near the city of Zumbo, located at the upper reaches of the Cahora Bassa reservoir in Mozambique (Hayashi et al.,2005). The largest tributary is the Chire river, the catchment of witch is mainly in Tanzania and Malawi, and includes the massive Lake Niassa. Others on the left or northern bank include the Luia river and the Revubue river, and on the right or southern bank are the Luenha river which drains from the north-eastern Zimbabwe.

Average annual rainfall in Mozambique part of the basin varies from less than 600 mm around Tete, to over 1400 mm along the northern border with Malawi. In Mozambique most of the basin area has a sparse very sparse population, however the population along the river is significant. The provincial capital of Tete is on the south bank of the Zambezi. Many thousands also live on the lands of Inhamgoma triangle along the Chire River to east of Mutarara. The delta is very little populated and access is difficult. A large commercial sugar cane operation is located in Marromeu in the upper delta (SMEC, 2004).

3.3.3 MAIN EFFECTS OF THE CAHORA BASSA IMPOUNDMENT

Both in advanced and in Developing Countries, the combined water and sediment management in artificial reservoirs is becoming a very serious and urgent issue that still needs a very defined methodological approach (Tate et al.,2000; Scodanibbio et al.,2005). Apart from the impact of dams on river hydrology (changes in the timing, magnitude and frequency of low and high flows, see Magilligan et al.,2005) and ecology (Baxter, 1977), the trapping of sediments by the reservoirs may give place to a number of negative consequences: besides the progressive reduction of the storage capacity, reservoir sedimentation produces important modifications of river morphology upstream and downstream of the dams (Brandt, 2000; Wang et al.,2007; Kondolf,1997; Zaghloul, 2006; Zhou et al.,2004). Different management

strategies could be implemented in order to mitigate those effects, for example the regular releases of sediments from the reservoir to the river (either by flushing or by mechanical means, Di Silvio, 2004a), which requires, in any case, an adequate water flow to mobilize the released material along the watercourse. In many situations, however, for structural, hydrological and/or economical reasons, the release of sediment is not possible and the impact of the reservoir on river morphology downstream could be very strong.

Quite a number of reports and papers were published in the past concerning the impact of the Kariba and the Cahora Bassa reservoirs on the Zambezi river system. Many of them are mainly focused on the ecological effects (biodiversity, fisheries, wetlands, etc) of these two impoundments (Bowmaker,1960; Attwell,1970; Hall et al.,1977; Du Toit,1984; Beilfuss et al.,1999; by the others), while very few addressed the problem of the morphological changes correlated to sediment and water loads altered by the presence of the two reservoirs that, as affirms Beilfuss et al. in 1999, "capture most of the sediment load of the upper and middle Zambezi systems, releasing clear, hypolimnetic waters downstream"; (Guy, 1980; Suschka et al.,1986; Beilfuss et al.,1999; Davies et al.,2000).

3.3.3.1 Siltation of the reservoir

Due to the lack of systematic quantitative studies of sediment transport rates, bathymetry measurement and monitoring sampling programme, is very hard to evaluate this phenomena. No quantitative estimate of the rate of sediment accumulation was published in the numerous reports which formed the basis for the design of the project (Bolton, 1984). Even during the operational period, no monitoring of silt accumulation has been (apparently?) carried on. A certain indication from the project design, however, is the relative small "dead" capacity chosen for the Cahora Bassa reservoir: 13 10^9 m^3 (HCB, 2004). Another useful information is that 15% of the Cahora Bassa's water comes from the undammed river Luangwa, which is known to carry a high silt load (the turbidity was measured in 36 ppm at the confluence with Zambezi, close to the CB reservoir (Hayashiet al., 2005), and a further 25% comes from other undammed rivers mainly off the Zimbabwean plateau (Bolton, 1978). Making different assumptions on the sediment production of the basin, the trapping capacity of the upstream Kariba reservoir and considering the sediment concentration occasionally measured on the tributaries of Cahora Bassa, Bolton (1984) estimated the total rate of sediment input to Lake Cahora Bassa in the range 20 to 200 x 10^6 m^3/year, namely with an uncertainty of 10 times. A more precise evaluation will be made in Sect.(3.5.5).

3.3.3.2 Changes in flow pattern

An in-depth study of the hydrological change in the Zambezi river system, in particular with reference to the delta environment, has been carried out by Beilfuss & Dos Santos in 2001, as part of a comprehensive program for the integrated development and ecological restoration of the lower Zambezi valley. It is not in the objectives of the present study to produce an extensive quantitative evaluation of the modifications in the flow pattern after the construction of Kariba (1958) and Cahora Bassa dam (1974). In any case, it is unquestionable fact that the damming of both Kariba and Cahora Bassa gorge has considerably changed the hydrological cycle of high and low flow.

From the data catalogue provided by DNA (National Directorate of Water in Maputo), that list several gauging station all along the Zambezi basin, only one station is still operating and could provide historical reliable discharge data. Tete gauging station E320, located next to the only bridge on the entire lower Zambezi some 135 Km downstream the dam, after the confluence of Luia river and just before the one with Revubue river, provides daily average discharge data from 1951. Data collected at this station until 2003, indicate that the presence of the two impoundments regulates the pattern of the monthly runoff, strongly augmenting its the minimum value (in September-October) and decreasing its maximum value (in February-March). As consequence the monthly runoff variation has a much lower amplitude and the discharges are more distributed all along the year changing the normal seasonal flow pattern, (Fig.3.6 and Table 3.3).

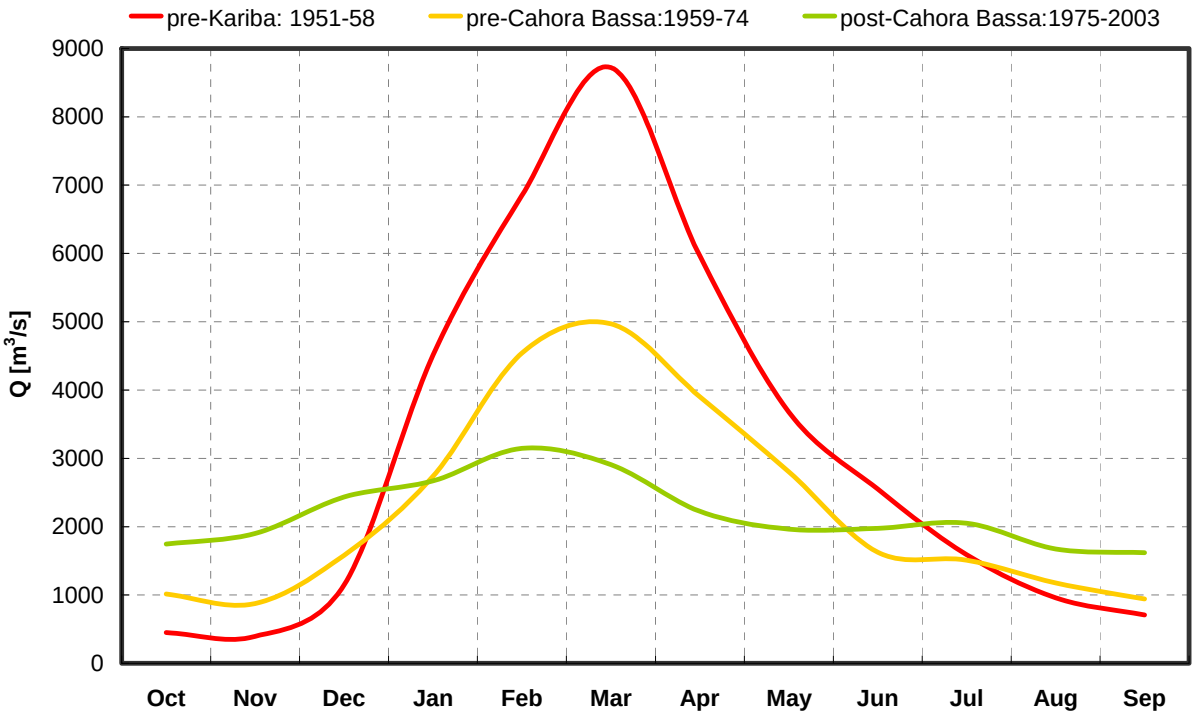

Figure 3.6: Monthly Average Discharge at Tete gauging station E320

	1951-1958	1959-1974	1975-2003
Minimum monthly average runoff [10^6 m^3]	1021	2261	4195
Maximum monthly average runoff [10^6 m^3]	23'360	13'310	7789
Difference [10^6 m^3]	22'338	11'049	3593
Mean value [10^6 m^3]	8161	6025	5748
Variance [10^6 m^3]	6995	3594	1181
January-March runoff [10^6 m^3], (% of the total annual runoff)	52'011 (53.1%)	31'629 (43.7%)	22'550 (32.7%)

Table 3.3: Variation of monthly average runoff before Kariba dam (1951-58), after Kariba and before Cahora Bassa dam (1959-1974) and after the construction of Cahora Bassa dam (1975-2003), Data derived from DNA – National Directorate of Water – Maputo, Mozambique.

3.3.3.3 Morphological changes

Very little information and measurement is available on sediment transport and river bed characteristics, but some considerations are possible. Suschka et al. (1986), Beilfuss et al., (1999) and Davies et al. (2000) tried to evaluate the morphological changes of the lower Zambezi river after the conclusion of Cahora Bassa dam, but without getting at the same outcome. In fact, while Suschka et al., in 1986 (ten years after the conclusion of the dam) affirm that "no evident changes in river bed configuration through aggradation or degradation have been measured and a much larger period will be necessary to find noticeable effects", Beilfuss in 1999 affirms that "in 1996 we observed the lower Zambezi river more than 2 m below bankful discharge in the delta during the period when peak floods normally occurred

(…); although there are no data on erosion and sedimentation on lower Zambezi, the widespread coastline erosion and mangrove dieback (perhaps 40%) in the delta may be resulting in part from the reduced sediment load"; Davies in 2000 emphasizes "the dramatic changes in the morphology of the river floodplain system". In their opinion, the constancy of flow imposed by Cahora Bassa dam (..) has transformed a flood-pulse driven river ecosystem, floodplain and coastal zone, into a series of confined channels. The removal of the sediment stores in the gorge zone (erosion), the incision of main flow channel with the stabilization of braid and bars in the transitional zone, the dominance of a single main channel that incises and conveys the majority of flow in the braided zone; the reduction of the Zambezi delta wetland mangrove swamp area and the increase the salt-water intrusion have been attributed to the impoundments (Chenje, 2000).

As observed in the introduction, in fact, the reduction of the sediment load and the curtailment of high flow tend to produce opposite effects which propagate in space after the construction of the dam. Unfortunately, at the moment no systematic evaluation of the morphological changes on the lower Zambezi due to the impact of both Kariba and Cahora Bassa dam, nor of the sediment dynamics all along the waterflow has been done. A numerical approach to these problems seems at the moment the only viable way of analysis.

3.4 MORPHOLOGICAL MODELS

Conventional morphological models, even if just one-dimensional, are too cumbersome for very long simulations (years, decades, centuries) at basin scale, especially if the river watershed is very large as in the case of the Zambezi river. Acceptable simplifications can be introduced in the one-dimensional equations that describe the waterflow (De St.Venant equations) along the hydrographic network. By contrast, the sediment movement at the erosion/deposition process, should accurately be described by considering a non-uniform material. At the basin scale, in fact, the sediment grainsize may vary over various orders of magnitude (from fine silt to boulders), while the transport in a given cross section presents a quite extended composition (including the so-called "wash-load", coming in suspension from distant slopes of the watershed). The "approximate" model (Di Silvio et al., 1989) applied in this chapter has been widely presented in Sect.(2.2).

3.5 MODEL IMPLEMENTATION

The morphological model based on the local uniform-flow hypothesis has been applied to the lower Zambezi river between the city of Zumbo, just upstream of the present reservoir of Cahora Bassa, down to the Indian Ocean, to investigate the morphological evolution of this river in the last century. The model simulates the hydrological variability of Q_{eq} (see Sect. 3.5.2) from 1907 up to 2000, both natural and due to the construction of Kariba dam (1958) and Cahora Bassa dam (1975). For the grainsize distribution (Sect. 3.5.3), have been utilized the data measured, along the main course and tributaries, by the Portuguese administration in 1963 (Brigada de Engenharia Hidráulica). For the initial topography of the Zambezi (Sect. 3.5.4), it has been used the survey of the reservoir site in 1963, as well the river widths extracted from the LANDSAT 7 images of 2002, while the river bottom bathymetry outside the reservoir has been reconstructed from the water slope configuration provided by the Digital Elevation Model HYDRO 1K (2000), (see Fig. 3.7). The few data regarding the sediment transport have been aggregated to calibrate the transport formula and to evaluate the input of sediments (Sect. 3.5.5).

As all the available data and information mentioned above are not chronologically synchronized, the initial river conditions (1907) has been reconstructed by means of the model itself, through an homogenizing data processes that, under adequate hypothesis, try to simulate and to reproduce the past: a sort of time-machine, in fact (Sect 3.5.9).

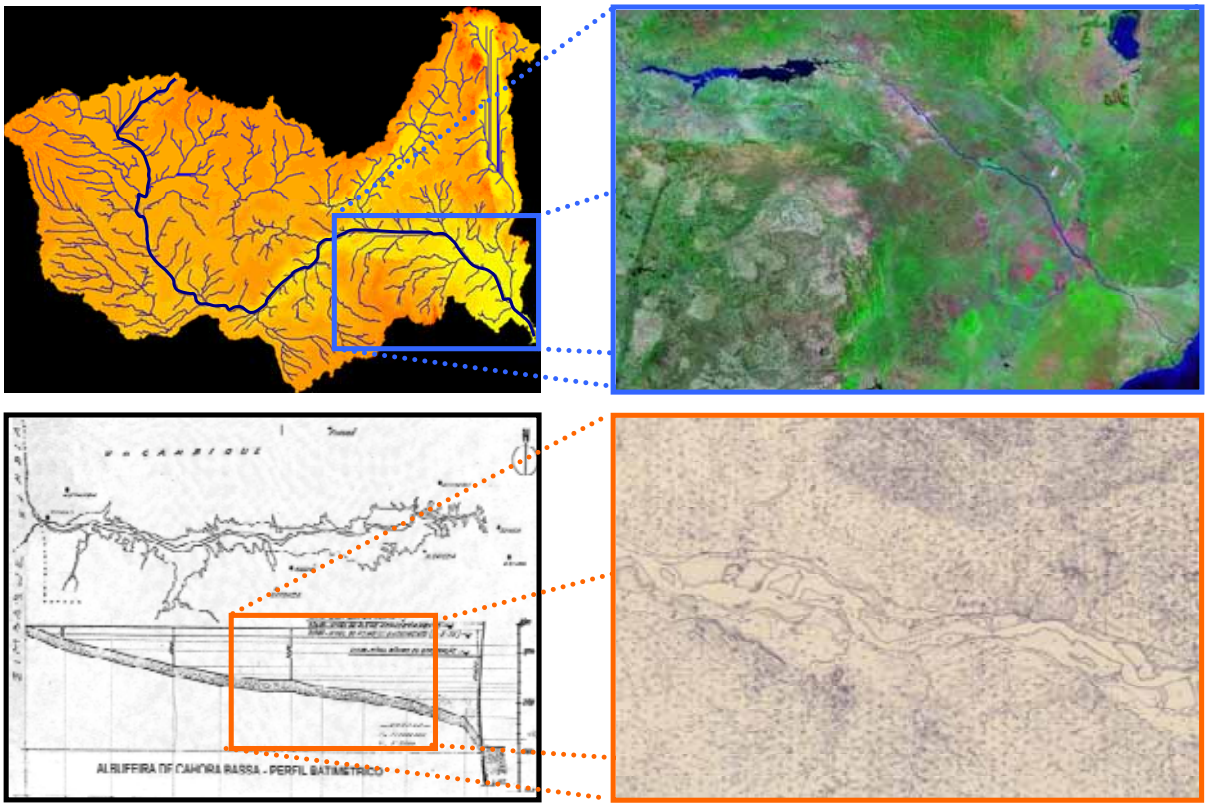

Figure 3.7: Digital Elevation Model (HYDRO1k, 2000, top left); satellite image of the Zambezi river basin in Mozambique (LANDSAT 7 2002, top right); bathymetry of the Cahora Bassa reservoir (HCB, 1963, bottom left); topography of the river prior to the submersion (1963, bottom right).

3.5.1 DATA NEEDS AND PROCESSING

As already mentioned, the main constraint for a reliable and realistic application of the model, is represented by the scanty and often uncertain measurements. These circumstances has obliged to complex operations of data processing to integrate, interpolate and extrapolate in space and time the few data available. In fact, due to a 17 years long civil war and to poor socio-economical conditions, the hydrometric monitoring network of the Mozambican part of the basin is very scarce and, apart from very few specific cases, no long-historical and systematic measures of flow, sediment transport and reservoir sedimentation measurements are available (Beilfuss et al., 1999). The Zambezi river basin is furthermore extended in eight different countries and no single authority has a complete database for all the catchment. This situation, however, is common to many rivers, especially (but not only) of Developing Countries (Sect.1.6).

3.5.2 HYDROLOGICAL DATA

For the application of the morphological model at one-year time-step, only the *equivalent* value of the river discharge is required, namely the constant water discharge Q_{eq} that annually convey the yearly sediment yield V_s.

The Cahora Bassa reservoir water balance has been implemented using monthly average inflow data from 1907 to 2003 provided by HCB (Hidroeléctrica de Cahora Bassa, the owner of the Cahora Bassa impoundment), while Beilfuss and Ara Zambeze (the Lower Zambezi Mozambican Authority) provide dam's daily discharge data from 1976 to 2003.

With reference to eq.(2.9):

$$P = M \cdot Q^m \tag{3.1}$$

we assume that the morphological quantities included in the parameter M do not substantially change during one year, while the duration curve of the water discharge is:

$$Q(t) = Q_0 \cdot \exp\left(\gamma \frac{t}{T_a}\right) \tag{3.2}$$

with T_a = 1 year. If γ is quite larger than 1, the yearly sediment yield is:

$$V_s = \int_{T_a} Q_s dt = M \cdot \frac{1}{m} \cdot Q_0^{m-1} \cdot V \tag{3.3}$$

with Q_0 maximum annual peak discharge and V total annual runoff, and the *equivalent* water discharge is:

$$Q_{eq} = \left(\frac{P}{M}\right)^{1/m} = \left(\frac{V_s}{M \cdot T_a}\right)^{1/m} = \left(\frac{Q_0^{m-1} \cdot Q_{med}}{m}\right)^{1/m} \tag{3.4}$$

For the computation of the input *equivalent* discharge, the monthly inflow measured at Cahora Bassa has been used from 1907 to 1975 (closure of the dam), while the dam's release

series has been used from 1976 to 2000, for the computation of the annul value (for each *i*-year) of $Q_{eq,i}$.

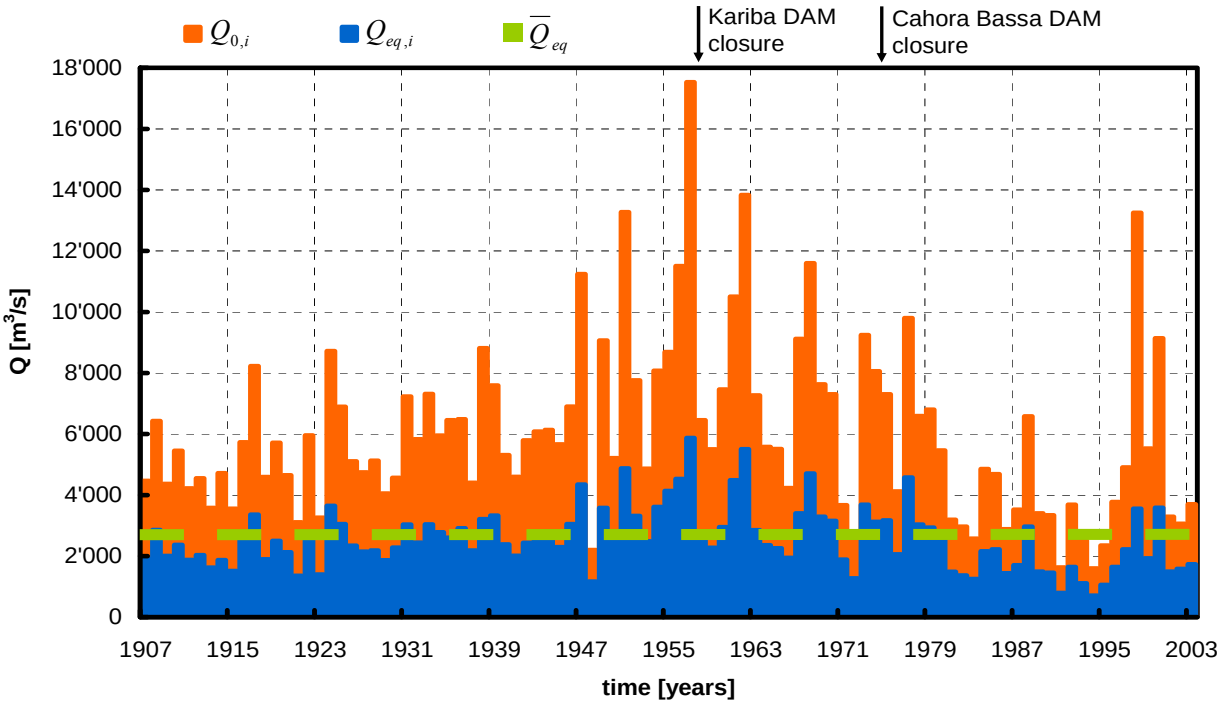

Figure 3.8: The maximum annual peak discharge $Q_{0,i}$, the respective value of the equivalent discharge $Q_{eq,i}$ and the average equivalent discharge $\overline{Q}_{eq}$, at the upstream boundary condition of the model.

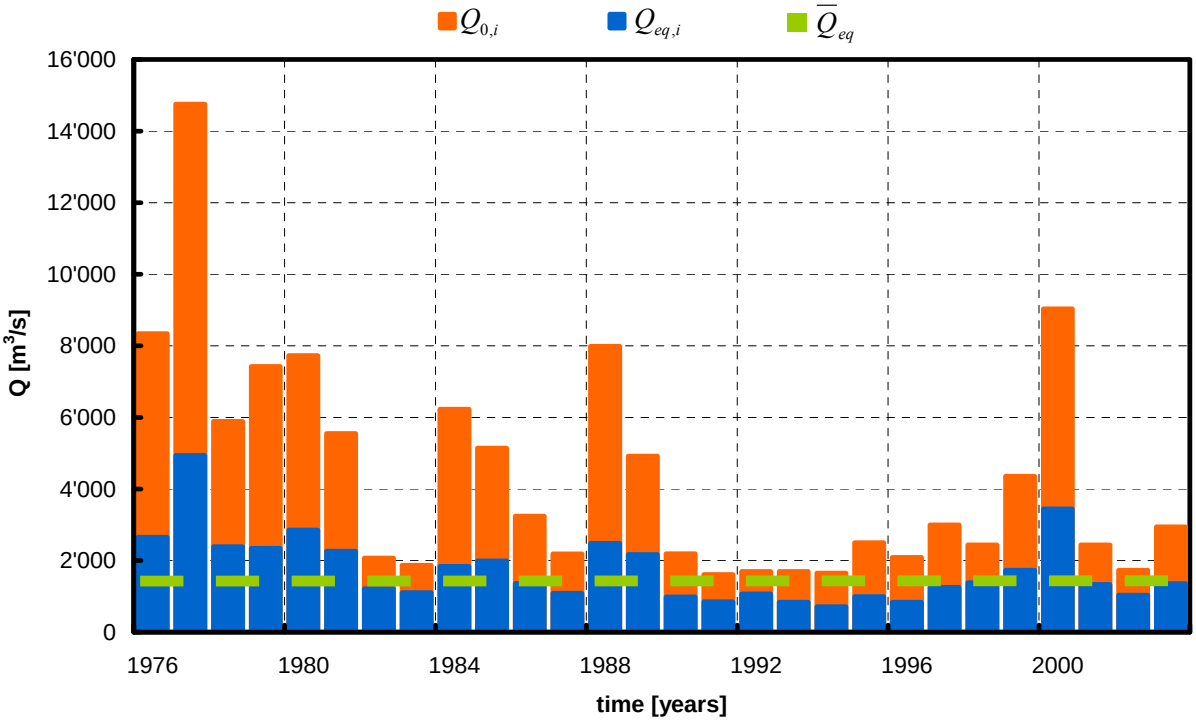

Figure 3.9: Maximum annual peak discharge $Q_{0,i}$, the respective value of the equivalent discharge $Q_{eq,i}$ and the average equivalent discharge $\overline{Q}_{eq}$ computed for the Cahora Bassa dam discharge series, from 1976 to 2003.

As regards the main tributaries of Zambezi (namely: Luangwa, just upstream of the reservoir, and Luia, Revubue, Luenha and Chire downstream of the dam), the respective value of the averaged $\overline{Q}_{eq}^{T}$ (where the space of averaging varies from river to river, see Table 3.4) have been derived from the mean monthly and mean maximum runoff series generated by Beilfuss et al. (2001), that revised and elaborated a great amount of data series collected from previous studies, but do not provides historical series. The annual value (for the *i*-year, from 1907 to 2003, permitting a complete overlapping with the hydrological series available for the main Zambezi system) of the $Q_{eq,i}^{T}$ of for the five tributaries are derived from $\overline{Q}_{eq}^{T}$, assuming the following proportion with the corresponding values of Zambezi ($Q_{eq,i}^{Z}$ and $\overline{Q}_{eq}^{Z}$)

$$Q_{eq,i}^{T} = \frac{Q_{eq,i}^{Z}}{\overline{Q}_{eq}^{Z}} \cdot \overline{Q}_{eq}^{T} \tag{3.5}$$

River	$\overline{Q}_{eq}^{Z,T}$ [m^3/s]	period of time
Zambezi - Cahora Bassa reservoir inflow	2554	1907 – 2003
Zambezi - Cahora Bassa dam outflow	1733	1976 – 2003
Luangwa	803	1955 - 1996
Luia	200	1975 – 2001
Revubue	158	1955 – 2000
Luenha	282	1960 - 1971
Chire	470	1952 - 1958

Table 3.4: $\overline{Q}_{eq}^{Z,T}$ values for Zambezi river (^{Z}) and main tributaries (^{T}), averaged on the specific period of time.

3.5.3 GRANULOMETRIC DATA

The samples have been taken from Zumbo to the Ocean, about every 15 km, and include a large part of the delta coastal profile and the final stretch of the tributaries (see Fig.3.10). The grainsize total extension has been splitted in four classes, as our morphological model requires, each one represented by the relative median diameter d_i (d_1=0.06·10^{-3} m; d_2=0.24·10^{-3} m; d_3=0.94·10^{-3} m; d_4=4.24·10^{-3} m). A representation of the initial bottom composition along the river is given in Fig. (3.11).

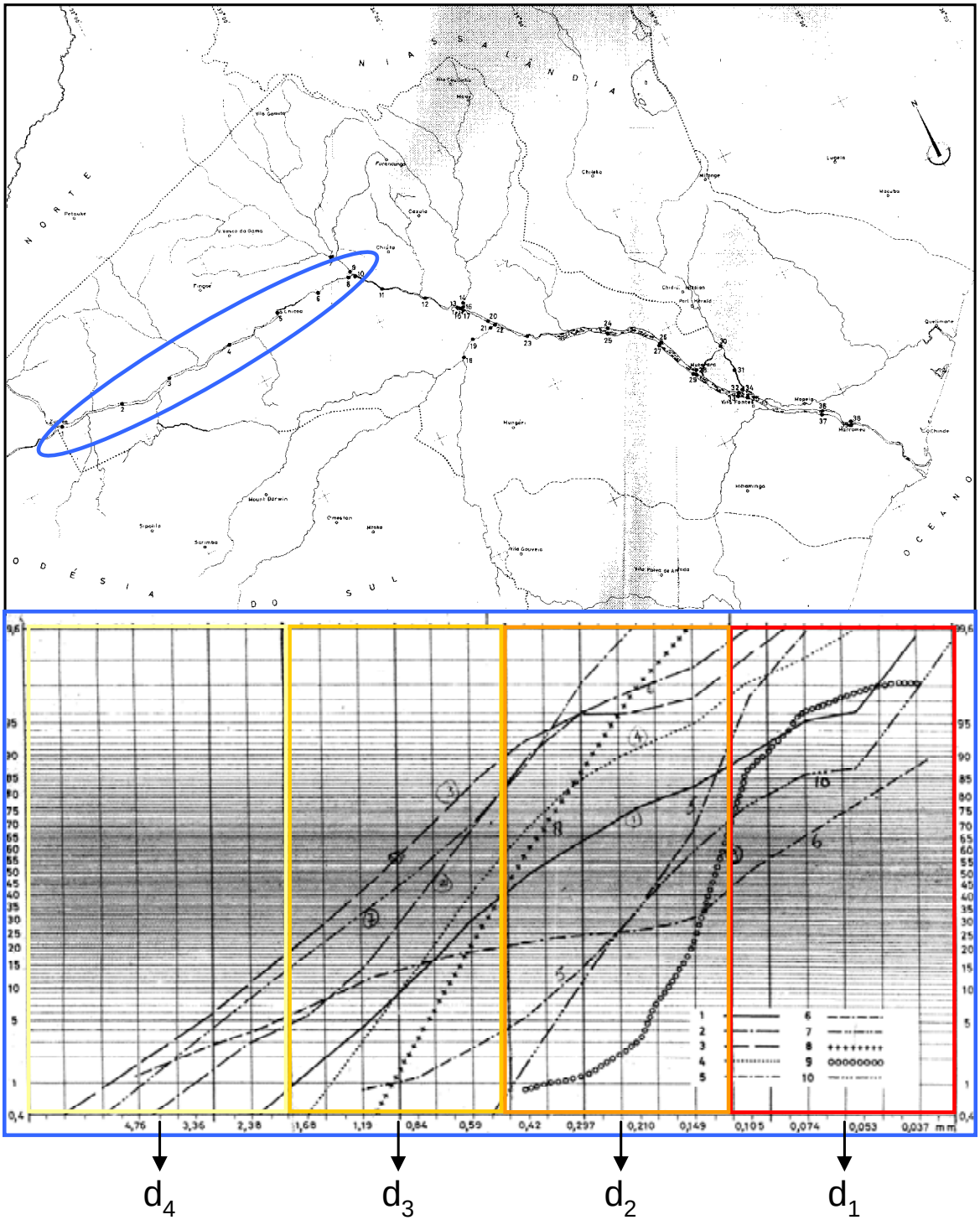

Figure 3.10: Localization of the granulometric survey made by MFPZ between Zumbo and the confluence with the Luia river (down, underline in blue), in 1962-64 (up); and the granulometric curves splitted in four granulometric classes, each one represented by the mean diameter d_i.

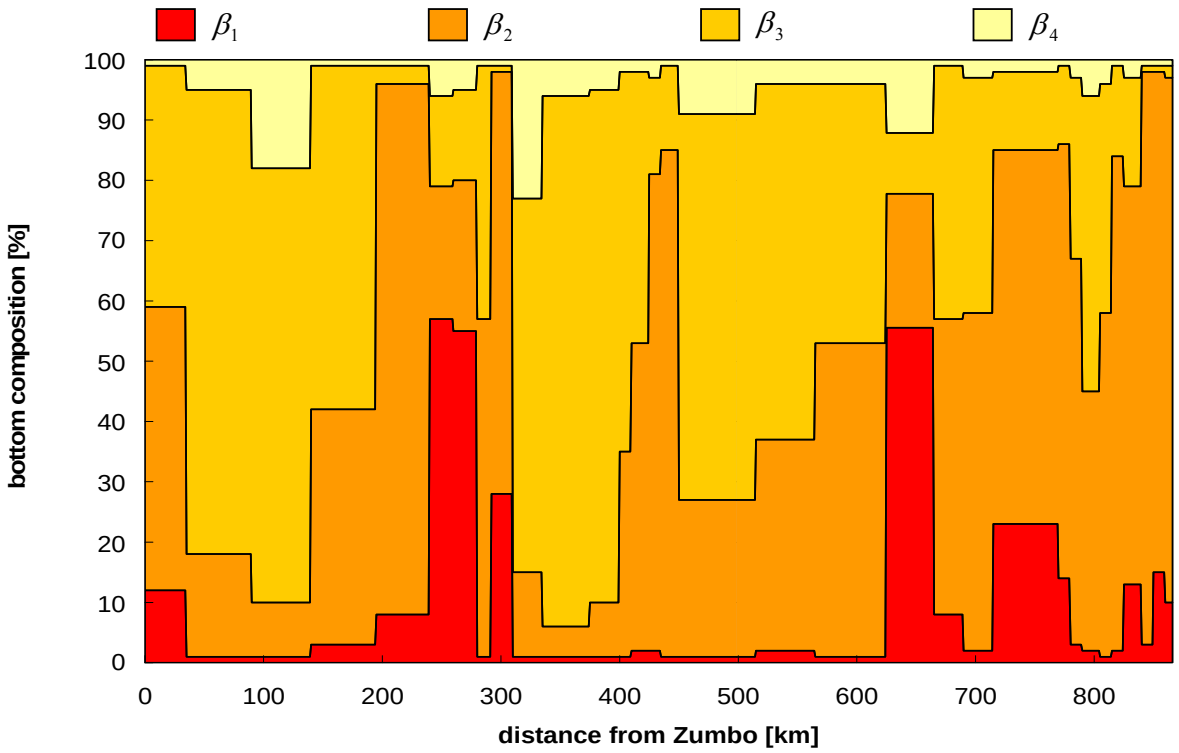

Figure 3.11: Percentage of presence in the bottom composition of the four granulometric classes selected (initial conditions).

3.5.4 TOPOGRAPHIC DATA

The basic river geometrical configuration (width and water slope of the main channel, as well as the ones of the main tributaries) has been reconstructed using different tools, depending on the reach considered, namely discriminating the reach of Zambezi river presently submerged by the Cahora Bassa reservoir - 260 km long - and the rest of the Zambezi river downstream the dam, down to the Indian Ocean, some 600 km long. For the first reach we used the ancient topographic maps, the only available before the inundation of the valley (HCB, 2004), for the rest of the river we used the LANDSAT 7 images and the Digital Elevation Model (DEM) HYDRO1k Africa. The ancient maps have a quite coarse scale (1:50'000), but still acceptable for a preliminary cartographic survey at the base resolution of 1km.

For details on the procedure used for reconstructing the river bathymetry from the averaged water slope configuration, see Sect.(2.3.1). The bottom profile configuration, indicating the input from the Zambezi and the various tributaries, as well as the localization of the Cahora Bassa reservoir, gorges and dam is so given in Fig.(3.12).

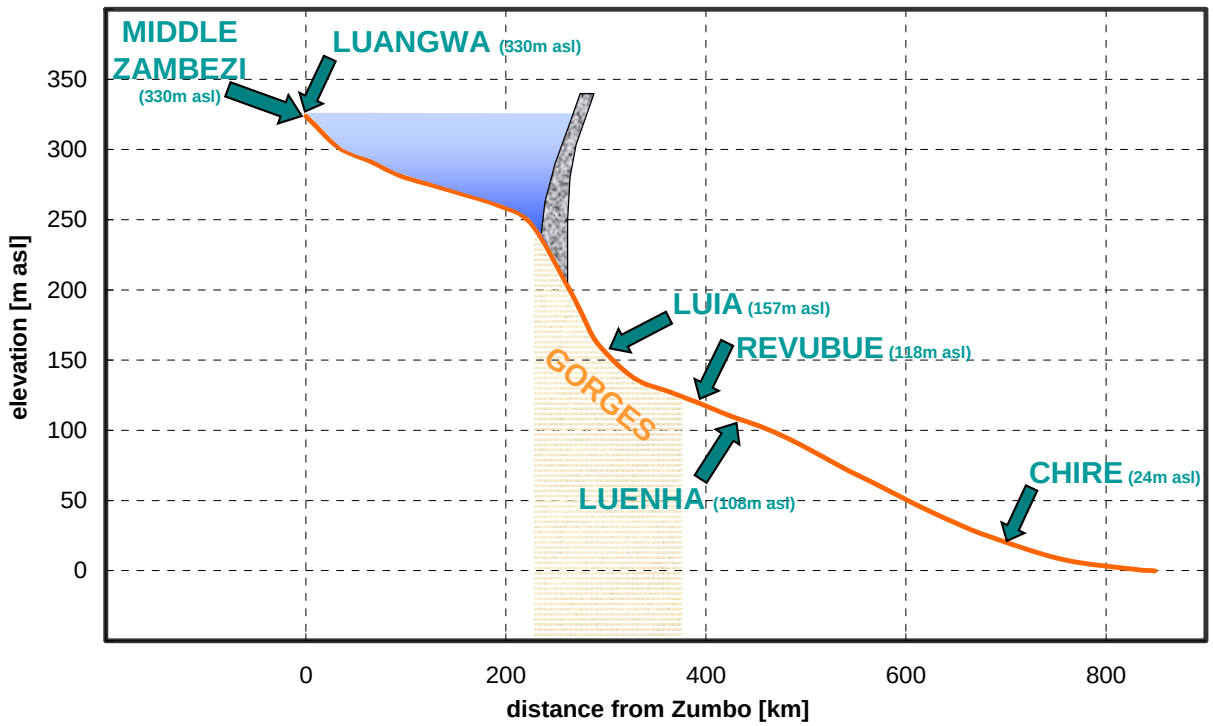

Figure 3.12:The lower Zambezi river longitudinal profile with its major tributaries in Mozambique, downstream the city of Zumbo. The reservoir of Cahora Bassa is also indicated.

3.5.5 SEDIMENT TRANSPORT DATA

As far as solid transport on the lower Zambezi river is concerned, as already remarked, the considerable lack of adequate information makes it impossible to give this subject a rigorous treatment (Bolton, 1983). In fact, the annual sediment transport entering the lower Zambezi from the main river upstream of the reservoir, as well as from the four main tributaries, is probably the most uncertain among the data necessary to run the 1-D model and to describe the erosion/deposition phenomena involved in the morphological development of the river basin (Suschka et al., 1986; Davies et al., 2000). However, a tentative evaluation of the total sediment yield (average value over years) at the upstream boundary of the Cahora Bassa reservoir (city of Zumbo) has been done through the sediment transport formula (eq.2.9). The formula itself has been calibrated by using the values of the suspended sediment survey made by Hall et al. in 1977, as well as the suspended sediments and bed load sampling made by the Portuguese administration (BEH-MFPZ, 1964).

A turbidity survey made by Hall et al.(1977) has been carried out during the biennium 1973-75 on the main Zambezi river and on the Luangwa river, which drains from Zambian plateau into the Zambezi River just upstream of the Cahora Bassa reservoir and seems to be the responsible of the bulk of sediment load that flows into the reservoir. These results are of

particular interest because they give sediment concentrations measured at a series of stations along the lower Zambezi from just upstream of the Luangwa confluence to a point in the delta. No details of the single measurements were published but only the maximum and minimum value of suspended sediment concentration in the main river and in some of the tributaries. As would expected the data show clear differences between sediment concentrations in the wet and dry seasons. The principal difficulties in interpreting and applying these results lie in shortcomings in the sampling method used, which provided no measurement of particle size distribution and would, in any case, have trapped only wash-load particles. Since samples were taken on only one occasion each month, it is not possible to relate the results to the pattern of river discharge (Bolton, 1983). However, assuming that the maximum value of sediment concentration occurs during the wet season (roughly from January to April), the minimum value during the dry season (from May to December), and coupling these values with the mean monthly equivalent discharge for the same stretch , we finally obtain an averaged value of 28.6 10^6 m^3/year of total sediment load as input to the lower Zambezi (for details of the calculation see Table 1.A, in Appendix A).

Another quite short time series of sediment transport measurements (in terms of tons per day), solid transport by both suspension (28 measures) and bed load (27 measures), has been done in the triennium 1962-64 by the former Portuguese administration (BEH-MFPZ, 1964) in the delta zone near the city of Marromeu. The survey has been carried on using two different turbidity samplers “Magistrato delle Acque” and “Neyrpic” for the suspended load, and a “BTMA Arnhem” sampler for the bed load. The outcomes point out the substantial difference between the order of magnitude of the two modes of transport: the bed load results, in fact, always less then 1% of the suspended load which seems to represent, in this way, the predominant mechanism, at least in the last stretch of the river. Moreover, considering that these two different series were not always simultaneous (only 9 measures, over 28), it is substantially impracticable the joint use of both series in the calibration procedure. The bedload data have therefore been neglected, taking into consideration only the suspended load as indicator of the total transport. It is important to note, however, that coupled with these measures, also a water discharge survey program was implemented at this gauging station. Table (3.5) provides the values utilized for the calibration procedure.

MFPZ Sect. 158, Marromeu [km785]		
Date	**Suspended load [m^3/s]**	**Water discharge [m^3/s]**
26.08.62	0.151	1900
23.09.62	0.133	1650
12.10.62	0.095	1500
19.12.62	0.762	3000
02.02.63	4.360	7700
03.02.63	3.966	7725
04.02.63	4.970	8020
06.02.63	5.876	7875
14.02.63	9.192	11’375
15.02.63	7.938	11’500
14.03.63	10.772	12’400
25.03.63	12.433	12’575
04.04.63	12.768	12’950
15.04.63	5.588	8900
21.06.63	0.533	3175
27.09.63	0.146	1575
29.10.63	2.598	4725
07.12.63	3.771	5775
02.01.64	3.621	n.d.
06.01.64	3.483	6175
15.01.64	6.713	8175
16.01.64	6.689	7700
08.02.64	2.198	n.d.
13.02.64	3.692	n.d.
15.02.64	3.575	5750
26.02.64	3.092	n.d.
20.08.64	0.083	1425
03.09.64	0.081	1350

Table 3.5: Series of suspended sediment load and water discharge measurements made by BEH-MFPZ, 1964.

3.5.6 CALIBRATION OF THE TRANSPORT FORMULA

The calibration of eq.(2.9) basically consists on the estimation of the coefficient α_T and the exponents *m, n, e, f, s* with respects to the measured and available values of $\underline{Q}$, $\underline{B}$, $\underline{i}$, $\underline{d_k}$, β_k and $\underline{P}$.

Since no morphological and geometrical information are available to characterize the river section at the Marromeu gauging station (in terms of bottom slope, section width and bottom composition) and in order to fit the solid transport formula (eq.2.9) with the measurements

executed in this location, we can only relate the total sediment load P (not divided in different classes P_k) to the water discharge Q through a power law relation (Syvitski et al., 2000):

$$\underline{P} = \sum_{k=1}^{N} \underline{P}_k = \sum_{k=1}^{N} \alpha_T \cdot \underline{\beta}_k \cdot \xi_k \frac{\underline{Q}^m \underline{j}^n}{\underline{B}^e d_k^f} = \alpha_T \frac{\underline{Q}^m \underline{j}^n}{\underline{B}^e} \sum_{k=1}^{N} \frac{\underline{\beta}_k \cdot \xi_k}{d_k^f} = M \cdot \underline{Q}^m \quad (3.6)$$

where the coefficient M includes in itself all the morphological and geometrical parameters ($\underline{j}$,$\underline{B}$, $\underline{d}_k$, $\underline{\beta}_k$), assumed to have remained constant during the biennium 1962-64.

The fitting procedure consists in the data interpolation with a non-linear least squares estimation method (Gavin, 1990; Ricci, 2006). This method, in fact, searches the best values for the vector of parameters φ (which consists, in our case, on the parameters m and M of eq.3.6) on minimizing the sum of residuals θ between the computed value $\underline{P}_i$ and the measurements y_i ($i=1,2,...n$, where n is the number of measures):

$$\underline{P}_i = M \cdot \underline{Q}_i^{\,m} = f(\underline{Q}_i, \varphi) \quad (3.7)$$

$$\vartheta = \sum_{i=1}^{n} \left[y_i - f(\underline{Q}_i, \varphi) \right]^2 = \min \quad (3.8)$$

The fitting is quite well (see Fig.3.14), and the value of the vector of parameters is the follow:

$\underline{P} = M\,Q^m$		
M	m	R
$1.69\ 10^{-6}$	1.67	0.98

Table 3.6: Results of the fitting procedure, determination of the parameters M and m that characterizes the formula of solid transport (eq.3.6).

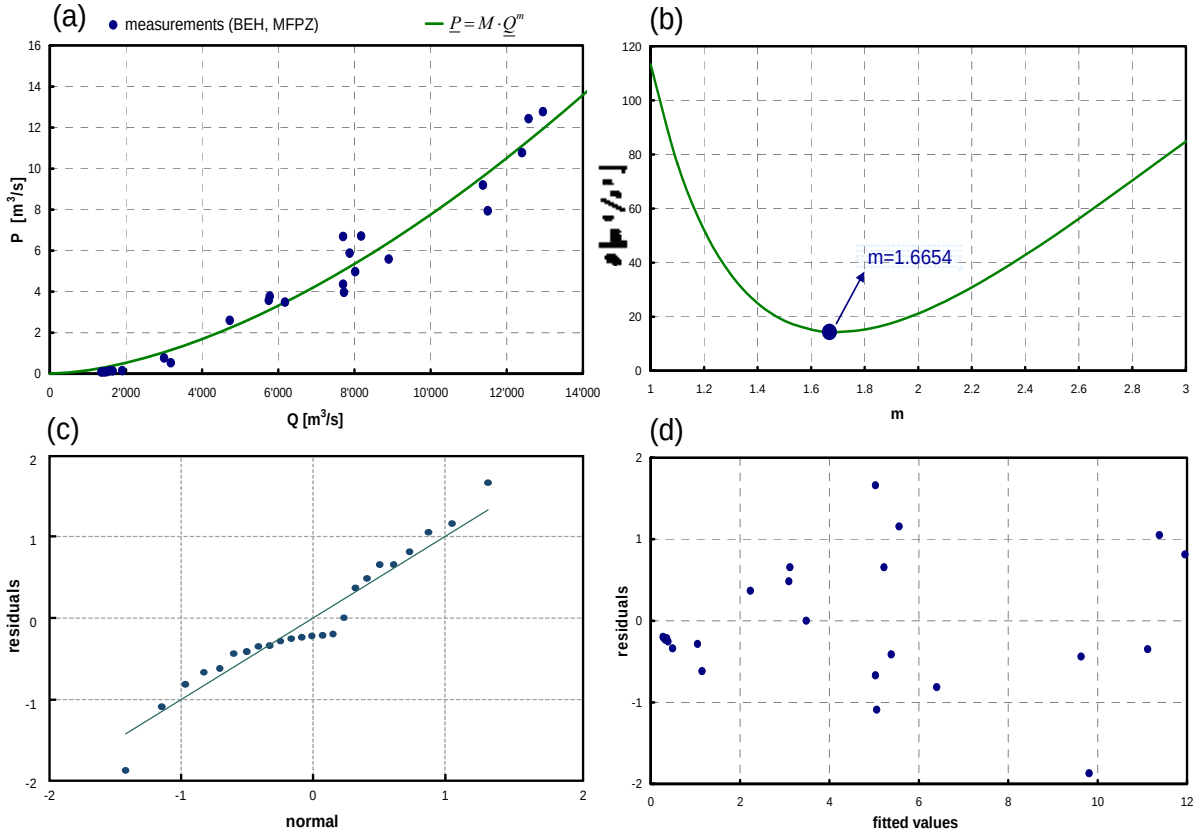

Figure 3.13: (a) fitting of the suspended sediment load and water discharge measurements with a power law curve (eq.3.6), with a non-linear least squares estimation method; (b) estimation of vector of parameters φ (the value of exponent m is plotted) by minimization of the sum of residuals ε between the estimated value $f(Q_i,\varphi)$ and the measurements y_i (eq.3.8); (c) *qq-plot*; (d) plot of residuals vs fitted values (Ricci, 2006).

The good quality of the fitting is demonstrated by the value of R obtained (0.98), where R is a measure of the "tightness" of the data points about the fitted line. An other confirmation comes from the *q-q plot* and the plot of residuals that are both statistical graphical techniques. The *q-q plot* is normally used to determine if two data sets come from populations with a common distribution. If the two sets come from a population with the same distribution the points should fall approximately along a 45 degree reference line, as Fig.(3.13, c) confirms. In this case we plotted the residuals's quantiles vs the standardized normal residuals to check if the assumption of normality is reasonable (residuals have to be normally distributed with average zero (white noise) and our test shows that the residuals are normally distributed with a level of (good) significance of 0.05). The plot of the residuals vs fitted values is used to detect any other relationship between the residuals and the fitted values, if the residuals follow a specific trend rather than a random scatter (Fig.3.13, d).

This first-step procedure permits to characterize the "power-law" version of solid transport formula (eq.3.6) through the parameters M and m. The others coefficients of eq.(2.9), namely

n, e, f are not independent ones but mutually related to *m* through the relations reported in Table (3.7) (Di Silvio, 2004b). The exponent *s* of eq.(2.7), expressing the magnitude of the hiding-exposure phenomena, has been assumed, for sake of simplification, equal to zero due to the relative limited amplitude of the grainsize composition extension of the bed (the ratio between the minimum and maximum value of the bottom grainsize diameter d_k is, in our case, 10^{-2}), coupled with thickness of the local maximum diameter d_k measured on the lower Zambezi by BEH-MFPZ (about 5mm). With these values, the hiding-exposure phenomena, namely the effect for each grainsize class *k* which reduces the larger mobility of smaller particles and vice-versa, seems to be negligible for the lower Zambezi river.

The second step of the calibration procedure consists on the determination of the coefficient α_T of eq.(2.9) which can not be computed with the Marromeu solid discharge survey, previously used, due to lack of precise hydrological and morphological data on that section, that prevents from applying this equation in the integral form (eq.2.9). The coefficient α_T, instead, has been determined using the total sediment load estimates with the data collected by Hall et al.(1977) close to the confluence between the Zambezi and the Luangwa river (Sect. 3.5.5), where hydrological and morphological data were less uncertain. In fact, by fixing the value of $V_s = 28.6\ 10^6$ m^3/year (and therefore *P*) as the annual suspended sediment load in input to the Cahora Bassa reservoir, where the morphological and hydrological configuration is known (in terms of bottom slope $\underline{j}$, section width $\underline{B}$, bottom grainsize composition ($\underline{\beta}_k$ and $\underline{d}_k$) and average equivalent discharge $\overline{Q}_{eq}$), the coefficient α_T has been computed simply applying eq.(2.9). In Table 3.7, the solid transport model (eq.2.9) parameters obtained with the fitting method presented above, are reported..

$\underline{P} = \sum_{k=1}^{N} \underline{P}_k = \sum_{k=1}^{N} \alpha_T \cdot \underline{\beta}_k \cdot \xi_k \frac{\underline{\underline{Q}}^m \underline{\underline{j}}^n}{\underline{B}^e d_k^f}$	
m	1.67
n = m	1.67
e = m-1	0.67
F = 3/2 (m-1)	1.00
s	0.00
α_T	0.0071

Table 3.7: Transport formula (eq.9) parameters obtained with the fitting method.

3.5.7 RIVER'S SCHEMATIZATION

With reference to the notion of *morphological box* in morphodynamic quasi-stationary equilibrium conditions (see Sect.2.4.1), the lower Zambezi river from Zumbo location (upstream reaches of the Cahora Bassa reservoir) down to the Indian Ocean, has been schematized in 27 homogeneous *morphological boxes* that correspond to the grid calculation of the model. Each cross-sections has been characterized by the morphological parameters measured at 1 km resolution (Table 2.A in Appendix D) and subsequently averaged in the *morphological box* immediately downstream (Table 3.8). The model's schematization also imposes that tributaries have to be introduced in the specific cross sections (see Fig.3.12). The morphological parameters measured at the "entering section" of the Zambezi and the tributaries are also shown in Table 3.8, indicated by letters *a, b, c, d, e, f*. Note that the morphological parameters have been measured in different periods (see Sect.3.5.9).

Morphological box **L**					**grainsize bottom composition**			
n°	**length [km]**	**active width [m]**	**stream width [m]**	**slope**	β_1	β_2	β_3	β_4
1 [(a) (b)]	32	998	3144	$6.87\ 10^{-4}$	0.12	0.47	0.40	0.01
2	32	928	2977	$3.62\ 10^{-4}$	0.02	0.20	0.74	0.05
3	32	1161	2822	$3.60\ 10^{-4}$	0.01	0.16	0.76	0.07
4	32	984	2549	$2.28\ 10^{-4}$	0.01	0.09	0.72	0.18
5	32	1056	2285	$2.17\ 10^{-4}$	0.02	0.28	0.63	0.07
6	32	787	1410	$2.02\ 10^{-4}$	0.03	0.39	0.57	0.01
7	33	666	1572	$3.52\ 10^{-4}$	0.08	0.84	0.08	0.01
8	35	164	283	$1.29\ 10^{-3}$	0.36	0.50	0.10	0.04
9	16	160	160	$1.37\ 10^{-3}$	0.55	0.25	0.15	0.05
10	16	162	162	$1.38\ 10^{-3}$	0.15	0.48	0.35	0.02
11 [(c)]	36	271	271	$6.23\ 10^{-4}$	0.15	0.42	0.32	0.12
12	36	725	725	$2.63\ 10^{-4}$	0.01	0.07	0.83	0.09
13	31	1234	1501	$2.43\ 10^{-4}$	0.01	0.08	0.86	0.05
14 [(d)]	31	1594	2256	$3.11\ 10^{-4}$	0.02	0.40	0.56	0.03
15 [(e)]	28	1336	2152	$1.91\ 10^{-4}$	0.01	0.74	0.22	0.03
16	28	806	1681	$3.49\ 10^{-4}$	0.01	0.26	0.64	0.09
17	28	2015	3627	$3.65\ 10^{-4}$	0.01	0.26	0.64	0.09
18	28	1748	3291	$3.86\ 10^{-4}$	0.02	0.33	0.60	0.05
19	28	1677	3163	$3.38\ 10^{-4}$	0.02	0.36	0.58	0.04
20	28	1484	3618	$3.92\ 10^{-4}$	0.01	0.52	0.43	0.04
21	28	1567	4049	$3.49\ 10^{-4}$	0.01	0.52	0.43	0.04
22	28	1510	3246	$3.26\ 10^{-4}$	0.49	0.25	0.14	0.12
23	28	1492	3492	$2.91\ 10^{-4}$	0.33	0.35	0.25	0.07
24 [(f)]	77	1235	3189	$2.41\ 10^{-4}$	0.14	0.58	0.26	0.02
25	76	845	2017	$9.19\ 10^{-5}$	0.09	0.62	0.26	0.03
26	18	1392	3923	$3.71\ 10^{-5}$	0.08	0.81	0.10	0.02

27	18	2807	4831	$-3.76\ 10^{-5}$	0.12	0.85	0.01	0.01
[(a)] middle Zambezi		909	909	$2.40\ 10^{-4}$	0.12	0.47	0.40	0.01
[(b)] Luangwa		296	296	$1.35\ 10^{-3}$	0.12	0.47	0.40	0.01
[(c)] Luia		181	181	$2.03\ 10^{-3}$	0.15	0.40	0.38	0.07
[(d)] Revubue		208	208	$2.52\ 10^{-3}$	0.01	0.27	0.64	0.08
[(e)] Luenha		229	229	$1.00\ 10^{-3}$	0.01	0.70	0.25	0.04
[(f)] Chire		186	186	$2.52\ 10^{-4}$	0.11	0.34	0.20	0.35

Table 3.8: Morphological parameters of the selected cross-sections (based on the concept of *morphological box*, see Sect. 2.4.1), including tributaries (5) and the middle Zambezi.

3.5.8 SEDIMENT INPUT FROM MIDDLE ZAMBEZI AND TRIBUTARIES

The model's schematization includes the main tributaries at the specific cross section, together with the middle Zambezi which is considered in the same way as a tributary at the upstream boundary of the river (see Fig.3.12). Their contributions to the main stream, both in terms of water and sediment discharge, is considered by the model through the application of a virtual "entering section" where local values of bottom slope i_f, river width B and grainsize composition β_k are properly selected for the computation of the prescribed annual sediment input (eq.2.9), as a function of the local equivalent discharge $Q_{eq}(t)$.

Erosional/depositional processes occurring on the main stream reproduced in the model have considerable effects on the morphology of the tributaries close to their confluence, and therefore on their sediment load contribution. Depending on the modifications that occurs on the main channel morphology (bed elevation Δz), caused by different reasons (flow regulation, natural aggradation/degradation processes, river diversions, etc.), tributaries adjusts their bed elevation in the vicinity of the junction to the main stream both by augmenting (local base level degradation) or diminishing (local base level aggradation) their bottom local slope i_f (Schumm, 1973; Germanoski et al., 1988; Brandt, 2000). The behaviour of the tributaries would have been explicitly taken into account if the watershed were entirely reproduced by the model. As it is not the case, some approximation is needed. We may assume, for example, that an increase of water flow or aggradation, and consequent base level raising , will only affect the tributaries for a limited extension, say up to a level where the backwaters curve intersects the original profile (Leopold et al., 1964).

As a crude approximation, the progressive aggradation/degradation of the tributary is assumed to develop in such way that (time-depending) slope in the final cross-section will

keep the same proportion with the (time-depending) average slope of the tributary. In order to consider the time- and space-variations of the main channel bottom elevation $\Delta z\ (t)$, the bottom slope $i_f\ (t)$ of each "entering section" is continuously updated during the computation:

$$i_f(t) = \frac{i_0}{I}\left(\frac{H_T - \Delta z(t)}{L_T}\right) \tag{3.9}$$

where i_0 is the initial value of $i_f\ (t=0)$, H_T (= const) is the elevation of the first fixed point along the tributaries (lake, gorges or, at least, divide), L_T is the distance between this point and the confluence and $I = H_T/L_T$ is the initial value of the averaged slope. The other morphological parameters of the "entering sections" (width and grainsize composition) are assumed to remain constant. By simplifying, the eq.(3.9) become:

$$i_f(t) = i_0\left(1 - \frac{\Delta z(t)}{H_T}\right) \tag{3.10}$$

	middle Zambezi	Luangwa	Luia	Revubue	Luenha	Chire
i_0	$2.52\ 10^{-4}$	$1.35\ 10^{-3}$	$2.03\ 10^{-3}$	$2.52\ 10^{-3}$	$1.00\ 10^{-3}$	$2.52\ 10^{-4}$
H_T [m]	388	839	237	380	1178	459
L_T [m]	791'860	942'694	74'000	105'000	391'715	518'009
I	$4.90\ 10^{-4}$	$8.90\ 10^{-4}$	$3.21\ 10^{-3}$	$3.63\ 10^{-3}$	$3.01\ 10^{-3}$	$8.87\ 10^{-4}$

Table 3.9: Local slope of the tributary in vicinity to the confluence with the main stream (i_0); H_T is the elevation of the first fixed point along the tributaries (lake, gorges or at least divide), L_T is the distance between this point and the confluence and $I = H_T/L_T$, for the tributaries (5) and the middle Zambezi.

3.5.9 HOMOGENIZATION OF THE DATA

The data utilized for the model implementation (Sect.3.5) have been measured in different periods of time. During the first half of 60'ies, in particular, the width B and the bottom elevation z have been measured at the reservoir site, while the bottom composition has been measured in 38 cross-sections all along the lower Zambezi and the main tributaries, from Zumbo to the Indian Ocean. For the period 2000-02, by contrast, the data of B and z are available from the DEM and the LANDSAT 7 images along from the Cahora Bassa dam downstream (with exception of the reservoir, covered by water).

The homogenization procedure consists in simulating the fluvial system evolution, first, in the forward time-direction and, subsequently, in the backward time-direction. In the forward simulation the data measured in the earlier period are utilized together with some approximate data, while in the backward simulation the data measured in the later period are also utilized with other approximate data. By eventually repeating the operation more than once, all the available information is transferred from one time to another with the purpose to reconstruct the "optimal" configuration with respect to all the available information. In particular, it has been reconstructed the configuration of the lower Zambezi at the beginning of the last century (1907), when hydrological measurements were started. In the homogenization procedure, the variation of water and sediment input due to the construction of Kariba dam (1958) and Cahora Bassa dam (1974) have been taken into account.

The procedure for backward simulation is reported in Appendix B.

3.6 MODEL APPLICATION

Although the model may in principle be applied to the entire Zambezi river at watershed scale, this would require a remarkable effort as far as its implementation is concerned. It has been mentioned that the Zambezi basin (some $1.38\ 10^6$ km^2) is extended in eight different countries and the necessary topographical, hydrological and sedimentological data (no matter if extremely coarse in quantity and quality) should be sought in many tens of agencies, offices and departments. This would require, in fact, a specific project with the collaboration of all the interested technical and administrative bodies.

On the other hand, it does not make much sense to carry on very long simulations (at geological scale) on a limited portion of the basin (albeit larger than $0.2\ 10^6$ km^2) like the lower Zambezi, because time- and space-domain should be somehow related. Some simulation performed over thousands of years, anyway, have shown that this part of the river seems to be subject to a long-lasting process of general progressive deposition which is apparently far from the equilibrium and is still slowing propagating in the downstream direction towards the Indian Ocean. Such a long type of simulations, however, should correctly be made by including all the sources of sediments, far then upstream from present boundary conditions of the model.

The attention has therefore been concentrated to relatively shorter simulations (100-200 years), in order to evaluate the morphological effects, at the present (quasi-equilibrium) situation, of Kariba's and (especially) Cahora Bassa's dams.

3.6.1 MEDIUM-TERM EFFECTS OF DAMS

The model has been applied for simulating the morphological behaviour of the lower Zambezi since 1907, namely the period following the commencement of systematic hydrological measurements at Cahora Bassa (Zumbo station). This has permitted to evaluate every year the "historical" equivalent discharge Q_{eq} entering the model, both from the Zambezi and (with some reasonable proportionality criterium) from the main tributaries, together with the corresponding annual sediment transport up to 2003.

Simulations have been carried on for another 100 years after present by assuming a synthetic hydrology with constant Q_{eq}, depending upon the configuration considered. The constant values of Q_{eq} have been obtained by averaging the historical Q_{eq} over different periods of time, from 1907 to 1958 (period before dams construction, natural configuration), from 1959 to 1974 (when only Kariba dam was in operation) and from 1974 to 2003 (after the completion of Cahora Bassa impoundment, therefore with both dams in operation).

The model clearly indicates the effects of the construction of Kariba (1958) and of Cahora Bassa (1974). Fig.(3.14) reports the bottom evolution along the 600 km river reach downstream Cahora Bassa following the year 1957 (just before the construction of Kariba dam), 1974 (just before the construction of Cahora Bassa dam), 2003 (last year with measured hydrological data) and 2100 (hundred year after present).

The three graphs in the figure indicate the different response of the bottom elevation, under three different hypothesis that correspond to the three different configurations considered: *no DAMS* (real configuration until 1958, hypothetic *natural* configuration in the following period), only *Kariba DAM* (real configuration only between 1958 and 1974, hypothetic in the following period) and *Kariba and Cahora Bassa DAMS* with both dams constructed (real configuration from 1974). In absence of dams (natural condition, bold line) it appears the progressive aggradation of the upper part of the river, downstream the gorges (from km 50 to km 200), where three tributaries enter the Zambezi. Along the intermediate reach, from km

200 to km 400, the aggradation rate is almost nil, and even a certain degradation is shown at Sect.16 (km 194); while a perceptible aggradation rate is again exhibited in the delta zone.

For the same Fig.(3.14) one may observe the effects of the dams, also on the light of the concept expressed by the "scale of Lane" (Fig.3.1) and also reported in Brandt (2000). The effect of Kariba alone is most evident in 1974, just before the construction of Cahora Bassa. With respect to the *natural* conditions, the bottom elevation with the dam appears to be higher (relative deposition), which is in fact the configuration anticipated by the scale of Lane: this is the effect of the equivalent waterflow (Q_{eq}) reduction, immediately transferred downstream, while the opposite effect of the sediment interception will require much more time to be perceived some 600 km downstream. On the other hand, the presence of Kariba in the year 2003 is almost totally hidden by the construction of Cahora Bassa. Being this dam just upstream of the river reach under consideration, the effects of sediment interception are rapidly felt in the first 100-150 km (namely just after the gorges which, before the dam, immediately discharged the sediments coming from upstream). By contrast, more than 25 years after the construction, the "instantaneous" opposite effect of the waterflow reduction due to Cahora Bassa (and even more Kariba) has been already adsorbed. But the time-depending consequences of the impoundments will be further clarified in Fig.(3.16).

Fig.(3.15) reports the contemporary evolution of grainsize composition corresponding to the bottom change discussed above. In absence of dam (bold line), one may observe, as expected, the *natural* long-term progressive fining of the bottom composition, which (according to the scale of Lane) generally accompanies deposition. According again to the scale, the *natural* fining is slightly reinforced in 1974 by the "instantaneous" reduction of the Q_{eq} due to the construction of Kariba. On the other hand, the opposite effects of waterflow and sediment input reduction, produced by the subsequent construction of two dams, cannot be easily distinguished. However, it appears quite clear the long-term relative attenuation of the *natural* grainsize fining, connected to the trapping of sediments, which apparently results to be the final prevailing mechanism according to the Lane's scale.

The time-history of the bottom elevation and bottom grainsize, reported in Fig.(3.16), confirms the observations above. In particular, the initial prevailing effects of waterflow reduction, rapidly propagating downstream, are very soon compensated (and eventually inverted) by the opposite effect of sediment trapping. It is also interesting to note the role

played by the long-term evolution of the river system (in the case of lower Zambezi, a general deposition accompanied by a progressive fining): the long-term process is initially and locally perturbed by the dam construction, but seems to reach relatively soon a new quasi-equilibrium configuration. The analytical evaluation of the effects of boundary conditions along a river reach (in terms of celerity and attenuation of their perturbation) may be found in Fasolato et al., (2007a).

Results of simulations for all the *morphological boxes* (from Zumbo to the Indian Ocean) are provided in Appendix C.

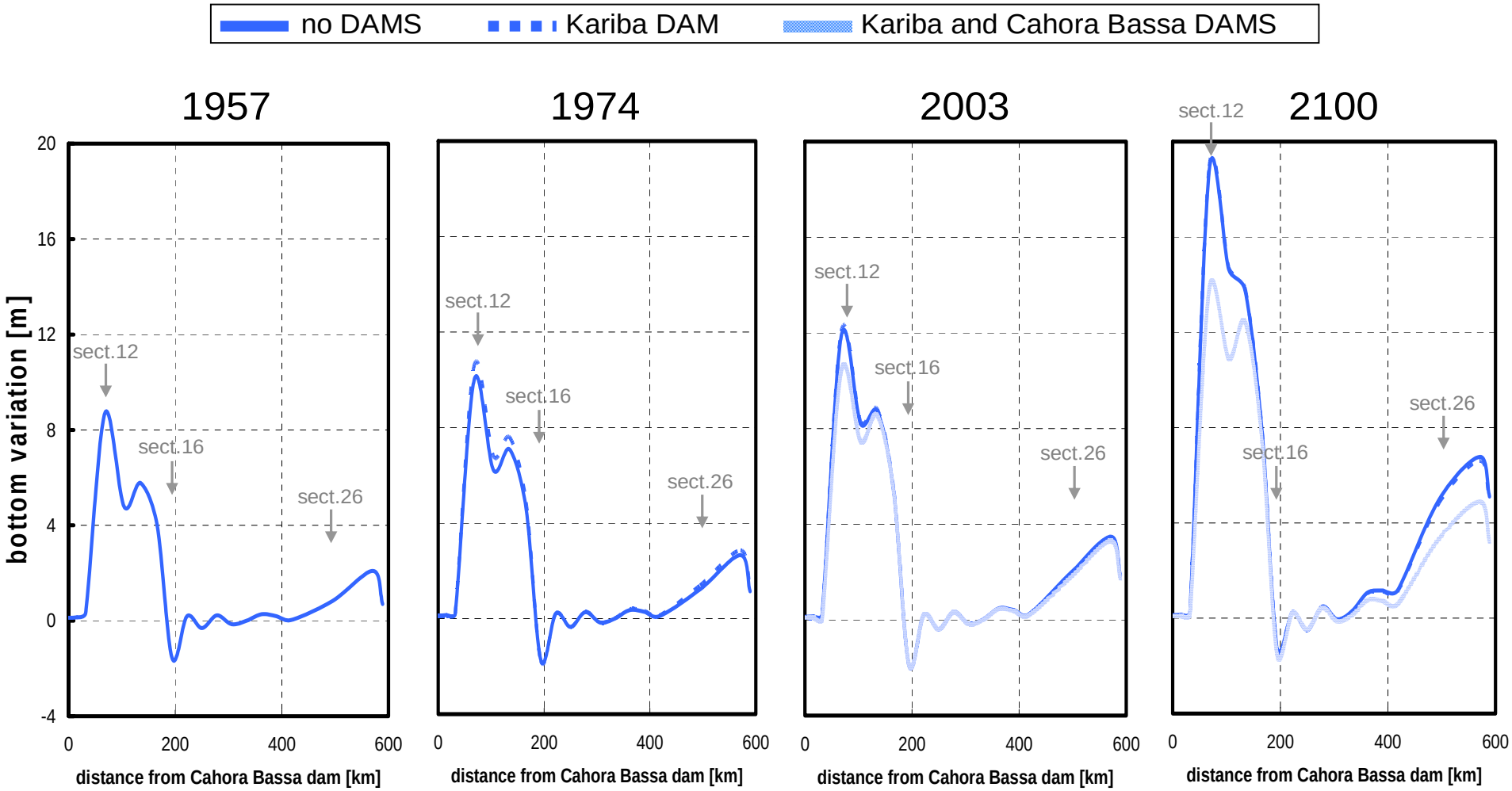

Figure 3.14: Results of simulations from 1907 configuration, in terms of bottom variation.

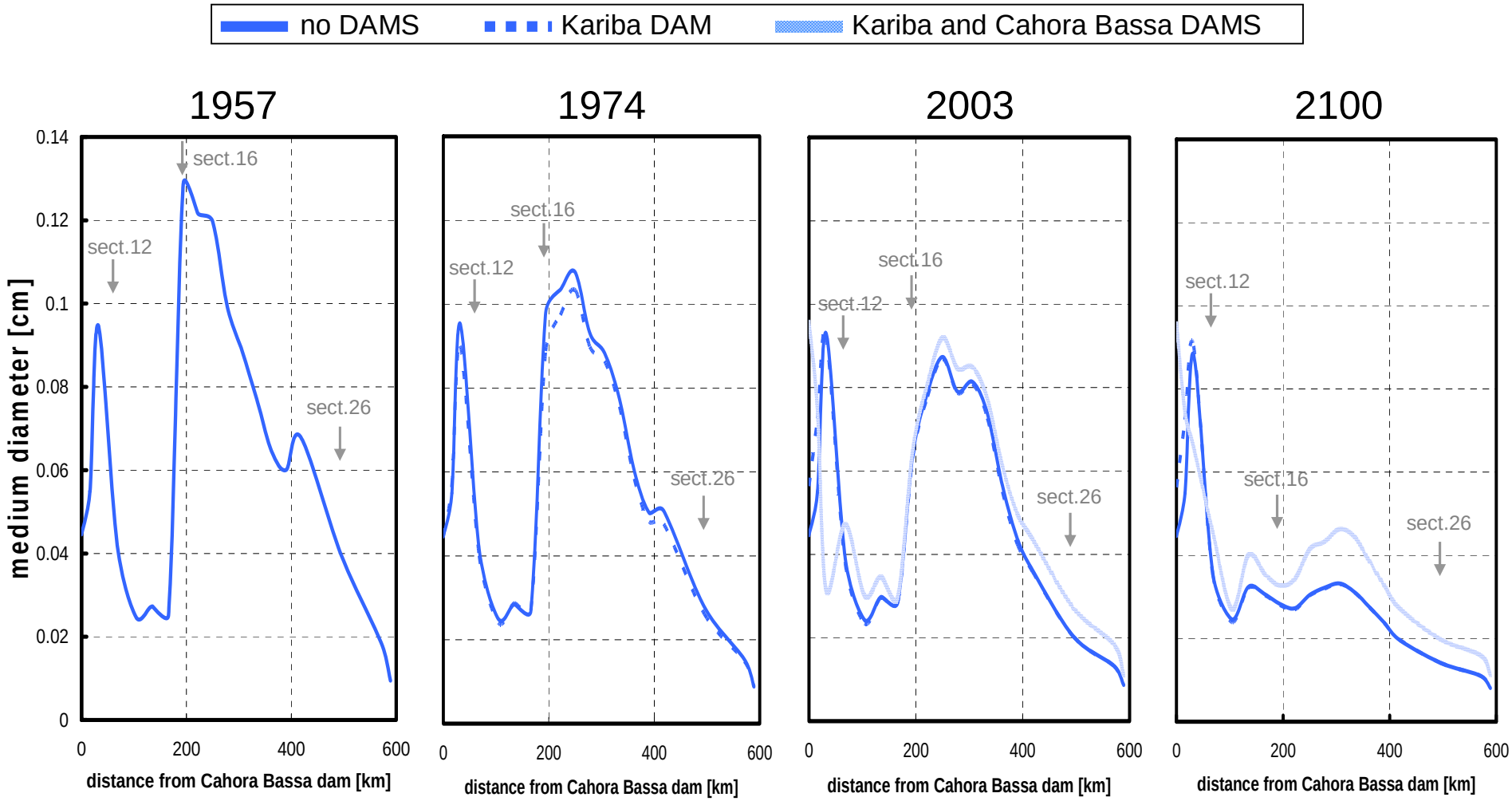

Figure 3.15: Results of simulations from 1907 configuration, in terms of grainsize variation.

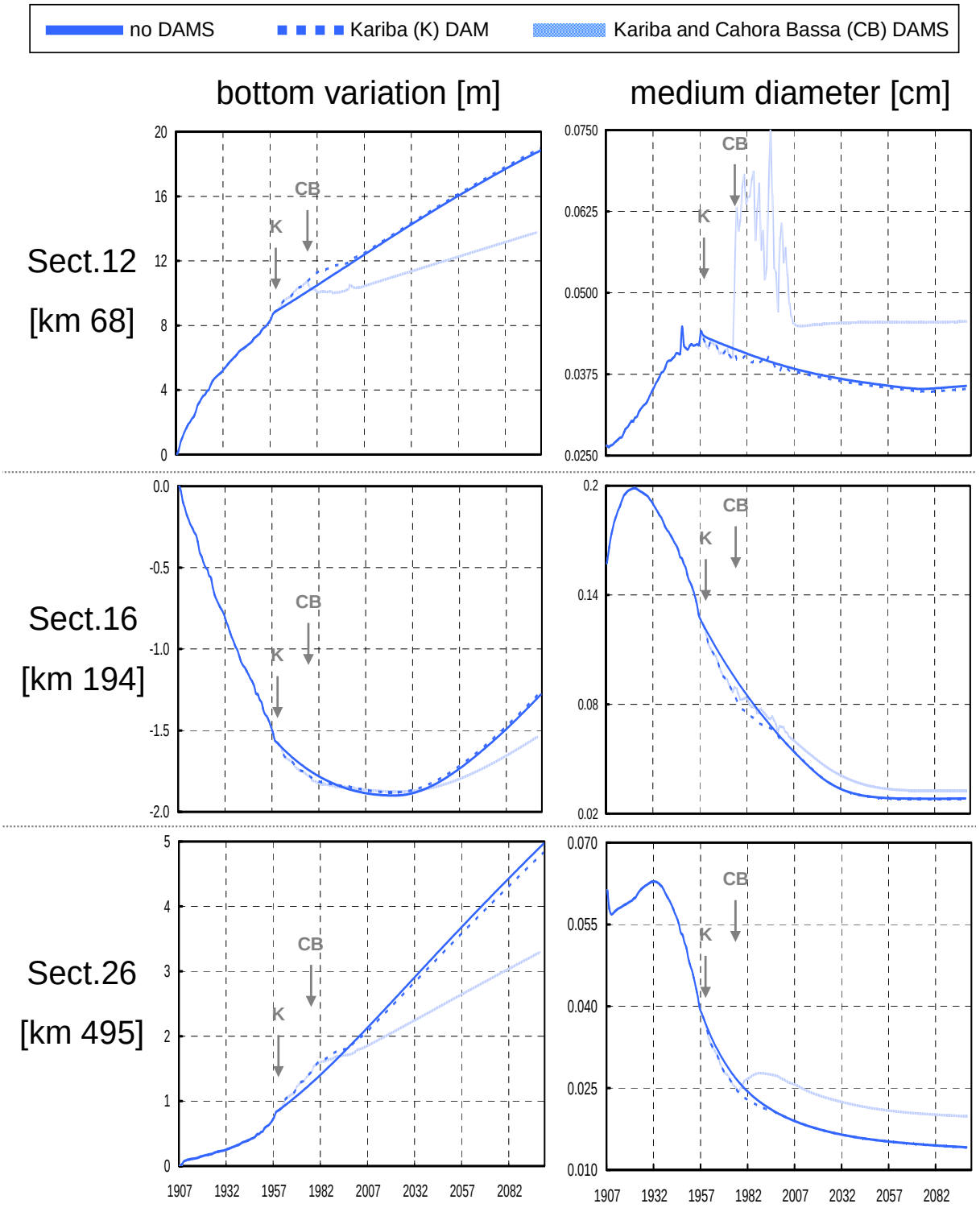

Figure 3.16:Results of simulations from 1907 configuration, in terms of bottom and grainsize variation in three sections downstream Cahora Bassa dam (distance are from Cahora Bassa dam).

3.6.2 COMPARISON BETWEEN COMPUTATIONAL RESULTS AND FIELD MEASUREMENTS AND ESTIMATIONS: DELTA EVOLUTION

Delta coastline evolution has been recognized as a crucial indicator of the magnitude of sediment transport yield in major rivers in the world. However, other complex physical mechanisms are involved in the evolution of the delta surface and morphology and extension besides sediment yield: erosion and redistribution by the sea, sea level fluctuations, subsidence, human intervention, etc. Different approaches have been developed to quantify evolution: aerial-photo, radar images, ground penetrating radar, sonar bathymetry, sediment sampling, grainsize distribution analysis, various mathematical models, etc. (Trebossen et al., 2005; Pelpola et al.,2004; Sun et al.,2002; Liu et al.,2000). Concerning the Zambezi delta evolution, Walford et al. (2005) calculated its solid sediment load history of the last 120Ma using seismic reflection profiles system, making some assumptions on the compaction history in order to construct isochore maps of solid sediment load and yield as a function of geological time. Walford et al. characterized three periods of elevated sediment flux: the first in Late Cretaceous times (90-65 Ma), the second in Oligocene times (34-24 Ma), and the last in Late Miocene times (10Ma) that can be attributed to the doubling of the Zambezi catchment area due to the capture of the upper part of the river (Nugent, 1990). In this last geological period (last 5Ma, that largely includes the human's induced effects on the river system), they estimated the annul sediment yield within the range of 6-13 10^6 m^3/year.

The predicted effects on the Zambezi delta system of the changes on both hydrological and sedimentological natural patterns, caused by dams impoundments, have been highlighted by recent studies of the Marromeu wetland system (e.g. Beilfuss et al., 1996, Anderson et al., 1990). By field ecological surveys analysis and aerial-satellite images comparison (from 1960 up to 2000), it was observed that delta is much drier at the end of the dry season than the natural (namely: pre-impoundment) conditions, with a reduction in wetland and open water areas, infestation of stagnant waterways with exotic vegetation, intrusion of saltwater, a reduction on grazing, fisheries and flood recession agriculture. Further, it was that the lower Zambezi river more than 2m below bankful discharge in the delta during the natural flooding period (Sect. 3.3.3.3).

It is unquestionable that the frequency, timing, magnitude, duration and sediment load of Zambezi river floods now differ greatly from historic flooding conditions (Bolton, 1983,

Suschka et al., 1986), but in fact, up to now, no quantitative and systematic evaluation of the effects of these phenomena on the delta coastline evolution has been carried on.

In this sense, a preliminary (but not exhaustive) evaluation of the delta shoreline evolution has been made, estimating the area extension of a reference surface (a single image (path 166, row 73) covers the entire Zambezi Delta) calculated from the 5 LANDSAT images, the only ones available for the last 35 years. In particular, we analyzed images taken from:

- LANDSAT MSS, 1972/09/24;
- LANDSAT MSS, 08/28/1979;
- LANDSAT TM, 06/14/1991;
- LANDSAT ETM+, 2000/07/16
- LANDSAT ETM+, 2004/11/08.

All the images has been georeferenced to the 2004 image and subsequently digitalized. A basic classification using various false-color combinations, distinguishing water (channel and sea) and soil cover has been implemented using ENVI software. The reference area extension has been finally computed with ArcView GIS software (see Fig.3.17; Table 3.10)

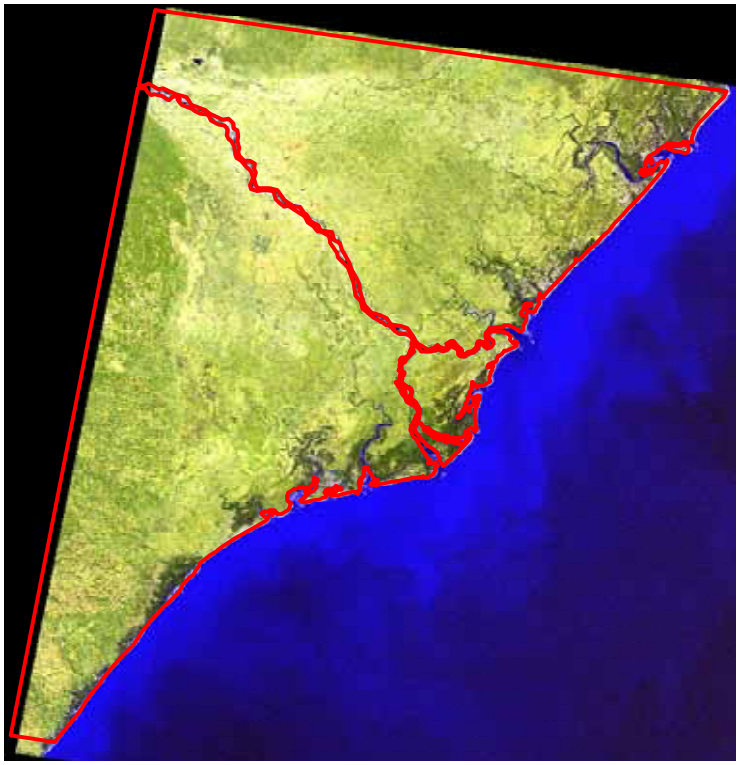

Figure 3.17: Edges of the reference area (in red) considered for the computation for the delta shoreline evolution trend (LANDSAT ETM+, 2000/07/16)

year	area [km^2]	loss/increase of area		
		diff. with the previous measurement [km^2]	rate [km^2/year]	cumulative from 1972 [km^2]
1972	13'920			
1979	13'903	-17.2	-2.2	-17.3
1991	13'881	-21.8	-1.7	-39.5
2000	13'905	23.7	2.4	-15.4
2004	13'894	-10.9	-2.2	-26.3

Table 3.10: Computation of the area of the Zambezi delta, pattern of variations over the considered period of time (1972-2004).

These limited and preliminary measures confirms in some way, the general negative trend of the delta area extension, with a loss of soil estimated in -2.2 km^2/year for the 1972-79 period, a less marked loss in the 1979-91 period (-1.7 km^2/year), an overturning of the erosion/deposition phenomena with an increase of area extension (attested in +2.4 km^2/year) for the period 1991-2000, and finally a substantial prevailing of the erosion process with a strong decrease of the delta area (-2.2 km^2/year). The delta shoreline evolution seems not to display a stable negative trend over the years, however up to now (2004 speaking), from the 1972 measurements, the erosion process seems to prevails against the depositional one, with an total loss of soil of more than 26 km^2.

Even if it is unquestionable that these variations do not depend only by the sediment yield pattern of the Zambezi river, it could be interesting and useful to compare the delta area evolution to the total sediment supply to the delta computed by the model in the last section of the river (Fig.3.18). While the influence of the Kariba dam seems not to be strong (there isn't any considerable difference before and after 1958), the model predicts a very variable pattern of sediment load for the period 1952-72, just before the Cahora Bassa dam construction: the sediment discharge varies between 0.5 and more than 3.5 10^6 m^3/year, apparently related to the corresponding interannual variation of Q_{eq} (note that sediment transport varies more than linearly). It is not clear the reason of these pulsations of Q_{eq}. In any case the heavy fluctuations of sediment discharge to the delta with consistent peaks value, could be the reason of the relative high delta surface extension measured on 1972. Apart of 1978/1988 events, when two consistent flood occurred on the lower Zambezi valley, from 1972 until 1995 the trend of the sediment supply to the delta is strongly negative: the average value of P decrease from 1.64 10^6 m^3/year to 0.95 10^6 m^3/year, that corresponds to a general and consistent decrease of the delta extension (averaged value of -1.9 km^2/year). Even if in the

following period (from 1995 until 2000) the model predicts a slight decrease of sediment supply (averaged value of 0.75 10^6 m^3/year) not correlated to the augmentation of the coastal area (+2.4 km^2/year), the peak of 2000 in sediment discharge could explain this increase. During the last period (from 2000 until 2004) the averaged sediment supply remains rather constant while the surface of the delta shows a strong decrease (-2.2 km^2/year), probably related to the relative strong coastal erosion of the sediment material stored on the delta area during the last floods (2000).

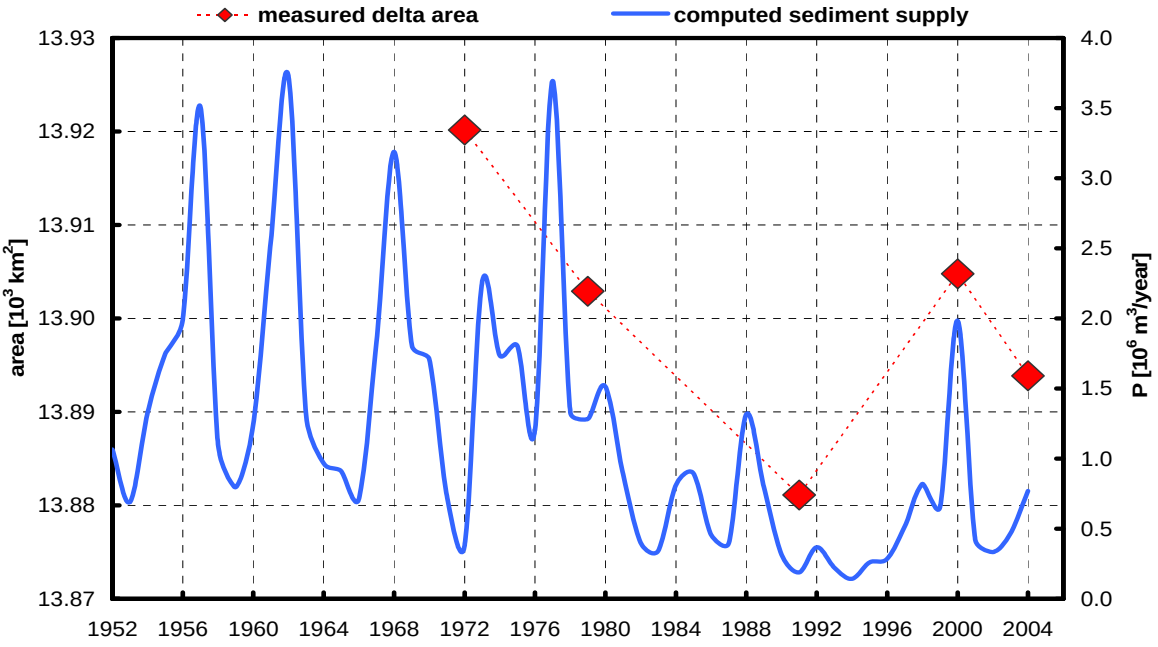

Figure 3.18: Comparison with the measured delta area extension (1972-2004) to the computed sediment supply to the delta site (1952-2004).

3.7 CONCLUSIONS

A simplified long-term morphodynamic model has been applied to the 860km lower reach of the Zambezi River, between Zumbo and the Indian Ocean, to evaluate the long-tem morphological effect of the presence of two very large impoundments, namely Kariba and Cahora Bassa dams.

Prior to the simulations, however, a considerable effort was made to adequately process the (scanty) available data. A innovative method has been implemented to reconstruct the river bathymetry (see Sect.2.4.1), to calibrate the solid transport formula and finally to homogenise the different time sequences of data, in terms of river topography and sedimentology. This

procedure permits to reconstruct the "optimal", or most plausible, past configuration with respect to all the data. In particular, it has been reconstructed the configuration of the lower Zambezi at the beginning of the last century (1907), when hydrological measurements were started.

The subsequent application of the model over a long period of time (centuries) indicates that the present lower Zambezi is not in equilibrium but is slowly aggrading, especially in its upper part closer to the sediment sources.

The presence of the dams (altering the natural waterflow pattern and intercepting the total amount of sediment coming from upstream) gives place to different and sometimes opposite effects that could in principle be explained according to the scale of Lane. The different celerities of perturbation in time and space, however, must be considered for a correct explanation of the effects. The presence of Kariba dam since 1958, with respect to the *natural* conditions, gives place to an "immediate" higher aggradation of the bottom elevation several hundreds kilometres downstream due to the reduction of the *equivalent waterflow* Q_{eq}, while the opposite effect of the sediment interception will require much more time to be perceived. The presence of the Cahora Bassa dam since 1974 has equally given place to a strong reduction of the sediment input to the river reach and to a less variable waterflow during the year. However, being this dam located at the upstream end of the river reach under consideration, the effects of sediment interception are rapidly felt in the first 100-150 km and progressively propagate towards the ocean. As a consequence, the "natural" long-term aggradation process of lower Zambezi has been slowed down, but it is still going on. From simulations carried on for some 100 years to present (till 2100), the combined effect of Cahora Bassa trapping of sediments and reduction of Q_{eq} seem to be the cause of reduction in bottom aggradation over the entire reach till the Indian Ocean. By contrast, the lower value of Q_{eq} due to the presence of Kariba seems to be much less important.

The results mentioned above seem to be confirmed when compared to the recent evolution of the Zambezi delta (1972-2004) indicates an apparent diminishing of the delta's surface, in correspondence to the reduction of the sediment output from the river. It should be noted, however, that five surveys are not enough to draw conclusions especially because the morphodynamics of the outer delta depends in a complex way also on the meteomarine conditions of the ocean.

Chapter 4

Conclusions and Further Developments

The knowledge of sediment budget at watershed scale and extended over long periods of time (historical scale), appears to be more and more important to predict and possibly mitigate the anthropogenic impact of large hydraulic works (especially dams) on fluvial, and adjacent coastal, system. Indeed, due to the gradually slow response of the fluvial systems to perturbations (Fasolato et al., 2007a), the effects of engineering interventions require long periods of time to propagate along the river down to the delta. Therefore, in principle, long simulations should correspondingly be performed over the entire watershed.

Simulations at watershed scale will provide, first of all, information on the overall evolution of the sediment budget components, often necessary before taking decisions regarding the river basin management. Moreover, this information may conveniently be used for prescribing the boundary conditions for 2-D / 3-D models of limited part of the river, for detailed morphological investigations.

The main difficulty for implementing a model at watershed scale is the scarcity of data (topographical, hydrological, granulometric and of sediment transport) distributed all over tha basin. For a detailed mode, moreover, the required data should be extremely dense and with high resolution power. This quantity and quality of data is virtually impossible to be obtained in economically developed countries, but even less, of course, in less affluent countries of Africa, Asia and Latin America. It is imperative, then, to develop a series of less demanding models, to be applied in such circumstances.

In the present thesis, in fact, a specific one-dimensional morphodynamic model has been developed, that only requires extremely simple and aggregated topographical data (easily available at accessible costs from satellite images) and quite coarse hydrological information (to be obtained by relatively crude hydrological models). The 1-D is based on a strong simplification of the waterflow (De St.Venant) equations, namely the hypothesis of instantaneous propagation of discharge and of averaged local uniform flow. The simplified model, by contrast, is quite accurate in reproducing the space- and time-changes of bottom grainsize composition and size fractions transport rates.

Part of this dissertation is devoted to establish the validity and limits of the simplified waterflow equations. While the first hypothesis is satisfied for flood waves much longer than the river reach comprised between tow main tributaries, the second hypothesis is valid for *morphological boxes* four times longer than the critical significant “width wave” of the river. The morphological box tends to be longer and longer with increasing Froude number, but is still acceptable even for slow lowland rivers like lower Zambezi.

The local uniform-flow hypothesis is very much faster than the complete model and susceptible to many interesting applications, especially useful for scarcely surveyed watersheds. The model, in fact, may also be used to supplement the few available data by interpolating / extrapolating them in time and space. This is especially necessary for multiplying the data regarding grainsize composition, almost invariably missing for long periods in many reaches of the river.

The model has been applied to the 600 km – long reach of the lower Zambezi, from the reservoir of Cahora Bassa to the Indian Ocean, for studying the effects of the Kariba and Cahora Bassa reservoirs on the river morphology. The model provides plausible results,

somehow confirmed by the five subsequent surveys of the delta region, carried out from 1972 to 2004. For a more reliable verification of the model, some other data would be necessary especially for better calibrating the sediment transport formula. Also the extension of the model to entire (or to a larger portion) of the Zambezi watershed would also very likely improve the model performances.

NOTATION

Symbol	Definition	Expression	Units	Symbol	Definition	Expression	Units
$\underline{Q}$	Water discharge		m^3/s	t	Non-dimensional temporal coordinate	$=t^*\underline{U}/\underline{H}$	-
A	Wetted cross section		m^2	α		$=1-F_r^2$	-
x^*	Dimensional space coordinate		m	F_r^2	Froude number	$=\underline{V}^2/g\underline{H}$	-
t^*	Dimensional time coordinate		s	E	Resistance coefficient	$=2g/\chi^2$	-
H	Local water depth		m	ε		$=3/2E\ F_r^2$	-
Z	Bottom elevation		m	η		$=(1-d)/(1+d)$	-
g	Gravity acceleration		m/s^2	d^*		$=d^{1-s}$	-
U	Flow velocity	$= Q/A$	m/s	η^*		$=(1-d^*)/(1+d^*)$	
j	Energy slope		-	S^*		$=1-\eta^{*2}$	-
B	Channel width		m	ψ	Sediment concentration	$=\underline{P}/\underline{Q}$	-
P_k	Solid discharge of k-th class		m^3/s	Δ	Relative mixing layer	$=\delta/\underline{H}$	-
δ	Active-layer thickness		m	b_c	Amplitude of river width perturbation		m
β_k	Percentage of k-th class		-	Ω		$=H/\lambda$	-
β_k^s	Percentage below active-lay		-	λ	Wavelength of the channel width		m
α_c	Coriolis coefficient (energy distribution)		-	L	Morphological box		m
β_c	Coriolis coefficient (momentum distribution)		-	E_r	Relative error ($Z_{steady} - Z_{uniform}$)		-
χ	Chézy coefficient		$m^{1/2}/s$	T_a	Reference time (for computation of Q_{eq})	$=1\ year$	s
d_k	Representative diameter of k-th cl.		m	γ	Irregularity coefficient		s
d	Ratio between diameters	$=d_1/d_2$		ζ	Admissible relative error		-
α_T	Transport formula coefficient		-	$\sigma_{\Delta x}$	Resolution (mean square error)		m
ξ_k	Hiding-exposure coefficient		-	$\varepsilon_{\Delta x}$	Steady model accuracy (mean square error)		m
Q_{eq}	Equivalent discharge		m^3/s	$\gamma_{\Delta x}$	Uniform model accuracy (mean square error)		m
$\underline{H}$	Reference water depth		m	$\lambda_{\Delta x}$	Uniform model relative error		-
$\underline{Y}$	Reference water elevation		m	$z^S{}_1$	Bottom elevation using steady flow model, obtained with a computational step of 1km		m
$\underline{Z}$	Reference bottom elevation		m	$z^S{}_{1,\Delta x}$	Bottom elevation using steady flow model, obtained with a computational step of 1km and averaged over Δx=L, L/2, L/4, L/8		m
$\underline{P}$	Reference sediment transport		m^3/s	$z^S{}_{\Delta x}$	Bottom elevation using steady flow model, obtained with a computational step of Δx=L, L/2, L/4, L/8		m
$\underline{i}_f$	Averaged bottom slope	$=-\partial\underline{Z}/\partial x^*$	-	$z^{uc}{}_{\Delta x}$	Bottom elevation using uniform flow model, obtained with a computational step of Δx=L, L/2, L/4, L/8		m
$\underline{i}_w$	Averaged water slope	$=-\partial\underline{y}/\partial x^*$	-	Q_0	Average annual flood peak		m^3/s
$\underline{i}$	Averaged energy slope		-	$Q_{0,i}$	Annual flood peak (i-year)		
$\underline{\beta_k}$	Averaged percentage of k-th class		-	V_0	Annual runoff volume		m^3
x	Non-dimensional spatial coordinate	$=x^*/\underline{H}$	-	Q_{med}	Annual average water discharge		m^3/s
m	Exponent of the transport formula			Q_{eq}	Equivalent discharge		m^3/s
n	Exponent of the transport formula			$Q_{eq,i}$	Annual equivalent discharge(i-year)		m^3/s
e	Exponent of the transport formula			$Q^T_{eq,i}$	Annual equivalent discharge(i-year) for the tributary T		
f	Exponent of the transport formula			$Q^Z_{eq,i}$	Annual equivalent discharge(i-year) for the main Zambezi		
s	Exponent of the hiding-exposure coefficient			V_s	Annual sediment runoff		m^3/year
M	Morphological coefficient of the transport formula (eq.3.1)			$S(x,t)$	Relevant quantity of the river (bottom elevation, medium diameter, etc..)		[..]
φ	Vector of solid transport formula parameters			$\Delta S'$	Computed difference between S(x, $t+\Delta t_{back}$) and S(x,t)		[..]
θ	Sum of residuals (fitting method)		m^6/s^2	ΔS	Real difference between S(x, $t+\Delta t_{back}$) and S(x,t)		[..]
H_T	Elevation of the first fixed point along the tributary		m	Δt_{back}	Evolution time of the backward-forward procedure		year
L_T	Distance between the fixed point and the confluence		m	$\Delta t'$	Evolution time of the backward-forward procedure for best fitting		year
y_i	Measurement of solid discharge		m^3/s	T		$=1-\Delta t'/\Delta t_{back}$	
				ω		$=1-\Delta S'/\Delta S$	

REFERENCES

Agarwal K.K. and Idiculla K.C., (2002). Reservoir sedimentation surveys using Global Positioning System, Central Water Commission Ministry of Water Resources New Delhi.

Anderson, J. & Dutton, P. & Goodman, P. & Souto, B. (1990). Evaluation of the wildlife resource in the Marromeu complex with recommendations for its further use. LOMACO, Maputo, Mozambique.

Armanini, A. & Di Silvio, G. (1988), A one-dimensional model for the transport of a sediment mixture in non-equilibrium condition, Journal of Hydraulic Research., 26 (3), 275-292.

Armanini, A. (1995), Non-uniform sediment transport: dynamics of the active layer, Journal of Hydraulic Research, 33 (5).

Attwell, R.I.G. (1970). Some effects of lake Kariba on the ecology of a floodplain of the mid-Zambezi valley of Rhodesia. Biological Conservation, 2 (3), 189-196.

Baker, B. (1880). The River Nile. Proc. Inst. Civ. Engrs., 50, 376.

Basson, G. (2004). Proposed Zambezi river Case Study for ISI: Africa. Confidential paper for IHP-UNESCO ISI Steering Committee. Paris.

Baxter, R.M. (1977). Environmental effects of dams and impoundments. Ann. Rev. Ecol. Syst., 8, 255-283.

Bates, P.D. & Anderson, M.G. & Baird, L. & Walling, D.E. & Simm, D. (1992). Modelling floodplain flow with a two dimensional finite element scheme. Earth Surface Processes and Landform. 17, 575-588.

Bates, P.D. & Anderson, M.G. & Hervouet, J.M. (1995). An initial comparison of 2-dimensional finite element codes for river flood simulation. Proc. Inst. Civ. Engrs. Water: Maritime and Energy 112, 238-248.

Baum, R.L. & Savage, W.Z. & Godt, J.W. (2002), TRGRS – A Fortran program for transient rainfall infiltration and Gps-based regional slope stability analysis, U.S. Geological Survey Open-File Report 02-424.

Beasley, D.B. & Huggins, L.F. & Monke, E.J. (1980). ANSWERS: A model for watershed planning, Trans. Am. Soc. Agric. Engrs. 23, 938-944.

Beilfuss, R.D. & Allan, D.G. (1996). Watled Crane and wetland surveys in the great Zambezi delta, Mozambique. Proceedings African Crane and Wetland training workshop, 345-354.

Beilfuss, R.D. & Davies, B.R. (1999). Prescribed flooding and wetlands rehabilitation in the Zambezi delta, Mozambique. An Int. Perspective on Wetland Rehabilitation, 143-158.

Beilfuss, R. & Dos Santos D. (2001). Patterns of Hydrological Change in the Zambezi Delta, Mozambique. Program for the Sustainable Management of Cahora Bassa Dam and the Lower Zambezi Valley. Working Paper #2. Direcção Nacional das Aguas, Maputo, Mozambique.

Beven, K. (1989). Changing ideas in hydrology – The case of physically based models. Journal of Hydrology. 105, 157-172.

Bolla Pittaluga, M. & Seminara, G. (2003). Depth integrated modelling of suspended sediment transport, Water Resources Research, 39 (5), 1137.

Bolton, P. (1978). The Control of Water Resources in the Zambezi Basin and its Implications for Mozambique. Occasional Paper on Appropriate Technology. School of Engineering Science, University of Edinburgh, Scotland.

Bolton, P. (1983). The regulation of the Zambezi in Mozambique: a study of the origins and impact of the Cabora Bassa Project, PhD Thesis. University of Edinburgh.

Bolton, P. (1984). Sediment deposition in major reservoir in the Zambezi basin. Proceeding of the Harare Symposium: Challenges in Africa Hydrology and Water Resources. IAHR Publ.n°144.

Bowmaker, A.P. (1960). A report on the Kariba lake area and Zambezi river prior to inundation, and the initial effects of inundation with particular reference to the fisheries. Report on the training center on fishery survey for the countries of African region. FAO Library Fiche AN:59986. Rome.

Brandt, S.A. (2000). Classification of geomorphological effects downstream of dams. Catena. 40, 375-401.

Brigada de Engenharia Hidraulica, Missão de Fomento e Povoamento do Zambeze (BEH-MFPZ), (1964). Vale do Zambeze: elementos de estudo, sedimentologia e reconheçimento de fundações. Plano geral de fomento e occupação. Anexos. Lourenço Marques (Maputo). Mozambique.

Bruk, S. (2003). Sediment research and social response: Regional Accents and the International Sediment Initiative of IHP. Proc. of the ICCORES-UNESCO Workshop: From watershed slopes to coastal areas: sedimentation processes at different scales, Venice, Dec. 2003.

Catuneanu, O. & Wopfner, H. & Eriksson, P.G. & Cairnecross, B. Rubidge, B.S. & Smith, R.M.H. & Hancox, P.J. (2005). The Karoo basins of south-central Africa. Journal of African Earth Sciences. 43, 211-253.

Centro Nacional de Cartografia e Teledetecção de Moçambique - Cenacarta (2000). Carta de Moçambique, escala 1:50,000 (various sheets). Maputo, Mozambique.

Chenje, M. (2000), State of the Environment Zambezi Basin 2000, SADC/IUCN/ZRA/SARDC, Maseru/Lusaka/Harare, 63.

Cotter, A.S. & Chaubey, I. & Costello, T.A. & Soerens, T.S. & Nelson, M.A. (2003). Water quality model output uncertainty as affected by spatial resolution of input data. Journal of American Water Resources Association (JAWRA) 39(4),977-986.

Coulthard, T.J. & Hicks, D.M. & Van De Wiel, M.J. (2007). Cellular modelling of river catchments and reaches: Advanteges, limitations and prospects. Geomorphology, 90, 192-207.

Davies, R.D. & Beilfuss, R.D. & Thoms, M.C. (2000). Cahora Bassa Retrospective, 1974-1997: effects of flow regulation on the Lower Zambezi River. Limnology in the developing word, 27, 1-9.

De Vries, M. (1993). Use of models for river problems, Studies and Reports in Hydrology Series, no. 51, UNESCO.

Di Silvio, G. & Peviani, M.A. (1989). Modelling Short- and Long-Term evolution of mountain rivers: an application to the torrent Mallero (Italy). Published at: International Workshop on fluvial hydraulics of mountains regions. Trent, Italy.

Di Silvio, G. (1991). Sediment exchange between stream and bottom: a four layer model. Int. Workshop on Grain Sorting in Rivers. Ascona (Switzerland), 21-25 Oct. 1991,163-192.

Di Silvio, G. & Marin, A. (1996a). Analytical approach to river morphodynamics : effects of space-and time-irregularities and grain-size non-uniformity. Commission of the European Communities, Directorate General XII for Science, Research and Development, Research and Technical Development Program in the Field of Environment, FRIMAR Project, Technical Report n. 2, 48.

Di Silvio, G. (1996b). Sediment yield estimates and prediction methods proceedings, Int. Conf. on Reservoir Sedimentation, vol. 2., Sect. v, 643-660, Ft. Collins, Colorado, 9-13 Sept.1996.

Di Silvio, G. & Marion, A. (1997), About delivery ratio: how does it change in time and space?, XXVII Congress IAHR., S.Francisco (USA), 10-15 Aug. 1997. Vol. D/b, 90-95.

Di Silvio, G. (2004a). Modelling long-term reservoir sedimentation for optimal management strategies. Proceedings of the 6th Int. Conference on Hydro-Science and Engineering, Brisbane (Australia), 30 May – 3 Jun. 2004.

Di Silvio, G. (2004b). Review of state-of-the-art research on erosion and sediment dynamics from catchment to coast (a Northern perspective). Meeting of the Task Force Group of ISI (International Sediment Initiative) of UNESCO-IHP. Paris, 23-24 Sept. 2004.

Di Silvio, G. (2006). Sediment sources and causes: Approaches to sediment yield evaluation Proceeding of the International Sediment Initiative Conference (ISIC). Khartoum, 12-15 November 2006, Sudan.

Du Toit, R.F. (1984). Some environmental aspects of proposed hydro-electric schemes on the Zambezi river, Zimbabwe. Biological Conservation, 28, 73-87.

Earth Resources Observation & Science (EROS), (2000). HYDRO1K Africa Documentation. Elevation Derivative Database. U.S. Geological Survey, Sioux Falls. U.S.A. http://edc.usgs.gov/products/elevation/gtopo30/hydro/.

Egiazaroff, I. V. (1965). Calculation of non-uniform sediment concentrations. Journal of Hydraulic Div., 91, 225–248.

Fasolato, G. & Ronco, P. & Di Silvio, G. (2007a). Boundary conditions in river morphodynamics. An analytical solution. Journal of Hydraulic Research (in revision).

Fasolato, G. & Ronco, P. & Di Silvio, G. (2007b). Validity of simplified one-dimensional models. Journal of Hydraulic Engineering ASCE (in revision).

Ferguson R.I.(1987). Accuracy and precision of methods for estimating river loads, Earth Surface Processes and Landforms, 12 (1), 95–104.

Fournier, F. (1960). Climat et Erosion. Presses Universitaires de France, Paris.

Galappatti, R. & Vreugdenhil, C.B. (1985). A depth-integrated model for suspended sediment transport. Journal of Hydraulic Research, 23, 4.

Gavin, J.S.R. (1990). Non linear estimation. Springer Series on Statistics, 189p.

Gee, D.M. & Anderson, M.G. & Baird, L. (1990). Large floodplain modelling. Earth Surface Processes and Landform. 15, 513-523.

Germanoski, D. & Ritter, D.F. (1988). Tributary response to local base level lowering below a dam. Regulated Rivers: Reservoir Management. 2, 11-24.

Golterman, H.L. (1983). Study of the relationship between water quality and sediment transport. UNESCO Technical Papers in Hydrology, n°26.

Grant, G. (2002). Emerging Issues for Water, Sediment, and Rivers: an International Cross-Cultural Comparison, Keynote Lecture, 9th International Symposium on the Interactions Between Sediments and Water, Banff Springs Hotel, Canada.

Gurnell, A.M. & Petts, G.E. (2002). Island-dominated landscapes of large floodplain rivers, an European perspective. Freshwater Biology. 47, 581-600.

Guy, P.R. (1980-81). River bank erosion in the mid-Zambezi valley, downstream of lake Kariba. Biological Conservation, 19, 199-212.

Hall, A. & Valente, I. & Davies, B.R. (1977). The Zambezi River in Mozambique: the physico-chemical status of the Middle and Lower Zambezi prior to the closure of the Cabora Bassa Dam, Freshwater Biology, 7, 187-206.

Hardy, R.J. & Bates, P.D. & Anderson, M.G. (1999). The importance of spatial resolution in hydraulic models for floodplain environments. Journal of Hydrology, 216,124-136.

Hayashi, H. & Clifford, M. & Banda, D. (2005). Cause of Turbidity in Luangwa River – Case of Dry Season. Proceeding of the XXXI IAHR Congress, Seoul, Korea, 11-16 Sept., 2005, 5335-5340.

Hidroeléctrica de Cahora Bassa (HCB), (2004). Various Technical Reports on Cahora Bassa Project. Songo. Mozambique.

Hidrotécnica Portuguesa (1967). Cahora Bassa undertaking (1st phase), Additament 2. Ministerio do Ultramar, Conselho Superior de Fomento Ultramarino, Grupo de Trabalho para o Zambeze. DNA Maputo, Mozambique.

Hirano, M. (1971). River bed degradation with armouring. Trans. of JSCE. 3(2).

Istituto Nacional de Geologia (ING), (1987). Carta Geologica, escala 1: 1'000'000. Ministerio dos Recursos Minerais. Mozambique.

Julien, P. & Shah, S. (2005). Sedimentation Initiatives in Developing Countries. Draft-Report for the International Sedimentation Initiative (ISI) of IHP-UNESCO. Colorado State University.

Kondolf, G.M. (1997). Hungry water: effects of dams and gravel mining on river channels. Environmental Management, 21 (4), 533-551.

Lahmeyer Int, EDF, Knight Piesold, 2001. Final Report on Meteorolgy, Hydrology and Sediment Transport. Mepanda Uncua and Cahora Bassa North Project. Republica de Moçambique, Maputo, doc.n°021.

Lane, E.W. (1955). The importance of fluvial morphology in hydraulic engineering. Proc. Am. Soc. Civil Eng., 81, 1-17.

Lee, D.S., R.D. Kingdon, J.M. Pacyna, A.F. Bouwman, and I. Tegen, (1999). Modelling base cations in European sources, transport and deposition of calcium. Atmos. Environ., 33, 224102256.

Leopold, L.B. & Wolman, M.G. & Miller, J.P. (1964). Fluvial processes in geomorphology. Freeman, San Francisco, 522p.

Liu, J.T. & Huang, J.S. & Hsu, R.T. & Chyan, J.M. (2000). The coastal depositional system of a small mountainous river: a perspective from grain-size distribution. Marine Geology, 165, 63-86.

Magilligan, F.J. & Nislow, K. H. (2005). Changes in hydrologic regime by dams. Geomorphology, 71, 61-78..

Maner, S.B. (1958) Factors affecting sediment delivery rates in the red hills physiographic area, Transactions of American Geophysics 39, 669–675.

Montgomery, D.R. & Dietrich, W.E. (1994). A physically based model for the topographic control on shallow landsliding, Water Resources Research, 30, 1153-1171.

Morgan, R.P.C. & Quinton, J.N. & Smith, R.E. & Govers, G. & Poesen, J.W.A. & Anerswald, K. & Chisci, G. & Torri, D. & Styczen, M.E. (1998). The European soil erosion model (EUROSEM): A process-based approach for predicting sediment transport from fields and small catchments. Earth Surface Processes and Landforms, 23, 527-544.

Morris, G.L. & Fan, J. (1998). Reservoir Sedimentation Handbook, McGraw-Hill, pp. 746.

Nearing, M.A. & Foster, G.R. & Lane, L.J. & Finker, S.C. (1989). A process-based soil erosion model for USDA, WEPP (Water Erosion Prediction Project technology), Trans. Am. Soc. Agric. Engnrs., 32, 1587-1593.

Nicholas, A.P. & Quine, T.A. (2007). Crossing the divide: Representation of channels and processes in reduced-complexity river models at reach and landscape scales. Geomorphology, 90, 318-339.

Nugent, C. (1986). Historical changes in the behaviour of the Zambezi river at Nyamuomba. Zimbabwe Sci. News, 20, 121-131.

Nugent, C. (1990). The Zambezi river: tectonism, climatic change and drainage evolution. Palaeogeography, Palaeoclimatology, Palaeoecology, 78, 55-69.

Ongley, E.D. (1982). Influence of season, source and distance on physical and chemical properties of suspended sediment. In: Recent Developments in the Explanation and Prediction of Erosion and Sediment Yields, Proc.Exeter Symp. July 1982. 371-384. IAHS Publ.n°137.

Orpen, J.L & Swain, C.J. & Nugent, C. & Zhou, P.P. (1989). Wrench-fault ant half-graben tectonics in the development of the Palaeozoic Zambezi Karoo basin in Zimbabwe - the “lower Zambezi” and “mid-Zambezi” basins respectively – and regional implications. Journal of African Earth Sciences. 8, (2/3/4), 215-229.

Parker, G. P. & Klingeman, P. C. (1982). On why gravel bed streams are paved. Water Resources Research, 18-5, 1409–1423.

Parker, G. & Paola, C. & Leclair, S. (2000). Probabilistic Exner sediment balance equation for mixtures with no active layer, Journal of Hydraulic Engineering - ASCE, 126, 818.

Peart, M. & Walling, D.E. (1982). Particle size characteristics of fluvial suspended sediment. In: Recent Developments in the Explanation and Prediction of Erosion and Sediment Yields, Proc.Exeter Symp. July 1982. 371-384. IAHS Publ.n°137.

Pelpola, C.P & Hickin, E.J. (2004). Long-term bed load transport rate based on aerial-photo and ground penetrating radar surveys of fan-delta growth, Coast Mountains, British Columbia. Geomorphology, 57, 169-181.

Petts, G.E. & Gurnell, A.M. (2005). Dams and geomorphology: Research progress and future directions. Geomorphology, 71, 27-47.

Proc. of the joint U.S.-Chinese Workshop on Sediment Transport and Environmental Studies, Marquette University, Milwaukee, Wis., July 2002 – Int. Journal of Sediment Research,18, (2), 2003.

Renschler, C.S. & Harbor, J. (2002). Soil erosion assessment tools from point to regional scales – the role of geomorphologists in land management research and implementation. Geomorphology, 47, 189-209.

Ricci, V. (2006). Principali tecniche di regressione con R. Lecture notes, vito_ricco@yahoo.it.

Roehl, J.E. (1962). Sediment source areas, and delivery ratios influencing morphological factors, International Association of Hydrological Sciences 59, 202–213.

Ronco, P. & Fasolato, G. & Di Silvio G. (2006). The case of Zambezi River in Mozambique: some investigations on solid transport phenomena downstream Cahora Bassa Dam. Proceeding of International Conference on Fluvial Hydraulics, Riverflow 2006. Lisbon, 1345-1354.

Ronco P. & Fasolato G. & Di Silvio G. (2007a). Simulating the profile evolution of large unsurveyed rivers: the case of Zambezi (Austral Africa). Proceedings of the 32nd IAHR Congress, Venice (CD).

Ronco P. & Fasolato G. & Di Silvio G. (2007b). Modelling evolution of bottom profile and grainsize distribution in unsurveyed rivers. Geomorphology, (in revision).

Ronco P. & Fasolato G. & Di Silvio G. (2008). Morphological effects of damming on lower Zambezi. Int. Journal of Sediment Research, (in revision).

SCC Brokonsult (Scandiaconsult), 2001. Final Report: Three Crossing Schemes. Consulting Services for Zambeze River Crossing at Caia in Mozambique. Ministerio das Obras Publica e Habitaçao, Republica de Moçambique. Maputo, 5.

Schumm, S.A. (1969). River metamorphosis. Proc. Am. Soc. Civ. Eng., J. Hydraul. Div. HY1, 255-273.

Schumm, S.A. (1973). Geomorphic thresholds and complex response of drainage system. In: Fluvial Geomorphology, Proceedings of the 4th Annual Geomorphology Symposia. Bimghamton, New York, George Allen and Unwin, Boston, 299-310.

Scodanibbio, L. & Manez, G. (2005). The World Commission on Dams: a fundamental step towards integrated water resources management and povery reduction? A pilot case in the lower Zambezi, Mozambique. Physics and Chemistry of the Earth, 30, 976-983.

SMEC (2004). Final Report – Zambeze River Basin Mozambique Flood Risk Analysis Project, Maputo. 2.

Shoko, D.S.M. & Gwavava, O. (1999). Is magmatic underplating the cause of post-rift uplift and erosion within the Cahora Bassa basin, Zambezi rift, Zimbabwe? Journal of African Earth Sciences. 28 (2), 465-485.

Sun, T. & Paola, C. & Parker, G. & Meakin, P. (2002). Fluvial fan delta: linking channel processes with large-scale morphodynamics. Water Resources Research, 38 (8), 1151.

Suschka, J. & Napica, P. (1986). Ten years after the conclusion of Cabora Bassa Dam. The impacts of large water projects on the environment: proceedings of an international symposium. Paris, UNEP/UNESCO. 171-203.

Starmans, G.A.N. (1950). The hydrology of the Tana river. Proc. Conference on Hydrology and Water Resources, Nairobi.

Strahkov, N.M (1967). Principles of Lithogenesis, vol.1, Olivier&Boyd, Edimbugh.

Sumi, T. & Hirose, T. (2002). Accumulation of Sediments in Reservoirs, EOLSS – Encyclopedia of Life Support Systems.

Sutherland, R.A. & Bryan, R.B. (2003) Variability of particle size characteristics of sheetwash sediments and fluvial suspended sediment in a small semiarid catchment, Kenya. Catena, 16(2), 189-204.

Syvitski, J.P. & Morehead, M.D. & Bahr, D.B. & Mulder, T. (2000). Estimating fluvial sediment transport: the rating parameters. Water Resources Research, 36 (9), 2747-2760.

Tate E.M. & Farquharson, F.A.K. (2000). Simulating reservoir management under the threat of sedimentation: the case of Tarbela dam on the river Indus. Water Resources Management, 14, 191-208.

Thomas, D.S.G. & Shaw, P.A. (1992). The Zambezi river: tectonism, climatic change and drainage evolution – is there really evidence for a catastrophic flood? A discussion. Palaeogeography, Palaeoclimatology, Palaeoecology. 91, 175-182.

Trebossen, H. & Deffontaines, B. & Classeau, N. & Kouame, J. & Rudant, J.P. (2005). Monitoring coastal evolution and associated littoral hazards of Frech Guiana shreline evolution with radar images. Geoscience, 337, 1140-1153.

Walford, H.L. & White, N.J. & Sydow, J.C. (2005). Solid sediment load history of the Zambezi Delta. Earth and Planetary Science Letters, 238, 49-63.

Walling, D.E. & Webb, B.W. (1983). The dissolved loads of rivers: a global overview. In: dissolved Loads of Rivers and Surface Water Quantity/Quality Relationships. Proc.Florence Symp. June 1981. 177-194, IAHS Publ. n°133.

Walling, D.E., (1984). The sediment yields of African rivers. Proc. of the Harare Symposium: Challenges in Africa Hydrology and Water Resources, 1984. IAHR Publ.n°144.

Walling, D.E. & Webb, B.W. (1988). The reliability of rating curve estimates of suspended sediment yield; some further comments. Sediment Budgets (Eds. Bordas, M:P:, Walling, D.E.). IAHS Publications no. 174, IAHS Press, Wallingford, U.K., 337-350.

Walling, D.E. & Webb, B.W. (1996). Erosion and sediment yield: global and regional perspectives, IAHS Publ.n° 236.

Wang, Z-Y. & Wu, B. & Wang G. (2007). Fluvial processes and morphological response in the Yellow and Weihe Rivers to closure and operation of Sanmenxia Dam. Geomorphology. 91 (1-2), 65-79.

White, W.R. (2001) "Evacuation of Sediments from Reservoirs" Thomas Telford Publishing, London, 2001

Wicks, J.M. & Bathurst, J.C. (1996). SHE-SED: A physically based, distributed erosion and sediment yield component for the SHE hydrological modelling system, Journal of Hydrology, 175 (1-4), 213-238.

Williams, J.R. and Berndt H.D., (1972). Sediment Yield Computed with Universal Equation, Journal of the Hydraulics Division, 98 (12), 2087-2098.

Wischmeier W.H. & Smith D.D. (1978). Predicting rainfall erosion losses a guide to conservation planning U.S.D.A. Washington, Agr. Handbook No. 557.

Wolock, D.M. & Price, C.V. (1994). Effect of Digital Elevation Model map scale and data resolution on a topography based watershed model. Water Resources Research. 30(11):3041-3052

World Meteorological Organization (WMO), (2005). WHYCOS Guidelines. WMO/TD-No.1282.

World Commission on Dams (WCD), (2000). Dams and Development - A New Framework For Decision-Making, Earthscan, London & Sterling, VA.

Wu, W. & Wang, S., Y. & Jia, Y. (2000). Non uniform sediment transport in alluvial rivers. Journal of Hydraulic Research, 38 (6).

Yang, X. (2005). Manual on sediment management and measurements. WMO, Operational Hydrology Report n°47, pp.176.

Zaghloul, S.S. (2006). Effects of Aswan High Dam on the Nile river regime at delta barrages area. Proceeding of the International Sediment Initiative Conference (ISIC). Khartoum, 12-15 November 2006, Sudan.

Zhang, W. & Montgomery, R. (1994). Digital Elevation Model grid size, landscape representation and hydrologic simulations. Water Resources Research. 30(4):1019-1028.

Zhou, Y. & Lu, X. & Huang, Y. & Zhu, Y. (2004). Anthropogenic impacts on the sediment flux in the dry-hot valleys of southwest China – an example of the Longchuan river. Journal of Mountain Science, 1(3) 239-249.

APPENDIX A: SUSPENDED SEDIMENT LOAD MEASUREMENTS (HALL ET AL., 1973-75)

Sampling Station		Oct	Nov	Dec	Jan	Feb	Mar	Apr	May	Jun	Jul	Aug	Sep	Total [10^6 m^3/year]
Rhodesia (Zambezi)	Q_{eq} [m^3/s]	287	288	1'025	2'149	4'739	4'372	3'754	2'637	1'734	895	541	377	
	Conc. [g/m^3]	64	64	64	344	344	344	344	64	64	64	64	64	
	Q_s [m^3/s]	0.018	0.018	0.066	0.739	1.630	1.504	1.291	0.169	0.111	0.057	0.035	0.024	
	V_s [10^3 m^3]	49.3	47.7	175.7	1'980.3	3'943.9	4'028.6	3'347.4	452.0	287.7	153.4	92.7	62.5	**14.6**
Luangwa	Q_{eq} [m^3/s]	237	290	638	1'157	1'547	1'407	1'034	696	528	440	360	302	
	Conc. [g/m^3]	54	54	54	1016	1016	1016	1016	54	54	54	54	54	
	Q_s [m^3/s]	0.013	0.016	0.034	1.175	1.572	1.429	1.050	0.038	0.029	0.024	0.019	0.016	
	V_s [10^3 m^3]	34.3	40.6	92.3	3'148.3	3'801.9	3'828.4	2'722.3	100.7	73.9	63.7	52.0	42.3	**14.0**
													Total sediment runoff in input – lower Zambezi	**28.6**
Chicoa	Q_{eq} [m^3/s]	525	578	1'663	3'306	6'286	5'779	4'788	3'333	2'263	1'335	901	679	
	Conc. [g/m^3]	89	89	89	490	490	490	490	89	89	89	89	89	
	Q_s [m^3/s]	0.047	0.051	0.148	1.620	3.080	2.832	2.346	0.297	0.201	0.119	0.080	0.060	
	V_s [10^3 m^3]	125.1	133.4	396.4	4'339.2	7'451.4	7'584.8	6'081.1	794.4	521.9	318.2	214.7	156.7	**28.1**
Tete	Q_{eq} [m^3/s]	541	607	1'783	3'571	6'684	5'779	4'910	3'392	2'304	1'363	922	696	
	Conc. [g/m^3]	70	70	70	588	588	588	588	70	70	70	70	70	
	Q_s [m^3/s]	0.038	0.043	0.125	2.099	3.930	3.398	2.887	0.237	0.161	0.095	0.065	0.049	
	V_s [10^3 m^3/year]	101.4	110.2	334.2	5'623.2	9'507.5	9'101.8	7'484.0	635.9	418.0	255.6	172.9	126.4	**33.9**

Table 1.A: computation of the total sediment runoff from the measures made by Hall et al. in the Zambezi catchment (1973-75).

APPENDIX B: DESCRIPTION OF THE BACKWARD-SIMULATION

The backward-simulation procedure permits to compute the river configuration at the time ($t - \Delta t_{back}$), from the river configuration (assumed to be known) at the time t, assuming that one knows the boundary conditions of the river from ($t - \Delta t_{back}$) to t. Let us call $S(x,t)$ any relevant quantity of the river at the time t, e.g. the bottom elevation $z(x,t)$ or the cumulative frequencies of bottom composition $F_k(x,t) = \sum_{i=1}^{k} \beta_k(x,t)$ with ($i=1,2,....k-1$); and let us compute now the regular (forward) evolution of the river from the time t to the time ($t + \Delta t_{back}$), by imposing as boundary conditions of the model the waterflow and the sediment input during the time interval ($t - \Delta t_{back}$) to t. If the evolution process was linear, the required quantity $S(x)$ at the backward instant ($t - \Delta t_{back}$) would be:

$$S(x, t - \Delta t_{back}) = S(x, t + \Delta t_{back}) - 2\Delta S' \qquad (1.A)$$

where $\Delta S'$ is the computed difference:

$$\Delta S' = S(x, t + \Delta t_{back}) - S(x, t) \qquad (2.A)$$

In general, however, the evolution tends to be progressively slower and slower with time: correspondingly the real difference ΔS:

$$\Delta S = S(x, t) - S(x, t - \Delta t_{back}) \qquad (3.A)$$

tends to be larger than $\Delta S'$ in eq.(2.A).

Indeed, if one starts again the forward simulation at ($t - \Delta t_{back}$) with $S(x, t - \Delta t_{back}) = S(x,t) - \Delta S'$ one finds that the best fitting between the new (computed) $S(x,t)$ and the original (measured) $S(x,t)$ takes place after an evolution time $\Delta t'$ quite shorter Δt_{back}. If one calls τ the relative difference:

$$\tau = \frac{\Delta t_{back} - \Delta t'}{\Delta t_{back}} = 1 - \frac{\Delta t'}{\Delta t_{back}} \tag{4.A}$$

and ω the relative difference:

$$\omega = \frac{\Delta S - \Delta S'}{\Delta S} = 1 - \frac{\Delta S'}{\Delta S} \tag{5.A}$$

one may assume for ΔS and Δt_{back} the same relative error $\tau = \omega$. The requested correction $\Delta S'$ is therefore :

$$\Delta S' = \frac{\Delta t'}{\Delta t_{back}} \Delta S \tag{6.A}$$

which may be used to predict the backwards quantities $S(x, t - \Delta t_{back})$ from eq. (1.A).

APPENDIX C: RESULTS OF SIMULATIONS

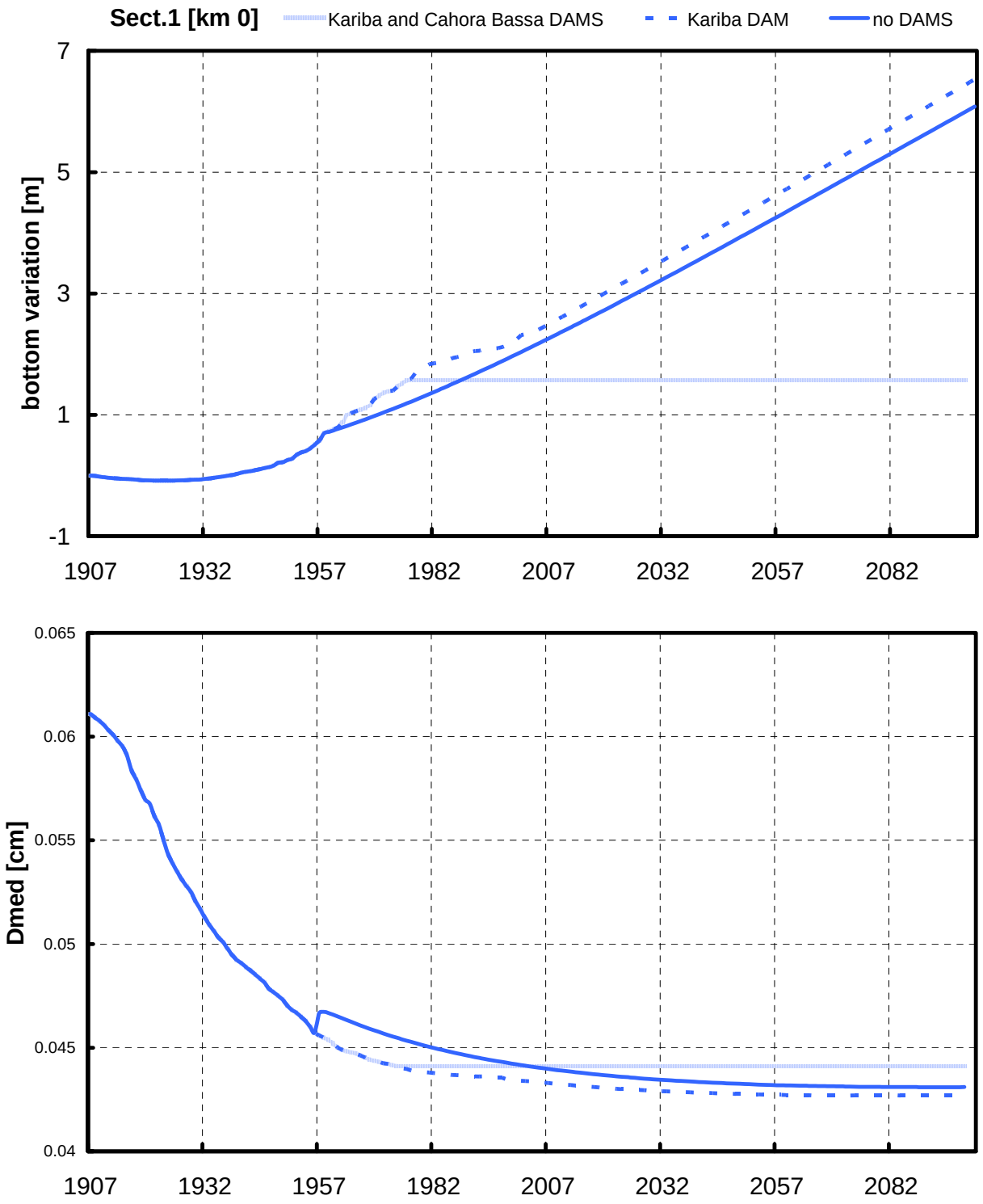

Figure 1.A: Results of simulations from 1907 configuration, in terms of bottom and grainsize variation in Morphological Box n°1 (distance are from Zumbo).

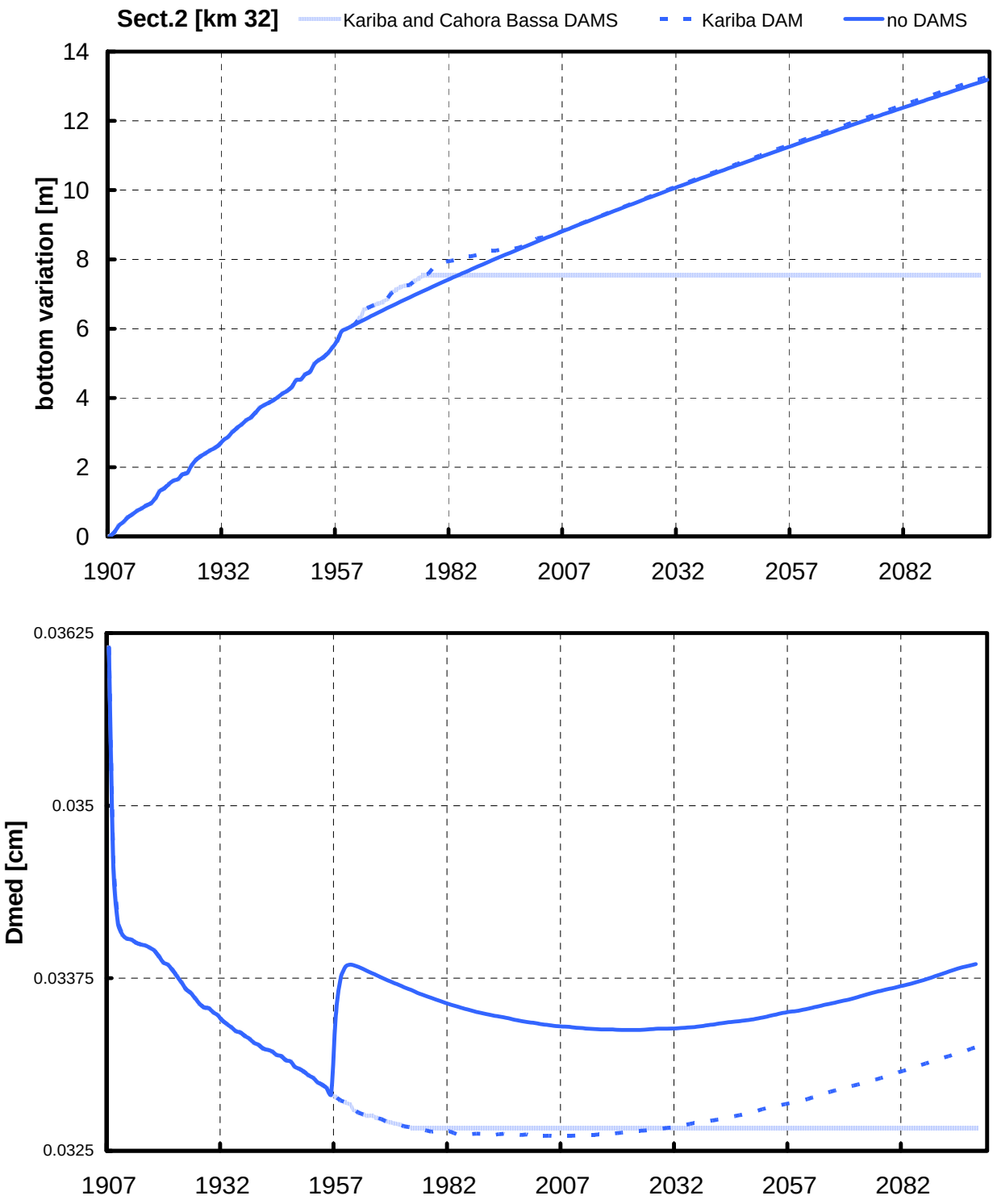

Figure 2.A: Results of simulations from 1907 configuration, in terms of bottom and grainsize variation in Morphological Box n°2 (distance are from Zumbo).

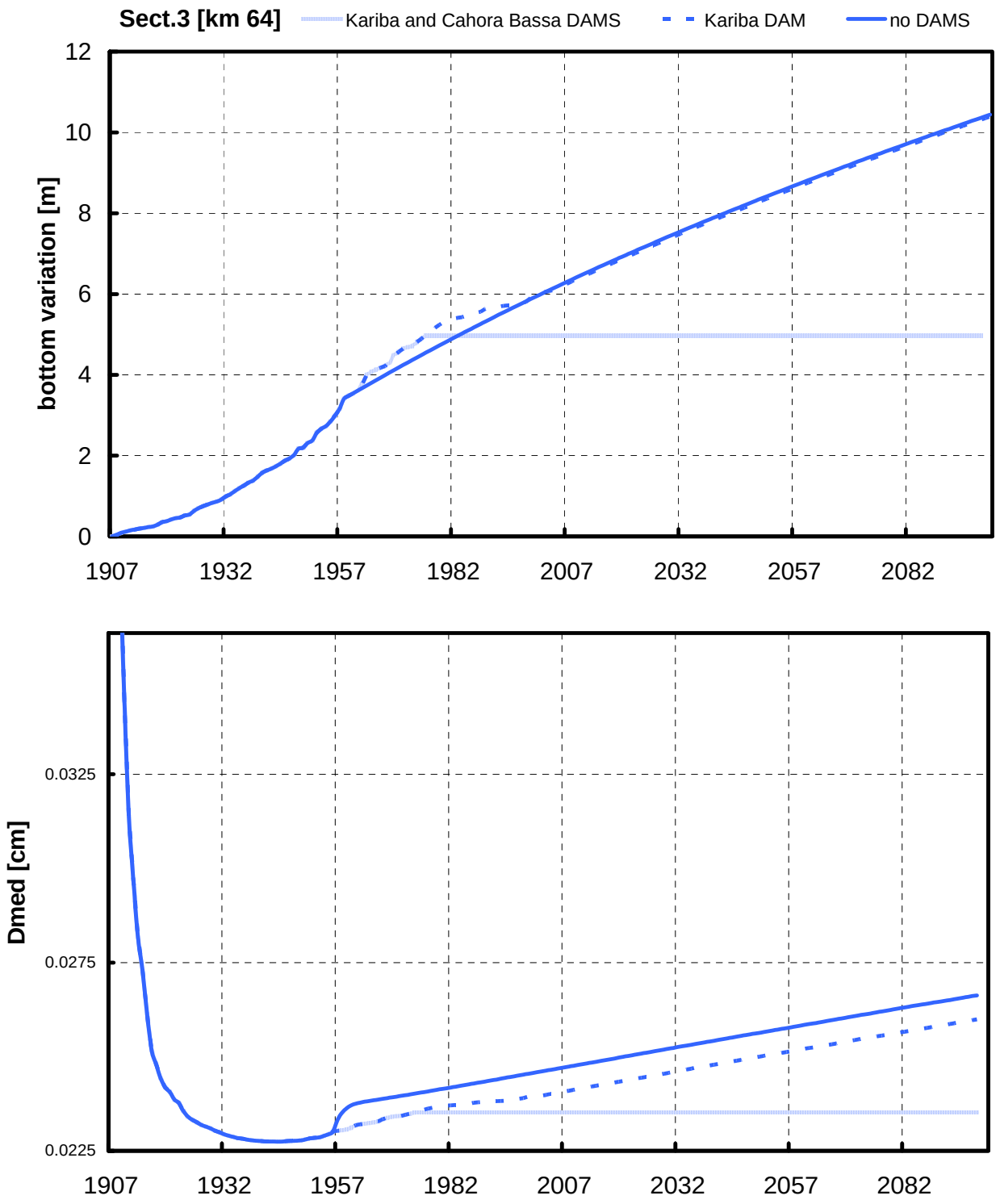

Figure 3.A: Results of simulations from 1907 configuration, in terms of bottom and grainsize variation in Morphological Box n°3 (distance are from Zumbo).

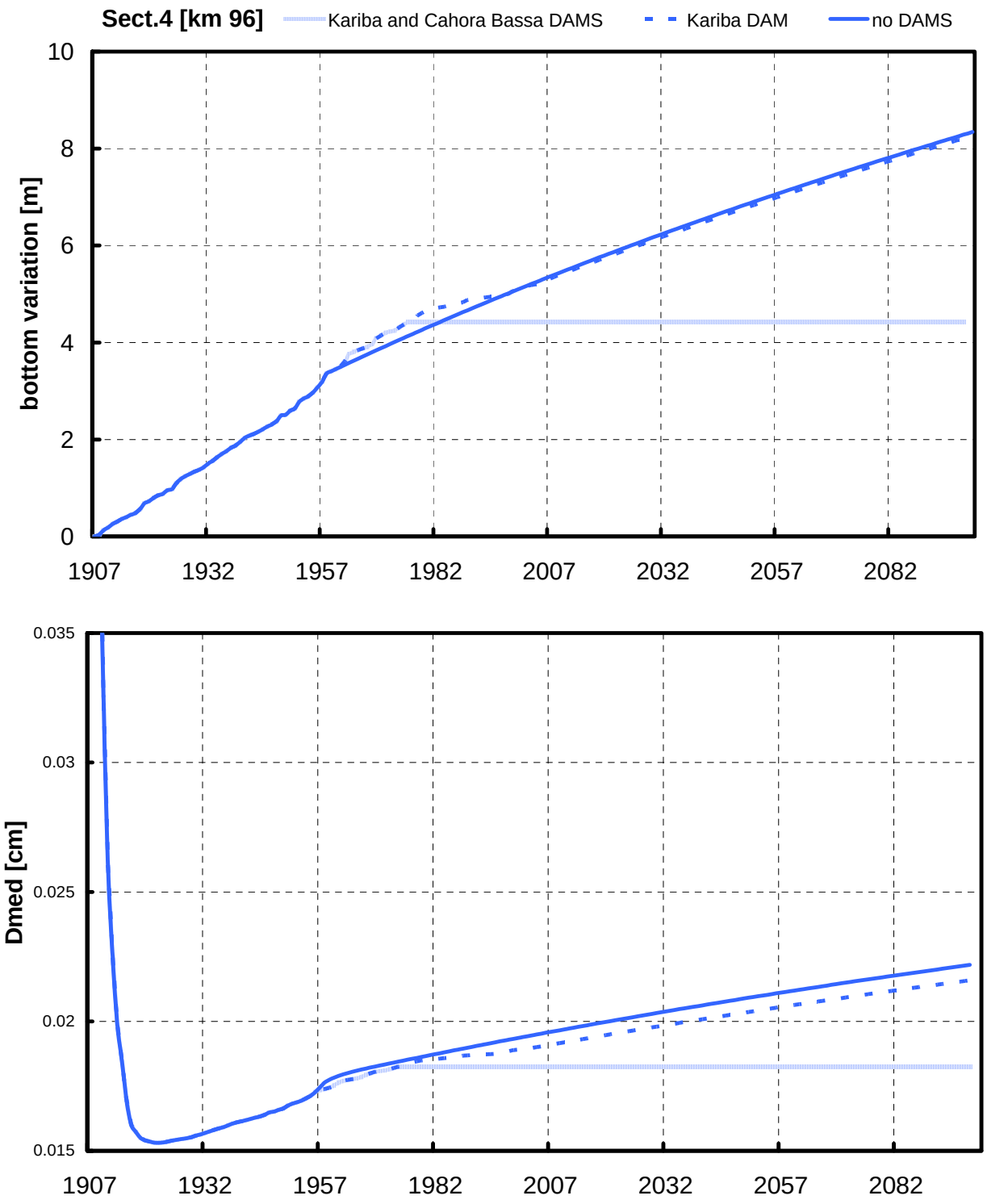

Figure 4.A: Results of simulations from 1907 configuration, in terms of bottom and grainsize variation in Morphological Box n°4 (distance are from Zumbo).

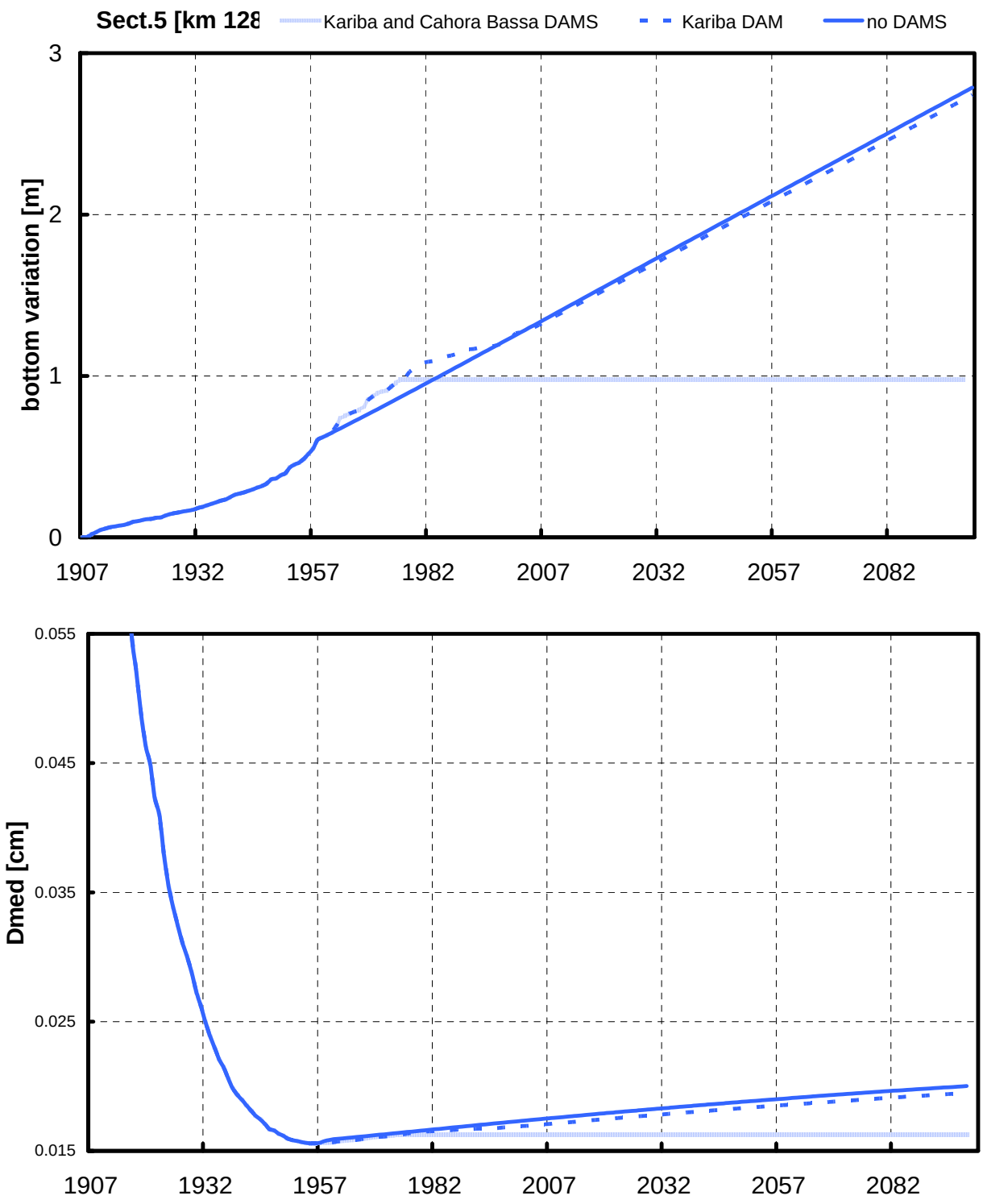

Figure 5.A: Results of simulations from 1907 configuration, in terms of bottom and grainsize variation in Morphological Box n°5 (distance are from Zumbo).

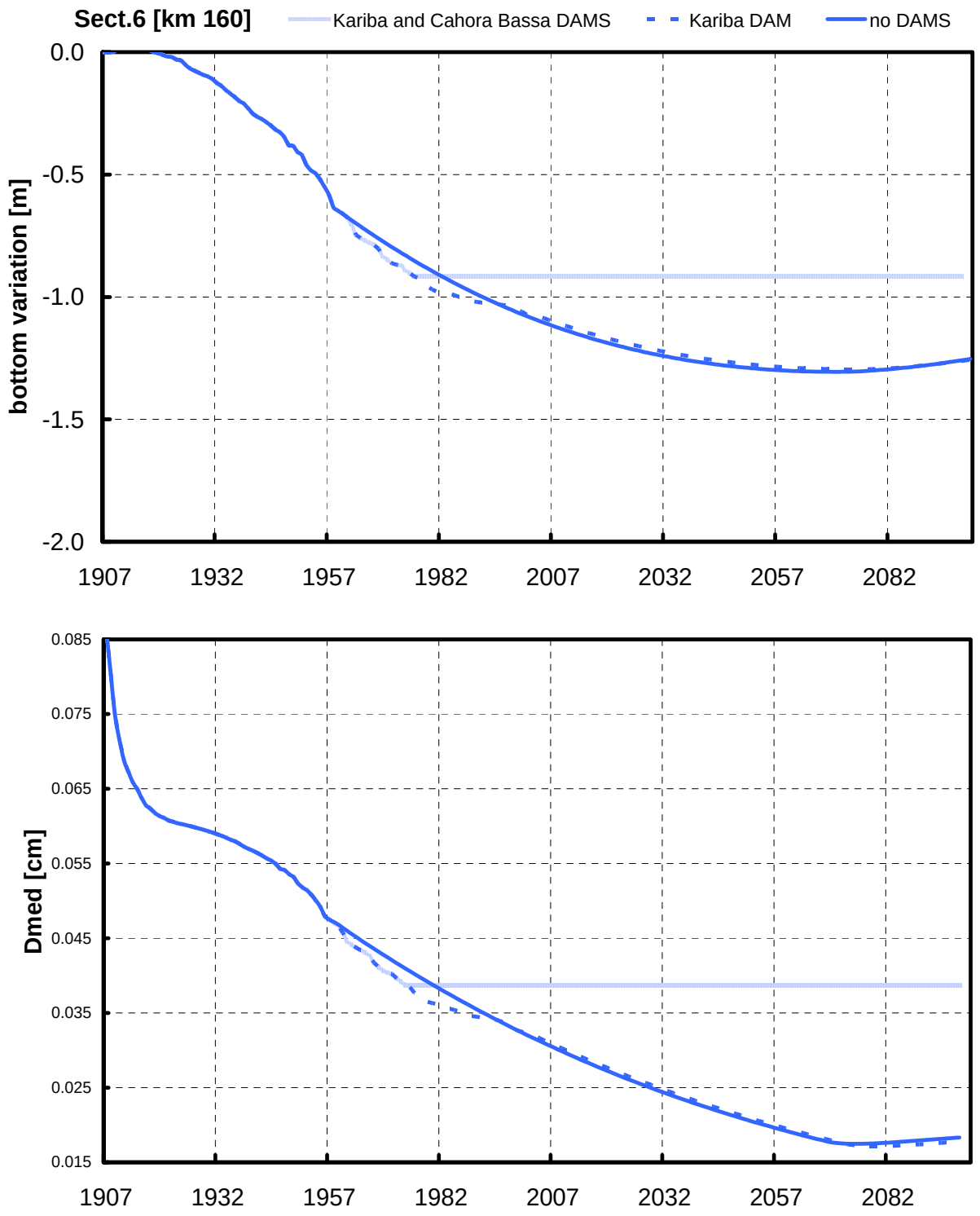

Figure 6.A: Results of simulations from 1907 configuration, in terms of bottom and grainsize variation in Morphological Box n°6 (distance are from Zumbo).

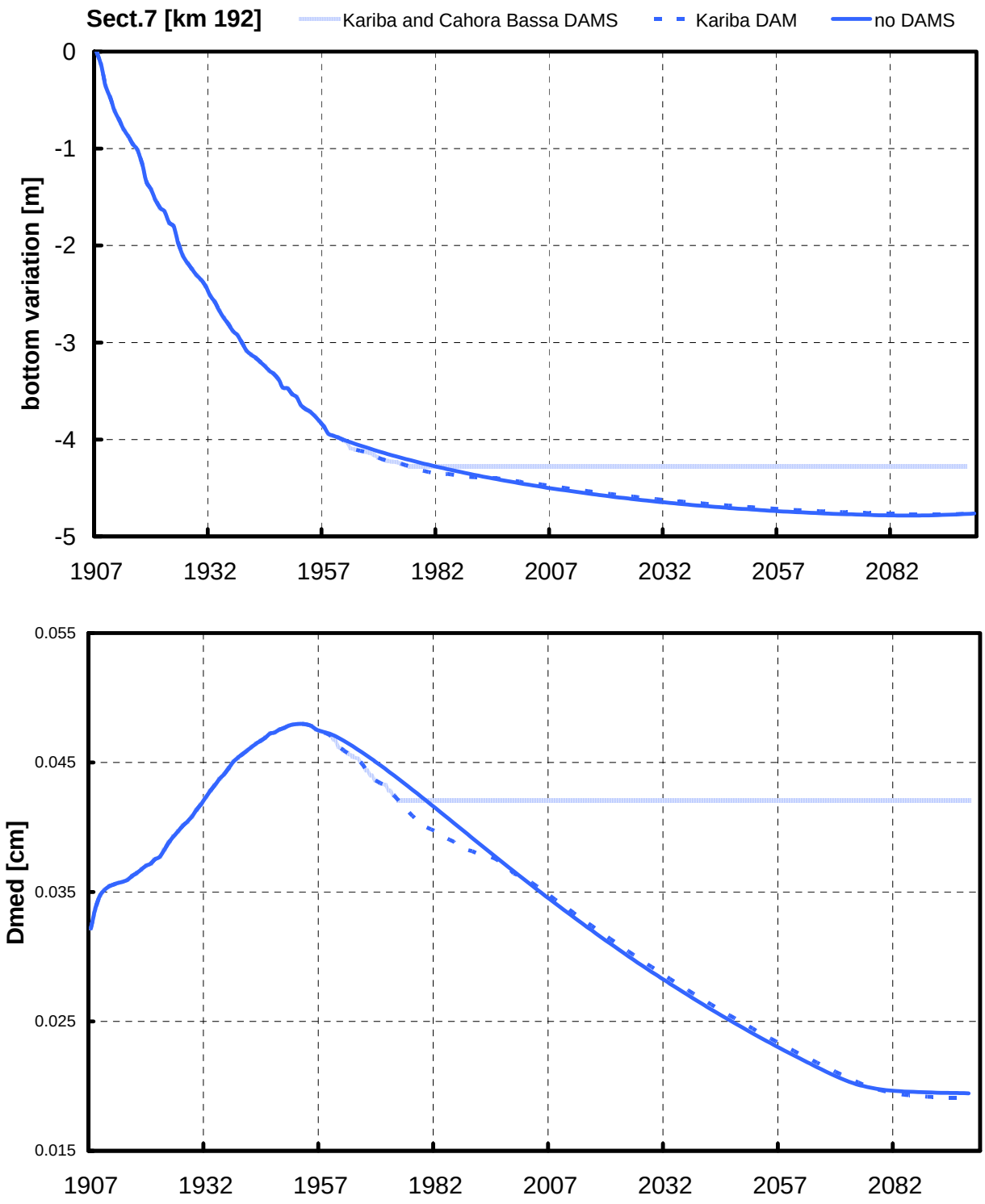

Figure 7.A: Results of simulations from 1907 configuration, in terms of bottom and grainsize variation in Morphological Box n°7 (distance are from Zumbo).

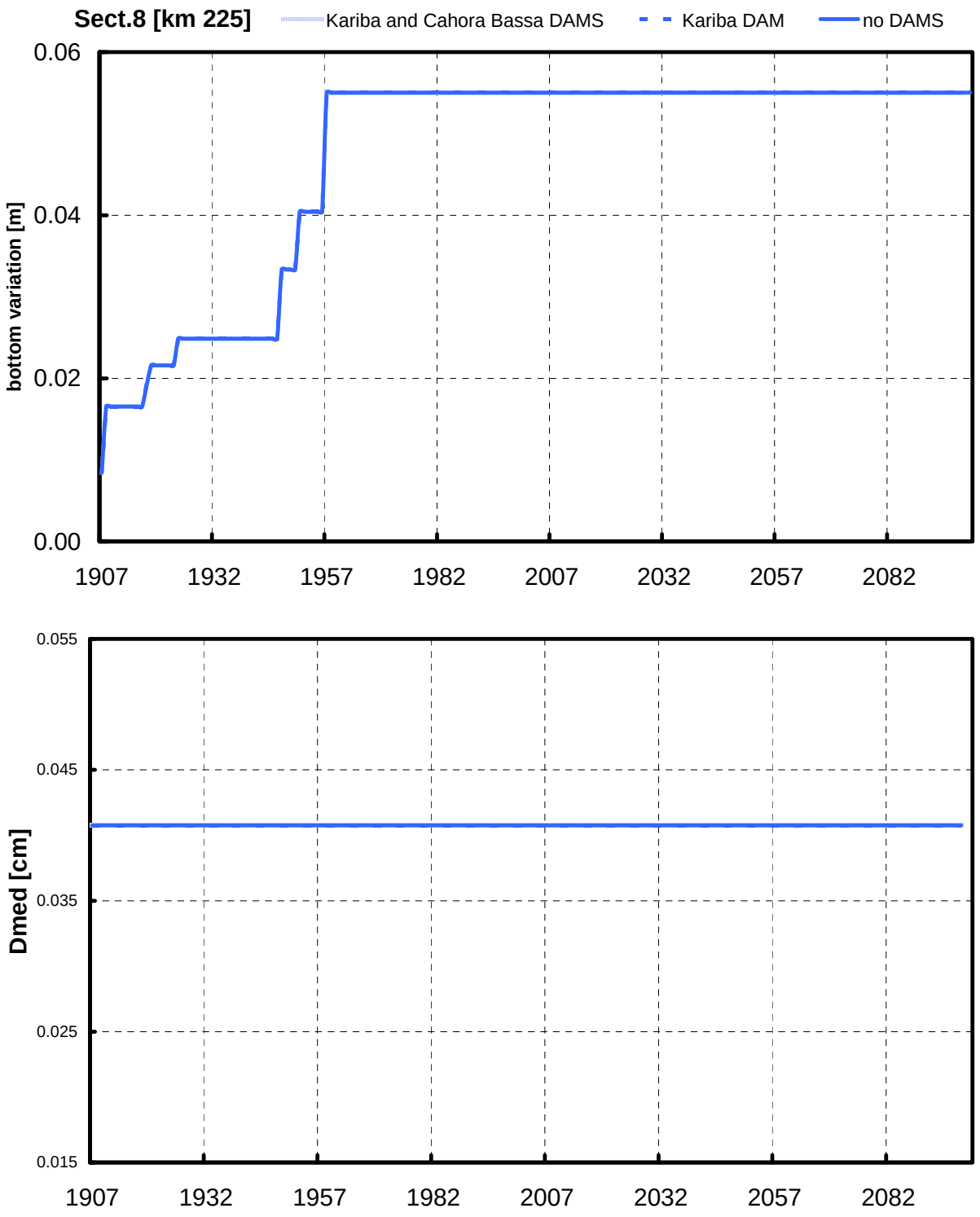

Figure 8.A: Results of simulations from 1907 configuration, in terms of bottom and grainsize variation in Morphological Box n°8 (distance are from Zumbo).

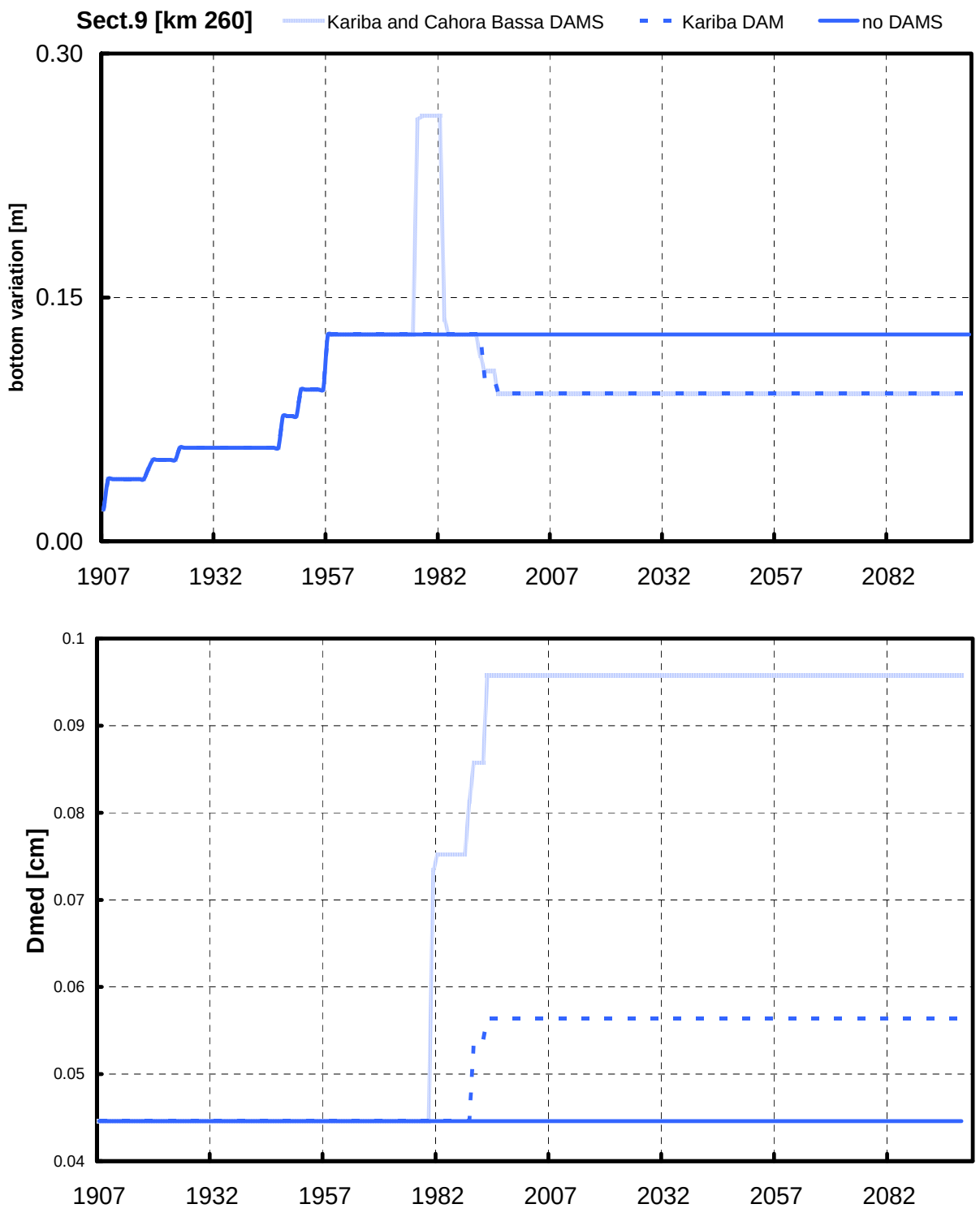

Figure 9.A: Results of simulations from 1907 configuration, in terms of bottom and grainsize variation in Morphological Box n°9 (distance are from Zumbo).

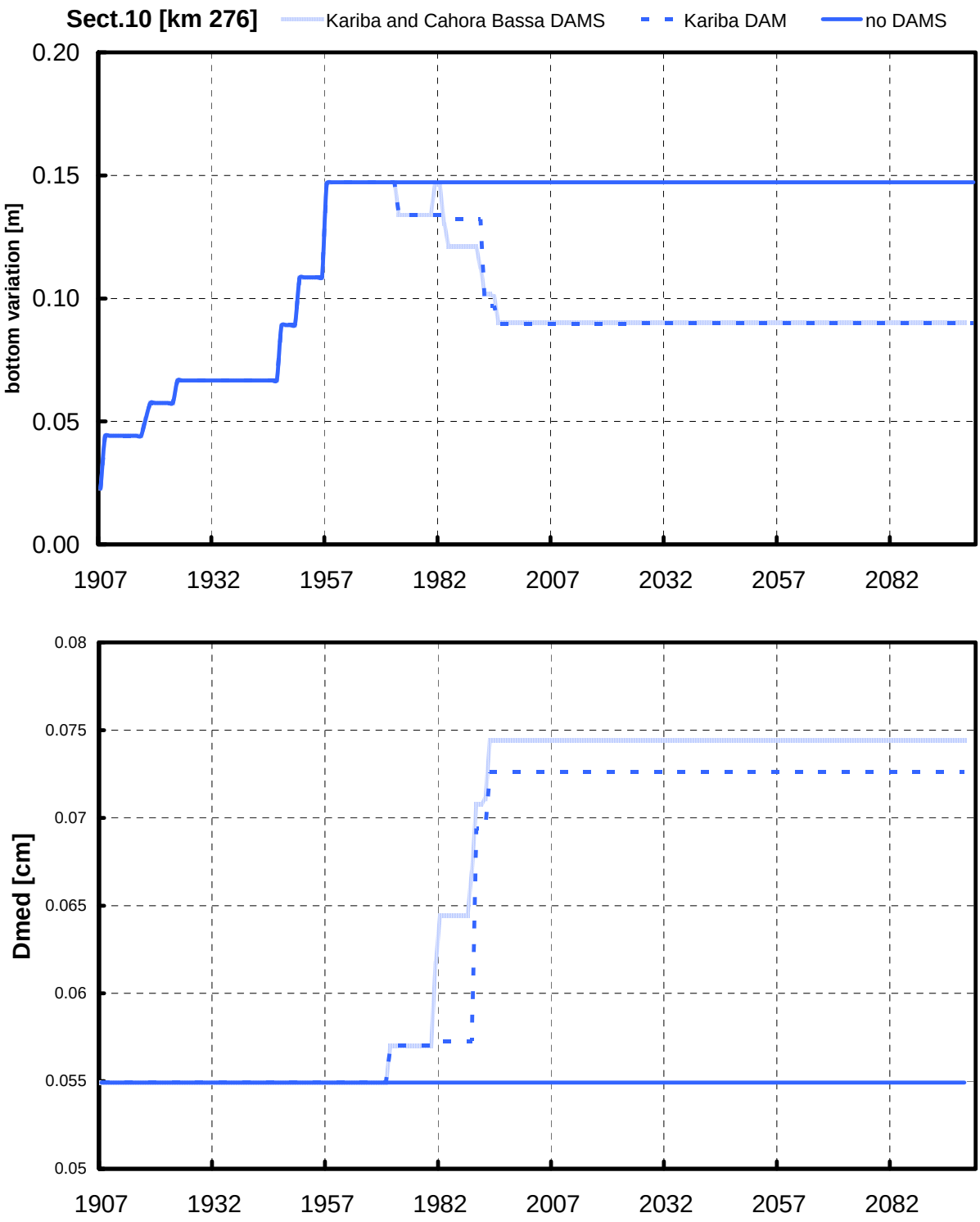

Figure 10.A: Results of simulations from 1907 configuration, in terms of bottom and grainsize variation in Morphological Box n°10 (distance are from Zumbo).

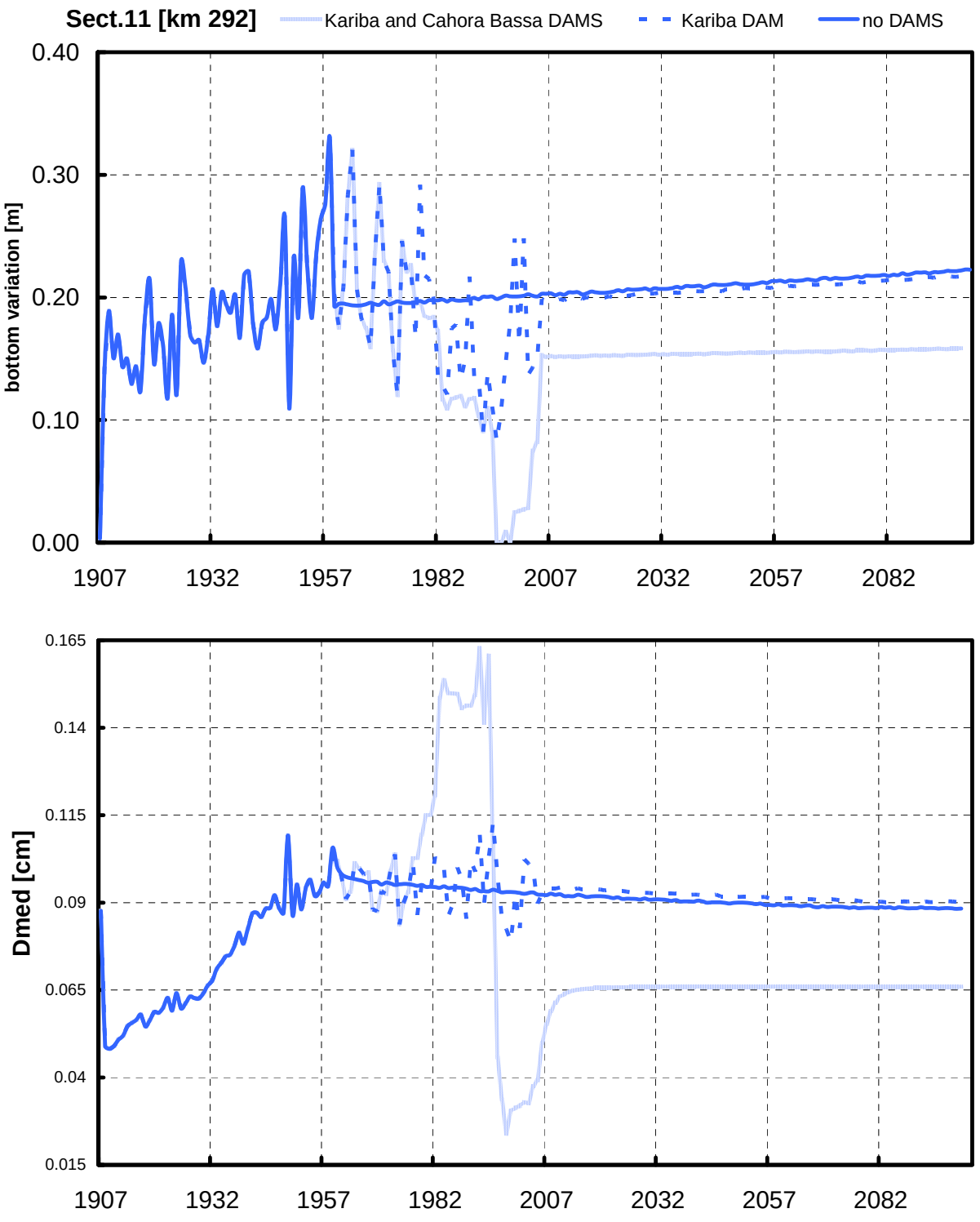

Figure 11.A: Results of simulations from 1907 configuration, in terms of bottom and grainsize variation in Morphological Box n°11 (distance are from Zumbo).

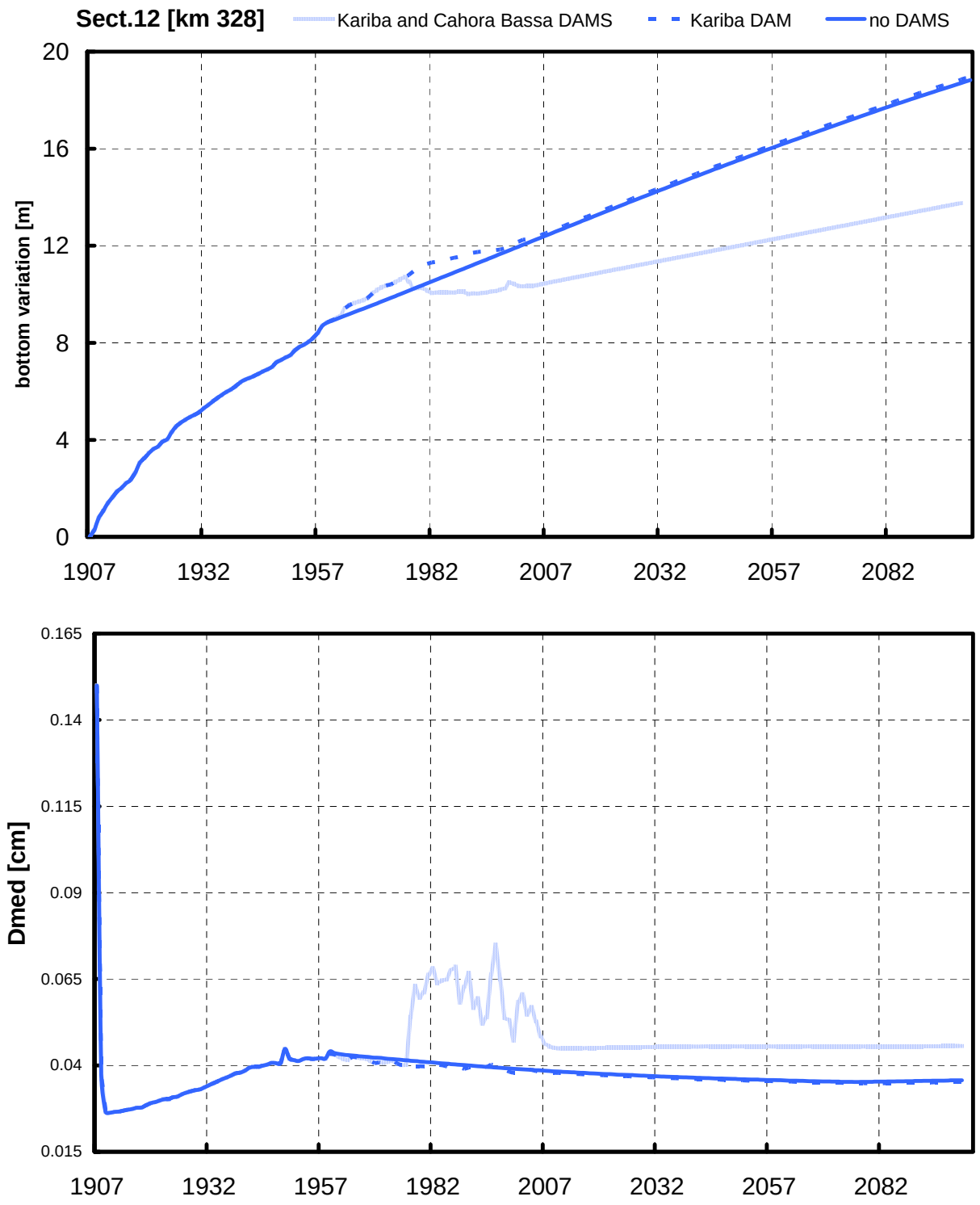

Figure 12.A: Results of simulations from 1907 configuration, in terms of bottom and grainsize variation in Morphological Box n°12 (distance are from Zumbo).

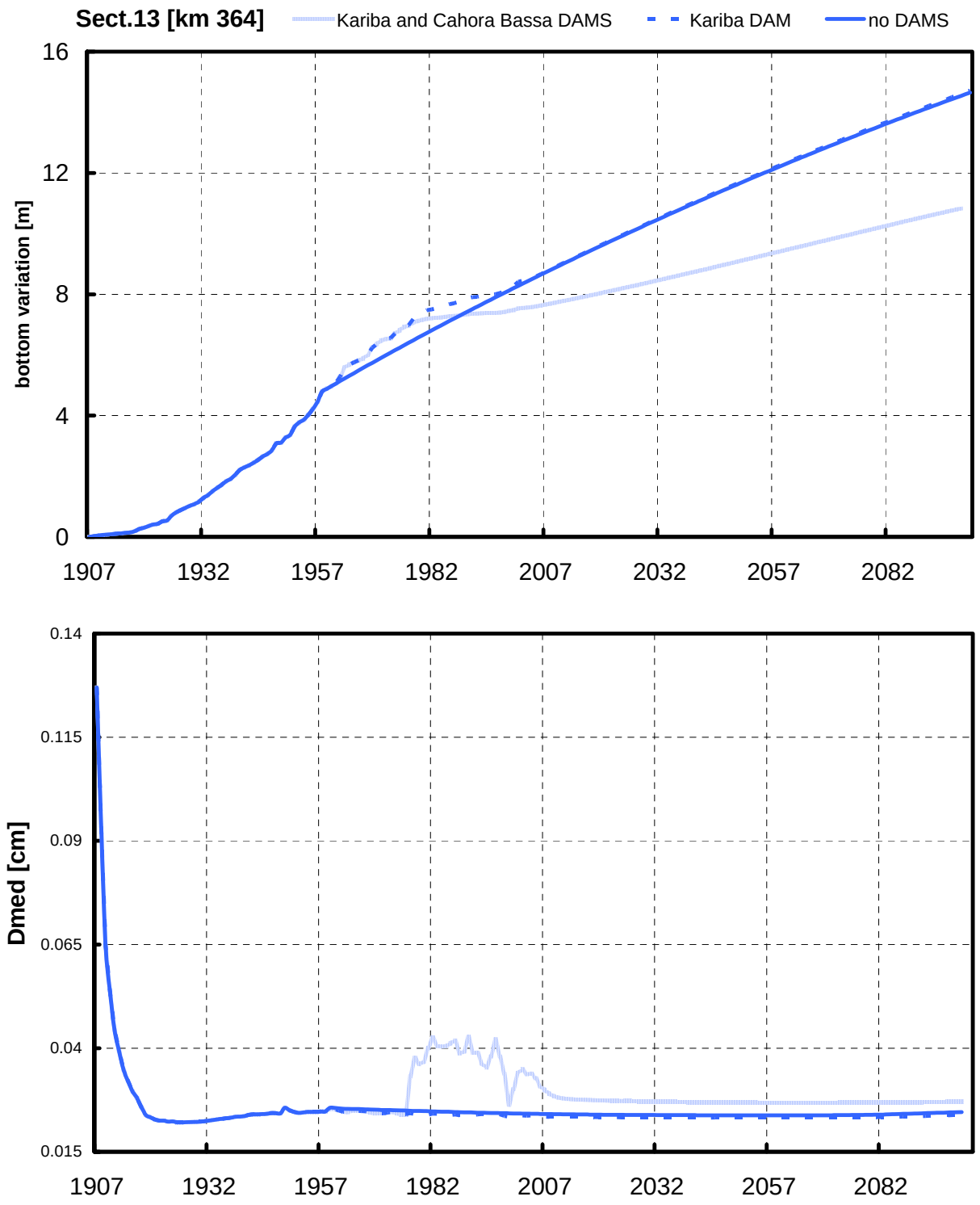

Figure 13.A: Results of simulations from 1907 configuration, in terms of bottom and grainsize variation in Morphological Box n°13 (distance are from Zumbo).

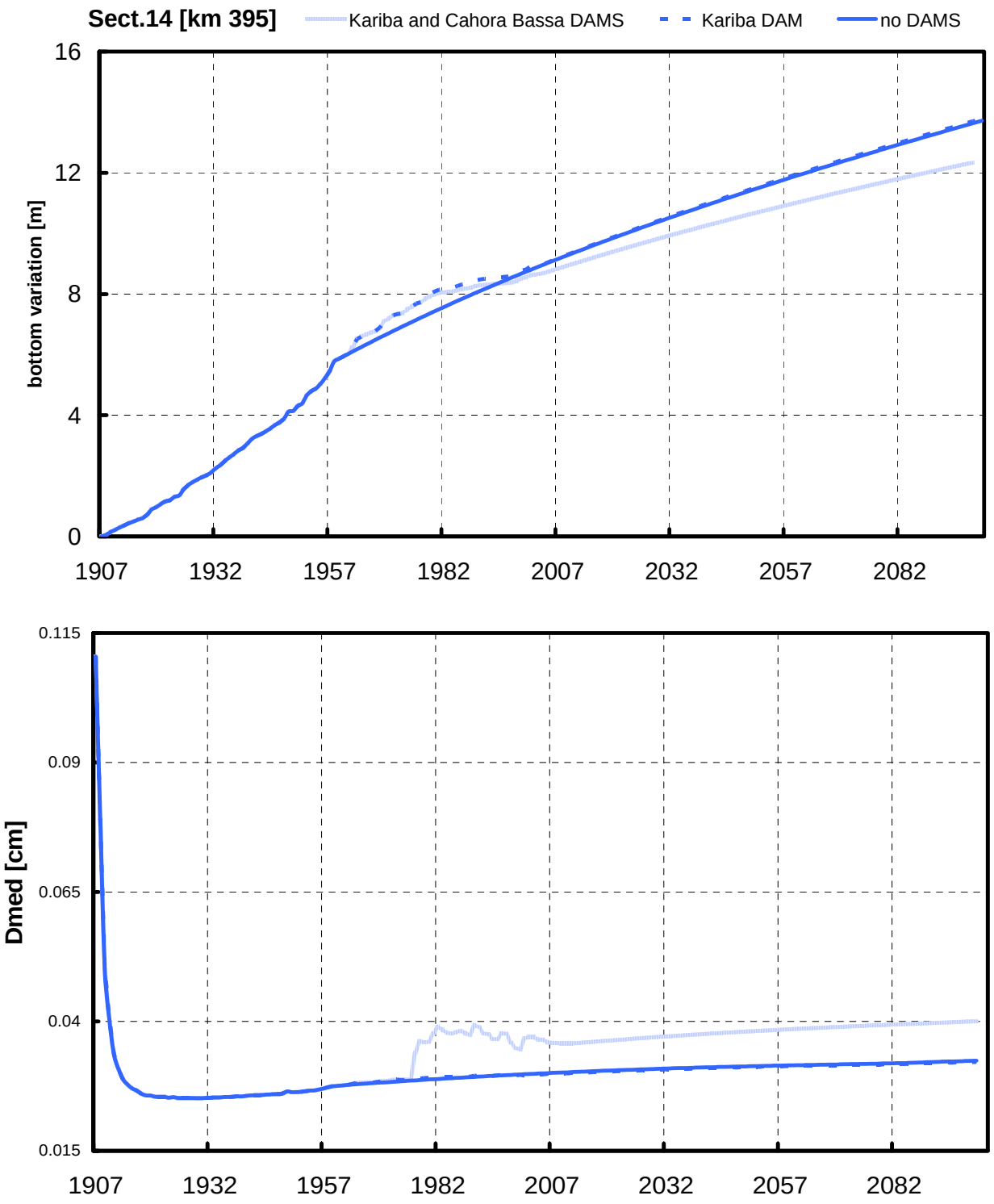

Figure 14.A: Results of simulations from 1907 configuration, in terms of bottom and grainsize variation in Morphological Box n°14 (distance are from Zumbo).

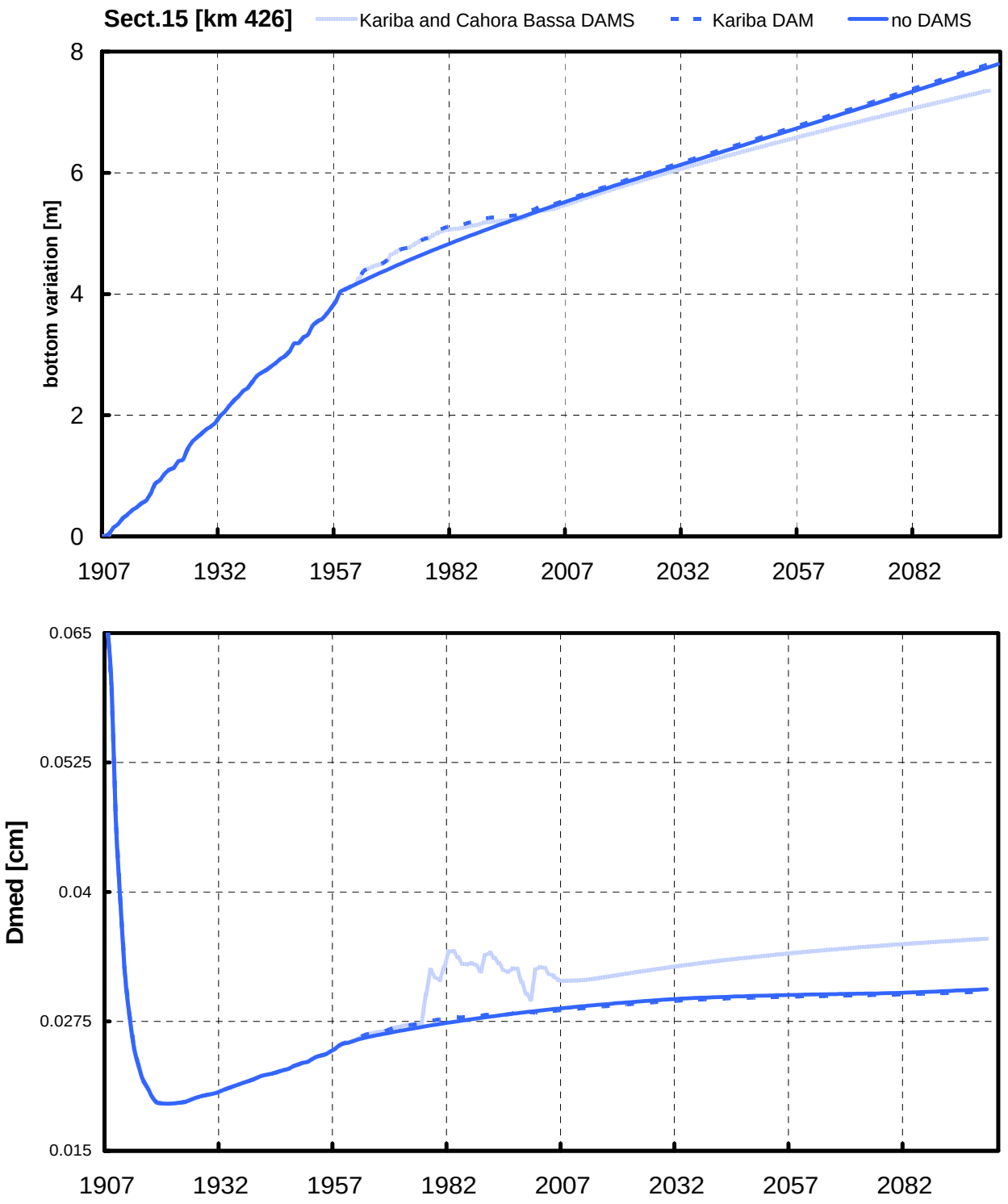

Figure 15.A: Results of simulations from 1907 configuration, in terms of bottom and grainsize variation in Morphological Box n°15 (distance are from Zumbo).

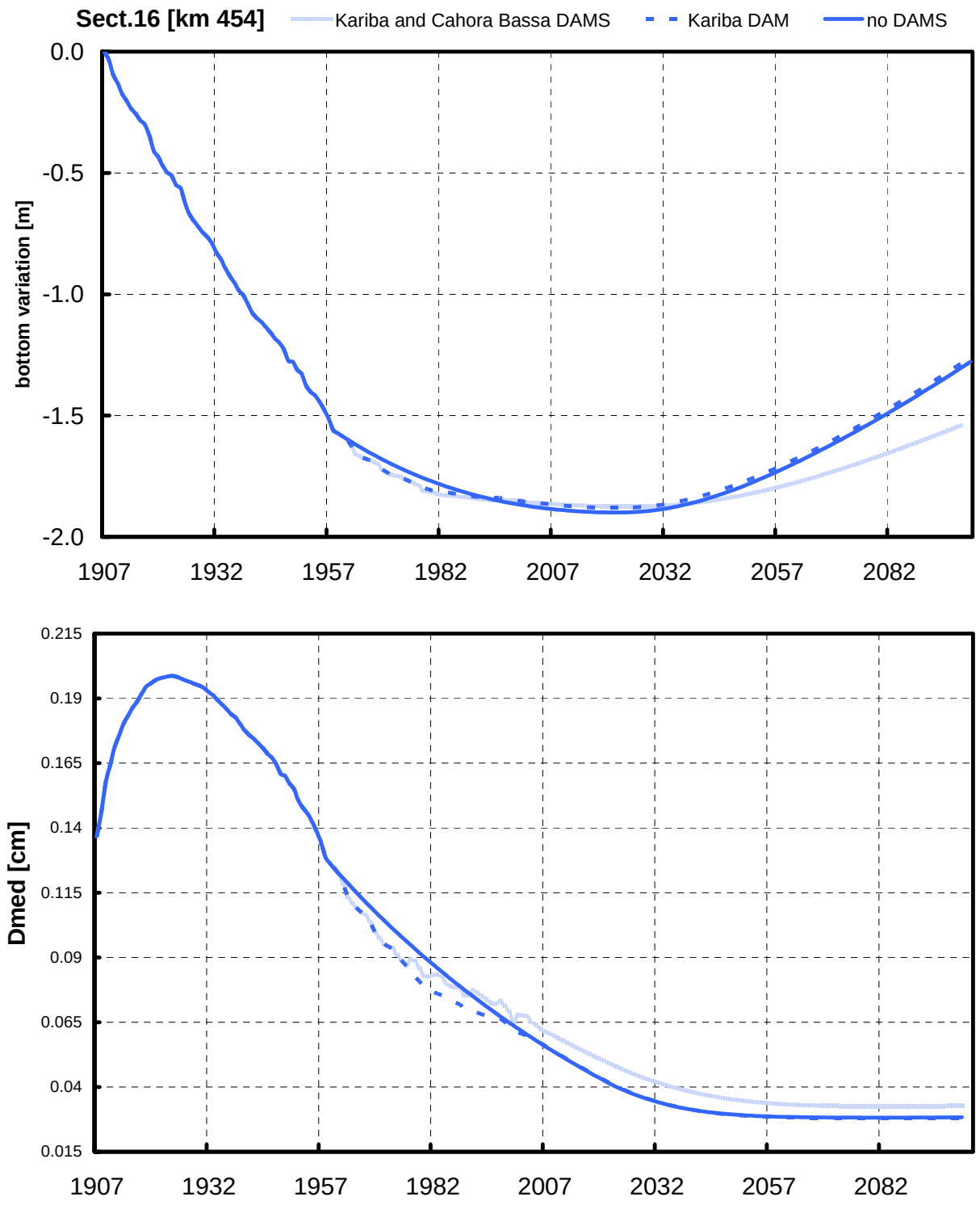

Figure 16.A: Results of simulations from 1907 configuration, in terms of bottom and grainsize variation in Morphological Box n°16 (distance are from Zumbo).

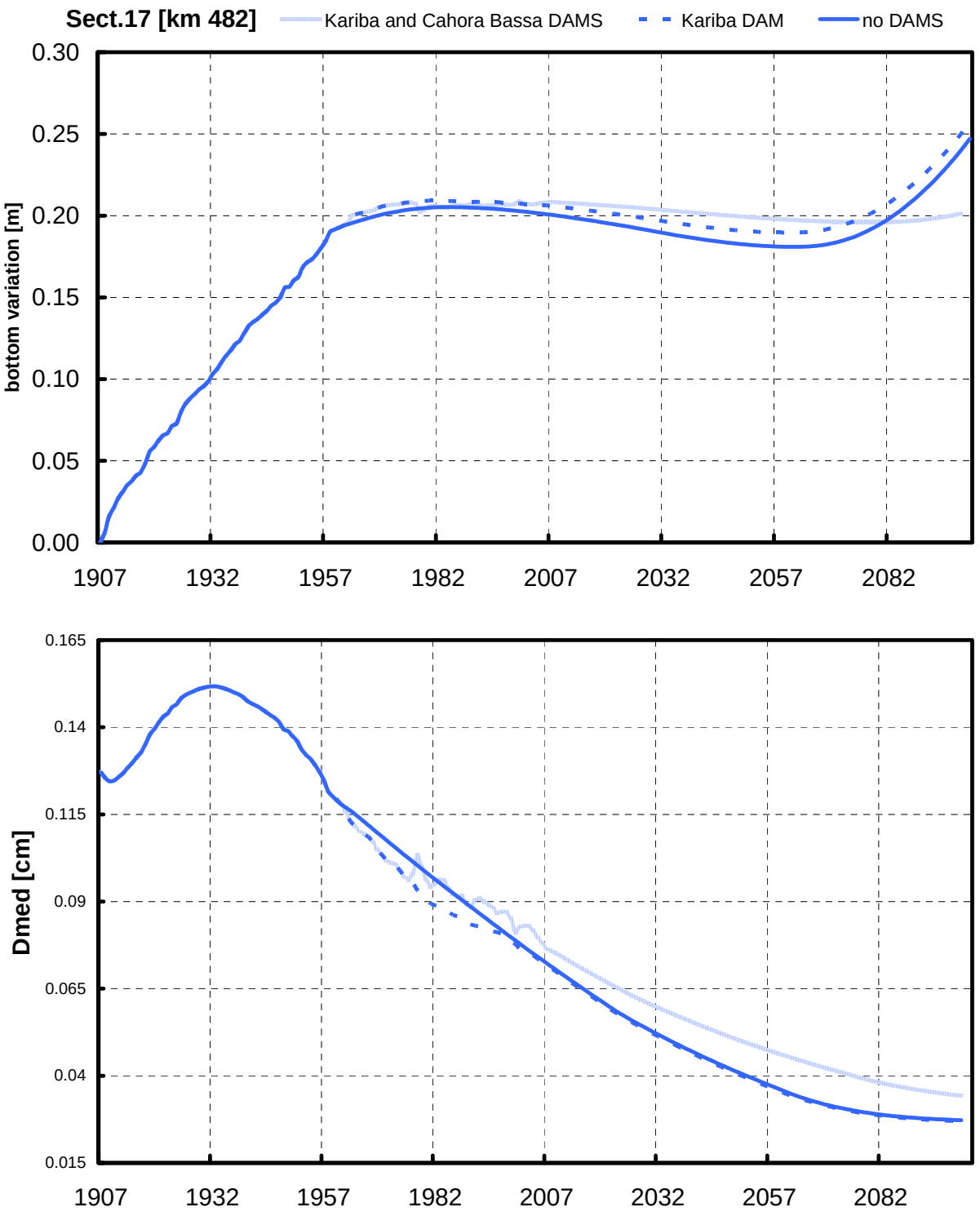

Figure 17.A: Results of simulations from 1907 configuration, in terms of bottom and grainsize variation in Morphological Box n°17 (distance are from Zumbo).

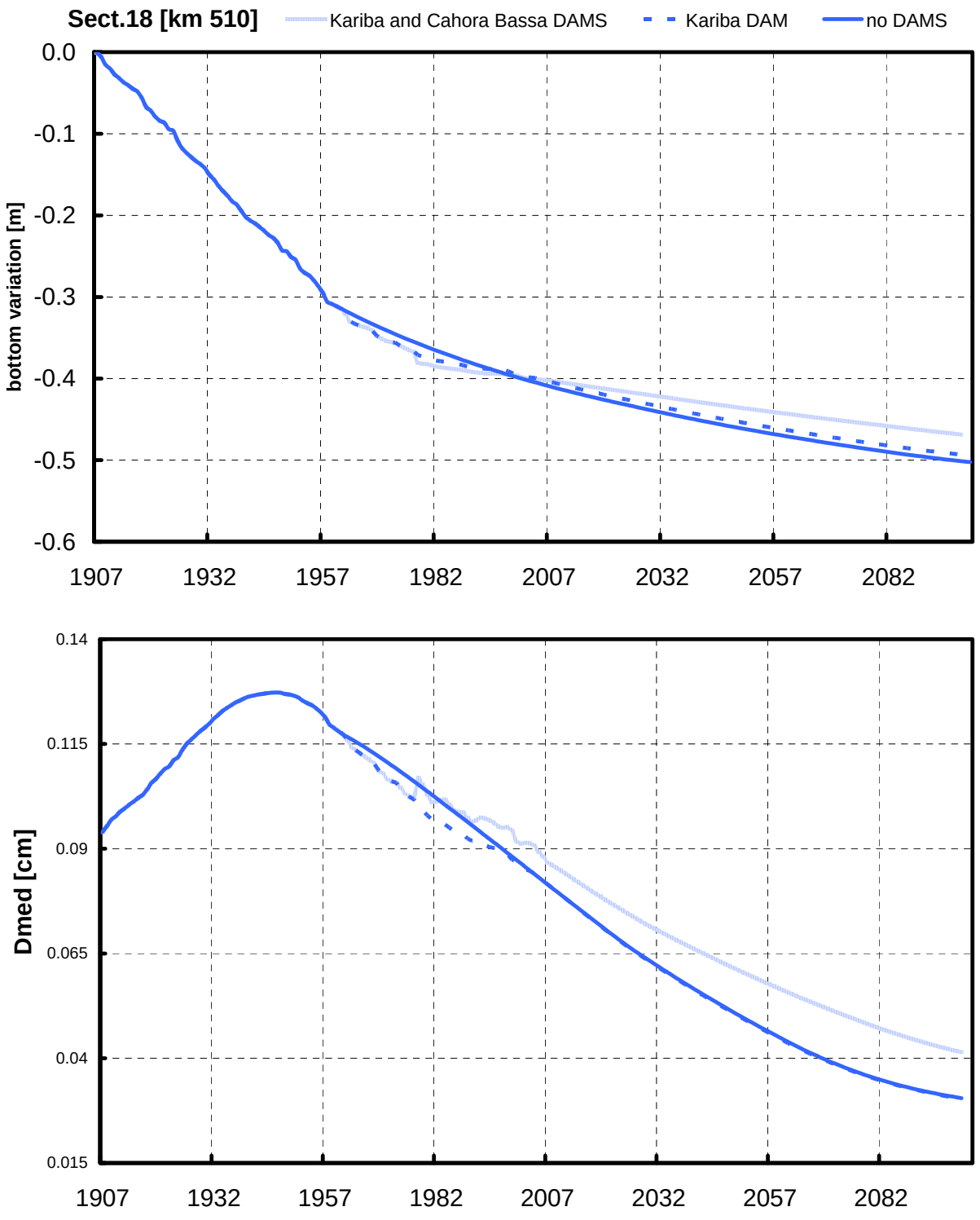

Figure 18.A: Results of simulations from 1907 configuration, in terms of bottom and grainsize variation in Morphological Box n°18 (distance are from Zumbo).

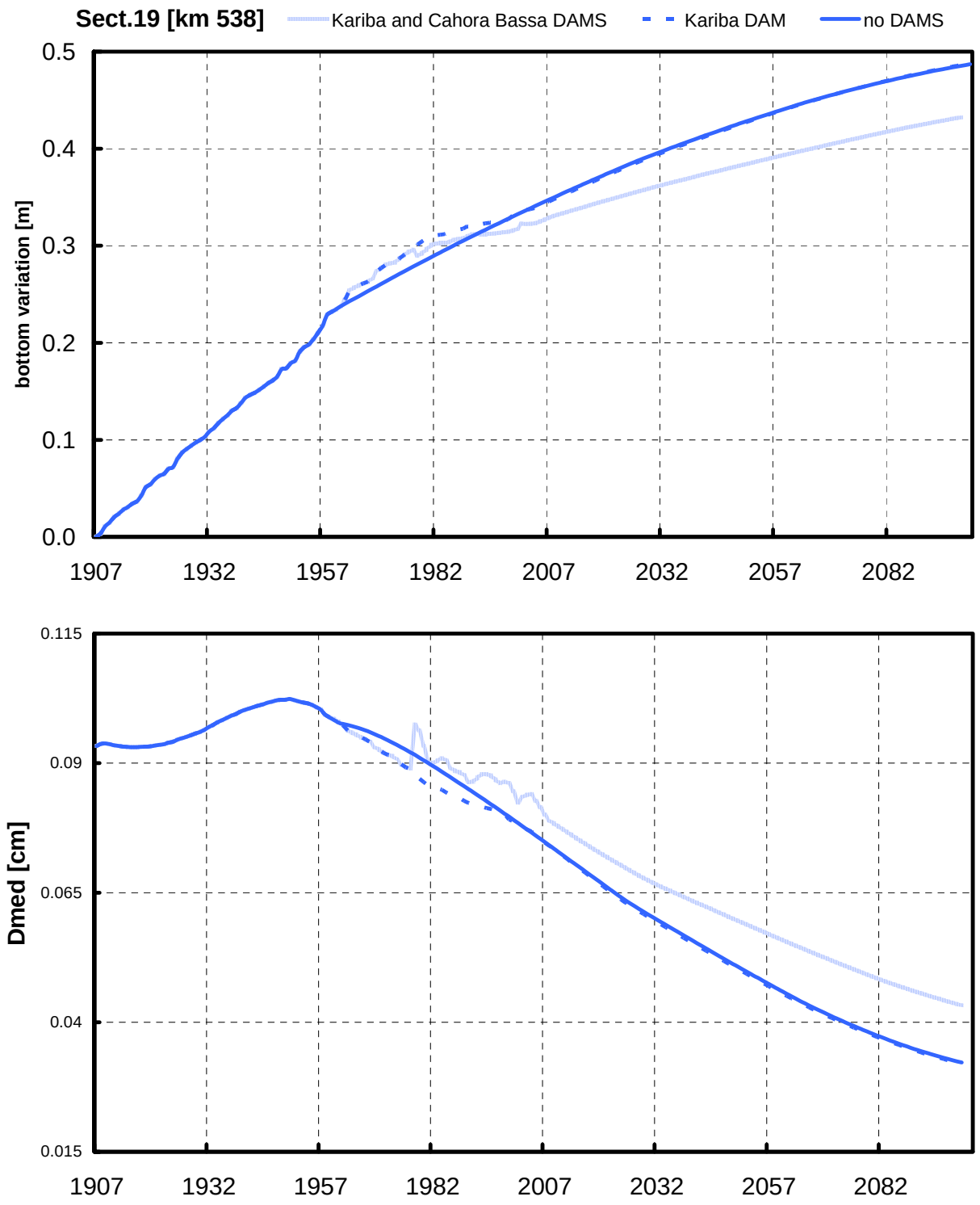

Figure 19.A: Results of simulations from 1907 configuration, in terms of bottom and grainsize variation in Morphological Box n°19 (distance are from Zumbo).

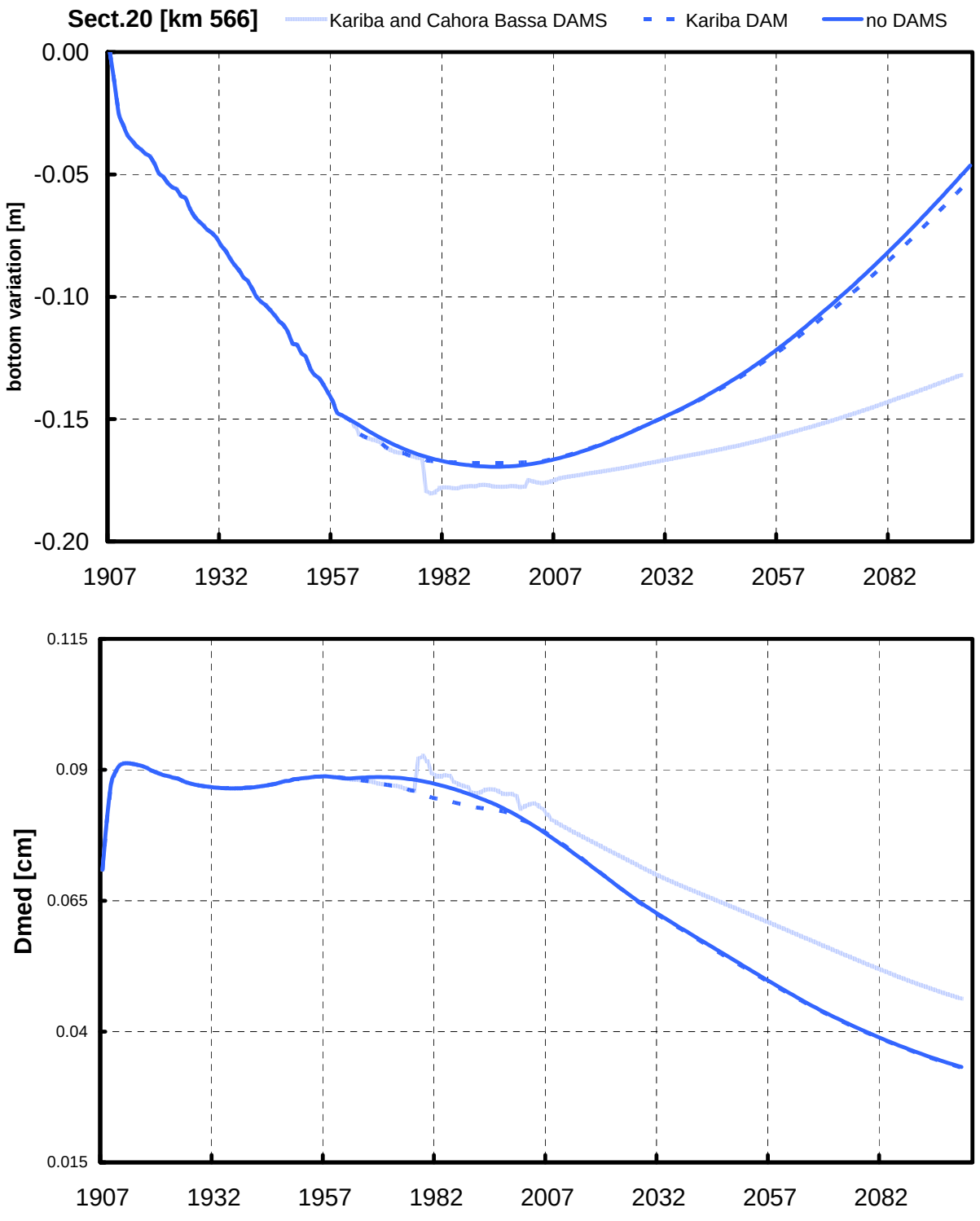

Figure 20.A: Results of simulations from 1907 configuration, in terms of bottom and grainsize variation in Morphological Box n°20 (distance are from Zumbo).

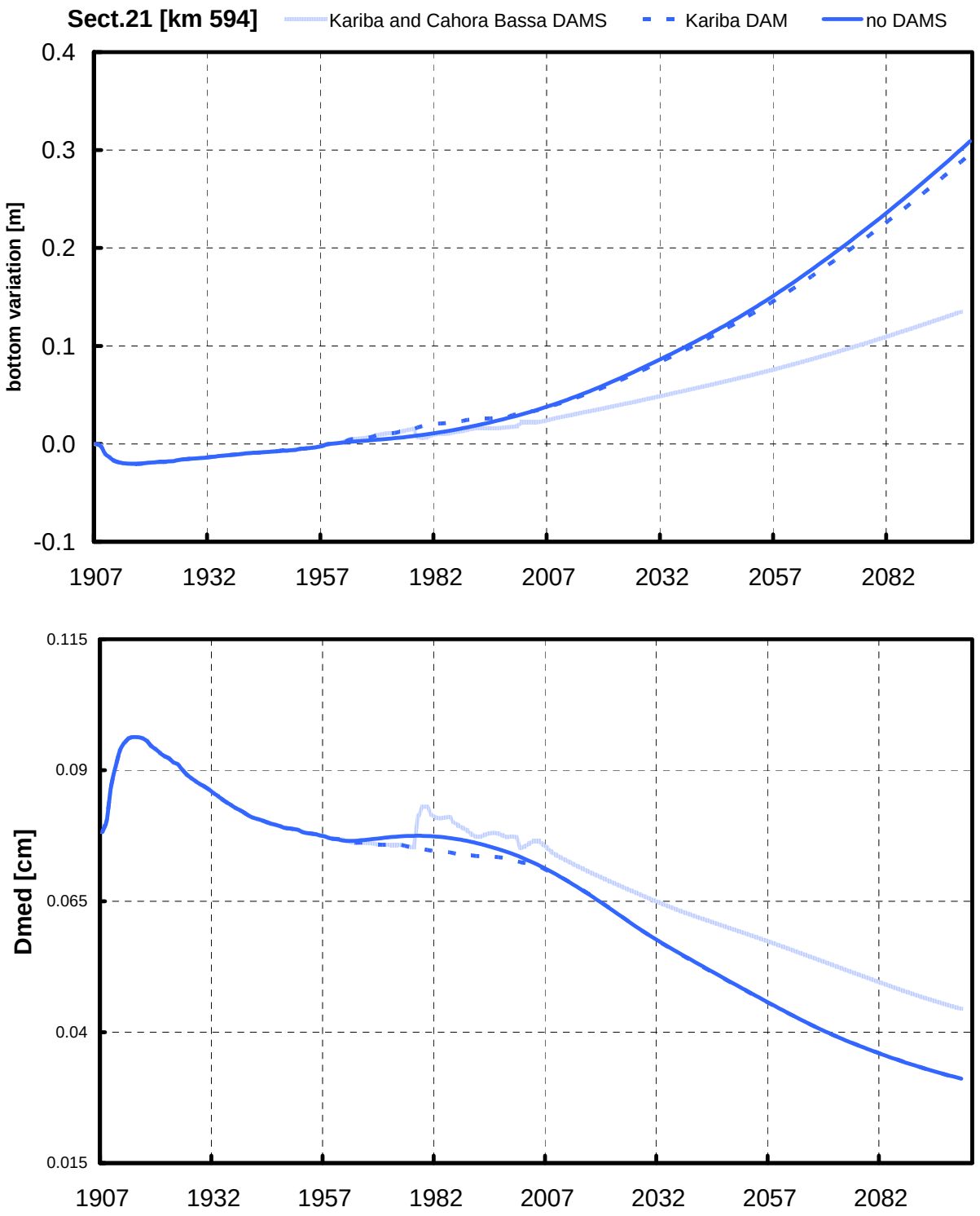

Figure 21.A: Results of simulations from 1907 configuration, in terms of bottom and grainsize variation in Morphological Box n°21 (distance are from Zumbo).

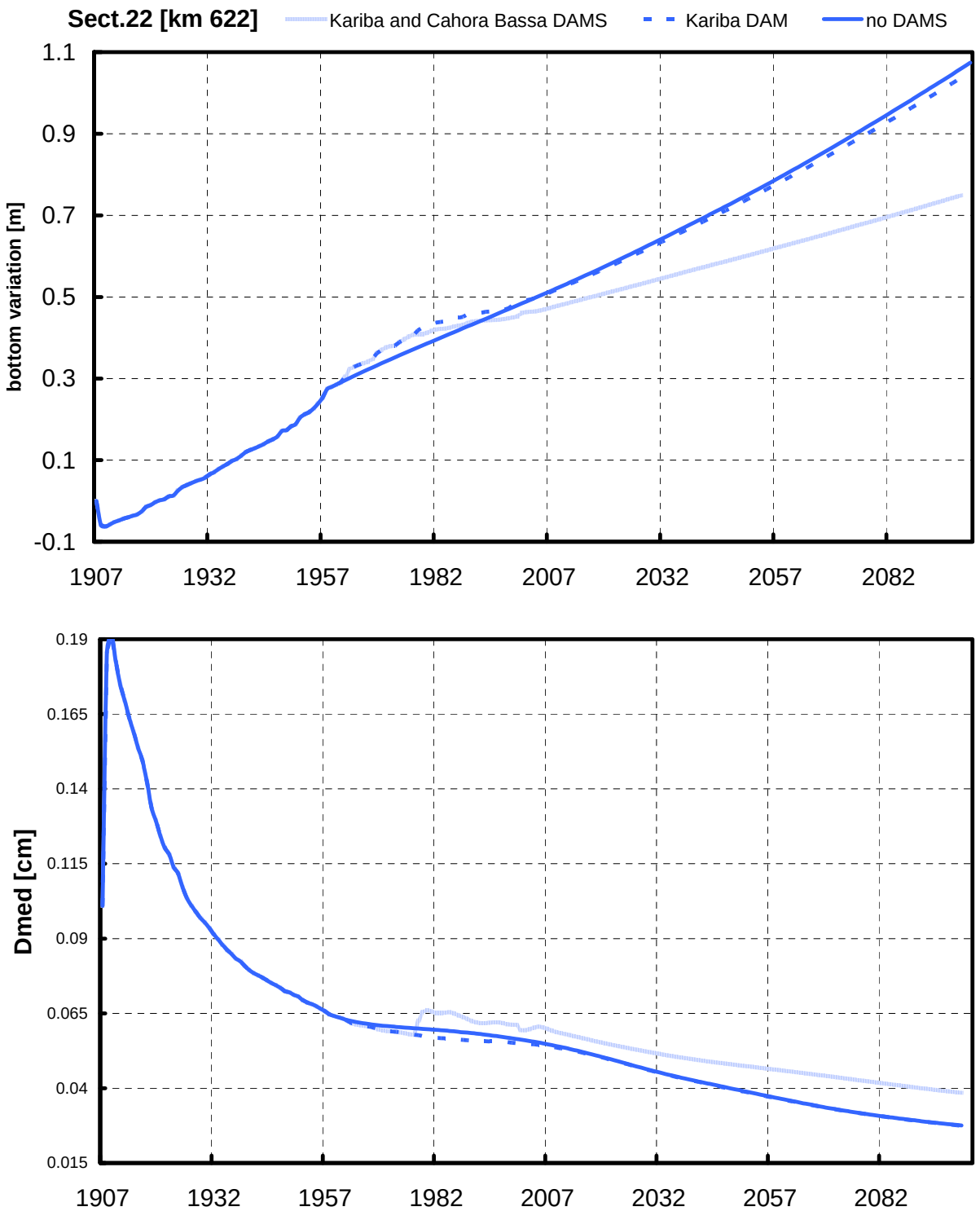

Figure 22.A: Results of simulations from 1907 configuration, in terms of bottom and grainsize variation in Morphological Box n°22 (distance are from Zumbo).

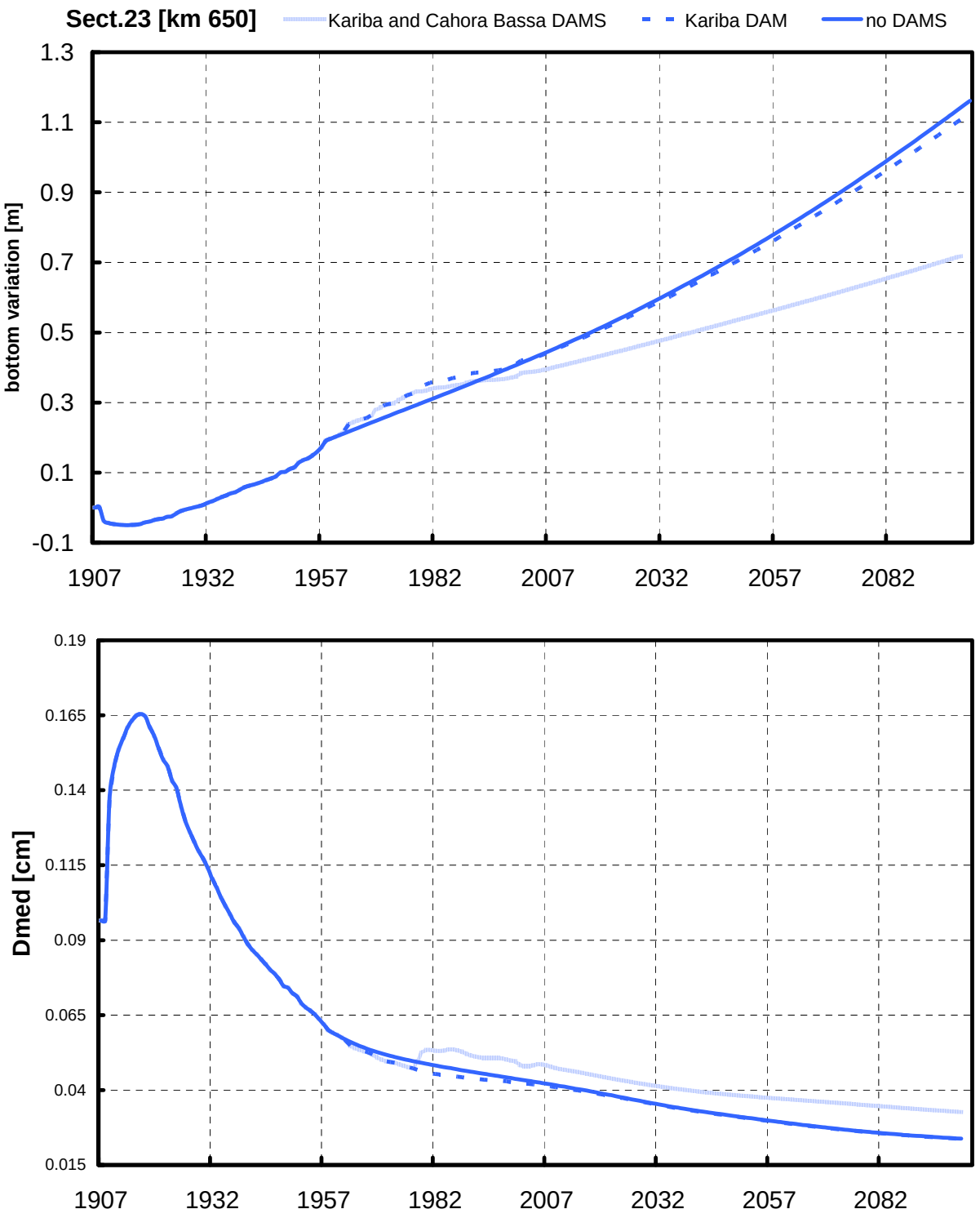

Figure 23.A: Results of simulations from 1907 configuration, in terms of bottom and grainsize variation in Morphological Box n°23 (distance are from Zumbo).

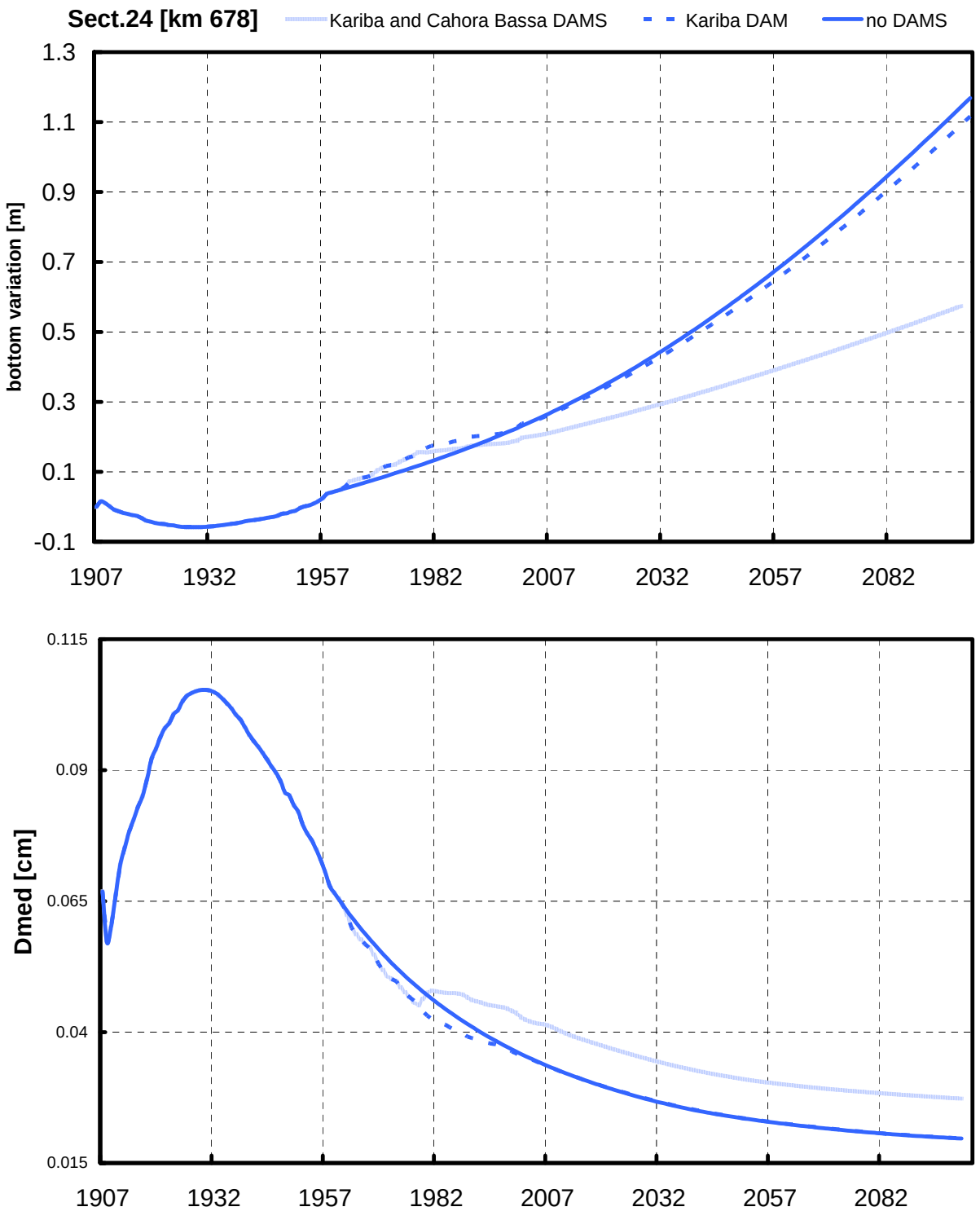

Figure 24.A: Results of simulations from 1907 configuration, in terms of bottom and grainsize variation in Morphological Box n°24 (distance are from Zumbo).

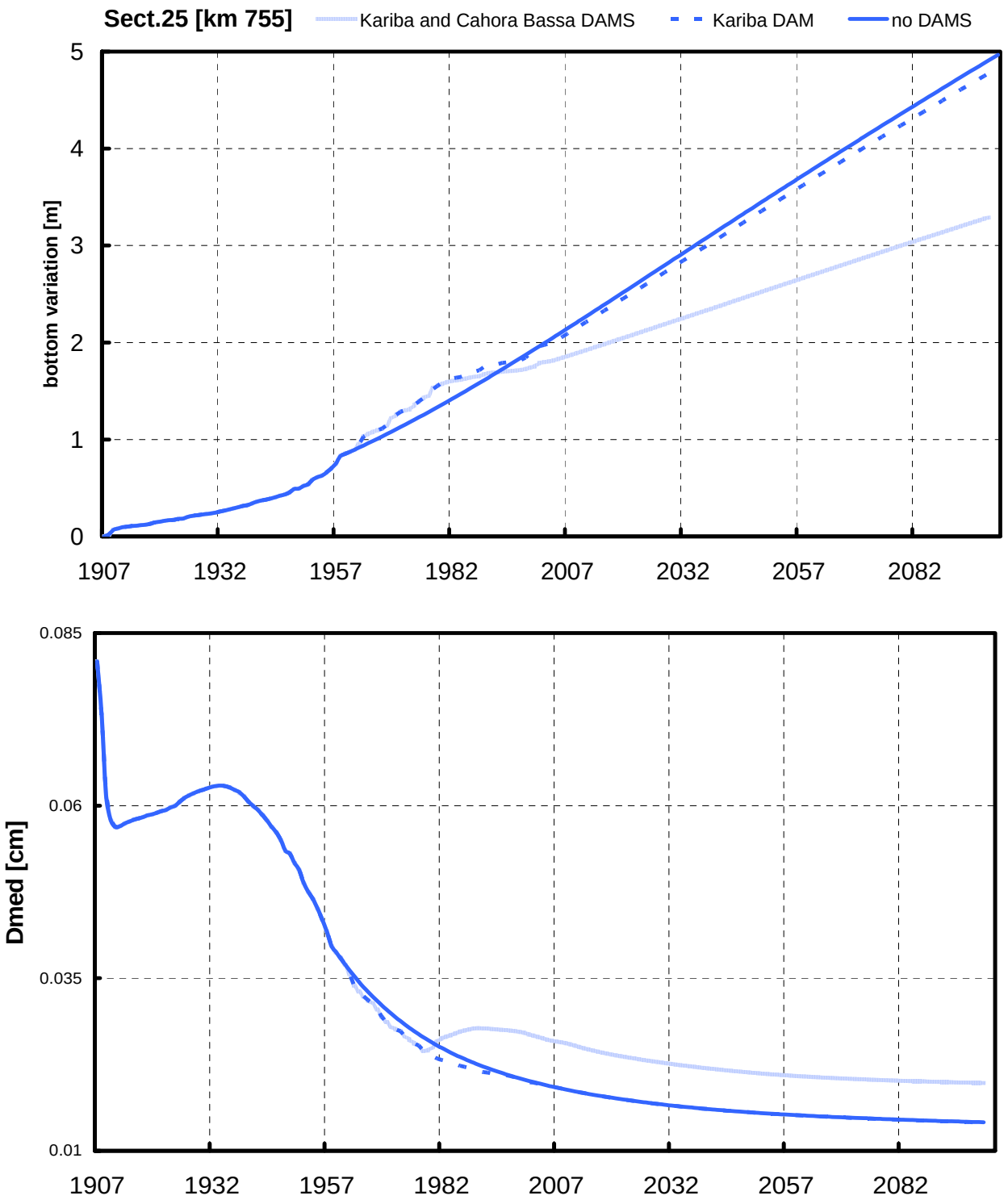

Figure 25.A: Results of simulations from 1907 configuration, in terms of bottom and grainsize variation in Morphological Box n°25 (distance are from Zumbo).

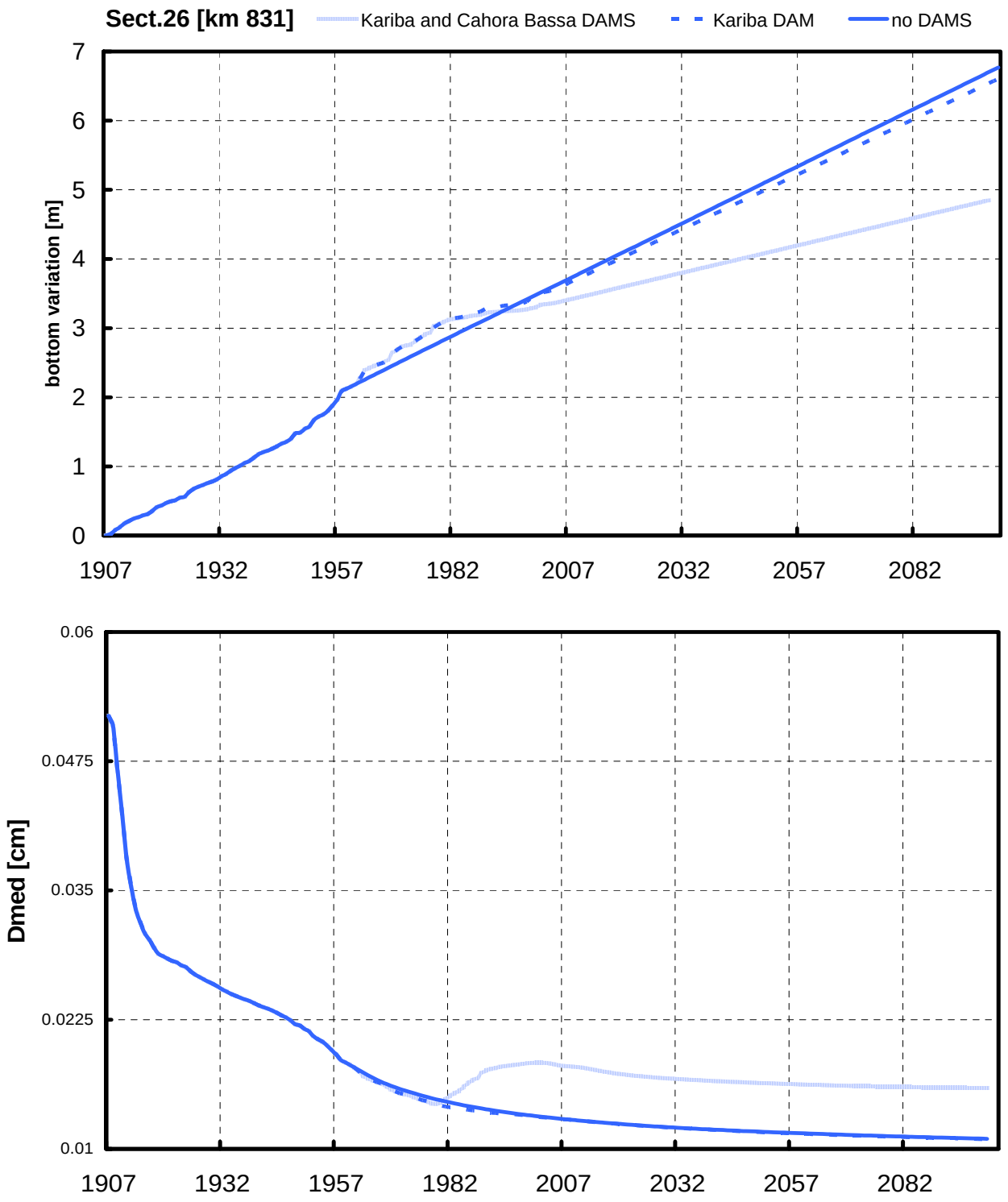

Figure 26.A: Results of simulations from 1907 configuration, in terms of bottom and grainsize variation in Morphological Box n°26 (distance are from Zumbo).

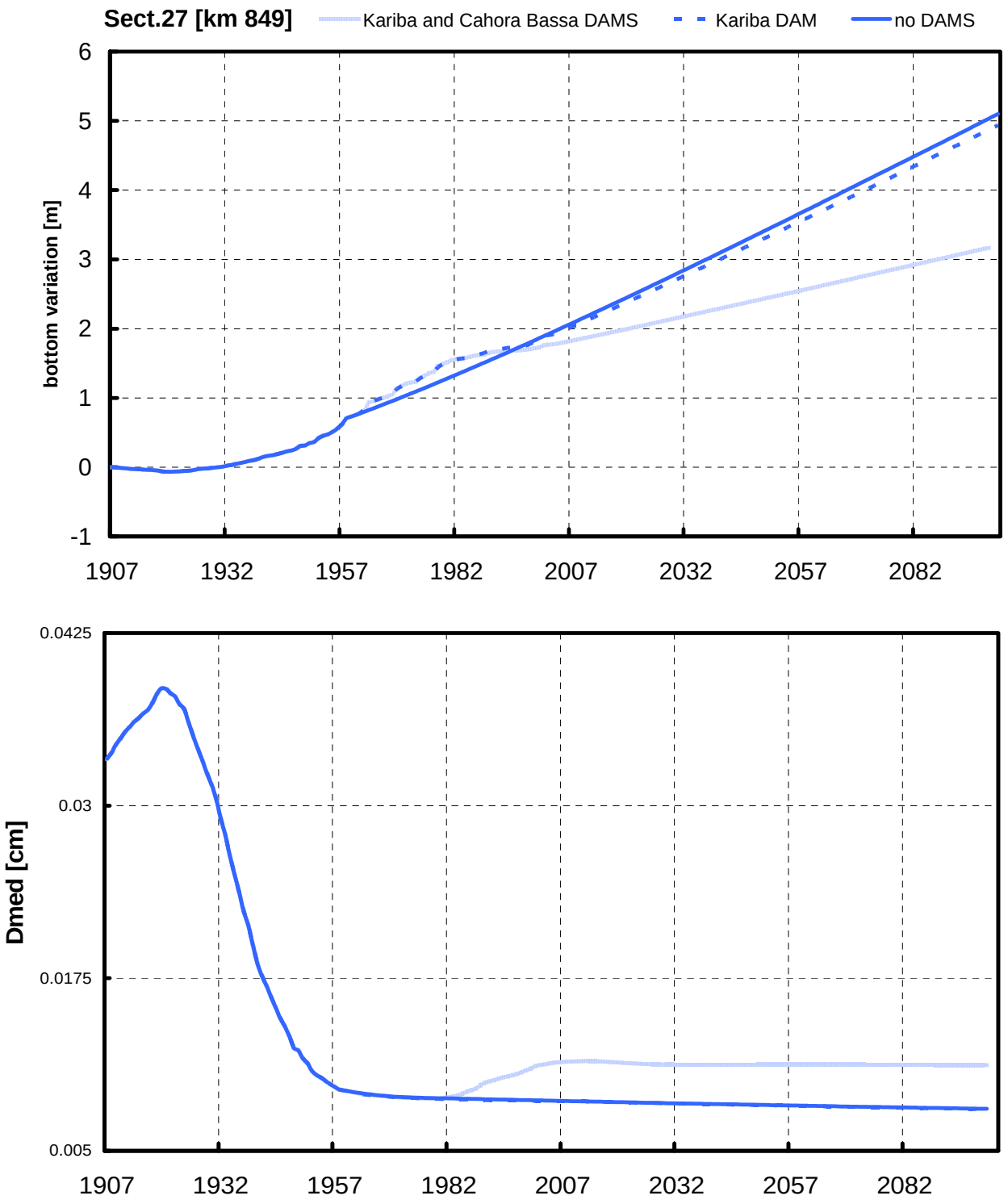

Figure 27.A: Results of simulations from 1907 configuration, in terms of bottom and grainsize variation in Morphological Box n°27 (distance are from Zumbo).

APPENDIX D: DATABASE AT 1 KM RESOLUTION

(the morphological boxes indicated in grey/white)

progressive distance from Zumbo[km]	active width [m]	stream width [m]	water slope i_w	bottom slope (reconstructed) i_f	bottom elevation [m a.s.l.]	water depth H [m] (1)	flow velocity U [m/s] (1)	Froude Number Fr(1)
0	562	975	7.95E-04	7.95E-04	323.87	2.18	2.08	0.450
1	337	1012	7.95E-04	7.95E-04	322.89	3.07	2.47	0.450
2	487	1250	7.95E-04	7.95E-04	322.40	2.40	2.18	0.450
3	550	1625	7.95E-04	7.95E-04	321.80	2.21	2.10	0.450
4	762	2000	7.95E-04	7.95E-04	321.39	1.78	1.88	0.450
5	1062	2375	7.95E-04	7.95E-04	321.09	1.43	1.68	0.450
6	1125	3250	7.95E-04	7.95E-04	320.49	1.37	1.65	0.450
7	1187	3625	7.95E-04	7.95E-04	319.89	1.33	1.62	0.450
8	1188	4000	7.95E-04	7.95E-04	319.20	1.32	1.62	0.450
9	1063	3875	7.95E-04	7.95E-04	318.35	1.43	1.68	0.450
10	1063	3750	7.95E-04	7.95E-04	317.67	1.43	1.68	0.450
11	1000	3625	7.95E-04	7.95E-04	316.90	1.49	1.72	0.450
12	750	3250	7.95E-04	7.95E-04	315.89	1.80	1.89	0.450
13	1000	2750	7.95E-04	7.95E-04	315.53	1.49	1.72	0.450
14	1150	3000	7.95E-04	7.95E-04	315.04	1.35	1.64	0.450
15	1313	3125	7.95E-04	7.95E-04	314.57	1.24	1.57	0.450
16	1125	3188	7.95E-04	7.95E-04	313.64	1.37	1.65	0.450
17	1100	3500	7.95E-04	7.95E-04	312.92	1.39	1.67	0.450
18	1313	3750	7.95E-04	7.95E-04	312.51	1.24	1.57	0.450
19	1250	3375	7.95E-04	7.95E-04	311.75	1.28	1.60	0.450
20	938	3625	7.95E-04	7.95E-04	310.65	1.55	1.76	0.450
21	1125	3875	7.95E-04	7.95E-04	310.21	1.37	1.65	0.450
22	1000	3938	4.43E-04	4.43E-04	309.36	1.81	1.41	0.336
23	938	4125	4.43E-04	4.43E-04	308.60	1.89	1.44	0.336
24	1013	3813	4.43E-04	4.43E-04	308.01	1.79	1.41	0.336
25	875	3625	4.43E-04	4.43E-04	307.14	1.97	1.48	0.336
26	1125	2875	4.43E-04	4.43E-04	306.79	1.67	1.36	0.336
27	813	3625	4.43E-04	4.43E-04	305.69	2.07	1.52	0.336
28	1438	2813	4.43E-04	4.43E-04	305.82	1.42	1.25	0.336
29	1088	3375	4.43E-04	4.43E-04	304.68	1.71	1.38	0.336
30	1000	3438	4.43E-04	4.43E-04	303.88	1.81	1.41	0.336
31	1188	4188	4.43E-04	4.43E-04	303.44	1.61	1.34	0.336
32	813	4375	4.43E-04	4.43E-04	301.88	2.07	1.52	0.336
33	813	4250	4.43E-04	4.43E-04	301.49	2.07	1.52	0.336
34	563	3625	4.43E-04	4.43E-04	300.66	2.65	1.71	0.336
35	750	3250	4.43E-04	4.43E-04	300.61	2.19	1.56	0.336
36	1125	3000	4.43E-04	4.43E-04	300.89	1.67	1.36	0.336
37	475	2938	4.43E-04	4.43E-04	299.34	2.97	1.81	0.336
38	938	2813	4.43E-04	4.43E-04	299.77	1.89	1.44	0.336
39	1125	2875	4.43E-04	4.43E-04	299.72	1.67	1.36	0.336
40	750	3063	4.43E-04	4.43E-04	298.66	2.19	1.56	0.336
41	1188	3125	4.43E-04	4.43E-04	299.05	1.61	1.34	0.336
42	1188	4000	4.43E-04	4.43E-04	298.67	1.61	1.34	0.336
43	1500	3875	3.60E-04	3.60E-04	298.83	1.48	1.15	0.303
44	1813	4563	3.60E-04	3.60E-04	299.00	1.30	1.08	0.303
45	1938	4875	3.60E-04	3.60E-04	298.84	1.25	1.06	0.303
46	1188	3750	3.60E-04	3.60E-04	297.11	1.73	1.25	0.303
47	1400	3125	3.60E-04	3.60E-04	297.10	1.55	1.18	0.303
48	938	2563	3.60E-04	3.60E-04	295.89	2.02	1.35	0.303
49	750	2438	3.60E-04	3.60E-04	295.17	2.34	1.45	0.303
50	1025	2813	3.60E-04	3.60E-04	295.27	1.90	1.31	0.303
51	1125	2813	3.60E-04	3.60E-04	295.06	1.79	1.27	0.303
52	688	2313	3.60E-04	3.60E-04	293.89	2.48	1.50	0.303
53	625	1813	3.60E-04	3.60E-04	293.39	2.65	1.54	0.303
54	600	1875	3.60E-04	3.60E-04	292.96	2.72	1.56	0.303
55	613	1438	3.60E-04	3.60E-04	292.59	2.68	1.55	0.303
56	500	2063	3.60E-04	3.60E-04	292.00	3.07	1.66	0.303
57	438	1688	3.60E-04	3.60E-04	291.50	3.36	1.74	0.303
58	638	1813	3.60E-04	3.60E-04	291.47	2.61	1.53	0.303
59	763	2250	3.60E-04	3.60E-04	291.30	2.32	1.44	0.303
60	688	2875	3.60E-04	3.60E-04	290.78	2.48	1.50	0.303
61	938	2688	3.60E-04	3.60E-04	290.84	2.02	1.35	0.303
62	725	2938	3.60E-04	3.60E-04	290.07	2.40	1.47	0.303
63	1088	3375	3.60E-04	3.60E-04	290.33	1.83	1.28	0.303
64	1500	3063	3.60E-04	3.60E-04	290.29	1.48	1.15	0.303
65	1438	2938	3.60E-04	3.60E-04	289.87	1.52	1.17	0.303

66	1438	2688	3.60E-04	3.60E-04	289.53	1.52	1.17	0.303
67	1438	2563	3.60E-04	3.60E-04	289.19	1.52	1.17	0.303
68	1000	2625	3.60E-04	3.60E-04	288.29	1.94	1.32	0.303
69	988	3125	3.60E-04	3.60E-04	287.94	1.95	1.33	0.303
70	1000	3063	3.60E-04	3.60E-04	287.62	1.94	1.32	0.303
71	1500	2813	3.60E-04	3.60E-04	287.92	1.48	1.15	0.303
72	1875	3000	3.60E-04	3.60E-04	288.07	1.27	1.07	0.303
73	1563	2625	3.60E-04	3.60E-04	287.33	1.44	1.14	0.303
74	1688	3063	3.60E-04	3.60E-04	287.15	1.37	1.11	0.303
75	1313	3000	3.60E-04	3.60E-04	286.34	1.61	1.21	0.303
76	1625	2625	3.60E-04	3.60E-04	286.40	1.40	1.12	0.303
77	688	2250	3.60E-04	3.60E-04	284.86	2.48	1.50	0.303
78	1125	2250	3.60E-04	3.60E-04	285.08	1.79	1.27	0.303
79	1125	2375	3.60E-04	3.60E-04	284.75	1.79	1.27	0.303
80	1125	2938	3.60E-04	3.60E-04	284.41	1.79	1.27	0.303
81	1750	3250	3.60E-04	3.60E-04	284.87	1.33	1.10	0.303
82	1188	3313	3.60E-04	3.60E-04	283.81	1.73	1.25	0.303
83	1375	3375	3.04E-04	3.04E-04	283.72	1.66	1.12	0.278
84	1750	3500	3.04E-04	3.04E-04	283.86	1.41	1.03	0.278
85	1750	3250	3.04E-04	3.04E-04	283.53	1.41	1.03	0.278
86	750	2375	3.04E-04	3.04E-04	281.90	2.48	1.37	0.278
87	1000	2875	3.04E-04	3.04E-04	281.89	2.05	1.25	0.278
88	750	3375	3.04E-04	3.04E-04	281.23	2.48	1.37	0.278
89	438	3500	3.04E-04	3.04E-04	280.49	3.55	1.64	0.278
90	438	4125	3.04E-04	3.04E-04	280.15	3.55	1.64	0.278
91	688	1750	3.04E-04	3.04E-04	280.14	2.63	1.41	0.278
92	500	1375	3.04E-04	3.04E-04	279.56	3.25	1.57	0.278
93	750	1375	3.04E-04	3.04E-04	279.54	2.48	1.37	0.278
94	750	2125	3.04E-04	3.04E-04	279.21	2.48	1.37	0.278
95	850	3750	3.04E-04	3.04E-04	279.00	2.28	1.32	0.278
96	1125	4125	3.04E-04	3.04E-04	278.78	1.89	1.20	0.278
97	875	3438	3.04E-04	3.04E-04	278.07	2.24	1.30	0.278
98	625	1438	3.04E-04	3.04E-04	277.37	2.80	1.46	0.278
99	563	563	3.04E-04	3.04E-04	277.03	3.01	1.51	0.278
100	688	688	3.04E-04	3.04E-04	277.08	2.63	1.41	0.278
101	688	688	3.04E-04	3.04E-04	276.87	2.63	1.41	0.278
102	1000	1000	3.04E-04	3.04E-04	277.29	2.05	1.25	0.278
103	563	1625	3.04E-04	3.04E-04	276.21	3.01	1.51	0.278
104	475	1688	3.04E-04	3.04E-04	275.83	3.36	1.60	0.278
105	538	2375	3.04E-04	3.04E-04	275.75	3.10	1.53	0.278
106	750	2875	3.04E-04	3.04E-04	275.97	2.48	1.37	0.278
107	1375	3250	3.04E-04	3.04E-04	277.01	1.66	1.12	0.278
108	1438	3375	3.04E-04	3.04E-04	276.93	1.61	1.11	0.278
109	875	2875	1.39E-04	1.39E-04	275.60	2.90	1.00	0.188
110	938	2125	1.39E-04	1.39E-04	275.52	2.77	0.98	0.188
111	1500	3375	1.39E-04	1.39E-04	276.43	2.03	0.84	0.188
112	1188	2750	1.39E-04	1.39E-04	275.60	2.37	0.91	0.188
113	1500	3063	1.39E-04	1.39E-04	276.02	2.03	0.84	0.188
114	1313	2750	1.39E-04	1.39E-04	275.44	2.22	0.88	0.188
115	975	2688	1.39E-04	1.39E-04	274.56	2.70	0.97	0.188
116	1413	2750	1.39E-04	1.39E-04	275.23	2.11	0.86	0.188
117	850	2875	1.39E-04	1.39E-04	273.90	2.96	1.01	0.188
118	1125	3500	1.39E-04	1.39E-04	274.24	2.46	0.92	0.188
119	1125	3250	1.39E-04	1.39E-04	274.04	2.46	0.92	0.188
120	1000	2125	1.39E-04	1.39E-04	273.58	2.66	0.96	0.188
121	1250	2250	1.39E-04	1.39E-04	273.88	2.29	0.89	0.188
122	1125	2625	1.39E-04	1.39E-04	273.42	2.46	0.92	0.188
123	1250	3625	1.39E-04	1.39E-04	273.46	2.29	0.89	0.188
124	850	3875	1.39E-04	1.39E-04	272.46	2.96	1.01	0.188
125	813	2688	1.39E-04	1.39E-04	272.18	3.05	1.03	0.188
126	875	2500	1.39E-04	1.39E-04	272.10	2.90	1.00	0.188
127	813	2750	1.39E-04	1.39E-04	271.77	3.05	1.03	0.188
128	750	3125	1.39E-04	1.39E-04	271.48	3.22	1.06	0.188
129	1225	2875	1.39E-04	1.39E-04	272.11	2.32	0.90	0.188
130	1225	2688	1.39E-04	1.39E-04	271.90	2.32	0.90	0.188
131	1275	2225	1.39E-04	1.39E-04	271.78	2.26	0.89	0.188
132	1038	2100	1.39E-04	1.39E-04	271.15	2.59	0.95	0.188
133	1063	2188	1.39E-04	1.39E-04	270.99	2.55	0.94	0.188
134	1000	2025	1.39E-04	1.39E-04	270.67	2.66	0.96	0.188
135	1500	2375	1.39E-04	1.39E-04	271.35	2.03	0.84	0.188
136	1250	2750	1.39E-04	1.39E-04	270.70	2.29	0.89	0.188
137	1438	2625	1.39E-04	1.39E-04	270.82	2.09	0.85	0.188
138	1375	2663	1.39E-04	1.39E-04	270.50	2.15	0.86	0.188
139	1000	1875	1.39E-04	1.39E-04	269.63	2.66	0.96	0.188
140	1250	1813	1.39E-04	1.39E-04	269.87	2.29	0.89	0.188
141	1000	2188	1.39E-04	1.39E-04	269.22	2.66	0.96	0.188
142	1063	2563	1.39E-04	1.39E-04	269.12	2.55	0.94	0.188
143	900	2738	1.39E-04	1.39E-04	268.63	2.85	1.00	0.188
144	875	2750	1.39E-04	1.39E-04	268.37	2.90	1.00	0.188
145	913	3125	1.39E-04	1.39E-04	268.23	2.82	0.99	0.188
146	875	2625	1.39E-04	1.39E-04	267.96	2.90	1.00	0.188
147	1125	2000	1.39E-04	1.39E-04	268.19	2.46	0.92	0.188

148	813	1750	1.39E-04	1.39E-04	267.43	3.05	1.03	0.188
149	1075	2000	1.39E-04	1.39E-04	267.69	2.53	0.94	0.188
150	875	1813	3.59E-04	3.59E-04	267.13	2.12	1.38	0.302
151	675	2125	3.59E-04	3.59E-04	266.57	2.52	1.50	0.302
152	1538	2375	3.59E-04	3.59E-04	267.88	1.45	1.14	0.302
153	900	2250	3.59E-04	3.59E-04	266.55	2.08	1.37	0.302
154	813	2125	3.59E-04	3.59E-04	266.19	2.22	1.41	0.302
155	1075	1875	3.59E-04	3.59E-04	266.44	1.85	1.29	0.302
156	1375	2188	3.59E-04	3.59E-04	266.76	1.57	1.19	0.302
157	1125	1875	3.59E-04	3.59E-04	266.12	1.79	1.27	0.302
158	900	1938	3.59E-04	3.59E-04	265.51	2.08	1.37	0.302
159	500	1500	3.59E-04	3.59E-04	264.59	3.08	1.66	0.302
160	638	1375	3.59E-04	3.59E-04	264.54	2.62	1.53	0.302
161	1000	1875	3.59E-04	3.59E-04	265.33	1.94	1.32	0.302
162	750	1750	3.59E-04	3.59E-04	264.40	2.35	1.45	0.302
163	750	1625	3.59E-04	3.59E-04	264.18	2.35	1.45	0.302
164	1250	1750	3.59E-04	3.59E-04	265.36	1.67	1.22	0.302
165	738	2000	3.59E-04	3.59E-04	263.69	2.37	1.46	0.302
166	1000	1500	3.59E-04	3.59E-04	264.20	1.94	1.32	0.302
167	500	1250	1.78E-04	1.78E-04	262.57	3.88	1.32	0.213
168	625	1188	1.78E-04	1.78E-04	262.70	3.35	1.22	0.213
169	888	1413	1.78E-04	1.78E-04	263.21	2.65	1.09	0.213
170	688	1375	1.78E-04	1.78E-04	262.42	3.14	1.18	0.213
171	875	1688	1.78E-04	1.78E-04	262.73	2.67	1.09	0.213
172	625	1875	1.78E-04	1.78E-04	261.80	3.35	1.22	0.213
173	1000	1625	1.78E-04	1.78E-04	262.63	2.45	1.04	0.213
174	750	1563	1.78E-04	1.78E-04	261.70	2.96	1.15	0.213
175	938	1688	1.78E-04	1.78E-04	262.00	2.55	1.07	0.213
176	1313	1625	1.78E-04	1.78E-04	262.83	2.04	0.95	0.213
177	813	1500	1.78E-04	1.78E-04	261.20	2.81	1.12	0.213
178	813	1938	1.78E-04	1.78E-04	260.97	2.81	1.12	0.213
179	1013	1438	1.78E-04	1.78E-04	261.31	2.43	1.04	0.213
180	975	1225	1.78E-04	1.78E-04	260.98	2.49	1.05	0.213
181	1125	1375	1.78E-04	1.78E-04	261.18	2.26	1.00	0.213
182	775	1500	1.78E-04	1.78E-04	259.97	2.90	1.14	0.213
183	625	1750	1.78E-04	1.78E-04	259.32	3.35	1.22	0.213
184	438	750	1.78E-04	1.78E-04	258.57	4.24	1.38	0.213
185	563	625	1.78E-04	1.78E-04	258.69	3.59	1.26	0.213
186	625	625	1.78E-04	1.78E-04	258.64	3.35	1.22	0.213
187	688	750	1.78E-04	1.78E-04	258.59	3.14	1.18	0.213
188	563	975	1.78E-04	1.78E-04	258.02	3.59	1.26	0.213
189	563	975	1.78E-04	1.78E-04	257.79	3.59	1.26	0.213
190	638	1313	3.00E-04	3.00E-04	257.78	2.78	1.44	0.277
191	638	1213	3.00E-04	3.00E-04	257.55	2.78	1.44	0.277
192	713	1313	3.00E-04	3.00E-04	258.07	2.58	1.39	0.277
193	675	1250	3.00E-04	3.00E-04	257.57	2.67	1.42	0.277
194	625	750	3.00E-04	3.00E-04	257.02	2.81	1.45	0.277
195	538	1375	3.00E-04	3.00E-04	256.36	3.11	1.53	0.277
196	513	1538	3.00E-04	3.00E-04	255.89	3.21	1.55	0.277
197	475	1750	3.00E-04	3.00E-04	255.39	3.38	1.59	0.277
198	750	2000	3.00E-04	3.00E-04	255.85	2.49	1.37	0.277
199	1125	1938	3.00E-04	3.00E-04	256.62	1.90	1.19	0.277
200	875	2063	3.00E-04	3.00E-04	255.46	2.25	1.30	0.277
201	688	2688	3.00E-04	3.00E-04	254.49	2.64	1.41	0.277
202	875	2000	3.00E-04	3.00E-04	254.68	2.25	1.30	0.277
203	563	1688	3.00E-04	3.00E-04	253.32	3.02	1.50	0.277
204	688	1813	3.00E-04	3.00E-04	253.32	2.64	1.41	0.277
205	938	2000	3.00E-04	3.00E-04	253.70	2.15	1.27	0.277
206	750	2375	3.00E-04	3.00E-04	252.73	2.49	1.37	0.277
207	688	2250	3.00E-04	3.00E-04	252.15	2.64	1.41	0.277
208	1000	2688	3.00E-04	3.00E-04	252.72	2.06	1.24	0.277
209	950	2813	3.00E-04	3.00E-04	252.18	2.13	1.26	0.277
210	1500	2063	3.00E-04	3.00E-04	253.27	1.57	1.08	0.277
211	1188	2000	3.00E-04	3.00E-04	252.14	1.83	1.17	0.277
212	575	1375	3.00E-04	3.00E-04	249.85	2.97	1.49	0.277
213	625	1725	3.00E-04	3.00E-04	249.61	2.81	1.45	0.277
214	488	1000	5.70E-04	5.70E-04	248.80	2.68	1.95	0.381
215	500	1000	5.70E-04	5.70E-04	248.45	2.64	1.94	0.381
216	500	750	5.70E-04	5.70E-04	248.06	2.64	1.94	0.381
217	438	688	5.70E-04	5.70E-04	247.47	2.88	2.03	0.381
218	500	813	5.70E-04	5.70E-04	247.28	2.64	1.94	0.381
219	438	1250	5.70E-04	5.70E-04	246.69	2.88	2.03	0.381
220	388	1250	5.70E-04	5.70E-04	246.15	3.12	2.11	0.381
221	438	1513	5.70E-04	5.70E-04	245.91	2.88	2.03	0.381
222	300	1500	5.70E-04	5.70E-04	245.10	3.71	2.30	0.381
223	288	288	5.70E-04	5.70E-04	244.67	3.81	2.33	0.381
224	375	375	5.70E-04	5.70E-04	244.55	3.19	2.13	0.381
225	313	313	5.70E-04	5.70E-04	246.47	3.61	2.27	0.381
226	288	350	5.70E-04	5.70E-04	244.71	3.81	2.33	0.381
227	225	338	5.70E-04	5.70E-04	242.13	4.49	2.53	0.381
228	175	363	5.70E-04	5.70E-04	239.82	5.31	2.75	0.381
229	263	513	5.70E-04	5.70E-04	240.52	4.05	2.40	0.381

230	363	575	5.70E-04	5.70E-04	241.43	3.27	2.16	0.381
231	300	600	5.70E-04	5.70E-04	238.91	3.71	2.30	0.381
232	238	263	5.70E-04	5.70E-04	236.33	4.33	2.48	0.381
233	213	375	5.70E-04	5.70E-04	234.56	4.66	2.58	0.381
234	175	625	5.70E-04	5.70E-04	232.53	5.31	2.75	0.381
235	150	625	5.70E-04	5.70E-04	230.77	5.88	2.89	0.381
236	150	363	5.70E-04	5.70E-04	229.55	5.88	2.89	0.381
237	125	350	5.70E-04	5.70E-04	227.79	6.64	3.08	0.381
238	138	375	5.70E-04	5.70E-04	226.85	6.23	2.98	0.381
239	138	325	5.70E-04	5.70E-04	225.63	6.23	2.98	0.381
240	113	175	5.70E-04	5.70E-04	223.87	7.13	3.19	0.381
241	100	150	5.70E-04	5.70E-04	222.38	7.71	3.31	0.381
242	125	150	5.70E-04	5.70E-04	221.72	6.64	3.08	0.381
243	138	213	5.70E-04	5.70E-04	220.77	6.23	2.98	0.381
244	150	250	5.70E-04	5.70E-04	219.83	5.88	2.89	0.381
245	138	225	5.70E-04	5.70E-04	218.34	6.23	2.98	0.381
246	125	275	5.70E-04	5.70E-04	216.85	6.64	3.08	0.381
247	113	238	2.31E-03	2.31E-03	215.37	4.47	5.08	0.767
248	113	188	2.31E-03	2.31E-03	214.15	4.47	5.08	0.767
249	113	188	2.31E-03	2.31E-03	212.94	4.47	5.08	0.767
250	125	213	2.31E-03	2.31E-03	211.99	4.17	4.90	0.767
251	125	125	2.31E-03	2.31E-03	210.78	4.17	4.90	0.767
252	150	150	2.31E-03	2.31E-03	210.11	3.69	4.61	0.767
253	119	119	2.31E-03	2.31E-03	208.21	4.31	4.99	0.767
254	113	263	2.31E-03	2.31E-03	206.86	4.47	5.08	0.767
255	150	150	2.31E-03	2.31E-03	206.46	3.69	4.61	0.767
256	125	125	2.31E-03	2.31E-03	204.70	4.17	4.90	0.767
257	125	125	2.31E-03	2.31E-03	203.49	4.17	4.90	0.767
258	126	126	2.31E-03	2.31E-03	202.30	4.14	4.88	0.767
259	112	112	2.31E-03	2.31E-03	200.76	4.50	5.09	0.767
260	184	184	1.37E-03	1.75E-03	201.32	3.83	3.62	0.590
261	167	167	1.37E-03	1.93E-03	199.57	4.09	3.74	0.590
262	141	141	1.37E-03	1.92E-03	197.64	4.58	3.95	0.590
263	116	116	1.37E-03	1.53E-03	195.72	5.23	4.23	0.590
264	108	108	1.37E-03	1.28E-03	194.19	5.46	4.32	0.590
265	112	112	1.37E-03	8.71E-04	192.91	5.33	4.27	0.590
266	135	135	1.37E-03	6.26E-04	192.04	4.71	4.01	0.590
267	169	169	1.37E-03	1.25E-03	191.42	4.06	3.73	0.590
268	174	174	1.37E-03	9.58E-04	190.17	3.98	3.69	0.590
269	193	193	1.37E-03	1.22E-03	189.21	3.72	3.56	0.590
270	200	200	1.37E-03	1.48E-03	187.99	3.63	3.52	0.590
271	194	194	1.37E-03	2.52E-03	186.51	3.70	3.55	0.590
272	142	142	1.37E-03	7.50E-04	183.99	4.56	3.95	0.590
273	170	170	1.37E-03	2.93E-04	183.24	4.04	3.72	0.590
274	219	219	1.37E-03	3.19E-03	182.95	3.41	3.42	0.590
275	136	136	1.37E-03	3.71E-04	179.77	4.69	4.00	0.590
276	186	186	1.37E-03	1.91E-03	179.39	3.81	3.61	0.590
277	157	157	1.37E-03	6.77E-04	177.48	4.26	3.81	0.590
278	185	185	1.37E-03	2.35E-03	176.81	3.82	3.61	0.590
279	137	137	1.37E-03	2.02E-03	174.45	4.68	4.00	0.590
280	103	103	1.37E-03	8.88E-04	172.43	5.63	4.39	0.590
281	122	122	1.37E-03	7.88E-04	171.54	5.05	4.15	0.590
282	145	145	1.37E-03	2.08E-03	170.76	4.50	3.92	0.590
283	108	108	1.37E-03	-1.68E-03	168.67	5.46	4.32	0.590
284	244	244	1.37E-03	3.69E-03	170.35	3.18	3.30	0.590
285	134	134	1.37E-03	1.52E-03	166.66	4.73	4.02	0.590
286	124	124	1.37E-03	-1.91E-03	165.14	5.00	4.13	0.590
287	270	270	1.37E-03	2.50E-03	167.04	2.97	3.19	0.590
288	215	215	1.37E-03	2.44E-03	164.55	3.46	3.44	0.590
289	162	162	1.37E-03	6.46E-04	162.11	4.17	3.77	0.590
290	192	192	7.55E-04	3.14E-03	161.47	4.55	2.93	0.439
291	107	107	7.55E-04	1.09E-03	158.32	6.70	3.56	0.439
292	160	160	7.55E-04	1.29E-03	157.24	5.40	3.19	0.439
293	109	109	7.55E-04	6.17E-04	155.94	6.95	3.62	0.439
294	115	115	7.55E-04	-1.68E-04	155.33	6.71	3.56	0.439
295	187	187	7.55E-04	6.92E-04	155.50	4.87	3.03	0.439
296	186	186	7.55E-04	2.73E-04	154.80	4.88	3.03	0.439
297	221	221	7.55E-04	1.15E-03	154.53	4.35	2.87	0.439
298	183	183	7.55E-04	5.04E-04	153.38	4.94	3.05	0.439
299	198	198	7.55E-04	1.44E-03	152.88	4.68	2.97	0.439
300	136	136	7.55E-04	4.87E-04	151.44	6.02	3.37	0.439
301	152	152	7.55E-04	8.00E-04	150.96	5.57	3.24	0.439
302	143	143	7.55E-04	1.81E-04	150.16	5.81	3.31	0.439
303	185	185	7.55E-04	3.51E-04	149.98	4.89	3.04	0.439
304	213	213	7.55E-04	2.19E-03	149.63	4.45	2.90	0.439
305	88	88	7.55E-04	5.04E-06	147.44	8.02	3.89	0.439
306	145	145	7.55E-04	4.35E-04	147.43	5.76	3.30	0.439
307	166	166	7.55E-04	1.40E-03	147.00	5.26	3.15	0.439
308	107	107	7.55E-04	6.92E-04	145.59	7.06	3.65	0.439
309	106	106	7.55E-04	6.84E-04	144.90	7.08	3.65	0.439
310	107	107	7.55E-04	5.52E-04	144.22	7.06	3.65	0.439
311	118	118	7.55E-04	2.61E-04	143.67	6.60	3.53	0.439

312	154	154	7.55E-04	8.00E-04	143.41	5.54	3.23	0.439
313	144	144	7.55E-04	9.72E-04	142.61	5.78	3.30	0.439
314	121	121	7.55E-04	-1.76E-04	141.63	6.51	3.50	0.439
315	193	193	7.55E-04	3.71E-06	141.81	4.77	3.00	0.439
316	250	250	7.55E-04	3.59E-04	141.81	4.01	2.75	0.439
317	277	277	7.55E-04	-5.29E-05	141.45	3.74	2.66	0.439
318	339	339	7.55E-04	-7.28E-04	141.50	3.27	2.48	0.439
319	457	457	7.55E-04	9.04E-04	142.23	2.68	2.25	0.439
320	439	439	7.55E-04	3.29E-03	141.32	2.75	2.28	0.439
321	222	222	7.55E-04	-1.07E-03	138.03	4.34	2.86	0.439
322	368	368	7.55E-04	-2.57E-04	139.10	3.09	2.42	0.439
323	447	447	2.75E-04	2.17E-03	139.36	3.81	1.62	0.265
324	870	870	2.75E-04	2.09E-03	137.19	2.44	1.30	0.265
325	987	987	2.75E-04	-2.64E-03	135.10	2.24	1.24	0.265
326	710	710	2.75E-04	1.37E-03	137.74	2.80	1.39	0.265
327	767	767	2.75E-04	1.57E-03	136.37	2.66	1.35	0.265
328	672	672	2.75E-04	6.53E-04	134.80	2.90	1.41	0.265
329	553	553	2.75E-04	-2.59E-04	134.15	3.30	1.51	0.265
330	722	722	2.75E-04	5.67E-04	134.40	2.77	1.38	0.265
331	629	629	2.75E-04	2.03E-04	133.84	3.03	1.44	0.265
332	652	652	2.75E-04	-5.59E-04	133.63	2.96	1.43	0.265
333	915	915	2.75E-04	9.00E-04	134.19	2.36	1.27	0.265
334	718	718	2.75E-04	1.03E-03	133.29	2.77	1.38	0.265
335	480	480	2.75E-04	-3.18E-04	132.26	3.63	1.58	0.265
336	667	667	2.75E-04	-8.68E-04	132.58	2.91	1.42	0.265
337	1028	1028	2.75E-04	1.17E-03	133.45	2.19	1.23	0.265
338	746	746	2.75E-04	5.68E-04	132.28	2.70	1.36	0.265
339	654	654	2.75E-04	9.94E-05	131.71	2.95	1.43	0.265
340	710	710	2.75E-04	1.06E-03	131.61	2.80	1.39	0.265
341	463	463	2.75E-04	-4.38E-04	130.56	3.72	1.60	0.265
342	688	688	2.75E-04	-7.79E-05	130.99	2.86	1.40	0.265
343	799	799	2.75E-04	3.75E-04	131.07	2.58	1.33	0.265
344	768	768	2.75E-04	2.15E-04	130.70	2.65	1.35	0.265
345	787	787	2.75E-04	9.94E-04	130.48	2.61	1.34	0.265
346	560	560	2.75E-04	1.21E-04	129.49	3.27	1.50	0.265
347	609	609	2.75E-04	-5.12E-04	129.37	3.10	1.46	0.265
348	857	857	2.75E-04	1.13E-03	129.88	2.47	1.30	0.265
349	587	587	2.75E-04	7.09E-05	128.75	3.17	1.48	0.265
350	652	652	2.75E-04	8.26E-04	128.68	2.96	1.43	0.265
351	478	478	2.75E-04	-1.10E-03	127.85	3.64	1.58	0.265
352	913	913	2.75E-04	8.39E-04	128.95	2.36	1.28	0.265
353	735	735	2.75E-04	-1.63E-04	128.12	2.73	1.37	0.265
354	874	874	2.75E-04	4.92E-04	128.28	2.44	1.29	0.265
355	805	805	2.75E-04	2.71E-04	127.79	2.57	1.33	0.265
356	807	807	2.75E-04	-2.47E-04	127.51	2.57	1.33	0.265
357	972	972	2.75E-04	-1.34E-04	127.76	2.27	1.25	0.265
358	1101	1101	2.75E-04	7.83E-04	127.90	2.09	1.20	0.265
359	941	941	2.75E-04	1.56E-03	127.11	2.32	1.26	0.265
360	534	534	2.75E-04	1.53E-04	125.55	3.38	1.53	0.265
361	573	573	2.75E-04	-4.65E-05	125.40	3.23	1.49	0.265
362	674	674	2.75E-04	-1.87E-05	125.44	2.89	1.41	0.265
363	767	767	2.75E-04	1.42E-04	125.46	2.66	1.35	0.265
364	808	808	2.75E-04	5.36E-04	125.32	2.56	1.33	0.265
365	609	753	2.75E-04	2.40E-04	124.79	3.10	1.46	0.265
366	637	671	2.75E-04	-1.58E-04	124.55	3.01	1.44	0.265
367	968	1054	2.75E-04	1.71E-04	124.70	2.27	1.25	0.265
368	1048	1223	2.75E-04	3.42E-04	124.53	2.16	1.22	0.265
369	997	1144	2.75E-04	5.13E-04	124.19	2.23	1.24	0.265
370	815	879	2.75E-04	1.61E-04	123.68	2.55	1.33	0.265
371	902	1214	2.75E-04	4.55E-04	123.51	2.38	1.28	0.265
372	765	797	2.75E-04	3.24E-04	123.06	2.66	1.35	0.265
373	728	745	2.75E-04	-5.47E-04	122.74	2.75	1.38	0.265
374	1358	1574	2.75E-04	1.03E-04	123.28	1.81	1.12	0.265
375	1490	2181	2.75E-04	4.81E-06	123.18	1.71	1.08	0.265
376	1697	2190	2.75E-04	-1.09E-04	123.18	1.56	1.04	0.265
377	1992	2318	2.75E-04	1.59E-04	123.28	1.41	0.98	0.265
378	2081	2278	2.75E-04	2.16E-04	123.12	1.37	0.97	0.265
379	2126	2530	2.75E-04	1.20E-03	122.91	1.35	0.96	0.265
380	1420	1826	2.75E-04	3.98E-04	121.71	1.76	1.10	0.265
381	1326	1523	2.75E-04	2.84E-04	121.31	1.84	1.13	0.265
382	1319	1699	2.75E-04	-2.91E-05	121.03	1.85	1.13	0.265
383	1553	1889	2.75E-04	1.99E-04	121.06	1.66	1.07	0.265
384	1611	1902	2.75E-04	6.37E-04	120.86	1.62	1.06	0.265
385	1334	1549	2.75E-04	5.96E-04	120.22	1.84	1.12	0.265
386	1089	1288	2.75E-04	-8.22E-05	119.63	2.10	1.20	0.265
387	1363	1621	2.75E-04	7.28E-05	119.71	1.81	1.12	0.265
388	1518	1873	2.75E-04	5.74E-04	119.63	1.68	1.08	0.265
389	1290	1515	2.75E-04	1.80E-04	119.06	1.88	1.14	0.265
390	1363	1461	2.75E-04	5.58E-04	118.88	1.81	1.12	0.265
391	1147	1365	2.75E-04	8.58E-04	118.32	2.03	1.18	0.265
392	700	755	2.77E-04	1.45E-04	117.46	2.82	1.40	0.266
393	800	1447	2.77E-04	-4.98E-04	117.32	2.58	1.34	0.266

394	1392	2465	2.77E-04	1.73E-05	117.82	1.78	1.11	0.266
395	1843	2607	2.77E-04	4.58E-04	117.80	1.53	1.03	0.266
396	1638	2283	2.77E-04	3.70E-04	117.34	1.66	1.07	0.266
397	1533	1893	2.77E-04	3.75E-04	116.97	1.73	1.10	0.266
398	1422	2145	2.77E-04	1.59E-04	116.60	1.82	1.12	0.266
399	1556	2194	2.77E-04	2.36E-04	116.44	1.72	1.09	0.266
400	1602	2015	2.77E-04	2.16E-04	116.20	1.68	1.08	0.266
401	1671	2442	2.77E-04	4.88E-04	115.98	1.64	1.06	0.266
402	1432	1641	2.77E-04	1.86E-04	115.50	1.81	1.12	0.266
403	1535	1867	2.77E-04	-3.89E-04	115.31	1.73	1.10	0.266
404	2289	3050	2.77E-04	4.71E-04	115.70	1.33	0.96	0.266
405	2069	2519	2.77E-04	3.72E-04	115.23	1.42	0.99	0.266
406	1962	2926	2.77E-04	5.28E-04	114.85	1.47	1.01	0.266
407	1678	2932	2.77E-04	-9.11E-05	114.33	1.63	1.06	0.266
408	2096	2628	2.77E-04	9.31E-04	114.42	1.41	0.99	0.266
409	1355	2269	2.77E-04	4.19E-05	113.49	1.88	1.14	0.266
410	1621	2169	2.77E-04	1.74E-04	113.44	1.67	1.08	0.266
411	1738	1943	2.77E-04	1.04E-04	113.27	1.59	1.05	0.266
412	1934	2339	2.77E-04	1.36E-04	113.17	1.48	1.01	0.266
413	2095	2410	2.77E-04	7.14E-04	113.03	1.41	0.99	0.266
414	1601	1838	2.77E-04	3.44E-04	112.32	1.68	1.08	0.266
415	1525	1939	2.77E-04	7.82E-05	111.97	1.74	1.10	0.266
416	1750	2318	2.77E-04	3.96E-04	111.89	1.59	1.05	0.266
417	1616	2194	2.77E-04	4.80E-04	111.50	1.67	1.08	0.266
418	1386	1915	2.77E-04	1.89E-04	111.02	1.85	1.13	0.266
419	1486	2516	2.77E-04	6.59E-04	110.83	1.77	1.11	0.266
420	1054	1734	2.77E-04	4.85E-06	110.17	2.23	1.24	0.266
421	1362	2208	2.77E-04	5.06E-04	110.17	1.88	1.14	0.266
422	1103	1715	2.77E-04	4.42E-06	109.66	2.16	1.22	0.266
423	1412	2643	2.77E-04	5.38E-04	109.65	1.83	1.13	0.266
424	1117	2569	2.77E-04	4.48E-04	109.12	2.14	1.22	0.266
425	923	2062	2.77E-04	5.18E-04	108.67	2.43	1.30	0.266
426	938	2216	2.77E-04	8.23E-04	108.15	2.56	1.33	0.266
427	505	1171	2.77E-04	-2.94E-04	107.33	3.86	1.64	0.266
428	958	1824	2.77E-04	-3.77E-06	107.62	2.52	1.32	0.266
429	1181	1976	2.77E-04	2.23E-04	107.63	2.19	1.23	0.266
430	1224	1978	2.77E-04	4.60E-04	107.40	2.14	1.22	0.266
431	1080	1574	2.77E-04	3.88E-04	106.94	2.33	1.27	0.266
432	991	1216	2.77E-04	3.65E-05	106.55	2.46	1.31	0.266
433	1183	1407	2.77E-04	2.25E-04	106.52	2.19	1.23	0.266
434	1224	1850	2.77E-04	4.64E-04	106.29	2.14	1.22	0.266
435	1075	1916	2.77E-04	4.24E-04	105.83	2.33	1.27	0.266
436	959	1518	2.77E-04	-3.01E-04	105.40	2.52	1.32	0.266
437	1417	1994	2.77E-04	3.00E-04	105.70	1.94	1.16	0.266
438	1399	2343	2.77E-04	2.67E-04	105.40	1.96	1.17	0.266
439	1407	1897	2.77E-04	4.77E-04	105.14	1.95	1.16	0.266
440	1248	1844	2.77E-04	1.49E-04	104.66	2.11	1.21	0.266
441	1350	1846	2.77E-04	9.38E-04	104.51	2.01	1.18	0.266
442	826	1730	2.77E-04	-2.01E-04	103.57	2.78	1.39	0.266
443	1206	1950	2.77E-04	6.68E-04	103.77	2.16	1.22	0.266
444	896	1825	2.77E-04	-1.49E-04	103.11	2.64	1.35	0.266
445	1234	2374	2.77E-04	-6.54E-04	103.26	2.13	1.22	0.266
446	1973	3329	2.77E-04	-4.07E-04	103.91	1.56	1.04	0.266
447	2516	3440	2.77E-04	1.24E-03	104.32	1.32	0.96	0.266
448	1748	2956	2.77E-04	-4.51E-05	103.07	1.69	1.08	0.266
449	2004	3023	2.77E-04	5.16E-04	103.12	1.54	1.03	0.266
450	1815	3183	2.77E-04	9.82E-04	102.60	1.65	1.07	0.266
451	1255	2262	2.77E-04	-6.72E-04	101.62	2.11	1.21	0.266
452	2008	2708	2.77E-04	5.50E-04	102.29	1.54	1.03	0.266
453	1792	2900	2.77E-04	-1.07E-03	101.74	1.66	1.07	0.266
454	1738	2562	2.77E-04	1.15E-03	102.81	1.69	1.08	0.266
455	2104	2989	2.77E-04	1.69E-04	101.66	1.49	1.02	0.266
456	1481	2660	2.77E-04	2.16E-03	101.49	1.89	1.14	0.266
457	835	1407	2.77E-04	4.58E-04	99.33	2.76	1.38	0.266
458	775	1279	2.77E-04	7.15E-04	98.88	2.90	1.42	0.266
459	627	1602	2.77E-04	1.13E-03	98.16	3.35	1.52	0.266
460	336	1167	2.77E-04	-5.28E-04	97.03	5.07	1.87	0.266
461	616	1540	2.77E-04	-1.07E-03	97.56	3.39	1.53	0.266
462	1080	2286	2.77E-04	1.70E-03	98.63	2.33	1.27	0.266
463	593	2092	2.77E-04	-1.17E-04	96.93	3.47	1.55	0.266
464	731	2311	2.77E-04	2.83E-04	97.05	3.02	1.45	0.266
465	732	2343	2.77E-04	8.39E-04	96.76	3.02	1.45	0.266
466	541	1259	2.77E-04	5.46E-05	95.92	3.69	1.60	0.266
467	620	1647	2.77E-04	5.94E-04	95.87	3.37	1.53	0.266
468	513	1800	2.77E-04	8.12E-05	95.27	3.83	1.63	0.266
469	582	1250	2.77E-04	-2.37E-05	95.19	3.51	1.56	0.266
470	688	1582	2.77E-04	-4.15E-04	95.22	3.14	1.48	0.266
471	929	1784	2.77E-04	1.25E-03	95.63	2.57	1.34	0.266
472	596	1502	2.77E-04	1.48E-04	94.38	3.46	1.55	0.266
473	643	1213	2.77E-04	3.81E-04	94.23	3.29	1.51	0.266
474	609	1065	2.77E-04	3.75E-04	93.85	3.41	1.54	0.266
475	578	1413	2.77E-04	3.19E-04	93.48	3.53	1.56	0.266

476	566	1275	2.77E-04	-1.09E-03	93.16	3.58	1.58	0.266
477	1039	1857	2.77E-04	1.07E-04	94.25	2.39	1.29	0.266
478	1099	1683	2.77E-04	2.06E-03	94.14	2.30	1.26	0.266
479	487	934	2.77E-04	-9.95E-05	92.08	3.96	1.66	0.266
480	619	1071	3.71E-04	-2.51E-04	92.18	3.06	1.68	0.307
481	803	1489	3.71E-04	-6.16E-04	92.43	2.58	1.54	0.307
482	1087	2179	3.71E-04	5.25E-05	93.04	2.10	1.40	0.307
483	1656	3535	3.71E-04	3.97E-04	92.99	1.59	1.21	0.307
484	1624	3630	3.71E-04	5.11E-04	92.59	1.61	1.22	0.307
485	1393	3788	3.71E-04	3.45E-04	92.08	1.78	1.29	0.307
486	1452	3643	3.71E-04	-2.06E-04	91.74	1.73	1.27	0.307
487	2473	3495	3.71E-04	4.75E-04	91.94	1.22	1.06	0.307
488	2306	4444	3.71E-04	1.88E-04	91.47	1.27	1.09	0.307
489	2638	4494	3.71E-04	3.92E-04	91.28	1.17	1.04	0.307
490	2615	4546	3.71E-04	5.06E-04	90.89	1.17	1.04	0.307
491	2392	4464	3.71E-04	7.40E-04	90.38	1.24	1.07	0.307
492	1760	3365	3.71E-04	6.27E-04	89.64	1.53	1.19	0.307
493	1326	3272	3.71E-04	-2.59E-04	89.02	1.84	1.31	0.307
494	2441	3374	3.71E-04	4.50E-04	89.27	1.23	1.07	0.307
495	2317	3401	3.71E-04	1.35E-04	88.82	1.27	1.08	0.307
496	2742	4147	3.71E-04	4.97E-04	88.69	1.14	1.03	0.307
497	2536	3556	3.88E-04	3.27E-04	88.19	1.18	1.07	0.314
498	2626	3799	3.88E-04	5.51E-04	87.87	1.15	1.06	0.314
499	2325	3461	3.88E-04	4.23E-04	87.31	1.25	1.10	0.314
500	2247	3527	3.88E-04	6.54E-04	86.89	1.28	1.11	0.314
501	1766	3225	3.88E-04	6.18E-05	86.24	1.50	1.21	0.314
502	2319	3183	3.88E-04	7.20E-04	86.18	1.25	1.10	0.314
503	1722	3466	3.88E-04	3.11E-05	85.46	1.52	1.22	0.314
504	2329	3644	3.88E-04	7.14E-04	85.42	1.25	1.10	0.314
505	1744	3422	3.88E-04	4.03E-04	84.71	1.51	1.21	0.314
506	1702	3560	3.88E-04	4.38E-04	84.31	1.54	1.22	0.314
507	1598	3394	3.88E-04	3.98E-04	83.87	1.60	1.25	0.314
508	1565	3564	3.88E-04	2.87E-04	83.47	1.63	1.26	0.314
509	1726	3970	3.88E-04	3.57E-04	83.19	1.52	1.22	0.314
510	1722	4092	3.88E-04	4.47E-04	82.83	1.53	1.22	0.314
511	1640	3618	3.88E-04	-6.10E-05	82.38	1.58	1.24	0.314
512	2264	3882	3.88E-04	3.98E-04	82.44	1.27	1.11	0.314
513	2250	3829	3.88E-04	2.59E-04	82.04	1.28	1.11	0.314
514	2430	3984	3.88E-04	5.82E-04	81.79	1.21	1.08	0.314
515	2161	3293	3.88E-04	3.77E-04	81.20	1.31	1.13	0.314
516	2176	3188	3.88E-04	7.94E-04	80.83	1.30	1.12	0.314
517	1612	2765	3.88E-04	4.16E-04	80.03	1.59	1.24	0.314
518	1573	3051	3.88E-04	6.49E-05	79.62	1.62	1.25	0.314
519	2022	3149	3.88E-04	4.19E-04	79.55	1.37	1.15	0.314
520	1978	3060	3.88E-04	1.31E-03	79.13	1.39	1.16	0.314
521	701	2998	3.88E-04	-2.83E-04	77.83	2.78	1.64	0.314
522	1632	2882	3.88E-04	1.92E-04	78.11	1.58	1.24	0.314
523	1905	3223	3.88E-04	6.13E-04	77.92	1.43	1.18	0.314
524	1592	3611	3.88E-04	1.19E-04	77.30	1.61	1.25	0.314
525	1966	3674	3.88E-04	5.73E-04	77.19	1.40	1.16	0.314
526	1710	3925	3.88E-04	2.33E-04	76.61	1.53	1.22	0.314
527	1925	3750	3.88E-04	8.11E-04	76.38	1.42	1.17	0.314
528	1337	3369	3.88E-04	2.87E-04	75.57	1.81	1.32	0.314
529	1478	3293	3.88E-04	2.15E-04	75.28	1.69	1.28	0.314
530	1717	2867	3.88E-04	6.52E-04	75.07	1.53	1.22	0.314
531	1351	2553	3.88E-04	1.79E-04	74.41	1.79	1.32	0.314
532	1640	2751	3.88E-04	3.47E-04	74.24	1.58	1.24	0.314
533	1697	2449	3.88E-04	4.67E-04	73.89	1.54	1.22	0.314
534	1588	3145	3.88E-04	6.66E-04	73.42	1.61	1.25	0.314
535	1202	3347	3.88E-04	7.01E-05	72.76	1.94	1.37	0.314
536	1643	3134	3.88E-04	1.06E-04	72.69	1.57	1.24	0.314
537	2035	3251	3.88E-04	5.50E-04	72.58	1.36	1.15	0.314
538	1825	3488	3.88E-04	7.31E-04	72.03	1.47	1.19	0.314
539	1362	3104	3.88E-04	1.65E-04	71.30	1.78	1.32	0.314
540	1619	3051	3.88E-04	1.37E-04	71.13	1.59	1.24	0.314
541	1912	3312	3.88E-04	8.07E-04	71.00	1.42	1.17	0.314
542	1352	3247	3.88E-04	-3.88E-05	70.19	1.79	1.32	0.314
543	1868	3104	3.88E-04	5.17E-04	70.23	1.44	1.18	0.314
544	1677	3231	3.88E-04	5.94E-04	69.71	1.55	1.23	0.314
545	1388	2961	3.88E-04	4.78E-04	69.12	1.76	1.31	0.314
546	1246	3068	3.88E-04	2.64E-04	68.64	1.89	1.35	0.314
547	1377	2757	3.88E-04	2.55E-05	68.38	1.77	1.31	0.314
548	1812	3148	3.88E-04	5.16E-04	68.35	1.47	1.20	0.314
549	1622	3039	3.88E-04	2.99E-04	67.83	1.59	1.24	0.314
550	1709	2418	3.51E-04	4.09E-04	67.53	1.58	1.18	0.299
551	1655	2208	3.51E-04	4.58E-04	67.13	1.62	1.19	0.299
552	1539	2162	3.51E-04	2.41E-04	66.67	1.70	1.22	0.299
553	1700	2424	3.51E-04	4.79E-04	66.43	1.59	1.18	0.299
554	1558	2948	3.51E-04	5.01E-04	65.95	1.69	1.22	0.299
555	1387	2921	3.51E-04	1.74E-04	65.45	1.82	1.26	0.299
556	1632	3202	3.51E-04	1.16E-04	65.27	1.63	1.20	0.299
557	1951	3063	3.51E-04	2.53E-04	65.16	1.45	1.13	0.299

558	2096	3191	3.51E-04	7.39E-04	64.90	1.38	1.10	0.299
559	1623	3423	3.51E-04	4.59E-04	64.16	1.64	1.20	0.299
560	1506	3740	3.51E-04	2.92E-04	63.71	1.72	1.23	0.299
561	1602	3790	3.51E-04	2.72E-05	63.41	1.65	1.21	0.299
562	2034	3753	3.51E-04	2.18E-04	63.39	1.41	1.11	0.299
563	2224	3724	3.51E-04	7.21E-04	63.17	1.33	1.08	0.299
564	1773	3841	3.51E-04	2.61E-04	62.45	1.55	1.17	0.299
565	1909	4235	3.51E-04	-3.78E-04	62.19	1.47	1.14	0.299
566	2595	4447	3.51E-04	1.80E-03	62.57	1.20	1.03	0.299
567	1116	3912	3.51E-04	-2.08E-04	60.77	2.11	1.36	0.299
568	1688	3482	3.51E-04	3.39E-04	60.98	1.60	1.18	0.299
569	1700	3824	3.51E-04	2.03E-04	60.64	1.59	1.18	0.299
570	1852	3801	3.51E-04	7.27E-04	60.43	1.50	1.15	0.299
571	1468	3535	3.51E-04	5.06E-04	59.71	1.75	1.24	0.299
572	1310	3465	3.51E-04	3.87E-04	59.20	1.89	1.29	0.299
573	1273	2573	3.51E-04	3.55E-04	58.81	1.93	1.30	0.299
574	1269	3570	3.51E-04	2.21E-04	58.46	1.93	1.30	0.299
575	1403	2932	3.51E-04	2.63E-04	58.24	1.81	1.26	0.299
576	1493	3575	3.51E-04	4.66E-04	57.97	1.73	1.23	0.299
577	1376	3474	3.51E-04	4.05E-04	57.51	1.83	1.27	0.299
578	1321	3134	3.51E-04	2.42E-04	57.10	1.88	1.29	0.299
579	1433	3571	3.51E-04	-5.17E-05	56.86	1.78	1.25	0.299
580	1845	3817	3.51E-04	1.01E-03	56.91	1.51	1.15	0.299
581	1174	3858	3.51E-04	-4.05E-05	55.91	2.04	1.34	0.299
582	1575	3532	3.51E-04	6.40E-04	55.95	1.67	1.21	0.299
583	1279	3487	3.51E-04	4.08E-04	55.31	1.92	1.30	0.299
584	1222	3053	3.51E-04	6.30E-05	54.90	1.98	1.32	0.299
585	1516	3109	3.51E-04	5.50E-04	54.84	1.72	1.23	0.299
586	1314	3222	3.51E-04	3.22E-04	54.29	1.89	1.29	0.299
587	1344	3827	3.51E-04	3.27E-04	53.96	1.86	1.28	0.299
588	1369	4257	3.51E-04	1.84E-04	53.64	1.84	1.27	0.299
589	1540	3927	3.51E-04	2.56E-04	53.45	1.70	1.22	0.299
590	1637	3913	3.51E-04	4.54E-04	53.20	1.63	1.20	0.299
591	1533	3689	3.51E-04	6.61E-04	52.74	1.70	1.22	0.299
592	1216	3910	3.51E-04	-1.03E-04	52.08	1.99	1.32	0.299
593	1681	4393	3.51E-04	6.01E-04	52.19	1.60	1.19	0.299
594	1434	5592	3.51E-04	1.74E-04	51.59	1.78	1.25	0.299
595	1633	5293	3.51E-04	5.10E-04	51.41	1.63	1.20	0.299
596	1455	5378	3.51E-04	4.37E-04	50.90	1.76	1.24	0.299
597	1359	5109	3.51E-04	1.36E-04	50.46	1.85	1.27	0.299
598	1600	4896	3.51E-04	3.52E-04	50.33	1.66	1.21	0.299
599	1599	4499	3.51E-04	6.67E-04	49.98	1.66	1.21	0.299
600	1245	4177	3.51E-04	5.74E-05	49.31	1.96	1.31	0.299
601	1575	4048	3.51E-04	3.92E-04	49.25	1.67	1.21	0.299
602	1529	4458	3.51E-04	1.35E-04	48.86	1.71	1.22	0.299
603	1772	4771	3.51E-04	3.90E-04	48.73	1.55	1.17	0.299
604	1728	4155	3.51E-04	1.24E-04	48.34	1.57	1.18	0.299
605	1983	3809	3.51E-04	4.45E-04	48.21	1.43	1.12	0.299
606	1878	3668	3.51E-04	5.22E-04	47.77	1.49	1.14	0.299
607	1687	4267	3.51E-04	1.05E-04	47.24	1.60	1.18	0.299
608	1963	4518	3.51E-04	5.37E-04	47.14	1.44	1.13	0.299
609	1755	4231	3.51E-04	5.41E-04	46.60	1.56	1.17	0.299
610	1543	3638	3.51E-04	7.40E-05	46.06	1.70	1.22	0.299
611	1854	4272	3.51E-04	7.17E-04	45.99	1.50	1.15	0.299
612	1444	3937	3.51E-04	5.07E-04	45.27	1.77	1.25	0.299
613	1269	3358	3.51E-04	9.11E-05	44.76	1.93	1.30	0.299
614	1561	3367	3.51E-04	2.78E-04	44.67	1.68	1.22	0.299
615	1643	3240	3.51E-04	6.39E-04	44.39	1.63	1.20	0.299
616	1320	2674	3.51E-04	3.43E-04	43.76	1.88	1.29	0.299
617	1329	2507	3.51E-04	4.83E-04	43.41	1.87	1.28	0.299
618	1181	2423	3.51E-04	2.79E-04	42.93	2.03	1.33	0.299
619	1262	3104	3.51E-04	-6.47E-05	42.65	1.94	1.31	0.299
620	1727	4054	3.51E-04	5.12E-04	42.71	1.57	1.18	0.299
621	1548	3941	3.51E-04	4.00E-04	42.20	1.69	1.22	0.299
622	1543	3206	3.51E-04	-1.57E-04	41.80	1.70	1.22	0.299
623	2028	3779	3.51E-04	8.53E-04	41.96	1.41	1.11	0.299
624	1484	3716	3.51E-04	2.32E-04	41.11	1.74	1.24	0.299
625	1572	3170	3.51E-04	7.36E-04	40.87	1.68	1.21	0.299
626	1147	2814	3.51E-04	-7.46E-05	40.14	2.07	1.35	0.299
627	1547	2956	3.51E-04	2.28E-04	40.21	1.69	1.22	0.299
628	1639	2822	3.51E-04	2.57E-04	39.98	1.63	1.20	0.299
629	1702	3300	3.51E-04	7.49E-04	39.73	1.59	1.18	0.299
630	1263	3530	3.51E-04	9.21E-05	38.98	1.94	1.30	0.299
631	1494	2958	3.51E-04	1.60E-04	38.89	1.73	1.23	0.299
632	1657	2973	3.51E-04	8.76E-04	38.73	1.62	1.19	0.299
633	1089	3312	3.51E-04	-4.61E-05	37.85	2.14	1.37	0.299
634	1461	3461	3.51E-04	6.32E-05	37.90	1.76	1.24	0.299
635	1721	3779	2.91E-04	6.85E-04	37.83	1.68	1.10	0.272
636	1347	4111	2.91E-04	1.40E-05	37.15	1.98	1.20	0.272
637	1658	3683	2.91E-04	5.44E-04	37.13	1.72	1.12	0.272
638	1429	3713	2.91E-04	4.73E-04	36.59	1.90	1.18	0.272
639	1272	3785	2.91E-04	2.57E-04	36.12	2.06	1.22	0.272

640	1335	3960	2.91E-04	4.45E-04	35.86	1.99	1.20	0.272
641	1206	3228	2.91E-04	1.65E-05	35.42	2.13	1.24	0.272
642	1514	2709	2.91E-04	3.21E-04	35.40	1.83	1.15	0.272
643	1511	2705	2.91E-04	5.42E-04	35.08	1.83	1.15	0.272
644	1284	2814	2.91E-04	-2.69E-04	34.54	2.04	1.22	0.272
645	1882	2998	2.91E-04	2.15E-04	34.80	1.58	1.07	0.272
646	1988	2820	2.91E-04	8.92E-04	34.59	1.53	1.05	0.272
647	1404	3163	2.91E-04	2.05E-04	33.70	1.92	1.18	0.272
648	1520	2543	2.91E-04	2.63E-04	33.49	1.82	1.15	0.272
649	1577	2891	2.91E-04	5.45E-04	33.23	1.78	1.14	0.272
650	1412	2980	2.91E-04	5.31E-04	32.68	1.92	1.18	0.272
651	1177	3026	2.91E-04	-4.28E-05	32.15	2.16	1.25	0.272
652	1495	2647	2.91E-04	3.65E-04	32.20	1.85	1.16	0.272
653	1420	2967	2.91E-04	1.96E-04	31.83	1.91	1.18	0.272
654	1508	2934	2.91E-04	3.59E-04	31.64	1.83	1.15	0.272
655	1439	4009	2.91E-04	6.61E-05	31.28	1.89	1.17	0.272
656	1652	3966	2.91E-04	3.58E-04	31.21	1.73	1.12	0.272
657	1584	4483	2.91E-04	5.97E-04	30.85	1.78	1.14	0.272
658	1286	4357	2.91E-04	3.57E-04	30.26	2.04	1.22	0.272
659	1218	3754	2.91E-04	3.02E-05	29.90	2.12	1.24	0.272
660	1467	4551	2.91E-04	1.71E-04	29.87	1.87	1.17	0.272
661	1579	3787	2.91E-04	2.80E-04	29.70	1.78	1.14	0.272
662	1585	3350	2.91E-04	1.31E-04	29.42	1.77	1.14	0.272
663	1737	3711	2.91E-04	3.12E-04	29.29	1.67	1.10	0.272
664	1713	3764	2.91E-04	1.18E-04	28.97	1.69	1.11	0.272
665	1876	3597	2.91E-04	5.61E-04	28.86	1.59	1.07	0.272
666	1613	3554	2.91E-04	1.71E-04	28.30	1.75	1.13	0.272
667	1725	3334	2.91E-04	7.78E-04	28.12	1.68	1.10	0.272
668	1252	3866	2.91E-04	2.49E-04	27.35	2.08	1.23	0.272
669	1288	3556	2.91E-04	-1.70E-04	27.10	2.04	1.22	0.272
670	1730	3741	2.91E-04	5.69E-04	27.27	1.67	1.10	0.272
671	1458	4044	2.91E-04	2.61E-04	26.70	1.88	1.17	0.272
672	1483	3410	2.91E-04	5.82E-04	26.44	1.86	1.16	0.272
673	1199	2935	2.91E-04	2.48E-04	25.85	2.14	1.25	0.272
674	1237	2912	2.91E-04	2.80E-05	25.61	2.09	1.23	0.272
675	1487	2624	2.61E-04	6.59E-05	25.58	1.92	1.12	0.258
676	1701	2806	2.61E-04	5.40E-04	25.51	1.75	1.07	0.258
677	1457	3107	2.61E-04	4.31E-04	24.97	1.95	1.13	0.258
678	1530	3918	2.61E-04	1.58E-04	24.54	2.06	1.16	0.258
679	1563	4213	2.61E-04	-4.12E-04	24.38	2.03	1.15	0.258
680	1929	3697	2.61E-04	6.20E-04	24.80	1.77	1.07	0.258
681	1693	3950	2.61E-04	1.16E-04	24.18	1.93	1.12	0.258
682	1750	3747	2.61E-04	8.95E-04	24.06	1.89	1.11	0.258
683	1353	3461	2.61E-04	6.23E-04	23.16	2.24	1.21	0.258
684	1115	3497	2.61E-04	3.19E-05	22.54	2.55	1.29	0.258
685	1222	3249	2.61E-04	3.17E-04	22.51	2.40	1.25	0.258
686	1162	3556	2.61E-04	-2.34E-05	22.19	2.48	1.27	0.258
687	1301	3364	2.61E-04	2.47E-04	22.22	2.30	1.22	0.258
688	1282	3170	2.61E-04	8.90E-04	21.97	2.32	1.23	0.258
689	888	3768	2.61E-04	-4.73E-04	21.08	2.97	1.39	0.258
690	1289	3448	2.61E-04	-4.60E-05	21.55	2.31	1.23	0.258
691	1442	2795	2.61E-04	6.84E-04	21.60	2.15	1.18	0.258
692	1168	2511	2.61E-04	7.01E-04	20.91	2.47	1.27	0.258
693	884	2805	2.61E-04	3.30E-05	20.21	2.98	1.39	0.258
694	990	2707	2.22E-04	-1.20E-04	20.18	2.91	1.27	0.238
695	1186	3015	2.22E-04	-3.01E-04	20.30	2.58	1.20	0.238
696	1487	3884	2.22E-04	-4.81E-05	20.60	2.22	1.11	0.238
697	1640	3927	2.22E-04	4.34E-04	20.65	2.08	1.07	0.238
698	1512	4952	2.22E-04	-5.29E-05	20.22	2.19	1.10	0.238
699	1669	4954	2.22E-04	2.46E-04	20.27	2.05	1.07	0.238
700	1650	4949	2.22E-04	7.06E-04	20.02	2.07	1.07	0.238
701	1364	4585	2.22E-04	7.94E-05	19.32	2.35	1.14	0.238
702	1443	4903	2.22E-04	-5.78E-04	19.24	2.26	1.12	0.238
703	1906	4667	2.22E-04	8.43E-04	19.82	1.88	1.02	0.238
704	1539	3224	2.22E-04	3.66E-04	18.97	2.17	1.10	0.238
705	1451	2713	2.22E-04	2.86E-04	18.61	2.26	1.12	0.238
706	1409	2845	2.22E-04	5.31E-04	18.32	2.30	1.13	0.238
707	1224	2930	2.22E-04	1.24E-04	17.79	2.53	1.18	0.238
708	1278	2813	2.22E-04	1.43E-04	17.67	2.45	1.17	0.238
709	1320	4338	2.22E-04	-1.98E-04	17.52	2.40	1.16	0.238
710	1560	4518	2.22E-04	1.37E-04	17.72	2.15	1.09	0.238
711	1606	4695	2.22E-04	5.28E-04	17.58	2.11	1.08	0.238
712	1423	4883	2.22E-04	9.22E-06	17.06	2.28	1.13	0.238
713	1543	5174	2.22E-04	9.61E-05	17.05	2.16	1.10	0.238
714	1612	5237	2.22E-04	6.06E-04	16.95	2.10	1.08	0.238
715	1384	4069	2.22E-04	5.69E-04	16.35	2.33	1.14	0.238
716	1177	3628	2.22E-04	1.55E-04	15.78	2.59	1.20	0.238
717	1212	3200	2.22E-04	-7.03E-05	15.62	2.54	1.19	0.238
718	1378	2912	2.22E-04	2.51E-04	15.69	2.33	1.14	0.238
719	1357	2839	2.22E-04	8.63E-04	15.44	2.36	1.15	0.238
720	978	3263	2.22E-04	6.46E-04	14.58	2.93	1.28	0.238
721	727	3284	2.22E-04	-5.08E-04	13.93	3.58	1.41	0.238

722	1148	3605	2.22E-04	4.86E-05	14.44	2.64	1.21	0.238
723	1245	3976	2.22E-04	-1.70E-04	14.39	2.50	1.18	0.238
724	1470	2806	2.22E-04	5.85E-04	14.56	2.24	1.11	0.238
725	1254	2316	2.22E-04	5.30E-04	13.97	2.49	1.18	0.238
726	1069	2752	2.22E-04	3.18E-04	13.44	2.76	1.24	0.238
727	1009	2700	2.22E-04	8.08E-04	13.13	2.87	1.26	0.238
728	663	2495	2.22E-04	-5.48E-05	12.32	3.80	1.45	0.238
729	821	2199	2.22E-04	-2.62E-04	12.37	3.30	1.35	0.238
730	1099	2241	2.22E-04	6.90E-05	12.64	2.71	1.23	0.238
731	1184	2421	2.22E-04	1.87E-04	12.57	2.58	1.20	0.238
732	1200	3143	2.22E-04	-2.22E-04	12.38	2.56	1.19	0.238
733	1455	2939	2.22E-04	3.89E-04	12.60	2.25	1.12	0.238
734	1353	2524	2.22E-04	8.33E-04	12.21	2.36	1.15	0.238
735	992	2408	2.22E-04	3.67E-04	11.38	2.91	1.27	0.238
736	904	2295	1.59E-04	-4.52E-04	11.01	3.46	1.17	0.201
737	1293	3080	1.59E-04	3.32E-04	11.46	2.72	1.04	0.201
738	1224	2964	1.59E-04	-7.07E-05	11.13	2.82	1.06	0.201
739	1391	2832	1.59E-04	5.01E-04	11.20	2.59	1.02	0.201
740	1223	2131	1.59E-04	9.97E-04	10.70	2.83	1.06	0.201
741	767	1913	1.59E-04	-6.73E-05	9.70	3.86	1.24	0.201
742	932	2191	1.59E-04	1.98E-04	9.77	3.39	1.16	0.201
743	942	2206	1.59E-04	-3.04E-04	9.57	3.37	1.16	0.201
744	1245	2376	1.59E-04	3.61E-04	9.88	2.79	1.05	0.201
745	1159	2307	1.59E-04	6.30E-04	9.52	2.93	1.08	0.201
746	917	1998	1.59E-04	-1.99E-06	8.89	3.43	1.17	0.201
747	1043	2001	1.59E-04	4.96E-04	8.89	3.14	1.12	0.201
748	879	1982	1.59E-04	4.99E-04	8.39	3.52	1.18	0.201
749	713	1874	1.59E-04	5.29E-04	7.89	4.05	1.27	0.201
750	530	1969	1.59E-04	-3.07E-04	7.37	4.94	1.40	0.201
751	835	1690	1.59E-04	7.67E-05	7.67	3.65	1.20	0.201
752	915	2074	1.59E-04	3.94E-04	7.60	3.43	1.17	0.201
753	811	2591	1.59E-04	1.67E-04	7.20	3.72	1.22	0.201
754	839	2322	1.59E-04	1.06E-03	7.03	3.64	1.20	0.201
755	878	2522	1.59E-04	1.34E-04	5.98	3.53	1.18	0.201
756	870	2399	1.59E-04	-9.07E-04	5.84	3.55	1.19	0.201
757	1113	2477	1.59E-04	1.07E-03	6.75	3.01	1.09	0.201
758	880	2415	1.59E-04	-5.87E-04	5.68	3.52	1.18	0.201
759	1046	2196	1.59E-04	-2.95E-04	6.27	3.14	1.12	0.201
760	1142	2267	1.59E-04	1.54E-03	6.56	2.96	1.08	0.201
761	794	2404	1.59E-04	6.36E-05	5.02	3.77	1.22	0.201
762	803	2273	1.59E-04	-3.44E-04	4.96	3.74	1.22	0.201
763	911	1271	1.59E-04	1.01E-03	5.30	3.44	1.17	0.201
764	692	1336	1.59E-04	1.16E-03	4.29	4.13	1.28	0.201
765	436	1146	1.59E-04	-1.31E-03	3.13	5.62	1.49	0.201
766	778	2171	1.59E-04	3.13E-04	4.45	3.82	1.23	0.201
767	727	2165	1.59E-04	-9.86E-04	4.13	4.00	1.26	0.201
768	989	2135	1.59E-04	1.68E-03	5.12	3.26	1.14	0.201
769	610	2081	1.59E-04	-4.19E-04	3.44	4.50	1.34	0.201
770	735	2228	1.59E-04	3.68E-04	3.86	3.97	1.26	0.201
771	671	1861	1.59E-04	-1.44E-03	3.49	4.22	1.29	0.201
772	1043	1876	1.59E-04	8.09E-04	4.94	3.14	1.12	0.201
773	873	1875	1.59E-04	5.23E-04	4.13	3.54	1.19	0.201
774	771	2049	1.59E-04	6.04E-05	3.60	3.85	1.24	0.201
775	781	2143	1.59E-04	2.88E-04	3.54	3.81	1.23	0.201
776	736	2340	1.59E-04	2.40E-04	3.26	3.97	1.26	0.201
777	703	2351	1.59E-04	-4.79E-04	3.02	4.09	1.27	0.201
778	843	2640	1.59E-04	-2.19E-04	3.49	3.62	1.20	0.201
779	920	1912	1.59E-04	1.93E-04	3.71	3.42	1.17	0.201
780	898	1661	1.59E-04	-3.52E-04	3.52	3.47	1.17	0.201
781	1007	1576	1.59E-04	1.83E-04	3.87	3.22	1.13	0.201
782	988	1730	1.59E-04	1.74E-03	3.69	3.26	1.14	0.201
783	593	1661	1.59E-04	-4.19E-04	1.95	4.58	1.35	0.201
784	719	1893	6.62E-05	-1.34E-03	2.37	5.39	0.94	0.130
785	1068	1952	6.62E-05	7.10E-04	3.72	4.14	0.83	0.130
786	921	1890	6.62E-05	8.02E-04	3.01	4.57	0.87	0.130
787	752	1844	6.62E-05	1.18E-03	2.20	5.24	0.93	0.130
788	493	1746	6.62E-05	-1.17E-03	1.03	6.94	1.07	0.130
789	800	2459	6.62E-05	-5.11E-04	2.20	5.02	0.91	0.130
790	948	2596	6.62E-05	-4.42E-04	2.71	4.48	0.86	0.130
791	1079	2125	6.62E-05	1.13E-03	3.16	4.11	0.83	0.130
792	831	3267	6.62E-05	9.29E-04	2.02	4.90	0.90	0.130
793	631	3262	6.62E-05	2.85E-04	1.09	5.88	0.99	0.130
794	587	2496	6.62E-05	-6.76E-04	0.81	6.17	1.01	0.130
795	775	2215	6.62E-05	2.18E-04	1.49	5.13	0.92	0.130
796	747	1910	6.62E-05	-1.13E-03	1.27	5.26	0.93	0.130
797	1043	2141	6.62E-05	1.43E-03	2.39	4.21	0.83	0.130
798	721	2399	6.62E-05	-4.37E-04	0.96	5.38	0.94	0.130
799	852	1937	6.62E-05	1.42E-03	1.40	4.82	0.89	0.130
800	533	2214	6.62E-05	-1.07E-03	-0.03	6.59	1.04	0.130
801	816	1941	6.62E-05	3.86E-04	1.05	4.96	0.91	0.130
802	747	2509	6.62E-05	-1.14E-03	0.66	5.26	0.93	0.130
803	1047	2295	6.62E-05	1.61E-04	1.80	4.20	0.83	0.130

804	1033	2073	6.62E-05	1.05E-03	1.64	4.24	0.84	0.130
805	803	1736	6.62E-05	8.67E-04	0.59	5.01	0.91	0.130
806	618	1217	6.62E-05	3.84E-04	-0.28	5.96	0.99	0.130
807	550	1293	6.62E-05	-1.30E-03	-0.66	6.45	1.03	0.130
808	889	1607	6.62E-05	3.52E-04	0.64	4.68	0.88	0.130
809	829	1724	6.62E-05	-1.20E-03	0.29	4.91	0.90	0.130
810	1142	2013	6.62E-05	1.19E-03	1.48	3.96	0.81	0.130
811	880	1532	6.62E-05	-1.01E-03	0.30	4.71	0.88	0.130
812	1149	1922	6.62E-05	9.56E-04	1.31	3.95	0.81	0.130
813	943	1701	6.62E-05	3.54E-04	0.35	4.50	0.86	0.130
814	882	1681	6.62E-05	8.35E-04	0.00	4.71	0.88	0.130
815	705	1442	6.62E-05	-7.73E-04	-0.84	5.47	0.95	0.130
816	916	1594	6.62E-05	7.14E-04	-0.06	4.59	0.87	0.130
817	768	2113	6.62E-05	6.08E-04	-0.78	5.16	0.92	0.130
818	646	1737	6.62E-05	-9.98E-04	-1.39	5.79	0.98	0.130
819	911	1467	6.62E-05	2.02E-04	-0.39	4.61	0.87	0.130
820	887	1626	6.62E-05	-1.38E-03	-0.59	4.69	0.88	0.130
821	1244	1816	6.62E-05	1.18E-03	0.79	3.74	0.79	0.130
822	983	1673	6.62E-05	1.36E-03	-0.39	4.38	0.85	0.130
823	679	1565	6.62E-05	-6.01E-04	-1.76	5.61	0.96	0.130
824	848	1696	6.62E-05	-1.14E-03	-1.16	4.83	0.89	0.130
825	1149	1767	6.62E-05	-1.90E-05	-0.01	3.95	0.81	0.130
826	1178	2349	6.62E-05	8.71E-04	0.01	3.88	0.80	0.130
827	992	2533	6.62E-05	-2.41E-04	-0.86	4.35	0.85	0.130
828	1075	2544	6.62E-05	2.31E-03	-0.62	4.13	0.83	0.130
829	543	2444	6.62E-05	-1.63E-04	-2.93	6.51	1.04	0.130
830	607	2200	6.62E-05	-1.76E-03	-2.77	6.04	1.00	0.130
831	1461	2246	6.62E-05	1.07E-04	-1.01	3.36	0.75	0.130
832	1441	3084	6.62E-05	-8.17E-05	-1.12	3.39	0.75	0.130
833	1513	3855	6.62E-05	5.18E-05	-1.04	3.28	0.74	0.130
834	1520	3901	6.62E-05	1.12E-03	-1.09	3.27	0.74	0.130
835	1013	3481	6.62E-05	-1.30E-03	-2.21	4.29	0.84	0.130
836	1670	4074	6.62E-05	4.12E-04	-0.91	3.07	0.71	0.130
837	1504	4190	6.62E-05	8.34E-04	-1.32	3.30	0.74	0.130
838	1135	3352	6.62E-05	-4.18E-04	-2.15	3.98	0.81	0.130
839	1368	4295	6.62E-05	2.92E-04	-1.73	3.51	0.76	0.130
840	1259	4833	6.62E-05	-2.46E-04	-2.03	3.71	0.78	0.130
841	1410	4336	6.62E-05	4.80E-04	-1.78	3.44	0.75	0.130
842	1211	4642	6.62E-05	4.39E-04	-2.26	3.81	0.79	0.130
843	1031	4795	6.62E-05	-6.83E-04	-2.70	4.24	0.84	0.130
844	1392	4137	6.62E-05	-4.37E-04	-2.02	3.47	0.76	0.130
845	1634	3982	6.62E-05	6.03E-04	-1.58	3.12	0.72	0.130
846	1376	4155	6.62E-05	-3.15E-04	-2.18	3.50	0.76	0.130
847	1559	3736	6.62E-05	6.62E-05	-1.87	3.22	0.73	0.130
848	1559	3512	6.62E-05	-2.55E-04	-1.93	3.22	0.73	0.130
849	1835	3271	6.62E-05	2.03E-04	-1.68	2.89	0.69	0.130
850	1623	3358	6.62E-05	1.47E-04	-1.88	3.13	0.72	0.130
851	1497	3825	6.62E-05	7.85E-05	-2.03	3.31	0.74	0.130
852	1478	3866	6.62E-05	-3.54E-05	-2.11	3.34	0.74	0.130
853	1636	3796	6.62E-05	-3.61E-04	-2.07	3.12	0.72	0.130
854	2296	4143	6.62E-05	3.53E-04	-1.71	2.49	0.64	0.130
855	1853	4452	6.62E-05	-3.90E-04	-2.06	2.87	0.69	0.130
856	2560	4693	6.62E-05	2.45E-04	-1.67	2.31	0.62	0.130
857	2283	4642	6.62E-05	4.02E-04	-1.92	2.50	0.64	0.130
858	1762	4106	6.62E-05	-2.73E-04	-2.32	2.97	0.70	0.130
859	2288	4533	6.62E-05	-1.44E-04	-2.05	2.49	0.64	0.130
860	2614	4911	6.62E-05	-2.73E-04	-1.90	2.28	0.61	0.130
861	3139	5488	6.62E-05	-5.03E-04	-1.63	2.02	0.58	0.130
862	4020	5855	6.62E-05	-5.07E-04	-1.13	1.71	0.53	0.130
863	4908	6149	6.62E-05	6.49E-05	-0.62	1.50	0.50	0.130
864	4909	6626	6.62E-05	-7.74E-06	-0.68	1.50	0.50	0.130
865	5024	6279	6.62E-05	2.14E-04	-0.68	1.48	0.49	0.130
866	4795	6972	6.62E-05	1.09E-04	-0.89	1.52	0.50	0.130

Table 2.A: database of the Zambezi river measured and computed with a space resolution of 1 km, in terms of local values of: river width (active and stream, taken form LANDSAT 7 and original cartography); water slope (from DEM); bottom slope and bottom elevation (reconstructed); water depth, flow velocity and Froude number (calculated).

(1) calculated with an average value of $\overline{Q}^{Z}_{eq} = 2554\, m^3/s$ at the upstream boundary